7-9-2009

Synthesis and coordination chemistry of new oxazoline and benzoxazole based ligands with lanthanides

Edicome Cornel Shirima

Follow this and additional works at: https://digitalrepository.unm.edu/chem_etds

Edicome Cornel Shirima
Candidate

Chemistry and Chemical Biology
Department

This dissertation is approved, and it is acceptable in quality
and form for publication:

Approved by the Dissertation Committee:

Robert J Paine   , Chairperson

[signature]

Lorraine Deck

[signature]

SYNTHESIS AND COORDINATION CHEMISTRY OF NEW OXAZOLINE AND BENZOXAZOLE BASED LIGANDS WITH LANTHANIDES

BY

EDICOME CORNEL SHIRIMA

B Sc (Hons), University of Dar es Salaam, 1991

DISSERTATION

Submitted in Partial Fulfillment of the
Requirements for the Degree of

**Doctor of Philosophy
Chemistry**

The University of New Mexico
Albuquerque, New Mexico

May, 2009

DEDICATION

To my beloved wife Adelaida Elias Shirima and our children Victoria E. Shirima and Emmanuel Salustianus Respicious.

ACKNOWLEDGMENTS

SYNTHESIS AND COORDINATION CHEMISTRY OF NEW OXAZOLINE AND BENZOXAZOLE BASED LIGANDS WITH LANTHANIDES

BY

EDICOME CORNEL SHIRIMA

ABSTRACT OF DISSERTATION

Submitted in Partial Fulfillment of the
Requirements for the Degree of

Doctor of Philosophy
Chemistry

The University of New Mexico
Albuquerque, New Mexico

May, 2009

SYNTHESIS AND COORDINATION CHEMISTRY OF NEW OXAZOLINE AND BENZOXAZOLE BASED LIGANDS WITH LANTHANIDES

BY

EDICOME CORNEL SHIRIMA

B Sc (Hons), Chemistry, University of Dar es Salaam, 1991-Tanzania

Ph.D., Chemistry, University of New Mexico, 2009-USA

ABSTRACT

In Chapter 1, a brief literature review on the chemistry of lanthanides (Ln) and actinides (An) is described. In addition, the coordination chemistry of lanthanides/actinides with various ligands comprised of organic backbones has also been described.

In Chapters 2 and 3 the syntheses of oxazoline and benzoxazole ligands is described. Both ligands contain a hard donor group (P=O) and the nitrogen (N) atom from the heterocycle as a relatively softer donor atom. In Chapter 2 the oxazoline ligand was synthesized in two steps reaction that involves substitution with Ph_2P group and oxidation of the phosphine into P=O by air. The target compound, 2-[(diphenylphosphinoyl)methyl]-4,5-dihydro-oxazole, **19** was fully characterized by spectroscopic methods. Single crystals suitable for X-ray diffraction of the target molecule were grown from a capped hot ethyl acetate solution for several hours. The coordination with lanthanides was demonstrated by isolation of a complex using Nd(III).

Single crystal X-ray diffraction analysis of the Nd(III) complex shows bidentate bonding via the P=O group and N donor atom.

In Chapter 3, a series of target benzoxazole based ligands **25a-25d** are described. All ligands contain the hard P=O and nitrogen (N) donor groups. These ligands have been fully characterized using elemental analysis, mass spectrometry and spectroscopic analysis. Single crystals suitable for X-ray diffraction studies for **25a-25d** were grown from different solvents. The coordination complexes were formed with Nd(III) and Yb(III). Single crystal X-ray diffraction studies were completed. Only **25a** complex with Nd(III) reveals bidentate coordination via P=O and N groups, the rest show monodentate coordination via P=O group only. In Chapter 4 a syntheses and coordination summary that is described in Chapters 2 and 3 is provided.

It is expected that some of the ligands prepared in this study may have the potential toward actinide(III) extraction, and this will be examined in future collaborative studies.

Table of Contents

CHAPTER 1

Coordination Chemistry of Lanthanides and Actinides

List of Abbreviations

An	Actinide ion
Bp	Boiling point
^{o}C	Celsius
Calcd	Calculated
$CDCl_3$	Deutarated chloroform
CMP	Carbamoylmethyl phosphonate
CMPO	Carbamoylmethyl phosphine oxide
DCM	Dichloromethane
DMSO	Deuterated dimethyl sulfoxide
EtOAc	Ethyl acetate
EtOH	Ethanol
Et_2O	Diethyl ether
g	Grams
HCl	Hydrochloric acid
Hz	Hertz
IR	Infrared spectroscopy
Ln	Lanthanide ion
MeOH	Methanol
M	Molarity
mol	Mole
m	Multiplate
mmol	Milli mole

mp	Melting point
NMR	Nuclear Magnetic Resonance
ppm	Parts per Million
ppt	Precipitate
THF	Tetrahydrofuran
TRUEX	Transuranium Extraction
s	singlet
t	triplate

List of Figures

xvii

xxii

List of Tables

Chapter 1

Coordination Chemistry of Lanthanides and Actinides

1.0 Introduction

This Chapter is a brief literature review on the chemistry of lanthanides (Ln) and actinides (An), related to their coordination behavior with various ligands specifically, those ligands with organic backbones. In subsequent chapters 2 and 3, the syntheses of organic ligands with hard phosphine oxide functional groups will be described together with studies of their coordination behavior with lanthanides. In order to get an insight on what is described in chapters 2 and 3, the general characteristics of lanthanides and actinides is important to know. The phosphine oxide functional group, as other oxygen or nitrogen containing functional groups, has a tendency of rendering ligands hemilabile and this property is useful in catalyst synthesis.[1] Ligands having these donor sites will be described in chapters 2 and 3 in relation to lanthanide (Ln) and actinide (An) recognition.

1.1 Lanthanides

The lanthanide series consists of 15 elements having atomic numbers from 57 to 71 (lanthanum to lutetium). These elements have special properties when compared to other elements in the periodic table. Previously, the placement of these elements in the periodic table was difficult due to their unique behavior. Currently, lanthanides are referred to as lanthanoids in many publications because the *suffix-ide* signifies that the element is negatively charged as chloride (Cl⁻), bromide (Br⁻), etc. These are f-block elements,[2-5] except lutetium, which is a d-block with the electronic configuration $[Xe]4f^{14}5d^{1}6s^{2}$.

Initially, lanthanides were classified as rare earth metals, although lanthanides are not as rare as originally thought. Several lanthanoid compounds have important uses in catalyst syntheses that are used in the production of petroleum and synthetic products. Lanthanides/lanthanoids are used in lamps, lasers, magnets, phosphors[6], motion picture projectors, and X-ray intensifying screens.[3] As mentioned above, lanthanide elements (Z=57-71) comprise the fifteen elements from $_{57}$La to $_{71}$Lu, but typically scandium (Sc) and yttrium (Y) are also included in this series as well due to their resemblance to lanthanides.[7, 8] For example, yttrium (Y), which lies above lanthanum in transition group IIIB, has a similar 3+ ion with a noble-gas electronic configuration:

Y^0 [Kr]$4d^1 5s^2$ $\longrightarrow$ Y^{3+} [Kr]. Its atomic and ionic radii have values that are close to those of terbium (Tb) and dysprosium (Dy).[8]

All lanthanides closely resemble lanthanum, with the following common properties. They are silvery-white metals that become dull/discolored when exposed to air due to formation of their oxides. The elements are soft metals, but their hardness increases with increasing atomic number. The ionic radii of lanthanides decrease along the period, a phenomenon called lanthanide contraction.[4] Their compounds are ionic, with coordination numbers 8, 9 and sometimes as high as 12, and most of them are strongly paramagnetic. Lanthanide atoms tend to lose three electrons, usually $5d^1$ and $6s^2$, to attain the most stable 3+ oxidation state.[1-4]

1.1.1 Electronic configuration and its impact on properties of lanthanides [4-9]

The accepted presentation of the electronic configuration of lanthanides is [Xe] $4f^n 5d^0 6s^2$. However, this format is not applicable to several lanthanides:

(a)   Cerium, where the sudden contraction and decrease in energy of the 4f orbital, after lanthanum, is not lowered enough to avoid filling of electrons in the 5d orbital. Therefore, the configuration of this element is [Xe] $4f^1 5d^1 6s^2$;

(b)   Gadolinium, where the stability of the half-filled 4f shell appears and it has the configuration [Xe] $4f^7 5d^1 6s^2$;

(c)   Lutetium, where the 4f shell is completely filled, ([Xe] $4f^{14} 5d^1 6s^2$).

The "lanthanide contraction," i.e., the decrease in atomic/ionic radius along the period, is caused by an increase in nuclear charge as electrons are added to the 4f subshell.[4] However, the shapes of 4f orbitals result in imperfect shielding of the $4f^n$ electrons. Each unit increase in nuclear charge produces a net increase in attraction for the electron charge cloud and each atom/ion shrinks slightly in comparison with its preceding elements. Due to the competition of these two factors, i.e., increase in nuclear charge as well as shielding effect of 4f electrons by $5s^2 5p^6$, the radii of lanthanide atoms/ions decrease across the period as observed with other elements in the periodic table.[4]

The atomic radii for europium and ytterbium atoms show a peculiar behavior by possessing higher than expected atomic radii. It has been suggested that most of the lanthanide metals exist in a lattice of Ln(III) ions ($4f^n$ configuration) with three electrons residing in a 5d/6s based conduction band. These atomic radii, therefore, vary in a manner similar to the variation found for the trivalent cations. However, Eu and Yb, both of which exist in the 2+ ion state, are proposed in the metal atoms to exist in their lattice as the larger 2+ cations with two electrons in a 6s conduction band.[7]

The ground state electronic configuration of the neutral lanthanum atom consists of a xenon core [Xe] with three electrons in the higher energy 5d and 6s orbitals. It has

been shown that both the energy and the orientation of the 4f orbital in space decrease immediately as the nuclear charge increases beyond $_{57}$ La.[10-12] For example, the nuclear binding energy of a single 4f electron drops from -0.95 eV for lanthanum atom to -5 eV for neodymium atom.[4] Therefore, although the 4f orbitals lie outside the xenon core for lanthanum atom, it is not occupied due to its higher energy but in neodymium 4f orbitals having relatively low energy are occupied. This is why the electronic configuration of $_{57}$La is $[Xe]5d^1 6s^2$ and $_{60}$Nd is $[Xe]4f^4 6s^2$.

The emission spectra data produced from atoms and ions have been used to assign the electronic configuration of elements.[13-15] The existence of a common 3+ oxidation state throughout the series in some cases requires the removal of f-electron, e.g., Pr^{3+} and Nd^{3+} (Table 1.1). The 2+ and 4+ oxidation states arise if the ion can attain an empty (f^0), half filled (f^7) or filled (f^{14}) subshell. For example, Ce^{3+}, a $4f^1$ ion, can be oxidized to Ce^{4+}, f^0, which is a stable oxidation state. This tendency makes Ce^{4+} a useful oxidizing agent. The Eu^{2+} ion ($4f^7$) is also easily formed.[4, 8]

Table 1.1: Ground–state "outer", Ln^{2+} and Ln^{3+} electronic configurations[4]

Element	symbol	Atomic number	Electronic configuration		
			Ln^{0}	Ln^{2+}	Ln^{3+}
Lanthanum	La	57	[Xe] $5d^{1}6s^{2}$	[Xe] $5d^{1}$	[Xe] $4f^{0}$
Cerium	Ce	58	[Xe] $4f^{1}5d^{1}6s^{2}$	[Xe] $4f^{2}$	[Xe] $4f^{1}$
Praseodymium	Pr	59	[Xe] $4f^{3}6s^{2}$	[Xe] $4f^{3}$	[Xe] $4f^{2}$
Neodymium	Nd	60	[Xe] $4f^{4}6s^{2}$	[Xe] $4f^{4}$	[Xe] $4f^{3}$
Promethium	Pm	61	[Xe] $4f^{5}6s^{2}$	[Xe] $4f^{5}$	[Xe] $4f^{4}$
Samarium	Sm	62	[Xe] $4f^{6}6s^{2}$	[Xe] $4f^{6}$	[Xe] $4f^{5}$
Europium	Eu	63	[Xe] $4f^{7}6s^{2}$	[Xe] $4f^{7}$	[Xe] $4f^{6}$
Gadolinium	Gd	64	[Xe] $4f^{7}5d^{1}6s^{2}$	[Xe] $4f^{7}5d^{1}$	[Xe] $4f^{7}$
Terbium	Tb	65	[Xe] $4f^{9}6s^{2}$	[Xe] $4f^{9}$	[Xe] $4f^{8}$
Dysprosium	Dy	66	[Xe] $4f^{10}6s^{2}$	[Xe] $4f^{10}$	[Xe] $4f^{9}$
Holmium	Ho	67	[Xe] $4f^{11}6s^{2}$	[Xe] $4f^{11}$	[Xe] $4f^{10}$
Erbium	Er	68	[Xe] $4f^{12}6s^{2}$	[Xe] $4f^{12}$	[Xe] $4f^{11}$
Thulium	Tm	69	[Xe] $4f^{13}6s^{2}$	[Xe] $4f^{13}$	[Xe] $4f^{12}$
Ytterbium	Yb	70	[Xe] $4f^{14}6s^{2}$	[Xe] $4f^{14}$	[Xe] $4f^{13}$
Lutetium	Lu	71	[Xe] $4f^{14}5d^{1}6s^{2}$	[Xe] $4f^{14}6s^{2}$	[Xe] $4f^{14}$

1.1.2 Oxidation states

As described in section 1.1.1, lanthanide chemistry is dominated by the 3+ oxidation state; however, in a few cases oxidation states of 2+ and 4+ can also be obtained. For example, it has been found that Ce(IV) and Eu(II) are stable in water and, they are strong oxidizing and reducing agents, respectively. Other Ln(IV) ions Ln = Pr, Tb and Ln(II) ions Ln = Nd, Eu, Dy, Tm, Yb also are formed in the solid state, but these are unstable in water.[4, 7-9]

The dominance of oxidation state 3+ is a result of the stabilizing effects exerted on different orbitals by increasing ionic charge. Basically, $6s^2$ and $5d^1$ electrons are removed first because the first three ionization potentials are relatively small.[4-9] After an ionic charge of 3+ has been obtained the 4f orbital becomes stable because the electrons remaining in the 4f orbitals are firmly attracted by the nucleus due to the imbalance between the positive charge of the nucleus and the remaining electrons. However, exceptions have been noted in cerium and praseodymium, which are at the beginning of the series, where the 4f orbitals are still at a comparatively high energy, i.e., less stable and can therefore lose a further electron. On the other hand terbium(IV) is easily formed due to the stability of the $4f^7$ configuration. The stabilizing effects of half, and completely filled, shells can be similarly used to explain the occurrences of the divalent state in europium(II) ($4f^7$) and ytterbium(II) ($4f^{14}$) as already noted.

The 3+ oxidation state is common to all lanthanides both in solid compounds and in solutions in water and other solvents. Very few solid compounds show the 4+ oxidation state, but only Ce^{4+} forms stable solid state compounds. Basically, all lanthanides can be obtained in the 2+ oxidation state when kept in solid alkaline earth

halide matrices, but dissolution in water lead to rapid oxidation to the 3+ oxidation state except europium(II) due to stabilization of half filled f-orbital (Eu[Xe]4f^7).[16-18]

The radii of the Ln^{3+} ions contract slowly from La^{3+} to Lu^{3+}. The decrease in ionic radii is caused by the increase in nuclear charge as electrons are removed from 5d^1 and 6s^2 valence orbitals. The common occurrence as Ln(III) is due to the fact that, once the valence s and d electrons have been removed, the f electrons are held tightly by the nucleus and do not extend beyond the xenon-like core as noted earlier. Studies[4] have also shown that the bonding interactions of Ln^{3+} ions are mainly attributed by the electrostatic attraction of ions. The same trend is also observed with actinide contraction among the 5f species, i.e., An^{3+}. It is also noted that the oxidation number determines the magnitude of the ionic radii, for example Sm^{2+}, Eu^{2+}, Tm^{2+} and Yb^{2+} have relatively larger ionic radii when compared to their corresponding Ln^{3+} ions. Similarly, Ce^{4+}, Pr^{4+} and Tb^{4+} show smaller ionic radii compared to the Ln^{3+} ions.

1.1.3 Coordination numbers and stereochemistry

Usually, the coordination number of a metal atom or ion in a complex is not determined by the composition of the solid because solvent molecules and species that are potentially ligands may fill spaces within the structure and do not form direct bonds to the metal ion. For example, single crystal X-ray diffraction analysis shows that Co^{2+} in $CoCl_2.6H_2O$ is not eight coordinate.[9] The structure contains the neutral complex $[Co(Cl)_2(OH_2)_4]$ with two outer sphere H_2O molecules that occupy specific positions in the crystal lattice. There are three fundamental factors that govern the coordination number of a complex. These are:

(1) the size of the central atom or ion;

(2) steric interactions between the ligands; and

(3) electronic interactions between the central atom or ion and the ligands.

This means that large central metal atoms/ions with small ligands favor higher coordination numbers while small central metal atoms/ions and bulky ligands favor low coordination numbers. Charged ligands also favor low coordination numbers due to the electrostatic interactions.[8, 9]

The range of coordination numbers and stereochemistry displayed by lanthanide ions is of particular importance to understanding some of the detailed chemistry described in the coming chapters. The stereochemistry of Ln^{x+} ion in a crystalline solid can be determined by using diffraction methods and spectroscopic techniques. However, these techniques are not used to determine the stereochemistry of Ln^{x+} complexes in aqueous solution due to the unknown degree of coordination by water molecules. In addition, there is competition of water molecules with other ligands in the complex. Only complexes formed with the strongest coordinating ligands can exist as separate chemical species in aqueous systems. [19, 20] The coordination number of 6 for Ln^{x+} ion is rare. Instead, larger coordination numbers of 7-12 are exhibited.[21-25] This is due to the increased space available around these larger cations.

As already noted above, strongly complexing ligands, usually chelating ligands, form complexes that can be isolated from aqueous solution as well, other types of complexes can be obtained in the same condition, however it has been observed that complexes with uncharged monodentate ligands, or ligands with donor atoms other than oxygen, must usually be prepared in the absence of water to avoid competition offered by water molecules. Complexes with coordination numbers below 6 are formed only with

8

very bulky ligands, and although the coordination number 6 is not very common but coordination numbers 7, 8 and 9 are common with lanthanides. Coordination numbers of 10 and higher are found with chelating ligands having small bite angles such as NO_3^- or SO_4^{2-}. [4, 8] Table 1.2 shows the impact of coordination number on the stereochemistry of the complexes formed.

Table 1.2 Coordination numbers and stereochemistries found with Ln $^{3+}$ ions[7]

Oxidation state	Coordination number	Stereochemistry
2	6	Octahedral
	8	Cubic
3	3	Pyramidal
	4	Tetrahedral, distorted tetrahedral
	6	Octahedral
	7	Capped trigonal prismatic
		Capped octahedral
	8	Dodecahedral, square ant prismatic
		Bicapped trigonal prismatic
	9	Tricapped trigonal prismatic
		Capped square antiprismatic
		Bicapped dodecahedral
		Irregular
	12	Icosahedral
4	6	Octahedral
	8	Cubic
		Square antiprismatic
	10	Complex
	12	Icosahedral

1.1.3.1 Coordination number 8

Coordination number 8 is commonly found for the large lanthanide ions. The two most common geometries are square antiprism and triangularly faced dodecahedral. The two structures slightly resemble each other.[25, 26-28] Examples of square antiprismatic arrangement (often distorted) are formed with the species like LnF_4, Ln = Ce, Tb[29], $[Ln(H_2O)_6Cl_2]^+$, Ln = Nd, Sm, Eu, Gd, Er[30, 31], $Ce(IO_3)_4$,[32] and $[Ce(CH_3CO \cdot CH=CO \cdot CH_3)_4]$.[33]

1.1.3.2 Coordination number 9

This coordination number is very common for larger Ln^{3+} ions. An example of the polyhedron under this coordination number is the symmetrical tricapped trigonal prism.[25] This coordination polyhedron is exemplified by the complexes of $[Ln(H_2O)_9]^{3+}$ as they appear in the crystalline ethyl sulfate salts $Ln(C_2H_5SO_4)_3 \cdot 9H_2O$,[34] the crystalline bromates $Ln(BrO_3)_3 \cdot 9H_2O$ (Ln=Nd)[35] and in the ions $[Ln(OH)_9]^{6-}$, as they appear in the crystalline trihydroxides (Ln = La, Pr, Nd, Sm, Gd, Dy).[36] The crystal lattices for $LnCl_3$, (Ln = La-Gd)[37, 38] also form symmetrically tricapped trigonal prismatic structures. Nine coordination is also exhibited by the molecular structures in the salts like $M^I [Ln(EDTA)(H_2O)_3] \cdot 5H_2O$.[39] (EDTA = ethylene diamine-N, N, N, N-tetraacetate; for $M^I = K^+$, Ln = La, Nd, Gd; for $M^I = Na^+$, Ln = La, Nd, Tb, Gd, Er; and when $M^I = NH_4^+$, Ln=Nd, Gd.[39]
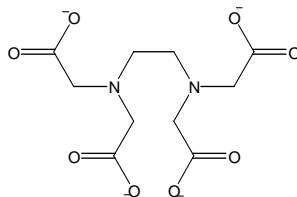
EDTA

Examination of the lanthanum and terbium complexes showed that the coordination polyhedron is defined by four oxygen atoms and the two nitrogen atoms from the $EDTA^{4-}$ ion and by three oxygen atoms from coordinated water molecules. Due to the large size of each Ln^{3+} ion, the $EDTA^{4-}$ ion is confined to a single hemisphere, and the water molecules appear in a second hemisphere.

1.1.3.3 Coordination number 10

Ten-coordinate complexes are limited to larger lanthanides as well as actinide ions due to steric hindrance of the complexing ligands. Two compounds are mentioned here as examples of 10-coordinate complexes [La(EDTA•H)(H$_2$O)$_4$] (EDTA•H = monoprotonated EDTA ion) [40] and [La(bipy)$_2$(NO$_3$)$_3$] (bipy = bipyridyl).[41] Both bipy and NO$_3^-$ coordinate in bidentate mode.

EDTA•H   bipyridyl
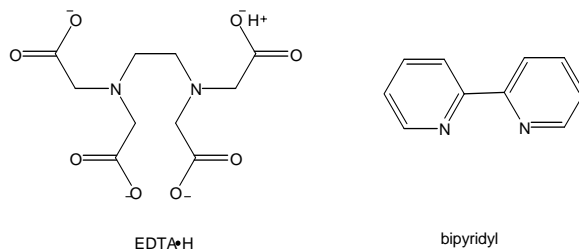
Referring to the above two complexes, the molecular structure of the [La(EDTA•H)(H$_2$O)$_4$] complex is comparable to [La(EDTA)(H$_2$O)$_3$]$^-$ [39] with an additional water molecule in the second hemisphere. The steric hindrance caused by the sexadentate EDTA•H^{3-} ligand and the larger size of the La^{3+} ion gives a distorted geometry of quasi-D$_{2d}$ dodecahedral geometry. The second complex [La(bipy)$_2$(NO$_3$)$_3$] is a bicapped dodecahedral geometry (D$_2$ symmetry) in which there are four donor nitrogen atoms from the bipyridyl molecules and six donor oxygen atoms from three bidentate nitrate groups.

1.1.4   General coordination chemistry of lanthanides[4-9]

The following features distinguish lanthanides from d-block metals in the area of coordination chemistry:

(i)   Lanthanides exhibit a wider range of coordination numbers (generally 7-12);

(ii)   Coordination geometries are more determined by ligand steric factors rather than by crystal field effects that dominate in d-block metals;

(iii)   They prefer anionic ligands with donor atoms of high electronegativity (e.g., O, F) as strong coordination is formed with hard donor atoms;

(iv)   They readily form hydrated complexes (Ln^{3+} exhibit high hydration energies) and this can lead to uncertainty in assigning coordination numbers;

(v)   The coordination chemistry of lanthanides is dominated by the (3+) oxidation state;

(vi)   They show less tendency to form $Ln =\!\!=\!\! O$ or $Ln \equiv N$ multiple bonds that are common for many transition metals and certain actinides;

(vii)   Water is generally a strong ligand. In aqueous media, other ligands compete with water for coordination with the Ln^{3+} ions. Once coordination has been established by water, displacement by another ligand is generally difficult. This behavior is illustrated in Chapter 3 whereby competition between a ligand and water is observed. Thus, only strong ligands, in particular those that are chelating, form complexes of sufficient thermodynamic stability to be isolated.

1.1.5   Donor atoms

Donor atoms are those atoms in Lewis base ligands that form a largely covalent bond or form dipole interaction to the central metal atom by donating a lone pair of electrons to the metal. For example, nitrogen is the donor atom when NH_3 acts as a ligand. The central metal atom or ion referred to as a Lewis acid is the acceptor or polarizing center. Considering d-block metal complexes, for example $[Co(NH_3)_6]^{3+}$, the central metal ion (Lewis acid), Co^{3+} ion, is surrounded by six NH_3 ligands.[4-9] The main concern in this section is to describe donor atoms which prefer forming complexes with f-block metals, specifically lanthanides. The literature[4] shows that complexes that are derived from ligands containing oxygen donor atoms are stable in solution and can be isolated easily. However, under certain conditions nitrogen, phosphorus and sulfur donor ligands also form complexes. In all cases a competition between donor atoms in ligands and solvent molecules have been observed, and thus the nature of the complex formed is determined to some degree by the solvent in which the reaction was done.[4]

For example, the ammoniates or amines $LnCl_3 \bullet xNH_3$ react with water to form insoluble hydrous oxides or hydroxides. Amines or diamines that are strongly basic give the same precipitates when added to aqueous Ln^{3+} salt solutions. More weakly basic amines do not react under comparable conditions. However, ethylenediamine (en) reacts with solutions of the anhydrous perchlorates (ClO_4^-) in anhydrous acetonitrile to form stable ions $[Ln(en)_4]^{3+}$ with an average enthalpy change of 61 kcal mole^{-1}. This indicates that the Ln-N bond is strong, but can only be formed in the absence of water due to competition with oxygen donor atom from water molecules.[20] Nevertheless, the formation of 1,10-phenanthroline (phen) and 2,2-bipyridyl (bipy) chelates, e.g. $Ln(phen)_2X_3$,

Ln(phen)(C$_2$H$_5$OH)X$_3$, Ln(bipy)$_3$X$_3$ (X = Cl, SCN, NO$_3^-$ or CH$_3$CO$_2^-$ from ethanol solutions, or terpyridyl (terpy) Ln(terpy)X$_3$(H$_2$O)n (X = Cl, NO$_3$, n = 0-3)[40, 42, 43] indicates that nitrogen is an important donor atom. Understanding this behavior is important in this study because ligands reported here have similar donors (nitrogen and oxygen).

It is also true that softer donor atoms, like sulfur, selenium, phosphorus, and arsenic can bind to the lanthanide ions under conditions of less competition.[44] On the other hand, the halide ions are common donors, as exemplified by their presence in the coordination spheres of a number of the species described in this section.

1.1.5.1 Phosphorus ligands

The chemistry of phosphorus(III) compounds is mainly concentrated on the lone pair of electrons and its availability for forming bonds. The coordination chemistry between phosphorus(III) based ligands and soft low-valent d-block transition elements have important use in the syntheses of catalysts. Examples of phosphorus ligands include bis-(diphenylphosphino)ethane, bis-(diphenylphosphine)methane, triethylphosphine, trimethylphosphine and triphenylphosphine.[9] The main difference between phosphorus(III) compounds from their nitrogen relatives is that the latter undergo inversion rapidly at room temperature, while inversion is slow in phosphines although both have a pyramidal structure.[49]

1.1.5.2 Tertiary phosphine oxide

Tertiary phosphine oxide ligands which are of interest in the current study are air stable compared to phosphines and they bond to hard acceptors, reflecting the nature of the harder oxygen donor atom. Known phosphine oxide ligands are numerous, and the purpose of this section is to give some examples to illustrate how they are synthesized,

explore some selected coordination compounds, and to provide applications of the oxides and their complexes. The phosphine oxide group combined with nitrogen functional groups produces chelating ligands that can be hemilabile. This property has been used in the synthesis of catalysts.[50, 51, 54]

1.1.5.2.1 Synthesis of tertiary phosphine oxides

Various strategies have been developed in the preparation of alkyl and aryl-substituted tertiary phosphine oxides. However, direct oxidation of alkyl phosphines by exposure to air is often not recommended since side products with P-O-C bonds may form.[51] A few illustrative examples highlight the different routes that may be used. The arylphosphine oxide **1** was synthesized in 26% yield from 4-diphenylphosphanyl-phenylamine using aqueous H_2O_2 in diethyl ether as solvent (Scheme 1).[52]

Scheme 1
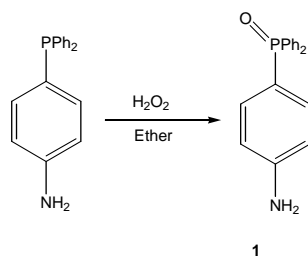
Alternatively, the above reaction was done using aqueous H_2O_2, in THF, at 0 $^\circ$C, and **1** was isolated in 49% yield (Scheme 2).[53]

Scheme 2
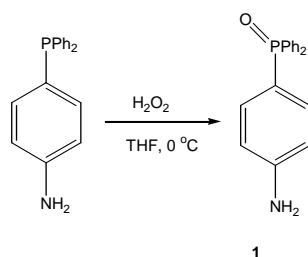
Several organophosphonates and phosphine oxide ligands have been prepared using Arbusov and Michaelis-Becker reactions. For example **2** (R= benzyl) was prepared in 67% yield using Arbuzov conditions (Scheme 3).[54]

Scheme 3

2
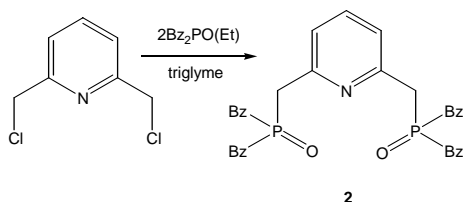
The synthesis of other derivatives have been reported using appropriate Grignard reagents, $R_2P(O)MgBr$, where R = ethyl, propyl, butyl, tolyl, etc.).[54] Alternatively, phosphorus oxychlorides, e.g., $R_2P(O)Cl$ or $RP(O)Cl_2$, can be used to prepare symmetrical phosphine oxides. Tetra-substituted calix[4]arene **3** can be prepared by initial treatment of *para-tert*-butylcalix[4]arene with NaH, followed by reaction with the highly reactive tosylated phosphine oxide $Ph_2P(O)CH_2O_3SC_6H_4Me-p$.[55]

3
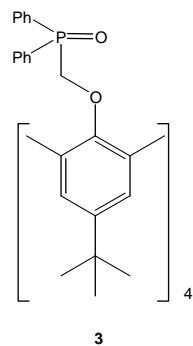
Ligand **4** (Scheme 4) can be prepared by lithiation of 6,6-dimethyl-2,2-bipyridine with lithium diisopropylamine (LDA), addition of $ClPPh_2$ and oxidation with $NaIO_4$ under phase-transfer conditions.[56]

17

Scheme 4
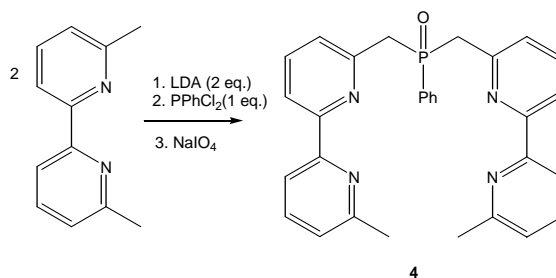
 Another way to use tertiary phosphines as precursors for synthesis of phosphine oxides is to quaternize them with alkyl halides, and then subject the quaternary ion to alkaline hydrolysis (usually 20-40% NaOH). One of the phosphorus substituents is eliminated as the hydrocarbon and the tertiary phosphine oxide is formed. Purification can be achieved either by recrystallization or chromatography. Compound **5** below was synthesized using this method .[57]
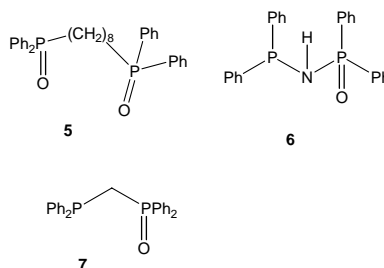
One problem, encountered in the synthesis of **6**, was poor control leading to double oxidation of both phosphorus centers when preparing mixed phosphine-phosphine oxide ligands. One interesting solution, developed by Grushin, is a catalytic method using simple Pd(II) salts in 1,2-dibromoethane under biphasic conditions. Adopting this method, **7** was prepared in high yield (>70%).[58] Unsymmetrical phosphorus ligands, $Ph_2P(X)CH_2P(Y)Ph_2$ where X, Y = lone pair, O, S or Se, have been synthesized by this method.[59]

1.1.5.2.2   Properties of tertiary phosphine oxides

Tertiary phosphine oxides are often crystalline, nontoxic solids that are easy to handle. In addition, phosphine oxides are highly polar and some are highly soluble in water. Some tertiary phosphine oxides can be reduced to phosphines using Si_2Cl_6 or $HSiCl_3$ and this constitutes an important reaction of these compounds. The oxygen atom of phosphine oxides can be exchanged with sulfur using Lawesson's reagent. Alternatively, tertiary phosphine sulfides can be prepared from the tertiary phosphine and elemental sulfur.[49]

Lawesson's reagent
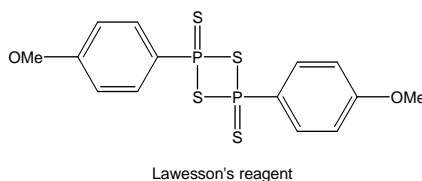
1.1.5.2.3   Coordination chemistry and catalytic uses of phosphine oxides

The coordination chemistry of phosphine oxides have been explored with many late transition metals, i.e., Ru, Co, Rh, Ir, Pd, Pt, Cu and Au,[50, 53, 56, 60-66] early transition metal,[67] lanthanide[54, 68, 69] and actinide[57, 70] ions. One interesting complex is **8** which is an extremely rare example of a d^8 metal center with a tetrahedral geometry.[63] Phosphine oxides have been used in the extraction of alkali, alkaline earth, and actinide metals,[71] in catalysis, e.g., in hydroformylation of alkenes,[72, 73] and epoxides,[64] carbonylation of methanol,[74] and as a useful crystallization aid .[75]

8
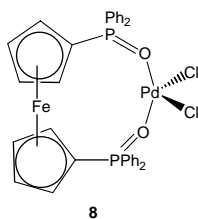
1.1.5.2.4 Effects of coordination on the properties of lanthanides ions

The effect of coordination on the properties of lanthanide ions is to reduce the amount of the cations in solution through complex formation. After complexation, the Ln^{3+} ions are shielded from external attack by surrounding ligands in the solution. Coordination of Ln^{3+} usually facilitates the extraction of these ions in organic solvents. Two cases of complexation are mentioned here as examples: $[Ln(diket)_3(H_2O)_{1-3}]$ (diket $= (CH_3)_2CO)_2$ and $[Ln(TBP)_3(NO_3)_3]$, $(TBP = n\text{-}Bu_3PO)$.[47, 48]

1.1.6 Applications

Coordination chemistry reported here finds its main application in separation of lanthanide ions through complex formation. The literature [4] shows that complexation also finds vital use in qualitative and quantitative determination of the lanthanide ions in solution. This branch of analytical chemistry of lanthanides has been reported by Woyski and Harris.[76] Two main aspects were described, one being the separation and determination of lanthanides as a group, and secondly, determination of the individual lanthanides. Considering the first case, materials containing lanthanides are dissolved either in acids or fused with sodium peroxide, carbonate, or pyrosulfate. In these cases lanthanide ions are recovered from solution by precipitation. Individual lanthanides from the precipitate are determined by varying their oxidation states. For example, cerium(IV) species are kinetically stable in aqueous solution and in this state of oxidation the element can be determined by oxidimetric titrations. Other lanthanides like europium and ytterbium can be recovered as sulfates after reduction to the 2+ oxidation state. Another importance of studying coordination chemistry of lanthanides is the development of modern techniques in purification of spent nuclear fuel (actinides) due to their

resemblance to lanthanides. However, it has been noted that many separation processes depend on the differences in acidity of the Ln^{3+} ions that occur with crystal radius changes.[78] In lanthanide ions, acidity is a measure of the ability to attract a negative charge or electron donor groups. Generally, acidity increases with a decrease in crystal/ionic radius. This means, high acidity, high complexation ability and low acidity are associated with weak complexation. Therefore, fractional separations of lanthanides/actinides can be designed to take advantage of changes in acidity. Studies[4] also show that regardless of the acidity, separation can be effected by one or some combination of experimental factors/methods outlined below:

1. Selective oxidation or reduction, i.e., one oxidation state is favored over another;

2. Changes in acidity in the same oxidation state depending on the size of crystal radius/ionic radius as described above;

    (a) fractional crystallization or precipitation from solution;

    (b) fractional thermal decomposition;

    (c) ion exchange;

    (d) solvent extraction; and

3. Differences in physical properties for a particular compound.

No single-step fractional separation of Ln/An is effective. Multiple separation steps must be used. Similarly, the relative efficiency of each step is given by the extent to which the separation factor α that describes that step exceeds 1. For example, two lanthanide ions Ln and Ln' that undergo change from an initial concentration condition

(1) to a new concentration condition (2), the separation factor sometimes, called partition coefficient, is defined by the following equations:

$$\alpha = \frac{{}^{c}Ln\,(2)/{}^{c}Ln'\,(2)}{{}^{c}Ln\,(1)/\,{}^{c}Ln'\,(1)} = \frac{{}^{c}Ln\,(2)\,{}^{c}Ln'\,(1)}{{}^{c}Ln\,(1)\,{}^{c}Ln'\,(2)}$$

(1)

or

$$\alpha = \frac{[Ln\,(2)]/[Ln'\,(2)]}{[Ln\,(1)]/\,[Ln'\,(1)]} = \frac{[Ln\,(2)]\,[Ln'\,(1)]}{[Ln\,(1)]\,[Ln'\,(2)]}$$

The size of α for a given technique of separation is related to the number of stages, or repetitions, of the step described required to effect a selected purification. The separation factor can be established only if the concentration of each lanthanide can be determined accurately, preferably by a technique that is both specific for each cation and does not destroy or alter the sample. Spectrophotometry procedures, based upon the characteristic absorption bands of the Ln^{3+} ions,[78-81] are generally the most useful in concentration determinations, since there exist for each absorbing cation bands that are both free from interference by other cations, and adhere to the Beer-Lambert relationship. The Beer-Lambert Law is defined mathematically as

$A = \varepsilon\, b\, c$ (2)

Whereby

A = absorbance

ε = molar absorbtivity with units L/mol cm

b = path length of the sample, that is, the path length of the cuvette in which the sample is contained, expressed in cm

c = concentration of the compound in solution, expressed in mol/L. Using this law, the concentration [C] can be determined in a given media/phase.

1.1.7 Solvent extraction

The solvent extraction process has been reported in a number of pioneering studies.[82-86] One of the pioneers, Warf, observed that cerium(IV) can be removed from Ln^{3+} ions with TBP.[84] This observation was followed by the work of Peppard and co-workers.[85] They showed that Ln^{3+} ions are selectively extracted from concentrated nitric acid media by TBP. The separation of the "first kilogram" of 95% pure gadolinium by Weaver[86] encouraged the use of solvent extraction process in the extraction of Ln/An ions.

The principles of solvent extraction and its application for separation of the lanthanide ions have been described.[87-89] For the distribution equilibrium

$$Ln \text{ (aq.)} \rightleftharpoons Ln \text{ (org.)} \tag{3}$$

where (aq.) represents the aqueous phase species and (org.) represents the organic phase species, can be described by a distribution ratio/partition coefficient (λ).

$$\lambda = {}^{c}Ln \text{ (org.)} / {}^{c}Ln \text{ (aq.)} \tag{4}$$

Therefore, for two lanthanides, Ln and Ln', using the two equations

$$\lambda = {}^{c}Ln \text{ (org.)} / {}^{c}Ln \text{ (aq.)} \tag{4 for Ln and}$$

$$\lambda' = {}^{c}Ln' \text{ (org.)} / {}^{c}Ln' \text{ (aq.)} \tag{4' for Ln'}$$

the separation factor α can be deduced (equation 5)

$$\alpha = \lambda/\lambda' = {}^{c}Ln \text{ (org)} \, {}^{c}Ln' \text{ (aq.)} / {}^{c}Ln' \text{ (org.)} \, {}^{c}Ln \text{ (aq.)} \tag{5}$$

The separation factor α depends on the type of extractant used. Two types of extractant have been used in the extraction processes the phosphorus-based ligands and non phosphorus-based.[87, 90] For the convenience of this study only the phosphorus based extractants are outlined:[4]

(1) the neutral orthophosphate esters, $(RO)_3PO$, organophosphonates, $(RO)_2RPO$, or phosphine oxides, R_3PO;

(2) the monoacido ortho-phosphate esters, $(RO)_2(HO)PO$, and organophosphonic acids, $(RO)(HO)RPO$;

(3) the diacido orthophosphate esters, $(RO)(HO)_2PO$, and organophosphonic acids, $(HO)_2RPO$.

Group R may be alkyl and /or aryl and may differ in a given compound. Selected compounds of this nature provide good efficiency in solvent-extraction separations for Ln^{3+} ions. Tri-*n*-butyl phosphate (TBP), the mostly used example of class (1) extractant, has shown to be stable toward hydrolytic cleavage when mixed with 16 M nitric acid. The reagent can be used undiluted as the organic phase[91] or diluted with kerosene or other hydrocarbon as the organic phase.[92, 93] In many situations, the distribution of Ln^{3+} ion between the two phases is not efficient at low aqueous nitric acid concentration, but at 16 M HNO_3, the extraction ability is maximized. In this case the extraction process is described by equation (6).

$$Ln^{3+} (aq.) + 3NO_3^- (aq.) + 3TBP (org.) \rightleftharpoons Ln(NO_3)_3 (TBP)_3 (org.) \qquad (6)$$

Several studies have shown that the extent of extraction increases with increasing atomic number due to decreasing crystal radius.[4] For example Peppard[4, 85] has summarized distribution ratios α, against nitric acid concentration, and logarithmic plots are linear as the nitric acid concentration approaches 16 M. Using equation (7), the constant Z (separation factor) increases with atomic number of the Ln^{3+} ion.

$$Log\ \lambda = Z\ log\ \alpha + constant \qquad (7)$$

Experiments revealed that separation is also possible on a large scale by using either column or mixer-settler systems.[94] It was also noted that separations are less efficient in chloride media because the chloride ion forms weaker complexes with the Ln^{3+} ions than the nitrate ion. This may result from monodentate coordination with Cl^- while NO_3^- exhibits bidentate coordination.

Class (2) extractants, such as di-(2-ethylhexyl) phosphoric acid (HDEHP), are less soluble in water but more stable than TBP toward acid hydrolysis and have been used in many separation processes.[95] HDEHP exists as a dimer in the organic phase, and the extraction reaction is in accordance to equation (8)

$$Ln^{3+}_{(aq.)} + 3(HDEHP)_{2(org.)} \rightleftharpoons Ln\left[H(DEHP)_2\right]_3 \ (org. + 3H^+_{(aq.)}) \qquad (8)$$
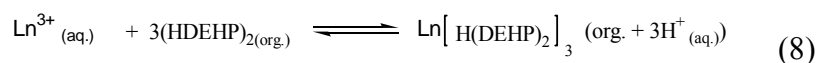
It is believed that chelated structures of the type shown below exist in the organic phase.[4, 95]
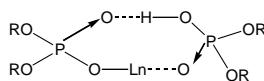
Di-(2-ethylhexyl) phosphoric acid is used considerably for large scale separations of the lanthanides. The average separation factors α, for other Ln^{3+} ions have been found to be nearly 2.5 and the advantage of this extractant is that extraction can be done in either chloride or sulfate media.[88]

Class (3) and (4) extractants are not described here because these have not been investigated extensively. Studies[90, 96] have shown that, other types of extractants can be employed in Ln^{3+} separations as well. To mention an example, long chain amines have been explored as liquid anion exchangers, but they are largely ineffective for lanthanide separations except for primary amines that can be used in sulfate systems.[96] However, the addition of polyaminopolycarboxylates improve separation with these extractants.

1.2   Actinides

The actinide series sometimes referred to as "actinons" or "actinoids," from thorium to lawrencium, follow actinium in the periodic table. The position of actinium, like that of lanthanum, signifies that it is sometimes included with actinides for comparative purposes. Historical development of actinides started recently. Before 1940 only the naturally occurring actinides, thorium, protactinium, and uranium, were known. The rest have been artificially made in laboratories. Manmade transuranium elements currently comprised 15% of all the known chemical elements.[97] The rare actinide, protactinium, was found in 1913 when K. Fajans and O. Göhring identified ^{234}Pa as an unstable member of the ^{238}U decay series:

$$^{238}_{92}U \xrightarrow{-\alpha} {}^{234}_{90}Th \xrightarrow{-\beta} {}^{234}_{91}Pa \xrightarrow{-\beta} {}^{234}_{92}U$$
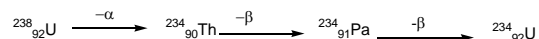
^{234}Pa was initially named brevium due to its short half-life (6.66 h). The more stable isotope of ^{231}Pa with a half-life of 32,800 years was discovered three years later by O. Hahn and L. Meitner and independently by F. Soddy and J. A. Cranston as a product of ^{235}U decay shown in the nuclear reaction equation: [97]

$$^{235}_{92}U \xrightarrow{-\alpha} {}^{231}_{90}Th \xrightarrow{-\beta} {}^{231}_{91}Pa \xrightarrow{-\alpha} {}^{227}_{89}Ac$$
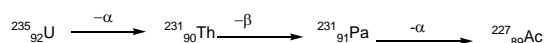
Because of its low natural abundance its chemistry was not immediately understood until 1960 when A. G. Maddock and co-workers collected 130 g from 60 tons of sludge which had accumulated during the extraction of uranium from UO_2 ores. This sample was distributed to several laboratories, from which the knowledge of the element's chemistry was developed. Usually, neutron capture by a heavy atom is accompanied by $^-\beta$ emission yielding the next higher atomic number element. This transformation is useful in the syntheses of new elements. E. Fermi and co-workers used the process shown below for

the formation of an atom with an atomic number 93 by neutron bombardment of ^{238}U. This process is described by the nuclear reaction equation:

$$^{238}_{92}U + ^{1}_{0}n \longrightarrow ^{239}_{92}U \xrightarrow{-\beta} ^{239}_{93}Np$$
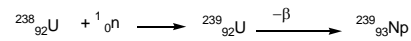
However, it was later discovered that this nuclear reaction led to fission products also, which produce lighter elements. In 1940, E. M. McMillan and P. H. Abelson managed to identify fission products and a short-lived isotope of element $_{93}$Np, having a half-life of 2.35 days. The element which follows immediately after uranium was named neptunium after Neptune, which is the next planet beyond Uranus. The remaining actinide elements were prepared in similar methods by various "bombardment" techniques over the next twenty years.[98, 99]

Table 1.3 The electron configuration of actinides [8]

Element	Symbol	Atomic Number	Half-life	Electronic configuration
Thorium	Th	90	1.40×10^{10} yrs	$[Rn]6d^2 7s^2$
Protactinium	Pa	91	3.28×10^4 yrs	$[Rn]5f^2 6d^1 7s^2$ or $[Rn]5f^1 6d^2 7s^2$
Uranium	U	92	4.47×10^9 yrs	$[Rn]5f^3 6d^1 7s^2$
Neptunium	Np	93	2.14×10^6 yrs	$[Rn]5f^4 6d^1 7s^2$ or $[Rn]5f^5 7s^2$
Plutonium	Pu	94	2.41×10^4 yrs	$[Rn] 5f^6 7s^2$
Americium	Am	95	432 yrs	$[Rn]5f^7 7s^2$
Curium	Cm	96	18.11 yrs	$[Rn]5f^7 6d^1 7s^2$
Berkelium	Bk	97	314 yrs	$[Rn]5f^9 7s^2$ or $[Rn]5f^8 6d^1 7s^2$
Californium	Cf	98	2.65 yrs	$[Rn]5f^{10} 7s^2$
Einsteinium	Es	99	20.5 days	$[Rn]5f^{11} 7s^2$
Fermium	Fm	100	100.5 days	$[Rn]5f^{12} 7s^2$
Mendelevium	Md	101	75 min.	$[Rn]5f^{13} 7s^2$
Nobelium	No	102	3.1 min.	$[Rn]5f^{14} 7s^2$
Lawrencium	Lr	103	27 seconds	$[Rn]5f^{14} 6d^1 7s^2$

1.2.1 Development of actinide coordination chemistry

The investigation of coordination chemistry of the actinide elements started after separation of uranium and thorium from pitchblende and thorite, respectively.[102, 103] The chemical properties of these elements such as redox reactions and stoichiometry of simple compounds such as oxides and halides were used to assign the position of actinides in the periodic table. The discovery of nuclear fission in 1938 encouraged further the development of coordination chemistry of actinides. Uranium–235 and plutonium–239 both undergo fission with slow neutron bombardment, making them suitable for use in weapons. Due to this important use, the development of large scale separation chemistry was designed to separate and purify these elements. Initially, the recovery processes employed precipitation techniques and latter followed by extraction from aqueous into nonaqueous solution by the use of organic extractants such as ethers, amines, or organophosphates. Since the separation of actinides from lanthanides was more sophisticated, new classes of extractants such as bifunctional and chelating ligands were developed.[104] Investigations of the nonaqueous coordination chemistry of the actinides began with the Manhattan project. This project aimed at developing the first nuclear weapon during the Second World War. Isotopic separation of uranium and plutonium involved distillation or centrifugation of volatile metal fluoride complexes. However, need for other separations led investigators to develop several new classes of compounds, including volatile alkoxide and borohydride complexes. The expansion of these interests was extended to include organometallic chemistry of the elements. This began in 1956 after the discovery of ferrocene that facilitated the preparation of the first cyclopentadienyl complexes of actinides.[104, 105]

1.2.2   Characteristics of actinides [100, 101]

The dominant characteristics of the actinides are manifested in their nuclear instability, as they exhibit radioactivity (α, β and γ-decay). All of these modes of decay become more pronounced (shorter half-lives) with the increase in atomic number. The metals are silvery in appearance as lanthanides, but have a variety of structures or allotropes. All except californium have more than one crystalline form. For example, plutonium has six different crystalline structures, and most of these are based on metallic close-packed arrangements. Structural variations among elements are due to the irregularities in metal radii which are a bit greater than the ones found in lanthanides. This might arise from different numbers of electrons contained in the metallic bands of the actinide elements. From actinium to uranium, the most stable oxidation state increases from 3+ to 6+. Comparatively, the ionic radius in a given oxidation state falls steadily which means that an "actinide contraction" exists, especially for the 3+ oxidation state, which is closely related to the lanthanide contraction.

1.2.3   Coordination number and geometries

Actinide ions have large ionic radii, and hence exhibit higher coordination numbers, and coordination numbers of 8-10 are common in this series. Similarly, coordination numbers 12 and 14 have been observed. Since the ionic radii decrease across the series, coordination numbers also decrease across the series/period for a given oxidation state for a given ligand. The table below lists examples of actinide complexes having different coordination numbers, with their respective geometries.[105-115]

Table 1.4 Coordination numbers and geometries of actinide complexes

Coordination Number	Complex	Coordination geometry
3	[U(N{SiMe$_3$}$_2$)$_3$]	Pyramidal
4	U(O-2,6-Bu$^t_2$C$_6$H$_3$)$_4$	Tetrahedral
5	[U(NEt$_2$)$_4$]$_2$	Distorted trigonal pyramidal
6	[UCl$_6$]$^{2-}$	Octahedral
7	[UCl(Me$_3$PO)$_6$]$^{3+}$	Distorted monocapped octahedron
8	(NEt$_4^+$)$_4$ [U(NCS)$_8$]$^{4-}$	Cube
9	[Th(C$_7$H$_5$O$_2$)$_4$(DMF)]	Monocapped square antiprism
10	Th(NO$_3$)$_4$[Ph$_3$P(O)]$_2$	*Trans*-octahedral
11	[Th(NO$_3$)$_4$(H$_2$O)$_3$]•2H$_2$O	Monocapped trigonal prism
12	[Th(NO$_3$)$_6$]$^{2-}$	Icosahedral
14	[U(BH$_4$)$_4$(THF)$_2$]	Bicapped hexagonal antiprism

1.2.4 Early actinide metals-Thorium to Plutonium

The chemistry of early actinide metals has been widely studied for several reasons with the main one being the availability of materials for study. Thorium and uranium, obtained from natural ores, have been examined for more than 100 years. Thorium, protactinium, and uranium are found in large quantities via extraction, while the

remaining early actinide elements, neptunium, and plutonium, are produced in nuclear reactors only.

A second reason that raised interest in the early actinide elements is their wide chemistry. For example, the chemical studies of the early actinides show that their oxidation states ranges from 3+ to 7+. The wide range of oxidation states is the motive for further development of chemical interest in the early actinides. However, this behavior also complicates the investigation of these elements. For example plutonium ions may exist in four different oxidation states (3+, 4+, 5+, and 6+) in the same solution.

Regardless of the two reasons mentioned above, another important interest in the chemistry of the early actinides is their technological importance. The importance of uranium and plutonium appears in their applications in nuclear power and radiothermal generators for deep space missions, e.g., space rockets. The production and use of nuclear materials in nuclear weapons motivated the development of the chemistry of these metals, from their separation and isolation to investigations of their behavior under biological conditions.[104]

1.2.5 Oxidation states

For thorium and uranium, the most stable oxidation state is 4+ (Th) and 6+ (U) both having a [Rn] configuration. After these, the most stable oxidation state becomes progressively lower until, in the second half of the series, the 3+ oxidation state becomes dominant. This means the highest oxidation state attainable by thorium, and the only one occurring in solution, is 4+. The second element in the series protactinium, with $[Rn]5f^26d^17s^2$ electronic configuration, shows an oxidation state of 5+ which is its most stable oxidation state due to stable [Rn] electronic configuration, and its reduction to 4+

requires very strong reducing agents such as Zn/H^+, $Cr(II)$, or $Ti(III)$, and the 4+ state in solution is immediately oxidized to 5+ by air. All in all, oxidation state 3+ is the one which, with the exceptions of thorium and protactinium, is displayed by all actinides. From uranium onwards, the resistance to oxidation in aqueous solution increases progressively with increase in atomic number and 3+ becomes the most stable oxidation state for americium and subsequent actinides (except nobelium having $[Rn]5f^{14}7s^2$ for which the f^{14} configuration gave greater stability on the 2+ state). Uranium(III) can be obtained by reduction of UO_2^{2+} or uranium(IV), either through electrolysis or with Zn amalgam[116] but is very unstable to oxidation, aqueous acids and even by pure water.[117]

Several complexes of neptunium(III) and plutonium(III) have been reported, but their instability limits the number of complexes, while for americium(III) the number of complexes prepared is limited mainly due to low availability of the element.[118]

1.2.6 General Characteristics

All early actinides possess a stable 3+ oxidation state in aqueous solution, except thorium and protactinium, but higher oxidation states of these elements are found to be more stable than 3+ even in the presence of oxygen. Trivalent compounds of the early actinides have similar structures to their trivalent lanthanide compounds, although their chemical reactions differ considerably, due to the ability of the actinides to act as reducing agents. There are very few examples of trivalent coordination compounds of thorium and protactinium. The early actinides possess large ionic radii with effective ionic radii ranges from 1.00-1.06Å in six coordinate metal complexes,[104, 120] and can therefore exhibit high coordination numbers in chemical compounds; 12-coordinate metal

centers are common and coordination numbers as high as 14 have been shown with these elements.

1.2.7 Simple donor ligands

Several complexes of actinides with simple donor ligands have been reported.[104] A short summary of selected complexes is provided in order to indicate the potential for coordination chemistry with the newly synthesized ligands reported in chapters 2 and 3.

(i) Ligands containing anionic group 15 donor atoms, e.g. $N(SiMe_3)_2{}^{-1}$

Complexes of the trivalent actinides with N-donor ligands are confined to bulky ligands that can provide kinetic stabilization. Complexes of An(III) with the above ligand have been generated for uranium, neptunium and plutonium [121-123] by using a metathesis reaction forming complexes of the type $An[N(SiMe_3)_2]_3$ whereby An = U, Np, Pu.

(ii) Ligands containing neutral group 15 donor atoms, e.g. NH_3

This ligand form complexes with uranium and plutonium when exposed to liquid or gaseous ammonia. Higher-coordinate complexes, e.g., $UCl_3 \bullet 7NH_3$, are found to be stable at lower temperatures. Above room temperature the complexes lose ammonia, e.g., $UCl_3 \bullet NH_3$. Similar behavior of Pu(III) with NH_3 have been reported, [124] e.g., $PuCl_3 \bullet 8NH_3$ and $PuI_3 \bullet 9NH_3$.

(III) Ligands containing anionic group 16 donor atoms, e.g., OH^-, NO_3^- and PO_4^{3-}.

The formation of complexes with these ligands involves hydrolysis and carbonate complexation with actinides.[104, 125] Plutonium(III) hydrolysis is not well examined because Pu(III) is readily oxidized to Pu(IV) in aqueous solutions, especially at neutral and basic pH. The first hydrolysis product, $Pu(OH)^{2+}$, was obtained in acid solution at pH *ca.* 3 with about 70% yield before oxidation to Pu(IV). This behavior has limited further

study of the complex.[126] The hydrolysis product of Np(III) has also been examined.[127] The hydroxide solids, $Pu(OH)_3 \cdot xH_2O$ and $Np(OH)_3 \cdot xH_2O$ are prepared by precipitation and are assumed to have similar structure with $Am(OH)_3$. Similarly, carbonates of An(III) appear to oxidize to An(IV) as the case observed with hydroxides of An(III).

Nitrates and Phosphates: An(III) nitrate species have been prepared by dissolution in nitric acid solution but they are unstable to oxidation. A plutonium nitrate has been prepared, analogous to the lanthanides nitrates and this was assumed to be $Pu(NO_3)_3$. However, due to its instability it was not characterized.[128] Neptunium and plutonium phosphates complexes are proposed to have the formula $An(H_2PO_4)_n^{3-n}$ (n = 1-4). If n = 1, the complex $[An(H_2PO_4)]^{2+}$ is formed. Nevertheless, these families of compounds have not been spectroscopically or structurally characterized.[129] For Pu(III), the blue, hexagonal $PuPO_4 \cdot 0.5H_2O$ has been prepared by precipitation from acid solution and heated to yield the anhydrate. Other binary, tertiary, and quartenenary phosphates have been prepared by Bamberger and co-workers and have been characterized by chemical analysis, Raman spectroscopy, and X-ray powder diffraction.[130]

(iv) Ligands containing neutral group 16 donor atoms

These types of ligands are based on the oxo-donor atom and are the most common in actinide coordination chemistry, due to their dominant use in separation chemistry of the f-elements. Citing an example of aqua species, a number of investigations of trivalent actinide ions in aqueous solution have been examined in order to identify the coordination environment of the metal center. Examination by luminescence, X-ray absorption (EXAFS), and NMR spectroscopy suggest that early actinides are probably bonded to nine water molecules.[131-135] The confirmation of this suggestion was done by

examining the crystal structure of $[Pu(H_2O)_9][CF_3SO_3]_3$, prepared by dissolving plutonium metal in triflic acid.[136] The X-ray crystallography result indicates that the plutonium ion in this complex is coordinated by nine water molecules arranged in an ideal tricapped trigonal prismatic geometry with Pu-O bond distances of 2.574(3)Å and 2.476(2)Å, respectively.[136]

1.2.8 Chelating ligands

These ligands bear more than one binding sites to form bidentate, tridentate or multidentate coordination spheres/sites. Two types of ligands are described:

(i) Multidentate donor ligands:

❖ Hydroxamates
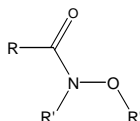
These can form complexes with An(III), but due to the high thermodynamic stability of the tetravalent actinide complexes, they are rapidly oxidized to An(IV) complexes. These complexes have been used for separating high and low valent actinides in nuclear fuel processing.[137, 141]

❖ Catecholate – These types of ligands have been used in forming complexes with americium(III) and plutonium(III). The importance of these ligands is that they have been used to remove actinides from humans via chelation.[138]

❖ 8-Hydroxyquinoline and derivatives: This ligand was found to form complexes with plutonium(III) in the form of $An(Ox)_3$ while complexes with uranium(III) and neptunium(III) oxidize rapidly into An(IV).

❖ Oxalate – $C_2O_4^{2-}$: The An(III) oxalates have been extensively used in actinide separation and purification, but the low solubility of $Pu_2(C_2O_4)_3 \cdot xH_2O$ limits its use. Dehydration of this complex produces an oxide, (PuO_2).[139]

(ii)   Macrocyclic ligands: Crown ethers

Two requirements have to be fulfilled to form stable complexes.

❖ The coordination sphere of the metal must be stabilized by both the crown ether and other anions such as NO_3^- and ClO_4^-. In addition the An(III) complex should posses a coordination number between seven or eight with crown ether.

❖ The net charge on the complex must be zero. This implies that the oxidation state of the An(III) must be neutralized by the anions in the complex. An example of crown ether ligand which has been used in forming complexes with uranium(III) is dicyclohexyl-18-crown-6 (dch-18-crown-6).[104] Complexes formed with uranium(III) were analyzed using EXAFS and single crystal X-ray diffraction, indicating that uranium(III) is bound in a *trans* manner within the complex.[140, 142]

1.3 Conclusion

In this chapter, some general chemistry of lanthanides and actinides has been outlined and that work provides a backdrop for new chemistry described in the following chapters. The objective in this study is to synthesize new ligands which show new coordination modes with lanthanides. It was anticipated that the chemistry would subsequentially provide useful liquid-liquid extraction performance toward lanthanide ions and ultimately actinide ions. By understanding the mode of coordination of the new ligands further it might be possible to design other ligand families.

1.4 REFERENCES

1. Shone, C. S.; Weinberger, D. A.; Mirkin, C. A. *Prog. Inorg. Chem.* **1999,** *48,* 233.

2. http://en.wikipedia.org/wiki/lanthanide.

3. http://chemistry.about.com/library/weekly/aa02230b.htm.

4. Bailar, J. C.; Emeleus, H. J.; Sir Nyholm, R.; Dickenson, A. F. *Comprehensive Inorganic Chemistry - lanthanide transition metal compounds* **1973,** *Vol. 4.*

5. **gpc.edu/.../PhysicalScience/Periodic-table.html.**

6. en.wikipedia.org/wiki/**Phosphor.**

7. Greenwood, N. N.; and Earnshaw, A. *Chemistry of the elements* **1984**, pp 1423, Pergamon Press.

8. Cotton, F. A.; and Wilkinson, G. F. R. S. *Advanced Inorganic Chemistry, A Comprehensive Text* **1972,** 3rd edition, pg. 1056.

9. Shriver, D. F.; Atkins, P. W.; Overton, T. L.; Rourke, J. P.; Weller, M. T.; and Armstrong, F. A. *Inorganic Chemistry* **2006**, 4th edition, pg 574, W. H. Freeman and Company, 41 Madison Avenue, New York, NY 10010.

10. Mayer, M. G. *Phys. Rev.* **1941**, *60,* 184.

11. Latter, R. *Phy. Rev.* **1955**, 99, 510.

12. Coulson, C. A.; and Sharma, C. S. *Proc. Phys. Soc. (London)* **1962**, 79, 920.

13. Meggers, W. F. *Science* **1947**, *105*, 514.

14. Russell, H. N.; and Meggers, W. F. *J. Research Natl. Bur. Standard* **1932,** *9,* 625.

15. Martin, W. C. *J. Opt. Soc. Am,* **1963,** *53,* 1047.

16. Asprey, L. B.; and Cunningham, B. B. *in progress in Inorganic Chemistry Vol. II,* Interscience Publishers, New York, **1960**, pp. 267.

17. Yocom, P. N. *in Lanthanide/Actinide Chemistry, Advances in Chemistry Series, American Chemical Society, Washington* **1967**, *Vol. 71,* pp 51.

18. Jørgensen, K. C. *J. Inorg. Nucl. Chem.* **1955,** *1,*301.

19. Birnbaum, E. R.; and Moeller, T. *J. Am. Chem. Soc.* **1969,** *91,* 7274.

20. Forsberg, J. H.; and Moeller, T. *Inorg. Chem.* **1969,** *8,* 883.

21. Moeller, T.; Martin, D. F.; Thompson, L. C.; Ferrus, R.; Feistel, G. R.; and Randal, W. J. *Chem. Rev.* **1965,** *65,* 1.

22. Moeller, T.; Birnbaum, E. R.; Forsberg, J. H.; and Gayhart, R. B. *in Progress in the Science and Technology of the Rare Earths (L. Erying, ed.), vol. 3, Pergamon Press, New York* **(1968),** pp 61.

23. Sinha, S. P. *Complexes of the Rare Earths, Pergamon Press, New York* (**1966).**

24. Moeller, T. *in Werner Centennial*, vol. 62, *Advances in Chemistry Series, American Chemical Society,* Washington, **1966,** pp 306.

25. Mnetterties, E. L.; and Wright, C. M. *Quart. Rev. (London),* **1967,** *21,* 109.

26. Hoard, J. L.; and Silverton, J. V. *Inorg. Chem.***1963,** *2,* 235.

27. Lippard, S. J. *in Progress in Inorganic Chemistry (Cotton, F. A. ed.) vol. 8,* Interscience Publishers, New York, **1967,** pp 109.

28. Lippard, S. J. *Inorg. Chem.* **1968,** *7,* 1686.

29. Zachariasen, W. H. *Acta Cryst.* **1949,** *2,* 388.

30. Marezio, M.; Plettinger, H. A.; and Zachariasen, W. H. *Acta Cryst.* **1961,** *14,* 234.

31. Belskii, N. K.; and Struchkov; Yu. T. *Krystallografinja* **1965,** *10,* 16.

32. Cromer, D. T.; and Larson, A. C. *Acta Cryst.* **1956,** *9,* 1015.

33. Matkovic, B.; and Grdenic, D. *Acta Cryst.* **1963,** *16,* 456.

34. Fitzwater, D. R.; and Rundle, R. E.; Krist, Z. **1959,** *112,* 362.

35. Helmholtz, L. *J. Am. Chem. Soc.* **1939,** *61,* 1544.

36. Schubert, K.; and Seitz, A., Z. *anorg.U. Allgem. Chem.* **1947,** *254*, 116.

37. Templeton, D. H.; and Carter, G. F. *J. Phys. Chem.* **1954,** *58,* 940.

38. Zachariasen, W. H. *Acta Cryst.* **1948,** *1,* 265.

39. Hoard, J. L.; Lee, B.; and Lind, M. D. *J. Am. Chem. Soc.* **1965,** *87,* 1612.

40. Lind, M. D.; Lee, B. K.; and Hoard, J. L. *J. Am. Chem. Soc.* **1965,** *87,* 1611.

41. Al-Karaghouli, A. R.; and Wood, J. S. *J. Am.Chem. Soc.* **1968,** *90,* 6548.

42. Basile, L. J.; Gronet, D. L.; and Ferraro, J. R. *Spectiochim. Acta 24A* **1968,** 707.

43. Sinha, S. P.; Naturforsch, Z. 20A **1965**, 552.

44. Bear, J. L.; Choppin, G. R.; and Quagliano, J. V. *J. Inorg. Nucl. Chem.* **1963,** *25,* 513.

45. Choppin, G. R.; and Martinez-Perez, L. A. *inorg. Chem.* **1968,** *7,* 2657.

46. Sakharova, N. N.; Doklady A. N. SSSR **1957,** *113,* 1073.

47. Sievers, R. E.; Eisentraut, K. J.; and Springer, C. S.; Jr. *Lanthanide/Actinide Chemistry, vol. 71, Advances in Chemistry Series, American Chemical Society, Washington* **1966,** pp 141.

48. Eisentraut, K. J.; and Sievers, R. E. *J. Am. Chem. Soc.* **1965,** *87,* 5254.

49. McCleverty, J. A.; and Meyer, J. T. *Comprehensive Coordination Chemistry II, Volume I, Fundamentals: Ligands, Complexes, Synthesis, Purification and Structure, Elsevier Pergamon, UK: Elsevier Ltd., The Boulevard, Langford Lane, Kidlington, And Oxford, OX5 IGB, UK. USA: Elsevier Inc.,525B street, suite 1900, San Diego, CA 92101-4495, USA.*

50. Slone, C. S.; Weinberger, D. A.; Mirkin, C. A. *Prog. Inorg. Chem.***1999,** *48,* 233.

51. Quin, L. D. *A Guide to Organophosphorus Chemistry; Wiley: New York* **2000.**

52. Whitaker, C. M.; Kott, K. L.; McMahon, R. J. *J. Org. Chem.* **1995,** *60,* 3499.

53. Bhattacharyya, P.; Slawin, A. M. Z.; Smith, M. B.; Woollins, J. D. *Inorg. Chem.* **1996,** *35,* 3675.

54. Gan, X. M.; Duesler, E. N.; Paine, R. T. *Inorg. Chem.* **2001,** *40,* 4420.

55. Dieleman, C.; Loeber, C.; Matt, D.; De Lain, A.; Fischer, J. *J. Chem. Soc. Dalton Trans.* **1995,** 3097.

56. Douse, L.; Charbonniere, L.; Cesario, M.; Ziessel, R. *New J. Chem.* **2001,** *25,* 1024.

57. Cristau, H. J.; Moucloet, P.; Dozol, J. F.; Rouquette, H. *Heteroatom Chem.* **1995,** *6,* 533.

58. Grushin, V. V. *Organometallics* **2001,** *20,* 3950.

59. Grim, S. O.; Walton, E. D. *Inorg. Chem.* **1980,** *19,* 1982.

60. Slawin, A. M. Z.; Smith, M. B.; Woollins, J. D. *J. Chem. Soc., Dalton Trans.* **1996,** 1283.

61. Slawin, A. M. Z.; Smith, M. B.; Woollins, J. D. *J. Chem. Soc., Dalton Trans.* **1996,** 4567.

62. Slawin, A. M. Z.; Smith, M. B.; Woollins, J. D. *J. Chem. Soc., Dalton Trans.* **1996,** 4575.

63. Yeo, J. S. L.; Vittal, J. J.; Hor, T. S. A. *Chem. Commun.* **1999,** 1477.

64. Weber, R.; Englert, U.; Ganter, B.; Keim, W.; Mothrath, M. *Chem. Commun.* **2000,** 1419.

65. Takahashi, Y.; Hikichi, S.; Akita, M.; Moro-oka, Y. *Chem. Commun.* **1999,** 1491.

66. Faller, J. W.; Patel, B. P.; Albrizzio, M. A.; Curtis, M. *Organometallics* **1999,** *18,* 3096.

67. Thorman, J. L.; Young, V. G. Jr.; Boyd, P. D. W.; Guzei, I. A.; Woo, L. K. *Inorg. Chem.* **2001,** *40,* 499.

68. Paine, R. T.; Bond, E. M.; Parveen, S.; Donhart, N.; Duesler, E. N.; Smith, K. A.; Nöth, H. *Inorg. Chem.* **2002,** *41,* 444.

69. Bond, E. M.; Duesler, E. N.; Paine, R. T.; Nöth, H. *Polyhedron* **2000,** *19,* 2135.

70. Aparna, K.; Krishnamurthy, S. S.; Nethaji, M. *J. Chem. Soc. Dalton Trans.* **1995,** 2991.

71. Le, Q. T. H.; Umetani, S.; Sasaki, T.; Tomita, T. ; Matsui, M. *Bull. Chem. Soc. Jpn* **1995,** *68,* 2867.

72. Le Gall, I.; Laurent, P.; Soulier, E.; Salaiin, J. Y.; des Abbayes, H. *J. Organomet. Chem.* **1998**, *567,* 13.

73. Ellis, D. D.; Harrison, G.; Orpen, A. G.; Phetmung, H.; Pringle, P. G.; de Vries, J. G.; Oevering, H. *J. chem. Soc. Dalton Trans.* **2000,** 671.

74. Wegman, R. W.; Abatjoglou, A. G.; Harrison, A. M. *J. Chem. Soc. Chem. Commun.* **1987,** 1891.

75. Etter, M. C.; Baures, P. W. *J. Am. Chem. Soc.* **1988**, *110,* 639.

76. Woyski, M. M.; and Harris, R. E. *Treatise on Analytical Chemistry* (Kolthoff, I. M. and Elving, P. J.; eds.) Interscience Publishers, New York, **1963,** Part II, section A, volume 8, pp. 1.

77. Moeller, T.; and Kremers, H. E. *Chem. Rev.* **1945,** *37,* 97.

78. Moeller, T.; and Brantley, J. C. *Anal. Chem.* **1950,** *22,* 433.

79. Moeller, T.; and Moss, F. A. *J. Am. Chem. Soc.* **1951,** *73,* 3149.

80. Banks, C. V.; and Klingman, D. W. *Anal. Chim. Acta* **1956,** *15,* 356.

81. Stewart, D. C.; and Kato, D. *Anal. Chem.* **1958,** *30,* 164.

82. Fischer, W.; Dietz, W.; and Jübermann, O. *Natur wissenschaften* **1937,** *25,* 348.

83. Appleton, D. B.; and Selwood, P. W. *J. Am. Chem. Soc.* **1941,** *63,* 2029, C. C. Templeton and J. A. Peterson, *J. Am. Chem. Soc.,* **1948,** *70,* 3967, C. C. Templeton, *J. Am. Chem. Soc.,* **1949,** *71,* 2187. Asselin, G. F.; Andrieth, L. F.; and Comings, E. W., *J. Phys . Colloid Chem.,* **1950,** *54*, 640.

84. Warf, J. C. *J. Am. Chem. Soc.* **1949,** *71,* 3257.

85. Peppard, D. F.; Faris, J. P.; Gray, P. R.; and Mason, G. W. *J. Phys. Chem.* **1953,** *57,* 294.

86. Weaver, B.; Kappelmann, J. A.; and Topp, A. C. *J. Am. Chem. Soc.***1953,** *75,* 3943.

87. Peppard, D. F. *in Progress and the Science and Technology of the Rare Earths* (L. Erying, ed.), Pergamon Press, New York **1964,** *1,* 89.

88. Silvernail, W. L.; and Goetzinger, N. J.; *in Kirk-Othmer's Encyclopedia of Chemical Technology* (A. Standen, ed.), 2nd edn. Interscience Publishers, New York, **1968,** *vol. 17,* pp 143.

89. Peppard, D. F.; *in the Rare Earths* (Spedding, F. H. and Daane, A. H., eds.), John Wiley, New York, **1961,** Chp. 4.

90. Weaver, B. *in Progress in the Science and Technology of the Rare Earths* (L. Erying, ed.), Pergamon Press, **1964,** *vol. 1,* pp 85-88, **1968,** *vol. 3,* pp 129.

91. Peppard, D. F.; Faris, J. P.; Gray, P. R.; and Mason, G. W. *J. Phys. Chem.* **1953,** *57,* 294.

92. Peppard, D. F.; Driscoll, W. J.; Sironen, R. J.; and McCrty, S. *J. Inorg. Nucl. Chem.* **1957,** *4,* 326.

93. Hesford, E.; Jackson, E. E.; and MacKay, H. A. C. *J. Inorg. Nucl. Chem.* **1959,** *9,* 279.

94. Bochinski, J.; Smutz, M.; and Spedding, F. H. *Ind. Eng. Chem.* **1958,** *50,* 157.

95. Peppard, D. F.; Mason, G. W.; Maier, J. L.; and Drscoll, W. J. *J. Inorg. Nucl. Chem.* **1957,** *4,* 334.

96. Rice, A.; and Stone, C. *U. S. Bur. Mines, Rept. Invest.* **1962,** 5923.

97. Greenwood, N. N.; and Earnshaw, A. *Chemistry of the elements, Pergamon Press Ltd.* **1984**, pp. 1450.

98. Seaborg, G. T. (ed.), *Transuranium Elements, Products of Modern Alchemy*, Dowden, Hutchinson and Ross, Stroudsburg **1978.**

99. Katz, J. J.; and Seaborg, G. T. *The Chemistry of the Actinide Elements, Methuen, London* **1957,** pp 508. An Early but authoritative summary uranium to element 102.

100. Lee, J. A.; and Waldron, M. B. The actinide metals, *vol. 7*, chp. 7, pp 221.

101. http://chemistry.about.com/library/weekly/aa022303c.htm

102. Klaproth, M. H. *Chem. Ann. (Crell) II* **1789,** 387.

103. Berzelius, J. J. *K. Sven. Vetenskapsakad. Handl.* **1829,** *9,* 1.

104. McCleverty, J. A.; and Meyer, T. J. *Comprehensive Coordination Chemistry II, Elsevier Pergamon publishers* **2004,** *3,* 190.

105. Stewart, J. L.; Anderson, R A. *Polyhedron* **1998,** *7,* 953.

106. Van Der Sluys, W. G.; Sattelberger, A.; Streib, W. E.; Huffman, J. C. *Polyhedron* **1989,** *8,* 1247.

107. Reynolds, J. G.; Zalkin, A.; Templeton, D. H.; Edelstein, N. M.; Templeton, L. K. *Inorg. Chem.* **1976,** *15,* 2498.

108. Zachariasen, W. H. *Acta Crystallogr.* **1948,** *1,* 268.

109. Bombier, G.; Forsellin, E. ; Brown, D.; Whittacker, B. *J. Chem. Soc. Dalton Trans.* **1976,** 735.

110. Countryman, R.; McDonald, W. S. *J. Inorg. Nucl. Chem.* **1971,** *33,* 2213.

111. Day, V. W.; Hoard, J. L. *J. Am. Chem. Soc.* **1970,** *92,* 3626.

112. Mazur-ul-Haque, Caughlin, C. N.; Hart, F. A.; van Nice, R. *Inorg. Chem.* **1971,** *10,* 115.

113. Ueki, T.; Zalkin, A.; Templeton, D. H. *Acta Crystallr.* **1966,** *20,* 836.

114. Alcock, N. W.; Esperas, S.; Bagnall, K. W.; Wang Hsian-Yun *J. Chem. Soc., Dalton Trans.* **1978,** 638.

115. Rietz, R. R.; Zalkin, A.; Templeton, D. H.; Edelstein, N. M.; Templeton, L. K. *Inorg. Chem.* **1978,** *17,* 658.

116. Barnard, R.; Bullock, J. I.; Gellatly, B. J.; and Larkworthy, L. F. *The chemistry of the trivalent actinides*. Part 2. Uranium(III) double chlorides and some complexes with oxygen donor ligands, JCS Dalton **1972,** 1932. J. Drozdzynski, A method of preparation of uranium (3+) compounds from solutions, *Inorg. Chim. Acta*, **1979,** *32*, L83-L85.

117. Bullock, J. I.; Storey, A. E.; and Thomson, P. *The chemistry of the trivalent actinoids*. Part 5. Uranium (III) complexes with bidentate organic amides, *JCS Dalton* **1979**, 1040.

118. Hulet, E. K. *Chemistry of the heaviest actinides*: Fermium, mendelevium, nobelium, and lawrencium.

119. Banks, R. H.; and Edelstein, N. M. *Synthesis and characterization of protactinium (IV), neptunium(IV), and plutonium(IV) borohydrides, lanthanide and Actinide Chemistry and Spectroscopy*, *ACS Symposium, Series 131, Am. Chem. Soc*., Washington **1980**, pp 331.

120. Shannon, R. D.; Prewitt, C. T. *Acta Crystallogr. Sect.B* **1969,** *25,* 925.

121. Anderson, R. A. *Inorg. Chem.* **1979,** *18,* 1507.

122. Clark, D. L.; Sattelberger, A. P.; Bott, S. G.; Vrts, R. N. *Inorg. Chem.***1989,** *28,* 1771.

123. Zwick, B. D.; Sattelberger, A. P.; Avens, L. R. Transuranium Organometallic Elements: The Next Generation. In *Transuranium Elements:* A half Century; American Chemical Society: Washington, D. C. **1992,** Chapter 25.

124. Cleveland, J. M.; Bryan, G. H.; Sironen, R. J. *Inorg. Chim. Acta* **1972,** *6,* 54.

125. Clark, D. L.; Hobart, D. E.; Neu, M. P. *Chem. Rev.***1995,** *95,* 25.

126. Kraus, K. A.; Dam, J. R.; Seaborg, G. T.; Katz, J. J.; Manning, W. M.; Eds.; McGraw-Hill: New York **1949,** IV-14B, p 466.

127. Lemire, R. J.; Fuger, J.; Nitsche, H.; Potter, P.; Rand, M. H.; Rydberg, J.; Spahiu, K.; Sullivan, J. C.; Ullman, W. J.; Vitorge, P.; Wanner, H. *Chemical Thermodynamics of Neptunium and Plutonium;* Elsevier: New York **2001,** *Vol. 4.*

128. Fuks, L.; Siekierski, S. *J. Radioanal. Nucl. Chem.* **1987,** *108,* 139.

129. Moskvin, A. I. *Soviet Radiochemistry* **1971,** *13,* 688.

130. Bamberger, C. E. *Solid Inorganic Phosphates of the Transuranium Elements. In Handbook on the Physics and Chemistry of the Actinides; Vol. 3,* Freeman, A. J.; Keller, C. Eds.; Elsevier: Amsterdam **1985,** pp 289.

131. Allen, P. G.; Bucher, J. J.; Shuh, D. K.; Edelstein, N. M.; Craig, I. *Inorg. Chem.* **2000,** *39,* 575.

132. Farkas, I.; Grenth, I.; Banyai, I. *J. Phys. Chem. A.* **2000,** *104,* 1201.

133. Conradson, S. D. *Appl. Spectrosc.* **1998,** *52,* 252A.

134. Kim, J. I.; Klenze, R.; Wimmer, H. *Eur. J. Solid State Inorg. Chem.* **1991,** *28,* 347.

135. Fuger, J.; Khodakovosky, I. L.; Sergeyeva, E. I.; Medvedev, V. A.; Navratil, J. D. *The Chemical Thermodynamics of Actinide Elements and Compounds;* IAEA: Vienna **1992,** Part 12.

136. Matonic J. H.; Scott, B. L.; Neu, M. P. *Inorg. Chem.* **2001,** *40,* 2638.

137. May, I.; Taylor, R. J.; Dennis, I. S. B.; Geoff,; Wallwork, A. L.; Hill, N. J.; Rawson, J. M.; Less, R. *J. Alloys Compd.* **1998,** 275.

138. Kappel, M. J.; Nitsche, H.; Raymond, K. N. *Inorg. Chem.* **1985,** *24,* 605.

139. Cleveland, J. M. *The Chemistry of Plutonium;* American Nuclear Society: La Grange Park, IL, USA **1979.**

140. Dejean, A.; Charpin, P.; Folcher, G.; Rigny, P.; Navaza, A.; Tsoucaris, G. *Polyhedron* **1987,** 6**,** 189**.**

141. Luca, De L.; Giaconelli, G; Taddei, M. *J. Org. Chem.* **2001,** *66,* 2534.

142. Crown ether-Wikipedia, the free encyclopedia.

Chapter 2

2.0 Synthesis and Coordination Chemistry of 2-[(diphenylphosphinoyl)methyl]-4,5-dihydro-oxazole, 19

2.1 INTRODUCTION

Ligand design for f-block metal ions is an important research area[1-7] and applications for this activity are found in efforts to develop improved separations for lanthanide and actinide ions found in nuclear waste and in medical isotope applications.[8-14] These separations are most often done by liquid-liquid extractions that employ a chemical agent that selectively coordinates to the metal ion in water and transports it to an organic phase. These agents are referred to as extractants. In order to develop useful ligands or extractants for the processing of f-elements, special properties must be present. These properties include:

1. stability toward heat and radiation;

2. stability toward basic and acidic solution conditions;

3. solubility in hydrocarbon process solvents;

4. formation of strong complexes;

5. rapid complexation kinetics ;

6. reversibility of the complexation process; and

7. selectivity for a particular metal ion over other ions.

The fundamental scientific issue in f-element ligand design involves the appropriate selection of donor atoms and their placement on an organic backbone that permits chelate interactions. For most f-element ions the ideal case is often different from that found for low-valent d-block ions and the term "inside-out" has been used to

describe f-block selective ligands. Namely, one looks to select a very hard donor atom to provide one or more primary donor-acceptor interactions with the f-block metal. A second, softer donor is often chosen to provide for selectivity in metal binding, e.g., to distinguish between Eu(III) and Am(III) in a mixture. Am(III) being somewhat softer than Eu(III) might be preferentially chosen by a hard/soft hybrid ligand.

In our research group, we have been interested in the aspect of the coordination chemistry of f-element cations that makes these ions distinct from d-block element cations. From a practical standpoint, this coordination chemistry controls the separations and waste treatment of these ions.[15-17]

There are a few success stories in the design of hybrid ligands for f-element ion separations. One involves the development of the carbamoylmethylphosphine oxides (CMPO), $R_2P(O)CH_2C(O)NR'_2$.[18-29] These ligands contain the hard donor phosphine oxide and the softer amide linked together so that bidentate, six-member chelate rings can be formed. With lanthanide and actinide ions, solid state complexes formed are usually bidentate in ligand connectivity except for the smallest lanthanides.[30-44] The ligand also turns out to be a good extractant and this property may result in part, from the hemilability, *vide infra* of the hybrid ligand. At high acid conditions, the P=O group is strongly bonded to the Ln(III) and the amide is dissociated, but it appears to facilitate phase transfer to an organic solution.

In previous efforts our group has designed several new hybrid f-element extraction ligands. These include multidentate ligand systems that contain both P=O and N-O donor groups. These donor functionalities are arranged to provide potentially bidentate or tridentate chelating interactions. Some of the multifunctional ligands

50

designed and synthesized are shown in structures **9-12** (Figure 2.1), the so-called NOPO,

9 and **11** and NOPOPO, **10** and **12** ligands.[45-55]

Figure 2.1 Molecular structures for NOPO and NOPOPO ligands
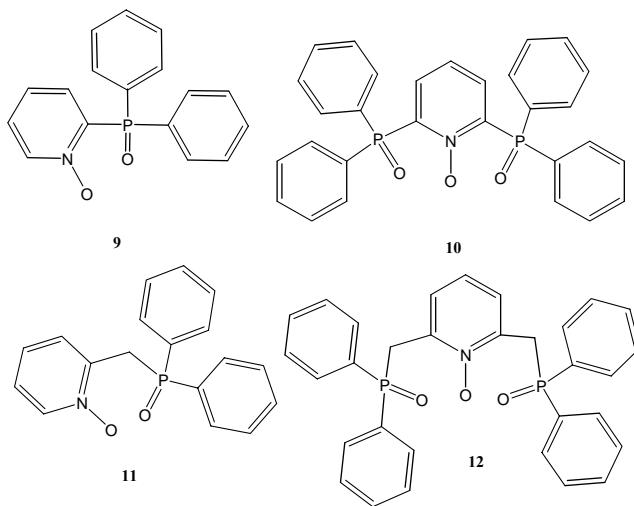
Here the P=O group provides the harder, primary donor center while the N-O provides

the softer/weaker, labile donor interaction. In addition, within this series there is an

increase in chelate ring size going from six in **9** and **10** to seven in **11** and **12**. Somewhat

surprisingly, it was discovered that the larger seven-member chelate structures are more

stable with Ln(III), Th(IV), Am(III), and Pu(IV) ions and examples of **11** and **12** are

amongst the best liquid-liquid extraction reagents for f-element metal ions.[52]

In this chapter, emphasis is directed to a new class of potentially bidentate hybrid

ligands that contain the 4,5-dihydro-oxazole ring **13** (Figure 2.2). Previous

investigations[56-58] have used this ring in the construction of soft hemilabile[59] ligands for

low-valent d-block ions.

Figure 2.2 Model structure for 2-oxazoline

13
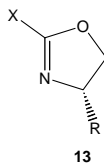
The term hemilability[56] refers to a class of ligands that contain both hard and softer donor groups. Such combinations provide for the formation of strong and weak interactions during metal ion coordination. This property has mainly been applied in the synthesis of ligands for homogeneous catalysts. The ease of dissociation of the weakly bonded donor site allows for substrate binding while the strongly bonded donor remains coordinated to the metal. In most cases the group X contains a soft donor center such as a phosphine (X=R_2P), pyridine or thiol (X=RS). The oxazoline ring offers two additional potential donor sites (C=N- and -O-). Many examples of the binding of **13** to low-valent, soft d-block metals have been reported in which the soft, X-based donor produces the kinetically inert attachment. In all of these cases the nitrogen donor of the oxazoline ring is reported to act as the labile donor.[56-66] A few specific classes of oxazoline-based ligands that have been developed are represented by structures **14-17,** (Figure 2.3).[56, 66]

Figure 2.3 Derivatives of oxazoline based ligands

14   **15**

16   **17**
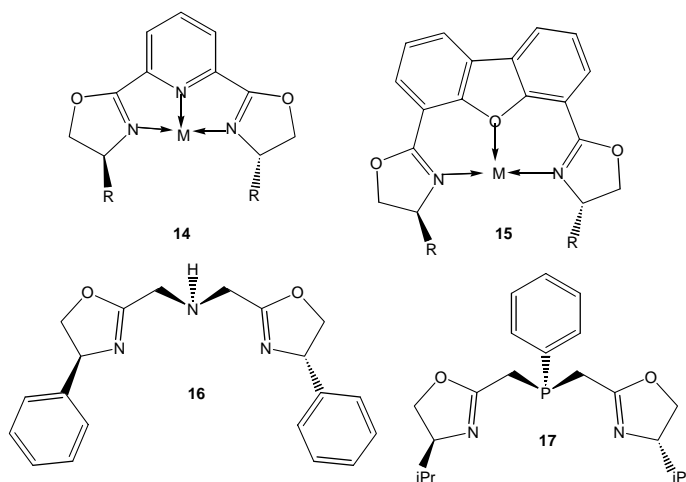
As will be detailed below, we were attracted by the possibility of building "inside-out" examples of ligands containing the oxazoline unit. We wished to determine if examples with X (Figure 2.2) containing a hard donor center could be prepared (Figure 2.4). If so, we wished to determine if the preference for N-binding over O-binding of the oxazoline persists with very hard acceptors.

Therefore, in this chapter, the syntheses of hybrid ligands that contain the 2-methyl-2-oxazoline fragment are described. Two functional groups, one the softer nitrogen from the 2-methyl-2-oxazoline ring and a P=O group substituted at the –CH$_2$-position, are employed. The study of the coordination chemistry with lanthanides is also outlined.

Figure 2.4 Example of "inside-out" oxazoline ligand
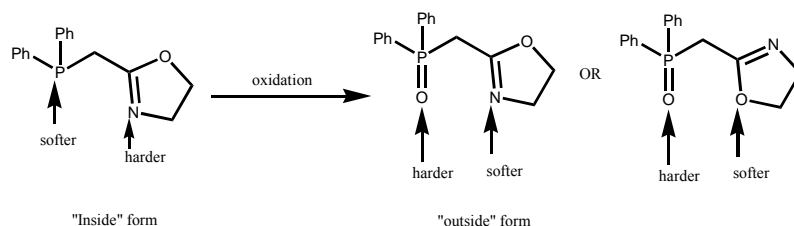
2.2 STATEMENT OF PROBLEM

So far, coordination chemistry of functionalized oxazoline ligands with low-valent, electron rich metals has been widely studied and oxazoline ligands have been used in the design of asymmetric ligands useful for forming homogeneous catalysts for selected organic transformations. However, coordination chemistry of the oxazoline ring and donor functionalized oxazoline rings with hard transition metal cations has scarcely been studied. Complexes with hard f-block metal ions are absent from the literature. The open question is: will a phosphoryl functionalized oxazoline ring incorporated in a ligand backbone act as either an N-donor or O-donor ligand toward an f-block metal ion?

2.3 EXPERIMENTAL

2.3.1 Synthesis of 2-[(diphenylphosphanyl)-methyl]-4,5-dihydro-oxazole, 18, and 2-[(diphenylphosphinoyl)methyl]-4,5-dihydro-oxazole, 19

Scheme 5
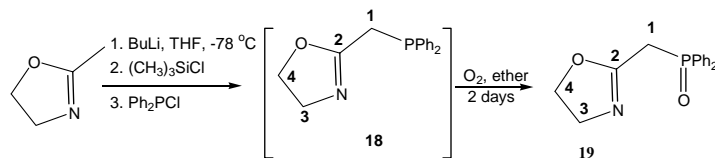
The synthesis of the phosphine precursor **18** has been reported by Braunstein and co-workers.[59] This method was repeated without modification to form compound **18**. A THF solution (5 ml) of 2-methyl-2-oxazoline (2.6 g, 30.8 mmol, 1 eq.) was added over a period of 10 min. with a cannula to a solution of BuLi in hexane (19.4 ml, 1.6 M, 30.8 mmol, 1 eq.) in a 250 ml flask containing dry THF (75 ml) at -78 $^{\circ}$C. The mixture was stirred under nitrogen for 1 h. The reaction mixture changed from colorless to yellow. Degassed (CH$_3$)$_3$SiCl (4 ml, 30.8 mmol, 1 eq.) was then added at the same temperature, to give a pale yellow mixture. After 1 h of stirring at -78 $^{\circ}$C, Ph$_2$PCl (5.5 ml, 30.8 mmol, 1 eq.) in THF (10 ml) was added followed by stirring overnight during which time the reaction mixture warmed to room temperature. The solvent was removed under reduced pressure leaving a yellow oil which was extracted with dichloromethane (100 ml), concentrated and put under vacuum for 5 days to give the phosphine intermediate **18** as a yellow solid. Yield: 3.8 g (46.7%); lit. 61%; mp 58-60 $^{\circ}$C.

Selected spectroscopic data for **18** are summarized here and typical ^{1}H NMR, and ^{31}P{^{1}H} NMR spectra are shown in Figures 2.5-2.6.

^{1}H NMR (250 MHz, 23 $^{\circ}$C, CDCl$_3$), δ (ppm): 3.0 (s, 2H, H$_1$), 3.6 (t, 2H, H$_3$, $^3J_{H-H}$ = 9.2 Hz), 3.9 (t, 2H, H$_4$, $^3J_{H-H}$ = 9.5 Hz), 7.2 (m, 6H, H-Ar), 7.3-7.4 (m, 4H, H-Ar).

^{31}P{^{1}H} (101.3 MHz, 23 ^{o}C, CDCl$_3$), δ (ppm): -16.9 (-CH$_2$-P).

Mass spectrum (ESI) *m/e* (fragment, relative intensity): [M+H$^+$] = 270.1058 and the calculated exact mass is 269.0970.

Efforts to obtain **18** in analytically pure form were unsuccessful, and the ^{31}P NMR indicates the presence of several minor impurities (Figure 2.6).

Figure 2.5 250 MHz ^{1}H NMR spectrum (CDCl$_3$) for 2-[(diphenylphosphanyl)-methyl]-4,5-dihydro-oxazole, 18
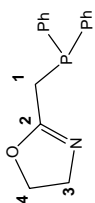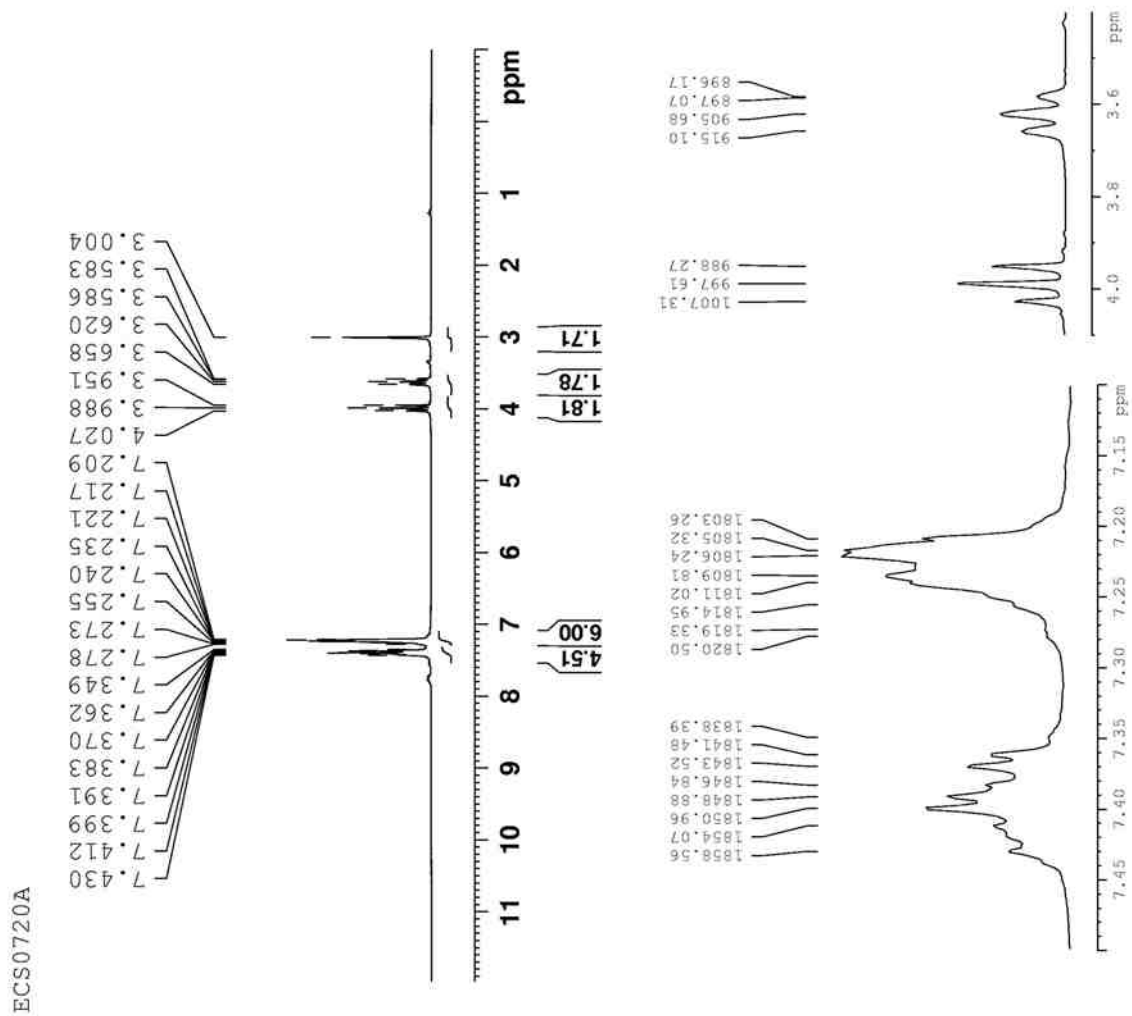
Figure 2.6 101.3 MHz ^{31}P{^{1}H} NMR spectrum (CDCl$_3$) for 2-[(diphenylphosphanyl)-

methyl]-4,5-dihydro-oxazole, 18
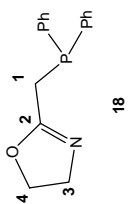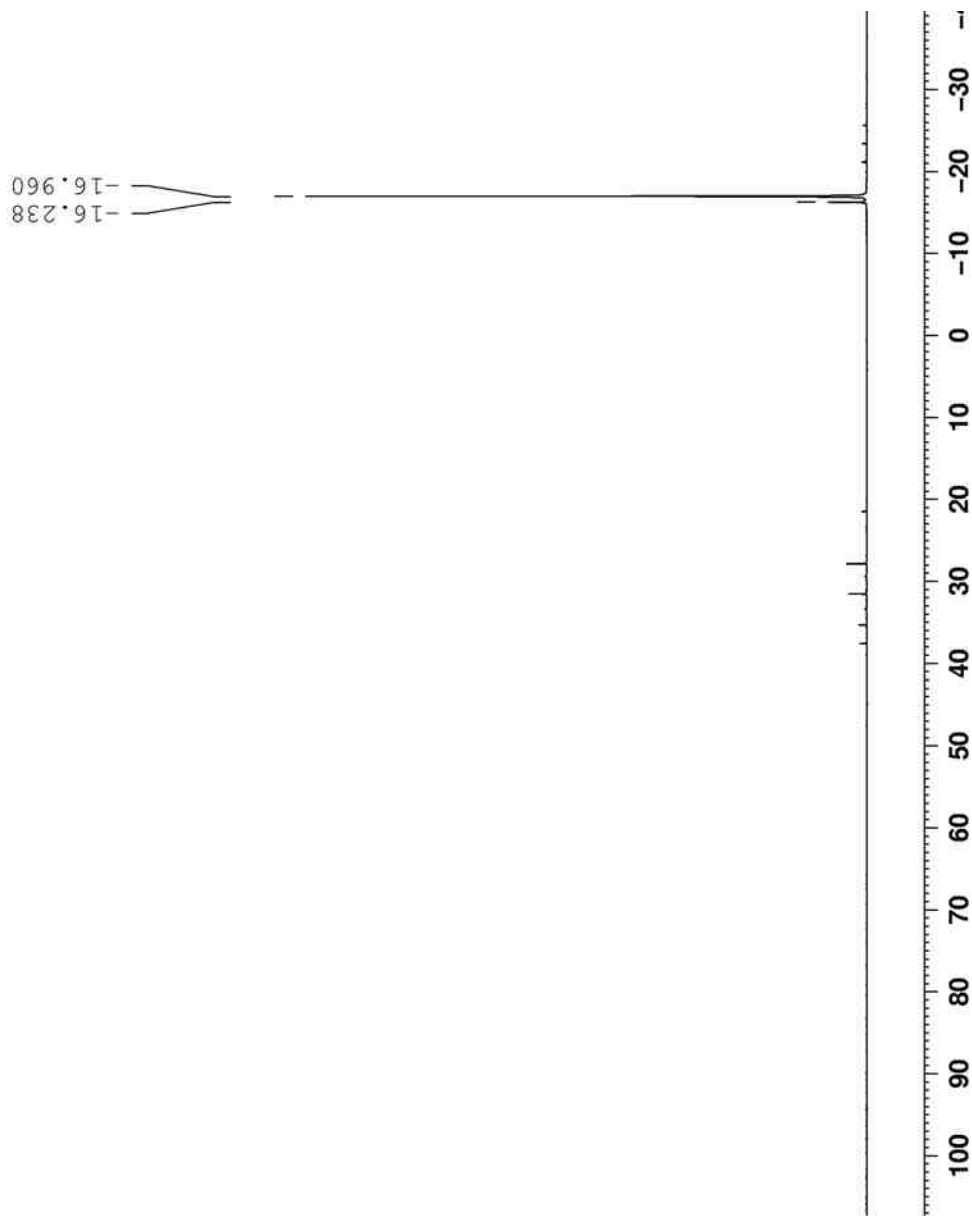
These data can be compared with data from the literature.[59]

Mp 59 $^{\circ}$C,

Infrared spectrum (CH$_2$Cl$_2$, cm^{-1}): 1660 (s, $v_{C=N}$).

^{1}H NMR (300.1 MHz, CDCl$_3$), δ (ppm): 3.05 (s, 2H,-CH$_2$-P), 3.75 (t, 2H, -CH$_2$-N, $^3J_{HH}$ = 9.4 Hz), 4.15 (t, 2H, -CH$_2$-O, $^3J_{HH}$ = 9.4 Hz), 7.20-7.50 (m, 10H, H-Ar).

^{13}C{^{1}H} NMR (50.3 MHz, CDCl$_3$), δ (ppm): 28.3 (d, P-CH$_2$, $^1J_{pc}$= 19.2 Hz), 54.7 (s, CH$_2$-N), 67.6 (s, –CH$_2$-O), 128.5 (d, o-aryl, $^2J_{pc}$= 7.0 Hz), 128.9 (s, p-aryl), 132.7 (d, $^3J_{pc}$= 19.7 Hz), 137.7 (d, $ipso$-aryl, $^1J_{pc}$= 14.1 Hz), 165.4 (d, C=N, $^3J_{pc}$= 7.0 Hz).

^{31}P{^{1}H} (121.5 MHz, CDCl$_3$): δ (ppm), -17.3 (s, -CH$_2$-P).

2.3.2 Synthesis of 2-[(diphenylphosphinoyl)methyl]-4,5-dihydro-oxazole, 19

Without isolation, the intermediate 2-[(diphenylphosphanyl)-methyl]-4,5-dihydro-oxazole, **18** was dissolved in ether and oxygen gas was bubbled through the solution for two days. The solvent was evaporated in vacuum, and the yellow oily product was purified by column chromatography: silica gel 70-230 mesh, 60Å, eluted with 95% CH$_2$Cl$_2$, MeOH followed by 90% CH$_2$Cl$_2$, MeOH. This provided **19** as a yellow solid. Yield: 5.1 g (58.2%) based on the starting material 2-methyl-2-oxazoline. Further purification was done by washing the product with CH$_2$Cl$_2$/hexane and followed by recrystallization from hot ethyl acetate to give colorless crystals: mp 128 - 130 $^{\circ}$C.

Elemental Analysis

Calculated for C$_{16}$H$_{16}$NO$_2$P (FW= 285.09 g/mole)   C, 67.36; H, 5.65; N, 4.91.

Found   C, 66.15; H, 6.01; N, 4.66.

Spectroscopic data for **19** are summarized here and typical spectra are displayed in Figures 2.7-2.14.

Infrared spectrum (KBr, cm^{-1}): 1659 (s, $\nu_{C=N}$), 1188 (s, $\nu_{P=O}$).

^{1}H (250 MHz, 23 $^{\circ}$C, CDCl$_3$), δ (ppm): 3.4 (d, 2H, H$_1$, $^2J_{H\text{-}P}$ = 14.6 Hz) 3.7 (t, 2H, H$_3$, $^3J_{H\text{-}H}$ = 9.4 Hz), 4.1 (t, 2H, H$_4$, $^3J_{H\text{-}H}$ = 9.1 Hz), 7.4-7.5 (m, 6H, H-Ar), 7.7-7.8 (m, 4H, H-Ar).

^{1}H (500 MHz, 23 $^{\circ}$C, CDCl$_3$ ^{31}P coupled), δ (ppm): 3.4 (d, 2H, H$_1$, $^2J_{H\text{-}P}$ = 14.6 Hz), 3.7 (t, 2H, H$_3$, $^3J_{H\text{-}H}$ = 9.4 Hz, d, $^5J_{H\text{-}P}$ = 3.6 Hz), 4.0 (t, 2H, H$_4$, ^3J = 9.5 Hz), 7.4-7.5 (m, 6H, H-Ar), 7.7-7.8 (m, 4H, H-Ar).

^{1}H (500 MHz, 23 $^{\circ}$C, CDCl$_3$ ^{31}P decoupled), δ (ppm): 3.4 (s, 2H, H$_1$) 3.7 (t, 2H, H$_3$, $^3J_{H\text{-}H}$ = 9.5 Hz), 4.0 (t, 2H, H$_4$, $^3J_{H\text{-}H}$ = 9.5 Hz), 7.4-7.5 (m, 6H, H-Ar), 7.8 (d, 4H, H-Ar, J = 8 Hz).

^{13}C{^{1}H} (62.9 MHz, 23 $^{\circ}$C, CDCl$_3$), δ (ppm): 32.5 (d, C$_1$, $^1J_{C\text{-}P}$ = 64.2 Hz), 54.8 (s, C$_3$), 68.2 (s, C$_4$), 128.9 (d, *ortho*-aryl, $^2J_{C\text{-}P}$ = 12.2 Hz), 131.5 (d, *meta*-aryl, $^3J_{C\text{-}P}$ = 9.7 Hz), 132.4 (d, *ipso*-aryl, $^1J_{C\text{-}P}$ = 100.9 Hz), 132.5 (d, $J_{C\text{-}P}$ = 2.5 Hz), C-Ar, 161.4 (d, C$_2$, $^2J_{C\text{-}P}$ = 7.4 Hz).

^{31}P{^{1}H} (101.3 MHz, 23 $^{\circ}$C, CDCl$_3$), δ (ppm): 28.1 (-CH$_2$-P=O).

Mass spectrum (ESI) *m/e* (fragment, relative intensity): [M+H$^+$] = 286.0988 and the calculated exact mass is 285.0919.

Figure 2.7 Infrared spectrum (KBr, cm^{-1}) for 2-[(diphenylphosphinoyl)methyl]-4,5-dihydro-oxazole, 19
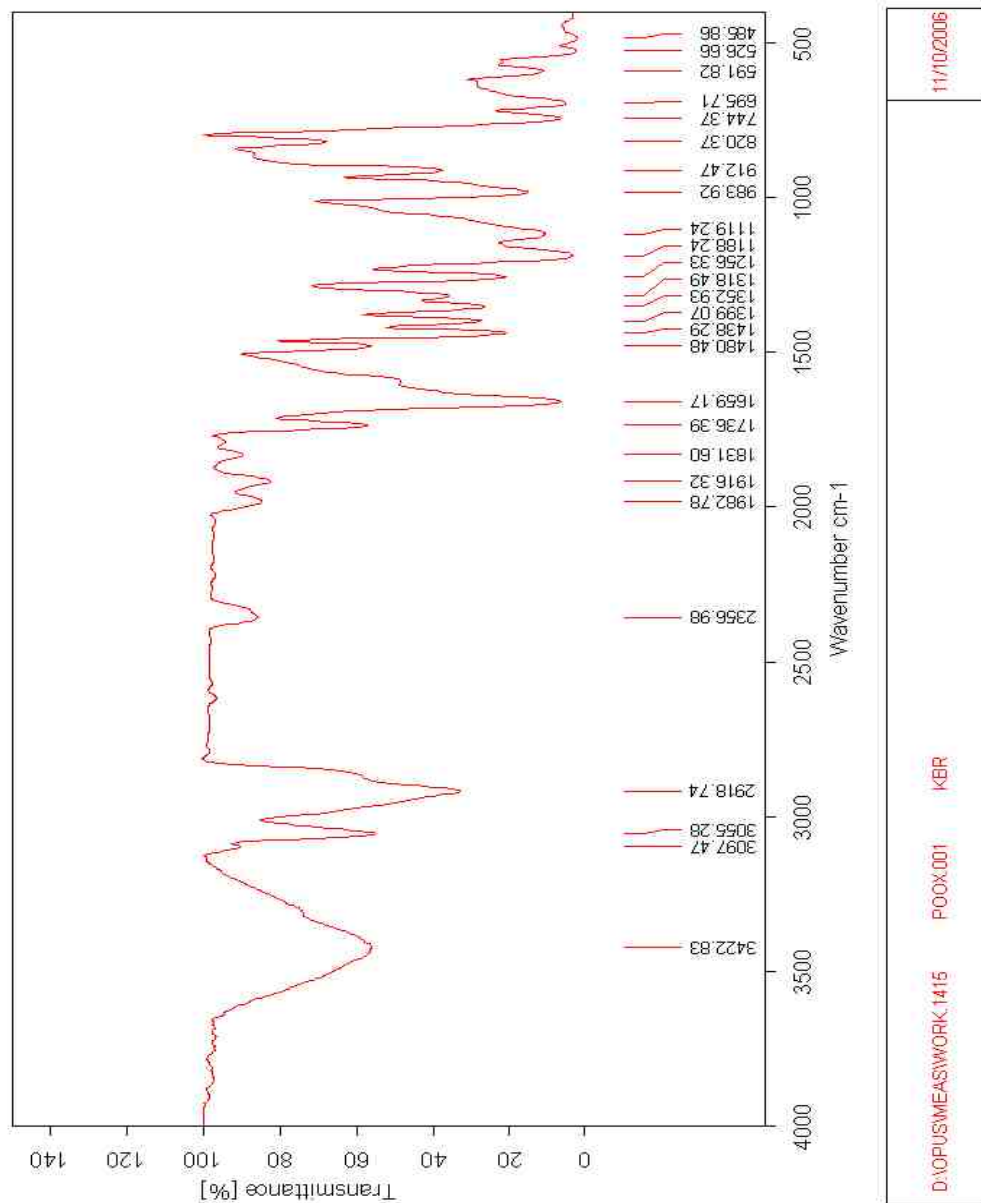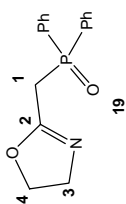
61
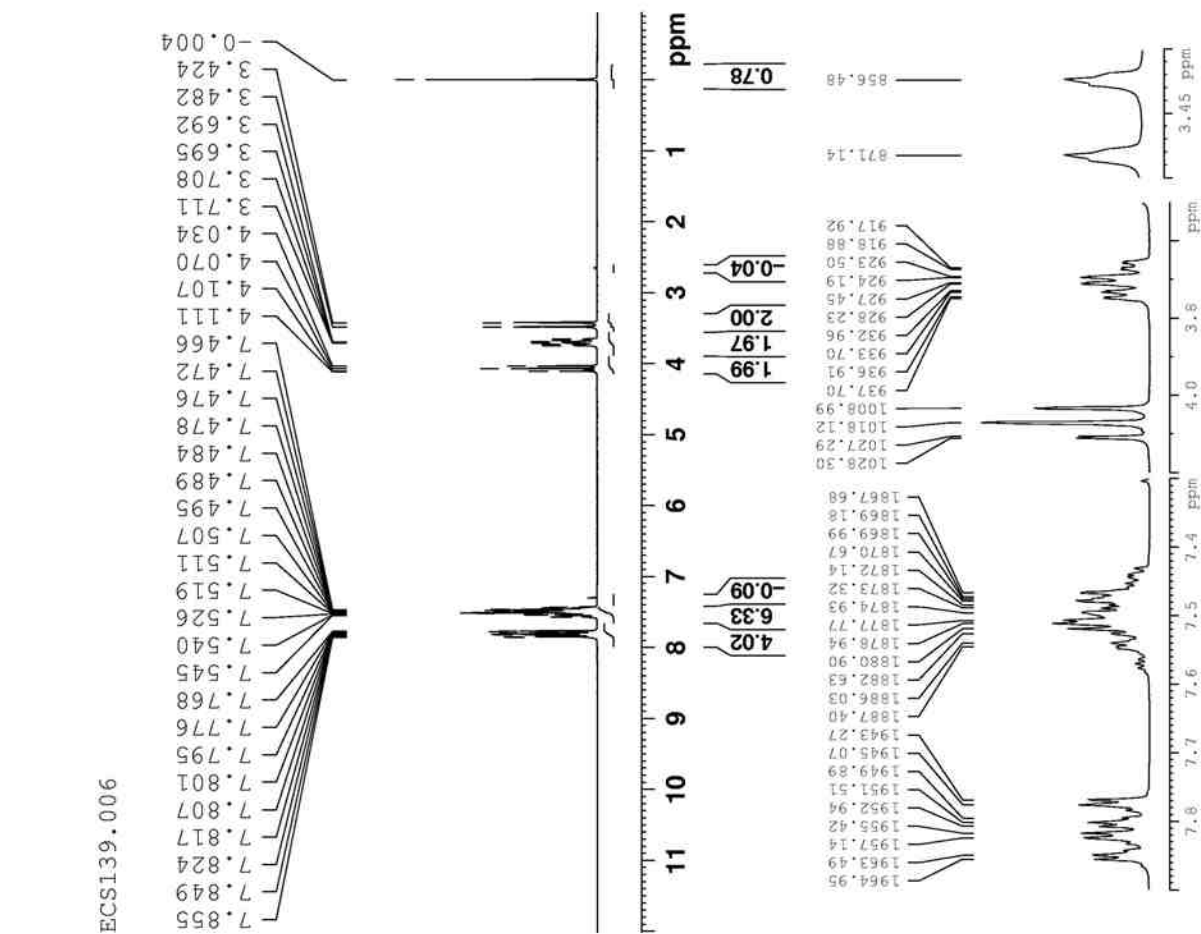
Figure 2.9 62.9 MHz ^{13}C {^1H} NMR spectrum (CDCl$_3$) for 2-[(diphenylphosphinoyl)methyl]-4,5-dihydro-oxazole, 19

−0.443
0.386

32.012
33.033

54.892
68.210
76.975
77.484
77.992

128.806
128.999
131.414
131.568
132.455
132.495
133.173
161.337
161.455

CHN115.013

2013.88
2078.13

8103.22
8115.39

8267.31
8277.01

8332.81
8335.31

8377.94

0 ppm
20
40
60
80
100
120
140
160
180
200

33 ppm
129 ppm
130
131
132
133

19
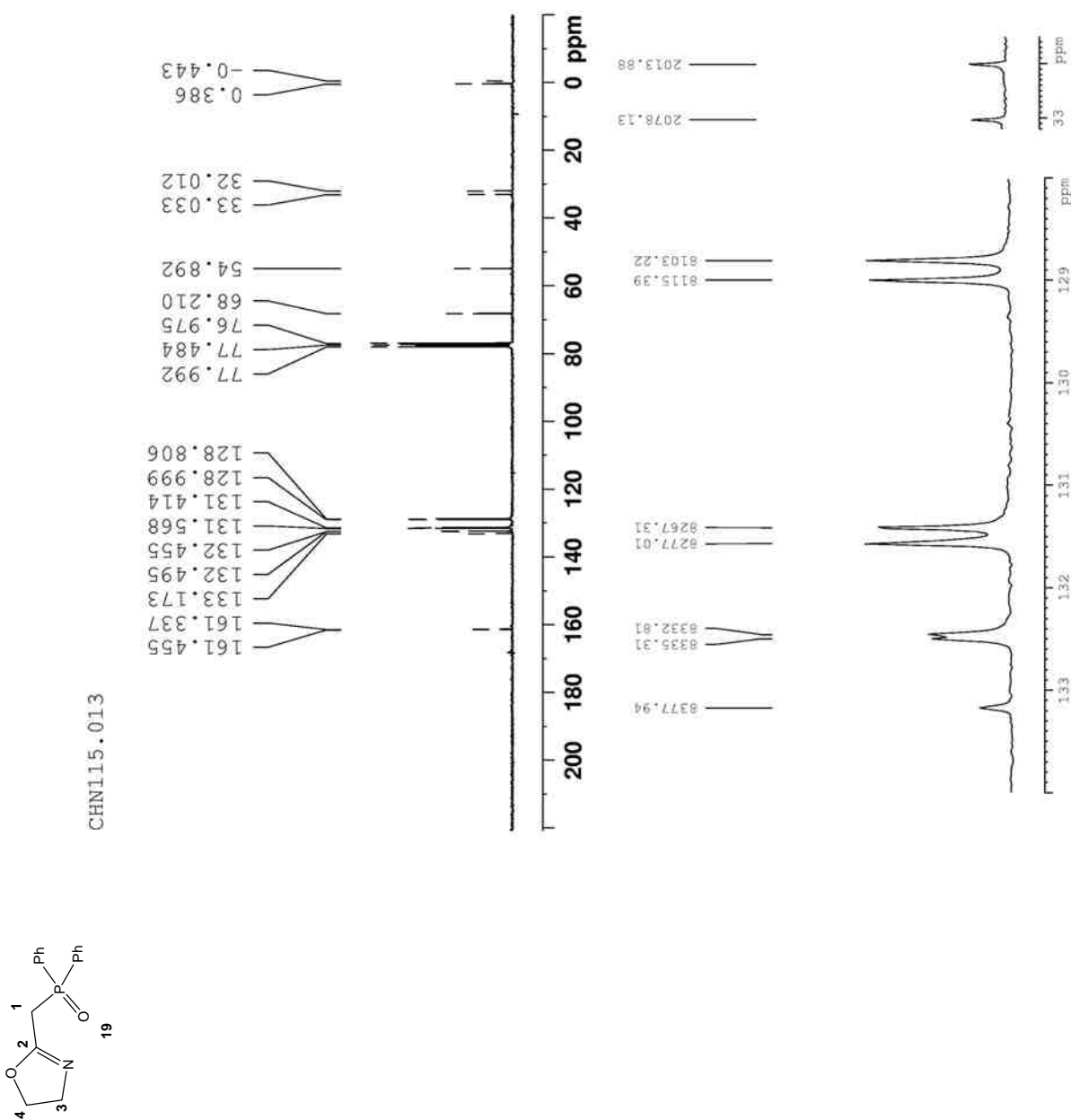
Figure 2.10 101.3 MHz ^{31}P{^{1}H} NMR spectrum (CDCl$_3$) for 2-[(diphenylphosphinoyl)methyl]-4,5-dihydro-oxazole, 19

28.123

CHN115.012
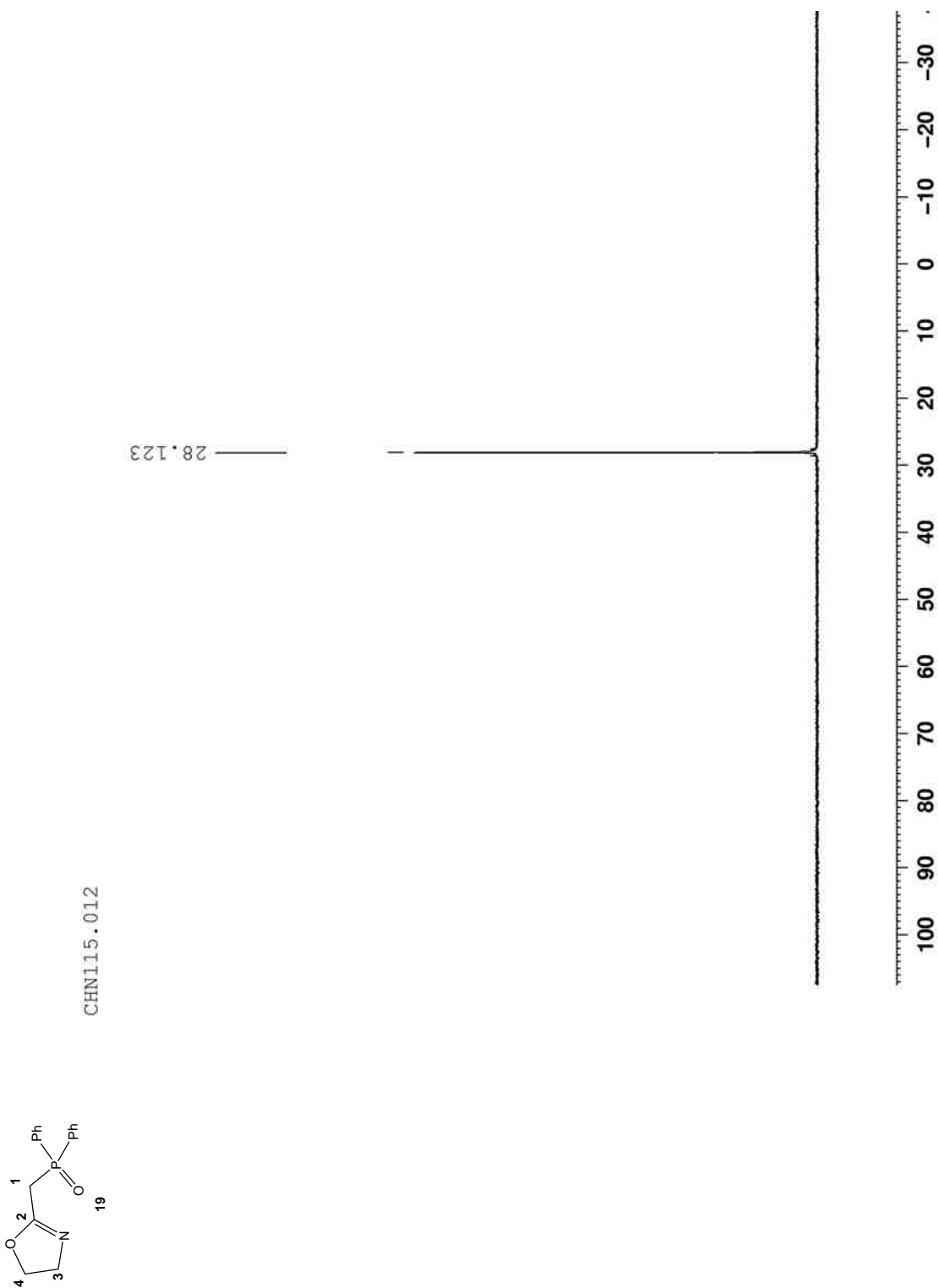
Figure 2.11 500 MHz ^{1}H NMR spectrum for 2-[(diphenylphosphinoyl)methyl]-4,5-dihydro-oxazole, 19 with ^{31}P coupling
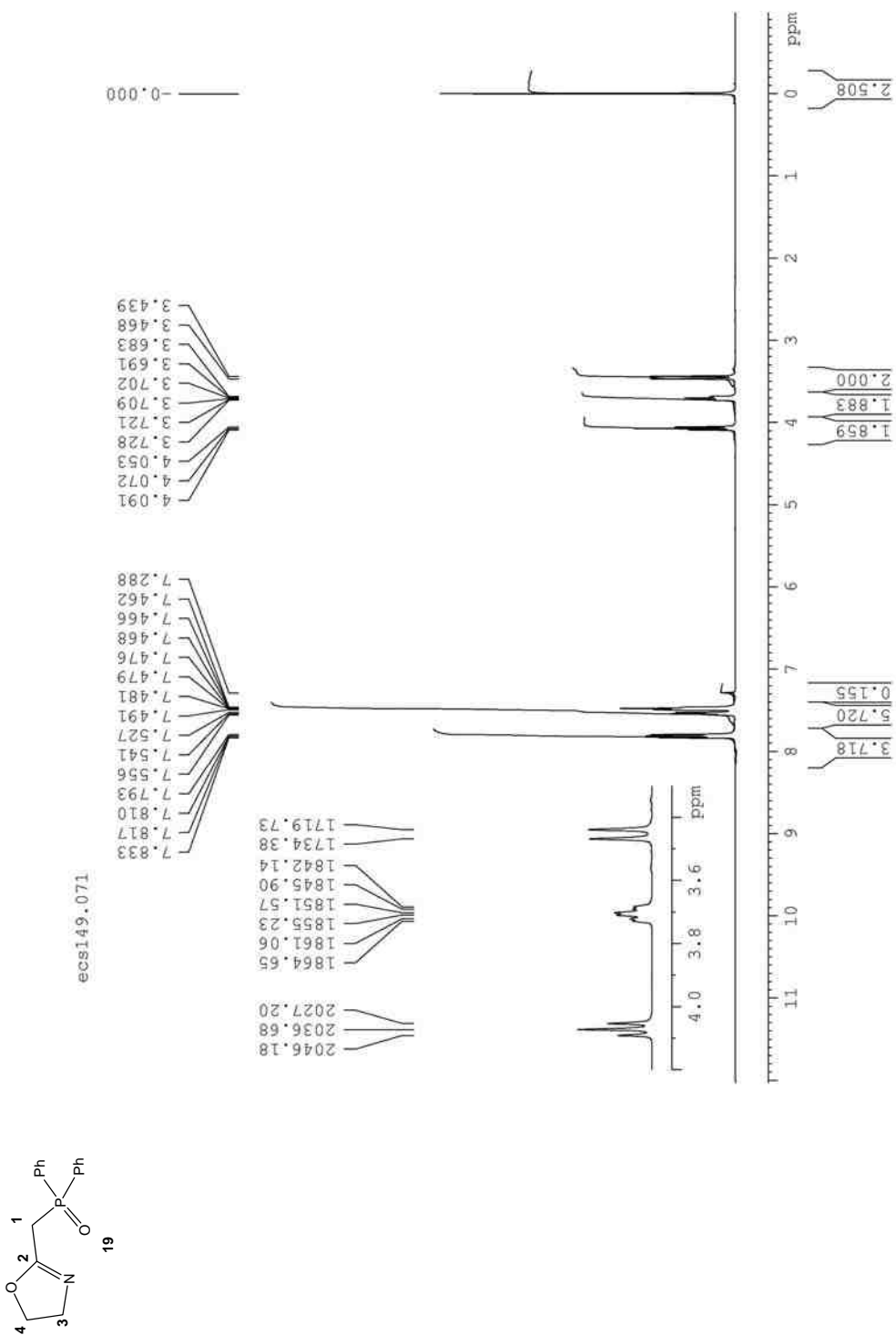
Figure 2.12 500 MHz ^{1}H NMR spectrum for 2-[(diphenylphosphinoyl)methyl]-4,5-dihydro-oxazole, 19 with ^{31}P decoupling
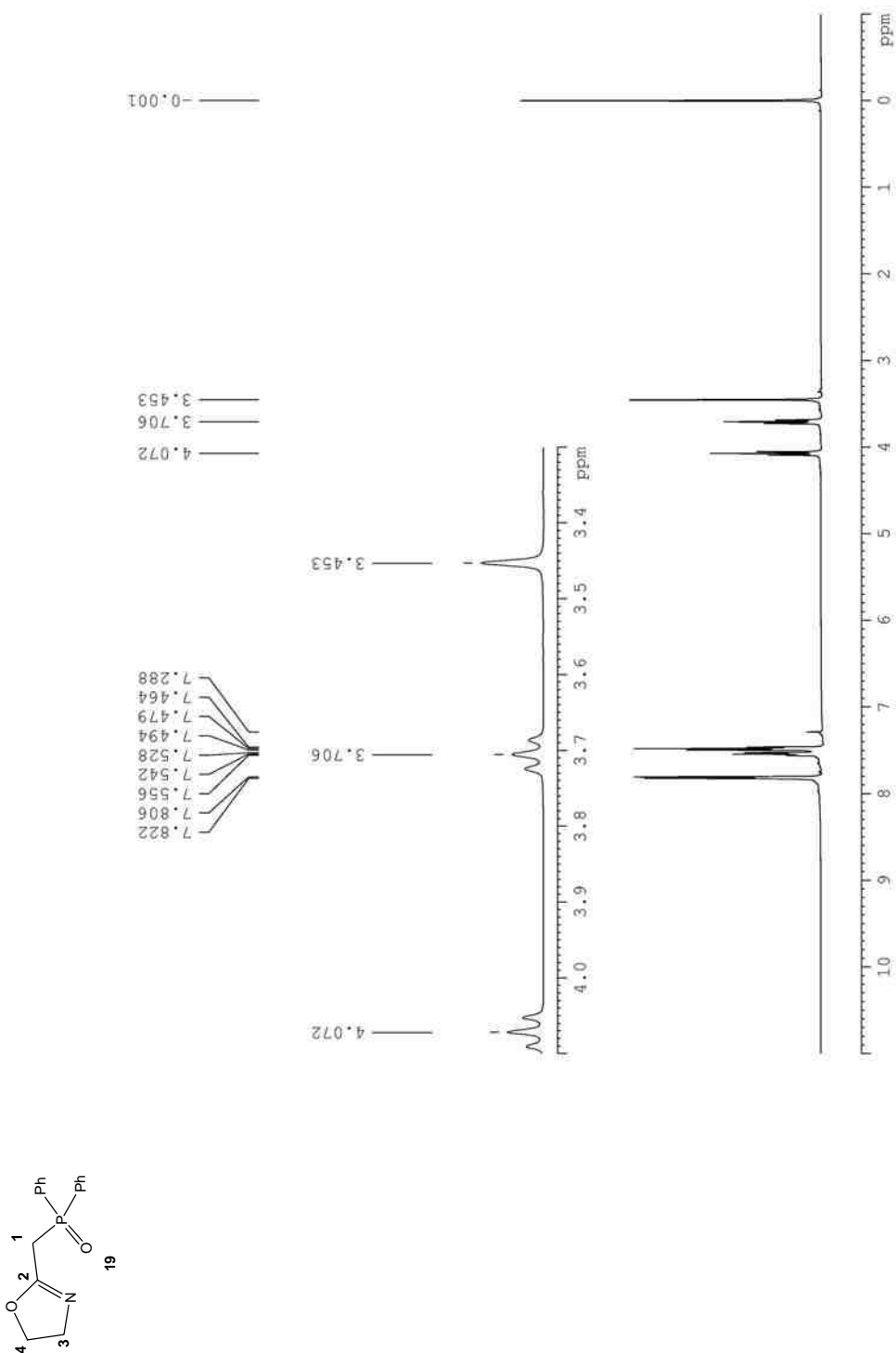
Figure 2.13 Comparisons between Figure 2.11 and 2.12

^{1}H NMR with ^{31}P{^{1}H} decoupling ^{1}H NMR with ^{31}P{^{1}H} coupling
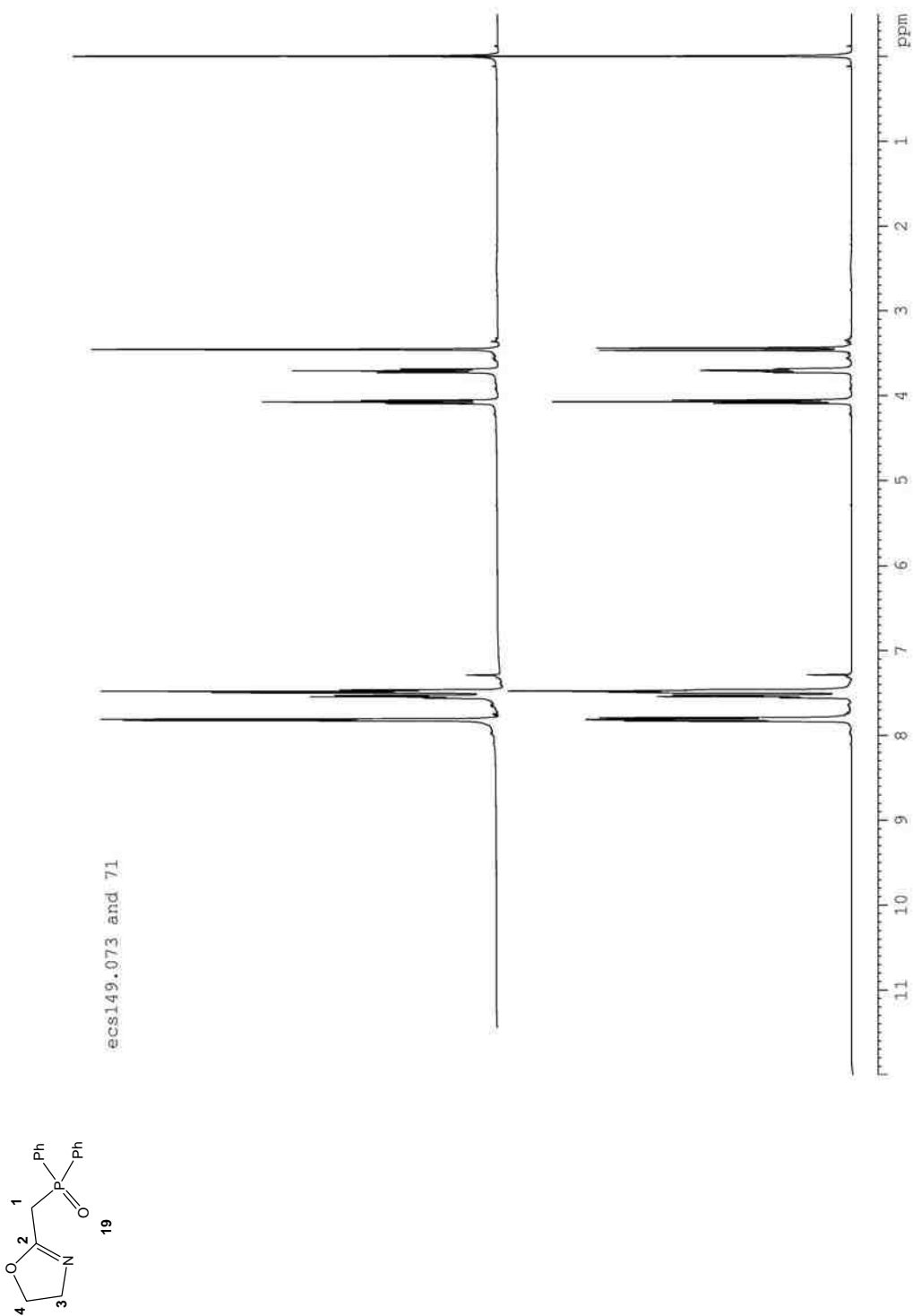
Figure 2.14 Expansion of Figure 2.13 to show the splitting of methylene protons at C$_1$, C$_3$, and C$_4$

^{1}H NMR with ^{31}P{^{1}H} decoupling ^{1}H NMR with ^{31}P{^{1}H} coupling
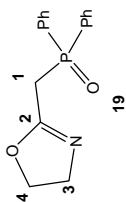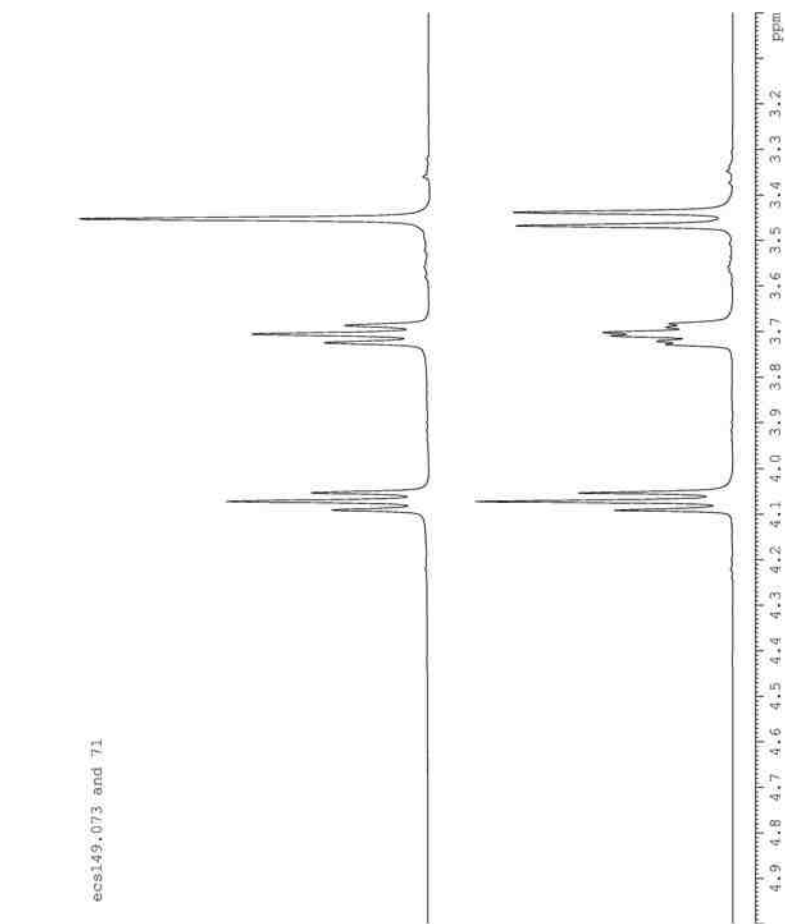
Single crystal X-ray structure determination for 2-[(diphenylphosphinoyl)methyl]-

4,5-dihydro-oxazole, 19

Single crystals suitable for X-ray crystal structure determination were grown from

a capped, hot ethyl acetate solution. Slow cooling, after several hours, gave colorless

crystals. The molecular structure is displayed in Figure 2.15. Crystal parameters are given

in Table 2.1 and bond lengths and angles are given in Table 2.2.

Figure 2.15 Molecular structure and atom labeling scheme for 2-

[(diphenylphosphinoyl)methyl]-4,5-dihydro-oxazole, 19
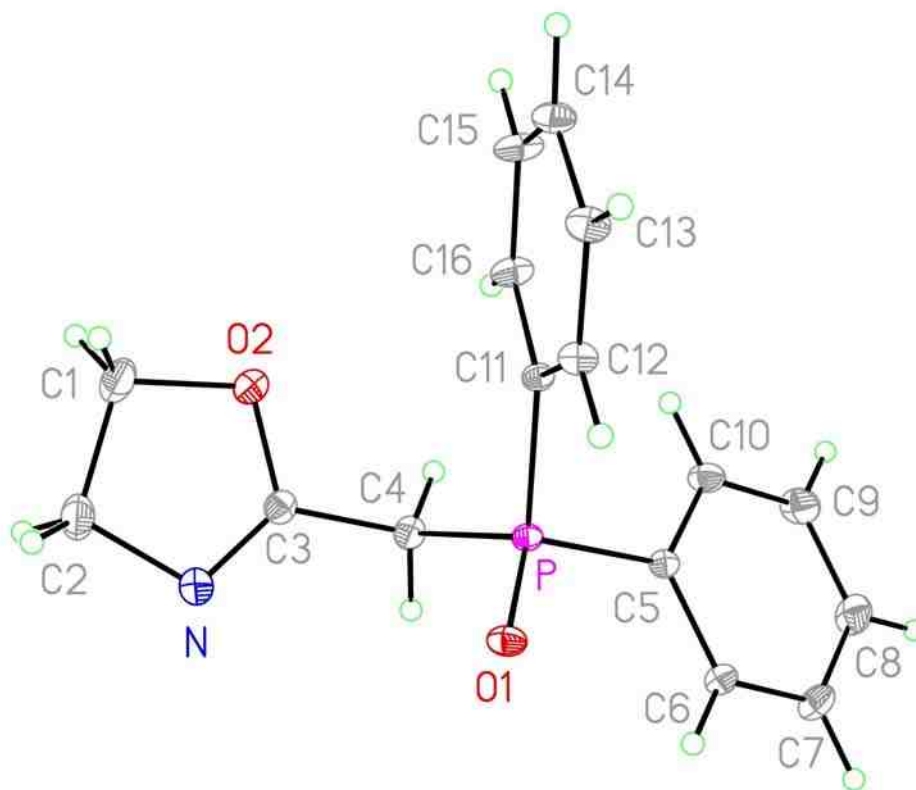
Table 2.1 Crystal parameters for 2-[(diphenylphosphinoyl)methyl]-4,5-dihydro-oxazole, 19

Empirical formula	$C_{16} H_{16} N O_2 P$
Formula weight	285.27
Temperature	223(2) K
Wavelength	0.71073 Å
Crystal system	Orthorhombic
Space group	P2(1)2(1)2(1)
Unit cell dimensions	a = 8.3623(6) Å $\alpha = 90°$.
	b = 11.2530(8) Å $\beta = 90°$.
	c = 15.5392(11) Å $\gamma = 90°$.
Volume	1462.25(18) Å^3
Z	4
Density (calculated)	1.296 Mg/m^3
Absorption coefficient	0.188 mm^{-1}
F(000)	600
Crystal size	0.46 x 0.44 x 0.42 mm^3
Theta range for data collection	3.19 to 31.11°.
Index ranges	-12<=h<=12, -16<=k<=16, -22<=l<=22
Reflections collected	39352
Independent reflections	4691 [R(int) = 0.0182]
Completeness to theta = 31.11°	99.7 %
Absorption correction	Semi-empirical from equivalents

Max. and min. transmission	0.920 and 0.910
Refinement method	Full-matrix least-squares on F^2
Data / restraints / parameters	4691 / 0 / 181
Goodness-of-fit on F^2	0.967
Final R indices [I>2sigma(I)]	R1 = 0.0275, wR2 = 0.0649
R indices (all data)	R1 = 0.0287, wR2 = 0.0657
Absolute structure parameter	0.00(6)
Largest diff. peak and hole	0.244 and -0.175 e.Å^{-3}

Table 2.2 Bond lengths [Å] and angles [°] for 2-[(diphenylphosphinoyl)methyl]-4,5-dihydro-oxazole, 19

P-O(1)	1.4865(8)
P-C(11)	1.7989(10)
P-C(5)	1.8042(11)
P-C(4)	1.8226(12)
O(2)-C(3)	1.3443(15)
O(2)-C(1)	1.4483(17)
N-C(3)	1.2528(17)
N-C(2)	1.475(2)
C(1)-C(2)	1.514(2)
C(3)-C(4)	1.4894(16)
C(5)-C(10)	1.3923(15)
C(5)-C(6)	1.3933(15)
C(6)-C(7)	1.3839(17)

C(7)-C(8)	1.374(2)
C(8)-C(9)	1.379(2)
C(9)-C(10)	1.3867(18)
C(11)-C(16)	1.3904(15)
C(11)-C(12)	1.3911(14)
C(12)-C(13)	1.3916(15)
C(13)-C(14)	1.3815(17)
C(14)-C(15)	1.3842(17)
C(15)-C(16)	1.3862(16)
O(1)-P-C(11)	112.42(5)
O(1)-P-C(5)	112.26(5)
C(11)-P-C(5)	107.99(5)
O(1)-P-C(4)	114.09(5)
C(11)-P-C(4)	107.29(5)
C(5)-P-C(4)	102.10(5)
C(3)-O(2)-C(1)	106.23(11)
C(3)-N-C(2)	106.57(13)
O(2)-C(1)-C(2)	103.65(12)
N-C(2)-C(1)	104.73(12)
N-C(3)-O(2)	118.61(12)
N-C(3)-C(4)	126.02(12)
O(2)-C(3)-C(4)	115.32(11)
C(3)-C(4)-P	115.78(9)

C(10)-C(5)-C(6)	119.50(10)
C(10)-C(5)-P	122.55(9)
C(6)-C(5)-P	117.89(8)
C(7)-C(6)-C(5)	120.11(11)
C(8)-C(7)-C(6)	120.28(12)
C(7)-C(8)-C(9)	119.93(13)
C(8)-C(9)-C(10)	120.74(13)
C(9)-C(10)-C(5)	119.43(12)
C(16)-C(11)-C(12)	119.20(9)
C(16)-C(11)-P	123.06(8)
C(12)-C(11)-P	117.74(8)
C(11)-C(12)-C(13)	120.45(10)
C(14)-C(13)-C(12)	120.12(10)
C(13)-C(14)-C(15)	119.39(10)
C(14)-C(15)-C(16)	120.93(11)
C(15)-C(16)-C(11)	119.86(10)

2.3.3 Coordination Chemistry

Preparation of Complexes

Scheme 6: Complex 20
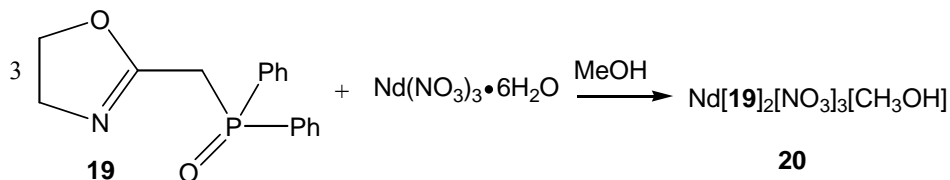
Neodymium nitrate hexahydrate (0.26 g, 0.58 mmol, 1 eq.) was dissolved in methanol (2 ml) and the ligand 2-[(diphenyl-phosphinoyl)methyl]-4,5-dihydro-oxazole (0.50 g, 1.7 mmol, 3 eq.) was dissolved in methanol (5 ml). The two were mixed together and stirred for 10 min. to give a white precipitate. The reaction mixture was further stirred for 1 h. The white solid was recovered by filtration, washed with cold methanol and left to dry on filter paper overnight. The mass of solid was 0.44 g (54% yield assuming the composition shown above): mp 145-147 ^{o}C. An infrared spectrum of **20** in KBr is shown in Figure 2.16 and it is overlaid with a spectrum of the free ligand **19** in Figure 2.17. Two diagnostic vibrations appear at 1646 cm^{-1} ($\nu_{C=N}$) and 1160 cm^{-1} ($\nu_{P=O}$) and these are shifted down-frequency from the corresponding vibrations in the free ligand: $\Delta\nu_{C=N}$ =12 cm^{-1}; $\Delta\nu_{P=O}$ =28 cm^{-1}.

Figure 2.16 Infrared spectrum (KBr, cm^{-1}) for Nd(19)$_2$(NO$_3$)$_3$[MeOH], 20
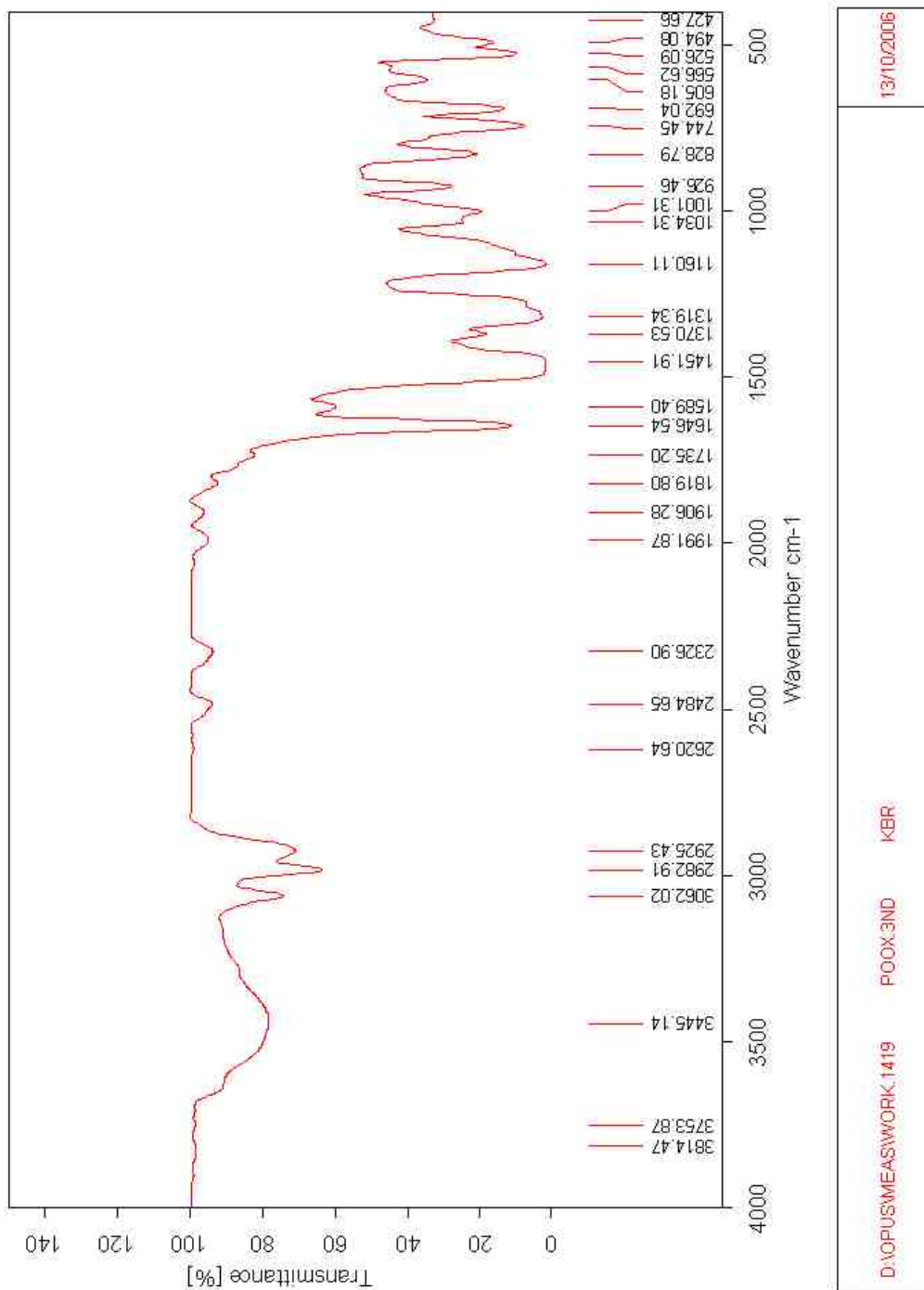
Figure 2.17 Infrared spectrum (KBr, cm^{-1}) for 2-[(diphenylphosphinoyl)methyl]-4,5-dihydro-oxazole, 19 superimposed with Nd(19)$_2$(NO$_3$)$_3$[MeOH]complex, 20
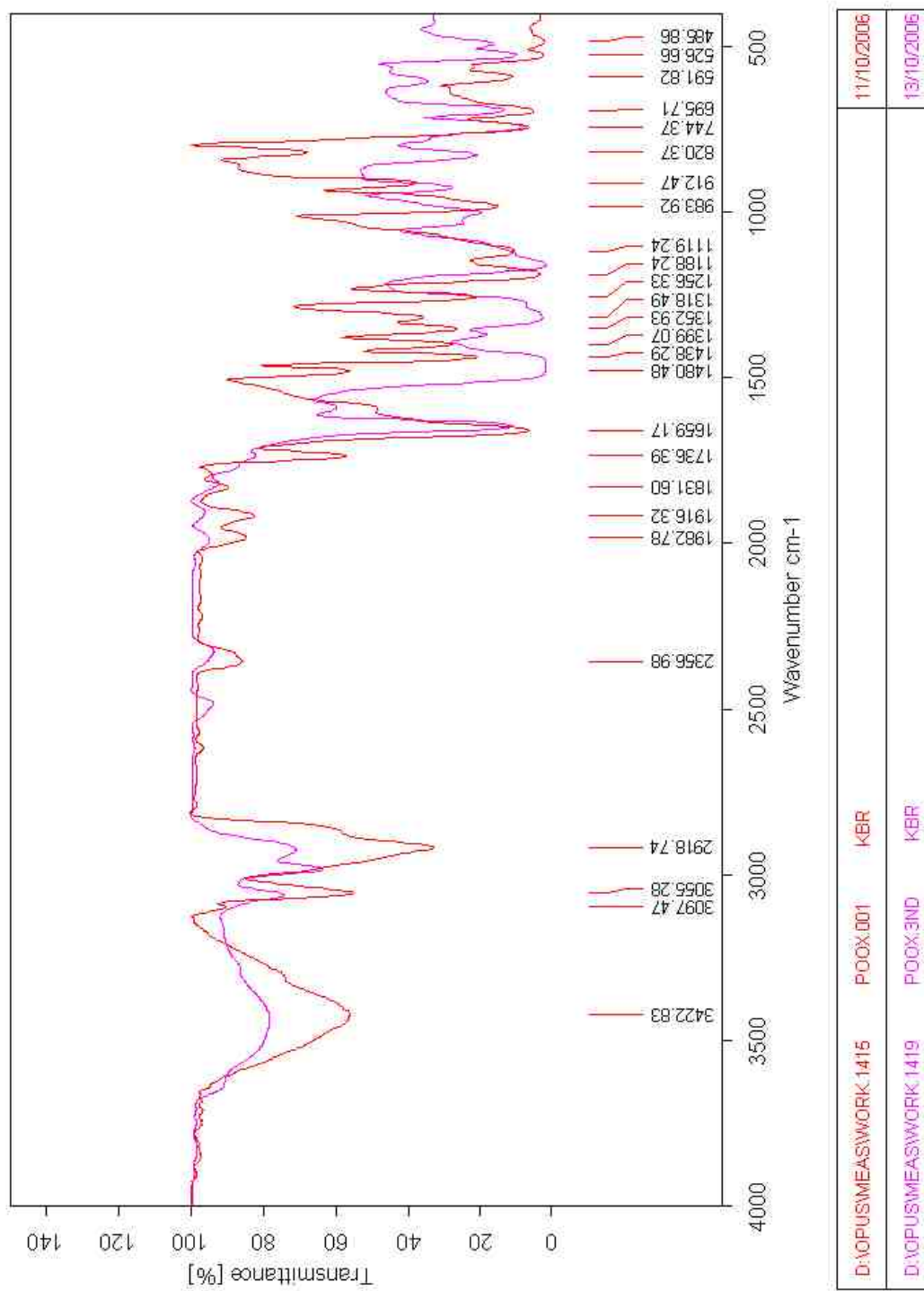
The complex was recrystallized by dissolving the white powder in hot methanol. This solution was left covered in a test tube at room temperature. After 2 h, colorless needles formed at the bottom of the test tube, methanol was decanted, crystals were washed (2 x 10 ml) using cold methanol and dried by blowing with nitrogen overnight. Colorless crystals of suitable quality for X-ray crystallographic analysis were obtained.

Elemental Analysis

Calculated $C_{33}H_{36}N_2$ Nd $O_{14}P_2$ C, 42.49; H, 3.89; N, 7.51; Nd, 15.46; P, 6.64.

Found   C, 42.32; H, 3.73; N, 7.47; Nd, 15.60; P, 6.27.

An X-ray crystal structure determination was completed and selected crystal parameters are summarized in Table 2.3. A view of the molecule is shown in Figure 2.18 and selected bond lengths are summarized in Table 2.4.

Figure 2.18 Molecular structure and atom labeling scheme for a single molecular unit of Nd(19)$_2$(NO$_3$)$_3$[MeOH], 20
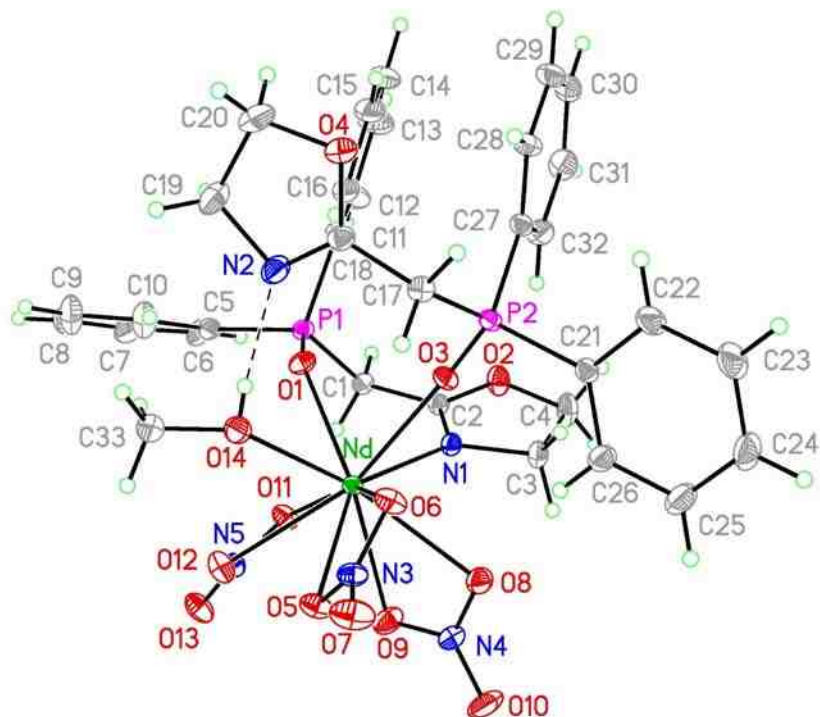
In an attempt to remove MeOH and produce a different type of coordination condition, the complex was redissolved in CH$_3$CN at room temperature, the resulting solution concentrated under vacuum and left to dry for 3 days. A white powder was formed, which was recrystallized by dissolving in CH$_3$CN and left to evaporate slowly at room temperature. After 5 days, colorless crystals formed. An X-ray crystal structure determination was completed and selected crystal parameters are presented in Table 2.3.

A view of the molecule is shown in Figure 2.19 and selected bond lengths are summarized in Table 2.4.

Figure 2.19 Molecular structure and atom labeling scheme for single molecular unit of Nd(19)$_2$(NO$_3$)$_3$, 21
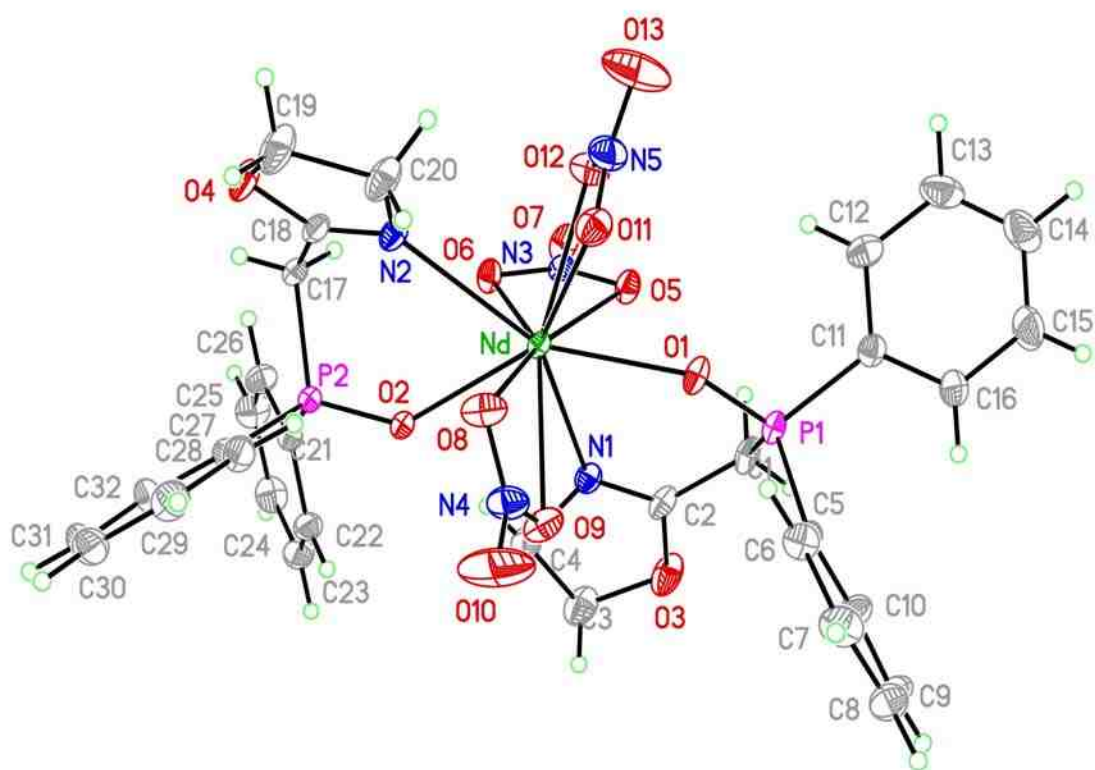
Table 2.3 Selected crystal parameters for Nd(19)$_2$(NO$_3$)$_3$[MeOH] and Nd(19)$_2$(NO$_3$)$_3$

Formula	Nd(19)$_2$(NO$_3$)$_3$[MeOH], 20	Nd(19)$_2$(NO$_3$)$_3$, 21
Formula Weight	932.85	900.81
Space Group	P2(1)/n	P-1
a, Å	16.0073(9)	12.1596(4)
B, Å	12.3024(7)	13.5689(4)
C, Å	19.1969(11)	13.8678(5)
α, deg.	90	63.3260(14)
β, deg.	97.846(2)	76.1590(14)
γ, deg.	90	64.0920(12)
Volume, Å^3	3745.0(4)	1836.44(10)
Z	4	2
Density, Mg/cm^3	1.654	1.629
T, K	223(2)	228(2)
R1^a [I>2δ(I)]	0.0175	0.0203
WR2^b [I>2δ(I)]	0.0435	0.0492

Table 2.4 Selected bond distances for Nd(19)$_2$(NO$_3$)$_3$[MeOH] and Nd(19)$_2$(NO$_3$)$_3$

Nd(19)$_2$(NO$_3$)$_3$[MeOH], 20		Nd(19)$_2$(NO$_3$)$_3$, 21	
Nd-O(3)	2.4136(9)	Nd-O(1)	2.3803(9)
Nd-O(1)	2.4274(9)	Nd-O(2)	2.4189(9)
Nd-O(14)	2.4466(11)	Nd-O(8)	2.5015(11)
Nd-O(9)	2.5492(11)	Nd-O(12)	2.5254(12)
Nd-O(8)	2.5702(10)	Nd-O(5)	2.5533(10)
Nd-O(5)	2.6034(10)	Nd-O(11)	2.5985(12)
Nd-O(12)	2.6055(11)	Nd-O(9)	2.6190(11)
Nd-O(6)	2.6263(11)	Nd-N(1)	2.6601(11)
Nd-O(11)	2.6493(10)	Nd-N(2)	2.6913(11)
Nd-N(1)	2.6554(11)	Nd-O(6)	2.7029(10)
P(1)-O(1)	1.4967(10)	P(1)-O(1)	1.4963(10)
P(1)-C(5)	1.7925(14)	P(1)-C(5)	1.7853(13)
P(1)-C(11)	1.7929(15)	P(1)-C(11)	1.7960(15)
P(1)-C(1)	1.8111(14)	P(1)-C(1)	1.7992(14)
O(2)-C(2)	1.3474(16)	P(2)-O(2)	1.5015(9)
O(2)-C(4)	1.4601(19)	P(2)-C(21)	1.7875(14)
N(1)-C(2)	1.2707(17)	P(2)-C(27)	1.7920(13)
N(1)-C(3)	1.4837(16)	P(2)-C(17)	1.8119(13)
C(1)-C(2)	1.4907(18)	N(1)-C(2)	1.2748(17)
C(1)-H(1A)	0.9800	N(1)-C(4)	1.476(2)
C(1)-H(1B)	0.9800	N(2)-C(18)	1.2740(17)

C(3)-C(4)	1.529(2)	N(2)-C(20)	1.4818(19)
C(3)-H(3A)	0.9800	O(3)-C(2)	1.3370(17)
C(3)-H(3B)	0.9800	O(3)-C(3)	1.455(3)
C(4)-H(4A)	0.9800	O(4)-C(18)	1.3443(16)
C(4)-H(4B)	0.9800	O(4)-C(19)	1.457(2)
C(5)-C(6)	1.385(2)	C(1)-C(2)	1.489(2)
C(5)-C(10)	1.393(2)	C(1)-H(1A)	0.99(2)
C(6)-C(7)	1.390(2)	C(1)-H(1B)	0.91(2)
C(6)-H(6)	0.9400	C(3)-C(4)	1.515(2)
C(7)-C(8)	1.374(3)	C(3)-H(3A)	0.88(3)
C(7)-H(7)	0.9400	C(3)-H(3B)	0.90(3)
C(8)-C(9)	1.377(3)	C(4)-H(4A)	1.00(2)
C(8)-H(8)	0.9400	C(4)-H(4B)	0.93(2)

2.4 RESULTS AND DISCUSSION

The target ligand **19** was prepared in two steps as described in Scheme 5.
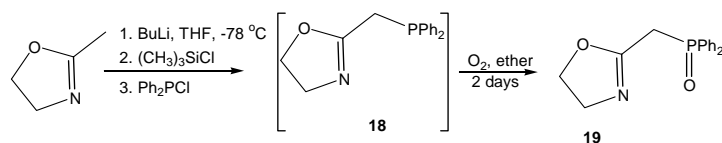
Although the synthesis for **18** has been described by Braunstein and co-workers,[59] the procedure, as outlined, was not reproducible in our laboratory. The Braunstein[59] workup involved removing the solvent, under reduced pressure, to give a yellow residue, which was triturated with hexane (2 x 10 ml) and Et_2O (2 x 20 ml) to remove residual THF and $(CH_3)_3SiCl$. The resulting yellow powder was then triturated with toluene (3 x 60 ml). The solution was filtered over Celite and a pale yellow solid was obtained after evaporation of toluene in vacuum. Finally, the product was crystallized from ethanol at -28 °C.[59]

In the current study, it was observed that the product **18** was slightly soluble in hexane, ether and toluene, but none of these solvents provided an effective extraction. Attempts to crystallize the yellow oil from ethanol were not successful. It was also discovered that product **18** is air sensitive and the compound is easily oxidized to **19** when left exposed to air. Therefore, an alternative workup was developed. The initial step was to synthesize compound **18** as described in the literature.[59] The workup was done by vacuum evaporation of the THF, followed by extraction of the residue using CH_2Cl_2 (100 ml). Vacuum evaporation of CH_2Cl_2 gave a pale yellow oil.

The high resolution mass spectrum (HRMS) for **18** shows an intense peak corresponding to [M+H$^+$] ion at *m/e* 270.1058 which is consistent with the proposed structure. No literature report of mass spectra data is available.

A singlet at -16.9 ppm is seen in the $^{31}P\{^1H\}$ 101.3 MHz, NMR spectrum which is shifted slightly downfield from the literature[59] value, which is -17.3 (s) for $^{31}P\{^1H\}$ (121.5 MHz, $CDCl_3$). The ^{31}P NMR spectrum also shows the presence of several minor impurities that were not identified.
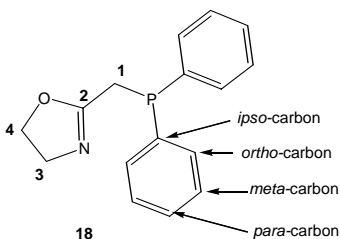
The ^1H NMR spectrum for **18** displays a singlet at 3.0 ppm that is assigned to the methylene protons on C_1. The literature value is 3.05 ppm.[59] The methylene protons at C_3 and C_4 are assigned to triplets at 3.6 and 3.9 ppm with coupling constants of $^3J_{H-H} = 9.2$ Hz and 9.5 Hz, respectively. The literature describes triplet resonances at 3.75 ppm and 4.15 ppm with $^3J_{H-H} = 9.4$ Hz in both cases. Resonances observed in the range 7.2 -7.4 ppm are assigned to aromatic protons, and these compare against values reported in the literature[59] in the range 7.2 -7.5 ppm.

A pure sample of compound **18** was not obtained in the current study due to its affinity with oxygen and other uncharacterized side products formed during the formation of compound **18** as shown in both ^1H NMR and $^{31}P\{^1H\}$ NMR spectra (Figure 2.5 and 2.6).

The oxidation of **18** was best accomplished by dissolving it in Et_2O and bubbling oxygen into the solution for two days. Purification of the crude product, **19,** was done as described in the experimental section, and it was crystallized from hot ethyl acetate.

Difficulties were encountered obtaining analytically pure samples of **19** and satisfactory CHN analyses were never obtained. By this method the yield was 58%.

Oxidation of **18** using H_2O_2/CH_3COOH and oxone led to disruption of the heterocyclic ring. An IR spectrum for this product shows the absence of a C=N band. In the course of this study, it was also found that the oxazoline ring is unstable in 1M HCl. Oxidation of **18** dissolved in CH_2Cl_2 by sparging with oxygen gas gave a low yield perhaps due to low solubility of oxygen in CH_2Cl_2. The yield of **19** by these approaches was 7-30%.

19
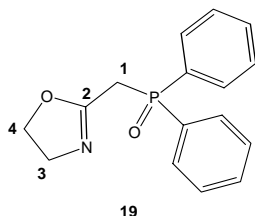
The formation of **19** has not been previously reported. The compound was isolated as a solid that provided analytical data. The elemental analysis for compound **19** shows a close correlation to the proposed structure suggesting a minor impurity. The mass spectrum showed an intense peak for $[M+H^+]$ at 286.0988 *m/e* which is consistent with the composition of compound **19**. In the IR spectrum two bands are diagnostic of the structure: $\nu_{P=O} = 1188$ cm^{-1} and $\nu_{C=N} = 1659$ cm^{-1}. The latter is essentially identical to the frequency in **18**: $\nu_{C=N} = 1660$ cm^{-1} reported in the literature.[59] These absorptions are similar to $\nu_{C=N}$ in several other molecules.[59, 69-73] The absorption band for P=O in compound **19** falls in the same range as $\nu_{P=O}$ bands seen in NOPO, NOPOPO and other ligands developed in our group. (Table 2.5).[47, 52-55, 67, 68]

A singlet at 28.1 ppm is seen in the $^{31}P\{^1H\}$ NMR spectrum for **19** which is shifted slightly upfield, from the resonance for NOPOPO at 31.3 ppm, and significantly downfield from the phosphine **18**.

Table 2.5 Comparative spectroscopic data for similar compounds containing P=O functional group[47, 55, 68]

Type of ligand	IR (cm^{-1}) P=O	^{1}H NMR for –CH$_2$- (ppm)	$^2J_{\text{H-P}}$ (Hz)	^{13}C NMR for –CH$_2$- (ppm)	$^1J_{\text{C-P}}$ (Hz)	^{31}P NMR (ppm)
NPO	1184	3.8	14.2	40.7	64.0	30.2
NOPO	1186	4.2	14.0	30.7	66.0	31.7
NPOPO	1195	3.7	14.0	41.4	65.2	34.0
NOPOPO	1195	4.1	13.8	31.4	67.0	31.3

NPO   NOPO

NPOPO   NOPOPO
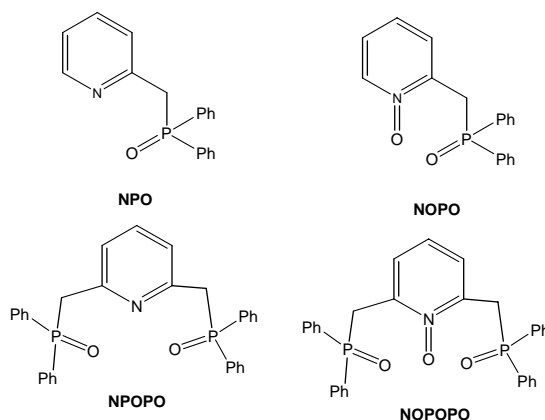
The ^{1}H NMR spectrum for compound **19** is consistent with the proposed structure. The resonance assigned to –CH$_2$P(O) appears as a doublet at 3.4 ppm with $^2J_{\text{P-H}}$ = 14.6 Hz. This can be compared with the value for the same structural feature in NOPOPO: 4.1 ppm, $^2J_{\text{P-H}}$ = 13.8 Hz. The methylene protons at C$_3$ and C$_4$ are assigned as triplets at 3.7 and 4.1 ppm respectively with coupling constants of $^3J_{\text{H-H}}$ = 9.4 Hz and 9.1 Hz. These data can be compared to data for compound **18** where C$_3$ and C$_4$ methylene protons appear as triplets at 3.6 ppm and 3.9 ppm respectively, with $^3J_{\text{H-H}}$ = 9.2 Hz and $^3J_{\text{H-H}}$ = 9.5 Hz. However, the C$_3$ proton triplet is also split into doublets as a result of

coupling with the ^{31}P nucleus. A ^{1}H NMR experiment, done with ^{31}P decoupling, confirmed that the C_3 and C_4 methylene protons appear as triplets. In addition, the C_1 protons appear as a singlet instead of a doublet (Figure 2.12). It is also noted that the triplet intensities for protons on C_3 and C_4 (Figure 2.14) are not the expected 1:2:1. That is the outer peaks in the triplets do not have equal heights. This is attributed to magnetic inequivalence leading to second order coupling.[76] A summary of ^{1}H NMR data is provided in Table 2.6. Resonances observed between 7.4 -7.8 ppm are assigned to aromatic protons.

Table 2.6 ^{1}H NMR for compound 19 with ^{31}P coupling and without coupling

^{1}H NMR WITH ^{31}P COUPLING			^{1}H NMR WITH ^{31}P DECOUPLING		
Position of the hydrogen on	Chemical shifts δ(ppm)	J (Hz)	Chemical shifts δ(ppm)	$^3J_{H-H}$ (Hz)	J_{H-P} (Hz)
C_3	3.7, triplet of doublets	$^5J_{H-P} = 3.6$ $^3J_{H-H} = 9.4$	3.7, triplet	9.5	-
C_4	4.0, triplet	$^3J_{H-H} = 9.5$	4.0, triplet	9.5	-
C_1	3.4, doublet	$^2J_{H-P} = 14.6$	3.4, singlet	-	-

The carbons common to both **NOPOPO** and **19** all appear at similar chemical shift ranges. For example, the C_1 resonance in the ^{13}C{^{1}H} NMR spectrum appears at 32.5 ppm for **19**. The corresponding resonance in NOPOPO appears at 31.4 ppm. Each is a doublet resulting from coupling to adjacent phosphorus with $^1J_{C-P} = 64.2$ Hz in **19** and 67 Hz in NOPOPO. The ^{13}C{^{1}H} NMR spectrum shows resonances at 54.8 ppm and 68.2 ppm for C_3 and C_4 compared to 54.7 ppm and 67.6 ppm in **18** reported in the literature.[59]

The aromatic carbons show $^{13}C\{^1H\}$ resonances between 128.9-132.5 ppm. As the case reported[59] with compound **18**, splitting of aromatic carbons was observed in compound **19** due to coupling with ^{31}P nucleus (Figure 2.9). This data is summarized in Table 2.7 and are compared to literature[59] data for **18**.

Table 2.7 Chemical shifts and coupling constants of aromatic carbons for compound 19 compared to 18

Compound 18	Compound 19
128.5 ppm, (doublet), *ortho*-carbon, $^2J_{C-P} =$ 7.0 Hz	128.9 ppm, (doublet), *ortho*-carbon, $^2J_{C-P} =$ 12.2 Hz
132.7 ppm, (doublet), *meta*-carbon, $^3J_{C-P} =$ 19.7 Hz	131.5 ppm, (doublet), *meta*-carbon, $^3J_{C-P} =$ 9.7 Hz
137.7 ppm, (doublet), *ipso*-carbon, $^1J_{C-P} =$ 14.1 Hz	132.4 ppm, (doublet), *ipso*-carbon, $^1J_{C-P} =$ 100.9 Hz

The $^{13}C\{^1H\}$ NMR data for compound **19** are not comparable to **18.** This indicates that the oxidation of compound **18** to **19** significantly alters the electron distribution within the molecule. However, the $^{13}C\{^1H\}$ NMR data for **19** are comparable to other arylphosphine oxide compounds previously reported in the literature.[77] For example the resonance 132.4 ppm (doublet) with $^1J_{C-P} = 100.9$ Hz assigned to *ipso*-carbon in **19** is comparable to similar resonance for (4-aminophenyl)diphenylphosphine oxide **(4ADPO)** that appears at 133.39 (doublet) with $^1J_{C-P} = 103.9$ Hz assigned to *ipso*-carbon. Resonances at 128.9 ppm and 131.5 ppm (doublets) with $^2J_{C-P} = 12.2$ Hz and $^3J_{C-P} = 9.7$ Hz assigned to *ortho* and *meta*-carbons in **19** falls in the same range when compared to

similar resonances in **4ADPO** that appear in the range of 128.30-133.77 ppm as doublets

with J_{C-P} in the range of 9.8-11.6 Hz.[77]
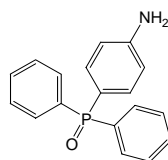
4ADPO

The resonance appears at 131.5 ppm, (doublet), J_{C-P} = 2.5 Hz for **19** presumably is the

long range coupling of *para*-carbon. The resonance for C_2 appears at 161.4 ppm as a

doublet with $^2J_{C-P}$ = 7.4 Hz. This compares with the reported[59] data for **18**: 165.4 ppm;

$^2J_{P-C}$ = 7.0 Hz.

Compound **19** was crystallized from hot ethyl acetate solution. The crystal and

molecular structure of **19** was determined by single crystal X-ray diffraction methods

(Figure 2.15). Table 2.1 shows crystal parameters for the structure and bond lengths and

angles are displayed on Table 2.2. Selected bond lengths P-O(1), 1.4865(8)Å, N-C(3),

1.2528(17)Å, and O(2)-C(3), 1.3443(15)Å are comparable to similar bond lengths

observed in benzoxazole ligand **25a** described in Chapter 3 with P=O, 1.4831(8)Å, O-C,

1.3571(14)Å, and C=N, 1.2925(15)Å. However, the C=N bond length for benzoxazole

ligand **25a** is longer than in compound **19**. This may be attributed by the aromatic nature

of compound **25a**.
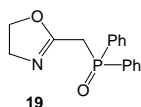
19

Oxazoline
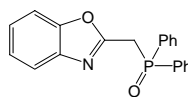
25a

Benzoxazole

The crystal structure of **19** shows that the torsion angle between the plane bonded to P=O

and N donor atoms is 71.6° indicating that the P=O and N are not oriented in the same

direction that signifies the coordination with Ln(III) may not be thermodynamically favored. In addition the intermolecular hydrogen bonding appears between C-H--O (Figure 2.20).

Figure 2.20 Intermolecular hydrogen bonding in compound 19
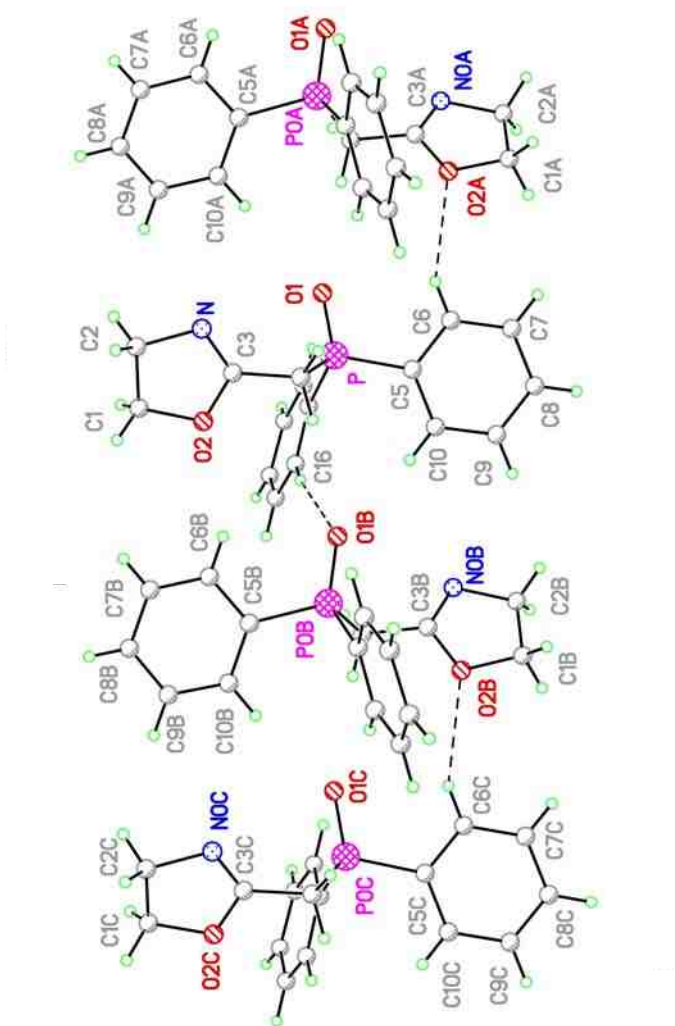
Alternative methods for synthesis of compound **19** were also examined.
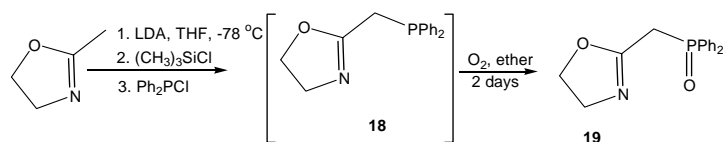
Adapting a method developed by Minami *et al.*, [74] using LDA prepared in *situ* from the combination of BuLi and diisopropyl amine,[74] the phosphine precursor compound **18** was formed. The crude phosphine was purified by column chromatography: silica gel 70-230 mesh, 60Å, eluted with 100% CH_2Cl_2, followed by 2.5–5% $MeOH/CH_2Cl_2$ to give the product as a pale yellow oil. Yield: 7.3 g (89%). However, both ^{1}H NMR and mass spectra analyses reveal the presence of the phosphine oxide **19** in addition to the phosphine **18** in the reaction mixture. Other uncharacterized products were also formed. The oxidation of this mixture by bubbling oxygen in ether solution for 2 days gave compound **19.** Purification of the crude product mixture gave pure **19,** 4.1 g (47.5% yield) based on the starting material, 2-methyl-2-oxazoline. The low yield may be attributed to the side products formed before and after oxidation. Previous work has shown that oxidation of phosphines by exposure to oxygen often leads to the formation of side products.[75] In this study such byproducts were not characterized. It is also pointed out that when Braunstein[59] attempted this reaction using LDA with different ratios without $(CH_3)_3SiCl$, he obtained the following results.
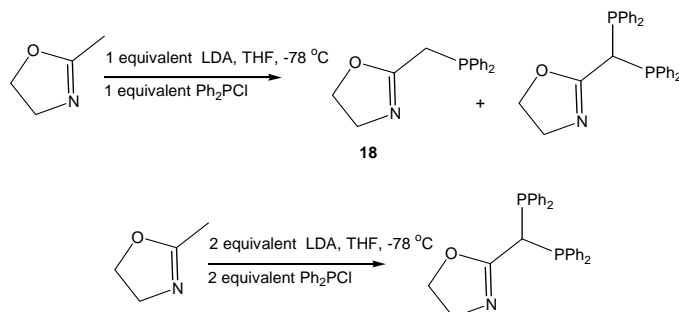
Braunstein claimed that $(CH_3)_3SiCl$ forms an N-silyl derivative with the oxazoline ring and steric hindrance prevents double substitution at the methylene position. Direct synthesis of **19,** using diphenylphosphinic chloride, $Ph_2P(O)Cl$, as shown below, was unsuccessful. Instead of forming compound **19**, other compounds that remain uncharacterized were formed.
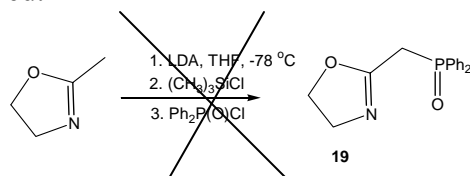
Coordination chemistry with **19** was attempted with $La(NO_3)_3 \bullet 6H_2O$, $Nd(NO_3)_3 \bullet 6H_2O$, $Er(NO_3)_3 \bullet 5H_2O$ and $La(OTf)_3 \bullet H_2O$. Only Nd(III) gave suitable crystals for single crystal X-ray crystallography. The others formed complexes but they were oils and powders that could not be crystallized. The Nd(III) complex was crystallized from hot MeOH to give colorless crystals. This complex was formed using 3:1 ligand to metal stoichiometry with an overall composition of $Nd(\mathbf{19})_2(NO_3)_3[MeOH]$. A single molecular unit of $Nd(\mathbf{19})_2(NO_3)_3[MeOH]$ is shown in Figure 2.18. The crystal structure shows one Nd atom bonded to two ligands both through P=O and one with an Nd-N bond, three nitrate ions each bonded through two oxygen atoms and one MeOH bonded through the oxygen atom. The terminal methyl group of the alcohol is disordered. The alcohol H is hydrogen bonded to the nitrogen of the monodentate ligand, which is bonded to Nd only through the P=O oxygen atom.

An attempt was made to remove the MeOH coordinated to Nd. Recrystallization was repeated from CH_3CN which gave colorless crystals. X-ray crystallographic analysis showed that both ligands bind in a bidentate chelating mode via one P=O and the nitrogen donor. The crystal structure of the complex shows that the torsion angle between

the plane bonded to P=O and N donor atoms in both ligands is 48.7° and 58.4°
respectively. When this data is compared to the torsion angle of the free ligand that is
71.6° indicates that in order to form complex a certain amount of energy must be applied
to reduce the angle between the P=O and N. The structure is shown in Figure 2.19. Table
2.8 shows selected bond distances for the two complexes for comparison.

Table 2.8 Comparison of bond distances between $Nd(19)_2(NO_3)_3[MeOH]$ and $Nd(19)_2(NO_3)_3$

Bonds	$Nd(19)_2(NO_3)_3[MeOH]$, 20	$Nd(19)_2(NO_3)_3$, 21
Nd-O(1)	2.4274(9)	2.3803(9)
Nd-O(2)	2.4136(9)	2.4189(9)
Nd-N(1)	2.6554(11)	2.6601(11)
Nd-N(2)	No coordination	2.6913(11)
P(1)-O(1)	1.4967(10)	1.4963(10)
P(2)-O(2)	1.4968(10)	1.5015(9)
N(1)-C(2)	1.2707(17)	1.2748(17)
N(2)-C(18)	1.4837(16)	1.476(2)

Comparison of these bond distances suggests that the coordination of one of the ligands
in complex **21** is more strongly bonded than the second ligand.

In complex **20** there are ten close contacts to central Nd atom (Figure 2.21). These
can be considered to form a distorted anti-prism which is capped on both square faces.
The square faces are formed by N1-O1-O12-O9, capped by O11 and O3-O8-O5-O14,
capped by O6.

Figure 2.21 Coordination polyhedron about Nd-bic-apped distorted square ant-prism for complex Nd(19)₂(NO₃)₃[MeOH], 20
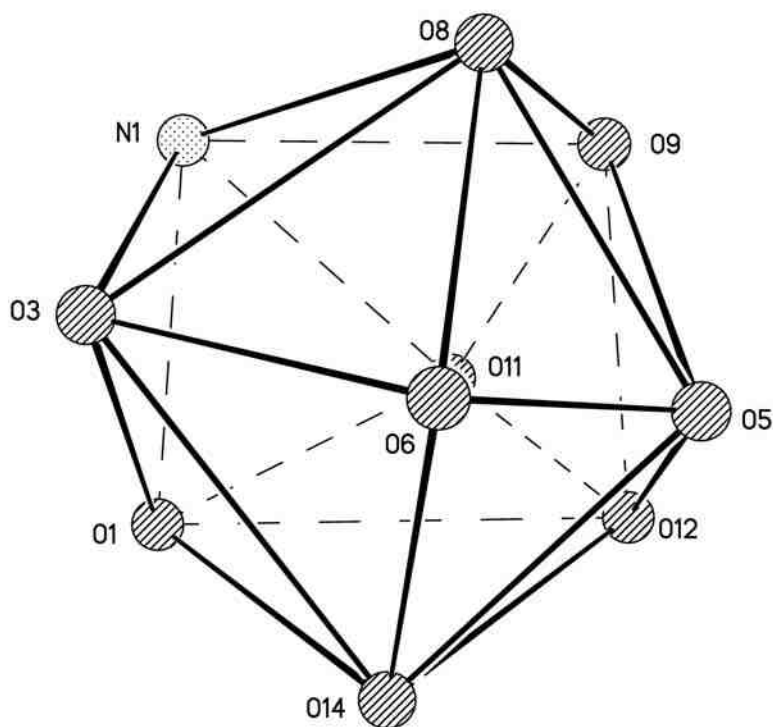
The Nd inner coordination sphere in complex **21** consists of 10 atoms: N1, N2, O1, O2, and the 3 bidentate nitrate groups through O5, O6, O8, O9, O11 and O12. This 10 vertex polyhedron looks like a sphenocorona, with two trapezo ideal faces and 12 triangular faces. The coordination number of Nd(III) is ten, (Figure 2.22 and 2.23)

Figure 2.22 Inner sphere coordination polyhedron for complex Nd(19)$_2$(NO$_3$)$_3$, 21 indicating coordination polyhedron of 10 vertices
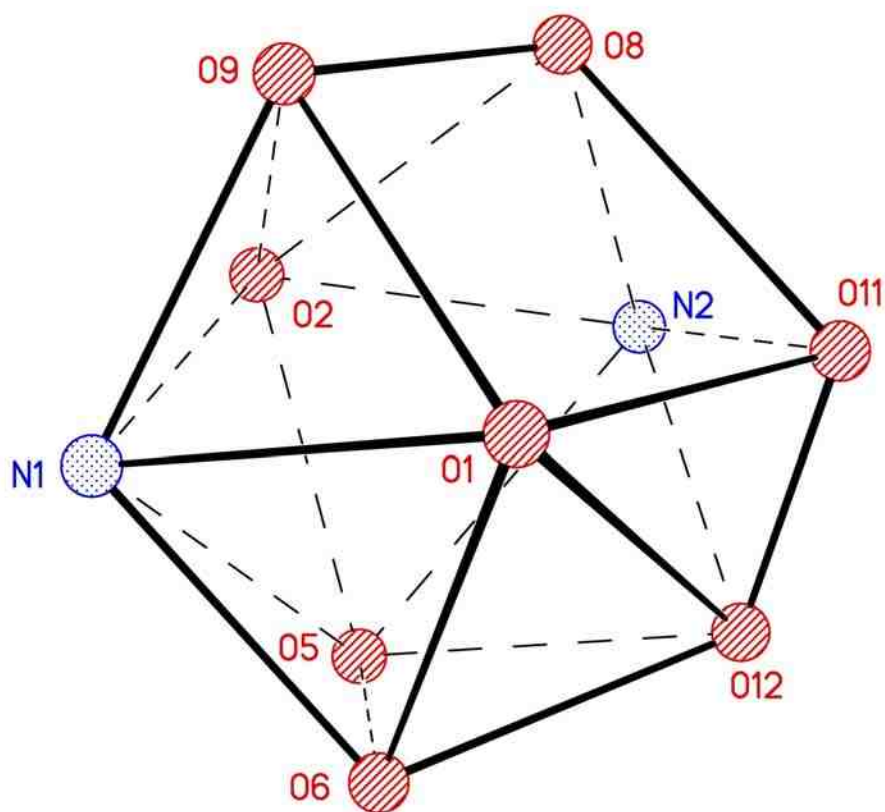
Figure 2.23 Inner sphere coordination polyhedron for complex Nd(19)$_2$(NO$_3$)$_3$, 21

The same as Figure 2.22 but with link O1—O12 omitted. Two trapezoidal faces make angle of 108 degrees, the expected angle is 102 degrees.
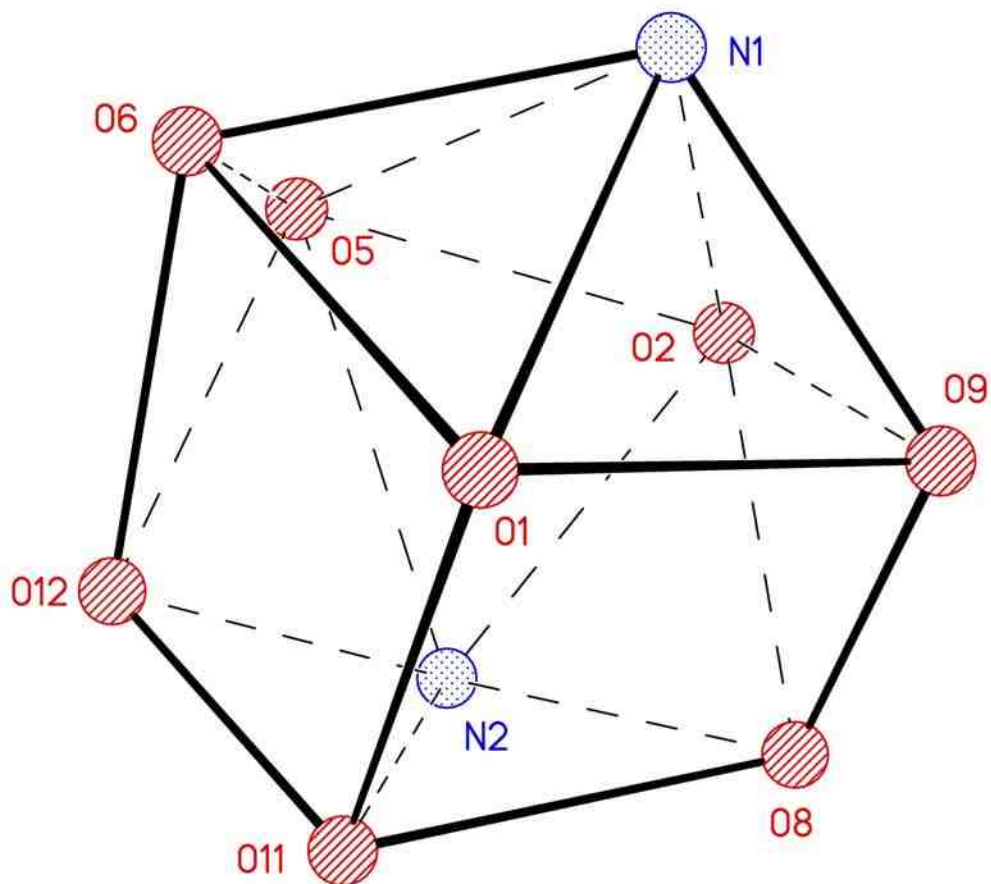
The three nitrate ions are coordinated to the central metal Nd(III) in an asymmetric bidentate fashion.

2.5 CONCLUSION

In this chapter, a synthesis of the trifunctional ligand **19** was developed, and the new molecule was fully characterized including the crystal structure. The objective in this study was to synthesize an oxazoline-based ligand related to the already developed[52-55] NOPO and NOPOPO ligands.[47, 68] The relationship being mainly based on the relatively softer donor nitrogen and a hardened P=O functionality. Three approaches were used in the synthesis of the target molecule, **19**. However, it was observed that, a two step synthesis using BuLi, $(CH_3)_3SiCl$ and Ph_2PCl gave the best yield (58%).

A crystal structure determination confirmed that the ligand can act as a bidentate chelate via nitrogen and P=O donor groups with $Nd(NO_3)_3$. Similarly it was shown that, the oxygen donor within the oxazoline ring is not used to form the chelate interaction with Nd(III).

It appears that when methanol is used as a solvent during coordination and crystallization of this complex, there is a competition between the oxygen from methanol and nitrogen donor from the ligand which prevents bidentate chelation on one ligand as shown in Figure 2.18. Nevertheless, the structure of this complex is stabilized by the hydrogen bonding between the O-H------N from the methanol and nitrogen from the ligand.

It was observed that the oxazoline-based ligand, is not stable in acidic medium and this makes **19** unsuitable for practical separation applications that require extractant stability in contact with 1-6 M HNO_3.[15-17] This led us to seek analogues of this compound having structural modifications which would convey stability in mineral acids i.e., the development of the benzoxazole ligands described in Chapter 3.

2.6 REFERENCES

1.   Hancock, R. D. *Prog. Inorg. Chem.* **1989**, *37*, 187 and references therein.

2.   Hay, B. P. *Coord. Chem. Rev.* **1993**, *126*, 177 and references therein.

3.   Hay, B. P.; Hancock, R. D. *Coord. Chem. Rev.* **2001**, *212*, 61 and references therein.

4.   Hay, B. P.; Firman, T. K. *Inorg. Chem.* **2002**, *41*, 5502 and references therein.

5.   Hay, B. P.; Dixon, D. A.; Vargas, R.; Garza, J.; Raymond, K. N. *Inorg. Chem.* **2001**, *40*, 3922.

6.   Hay, B. P.; Firman, T. K. *Inorg. Chem.* **2002**, *41*, 5502.

7.   Hay, B. P.; Firman, T. K.; Lumetta, G. J.; Rapko, B. M.; Garza, P. A.; Sinkov, S. I.; Hutchinson, J. E.; Parks, B.W.; Gilbertson, R. D.; Weakley, T. J. R. *J. Alloys and Compounds* **2004**, *374*, 416.

8.   Cohen, S. M.; Xu, J. D.; Radkov, E.; Raymond, K. N.; Botta, M.; Barge, A.; Aime, S. *Inorg. Chem.* **2000**, *39*, 5747; Johnson, A. R.; O'Sullivan, B.; Raymond, K. N. *Inorg. Chem.* **2000**, *39*, 2652; Sunderland, C. J.; Botta, M.; Aime, S.; Raymond, K. N. *Inorg. Chem.* **2001**, *40*, 6746; Hajela, S.; Botta, M.; Giraudo, S.; Xu, J. D.; Raymond, K. N.; Aime, S. *J. Am. Chem. Soc.* **2000**, *122*, 11228.

9.   Romanovski, V.V.; White, D. J.; Xu, J. D.; Hoffman, D. C.; Raymond, K. N. *Solv. Extr. Ion Exch.* **1999**, *17*, 55; Zhao, P. H.; Romanovski, V. V.; Whisenhunt, D.W.; Hoffman, D. C.; Mohs, T. R.; Xu, J. D.; Raymond, K. N. *Solv. Extr. Ion Exch.* **1999**, *17*, 1327; Xu, J.D.; Raymond, K.N. *Inorg. Chem.***1999**, *38*, 308; Xu, J. D.; Radkov, E.; Ziegler, M.; Raymond, K. N. *Inorg. Chem.* **2000**, *39*, 4156; Paquet, F.; Montegue, B.; Ansoborlo, E.; HengeNapoli, M. H.; Haupert, P.;

Durben, P. W.; Raymond, K. N. *Int. J. Rad. Biol.* **2000**, *76*, 113; Durben, P. W.; Kullgren, B.; Xu, J.; Raymond, K. N. *Intl. J. Rad. Biol.* **2000**, *76*, 199; Xu, J.; Durbin, P.W.; Kullgren, B.; Ebbe, S. N.; Uhlir,. L. C.; Raymond, K. N. *J. Med. Chem.* **2002**, *45*, 3963.

10. Nash, K. L. "Separation Chemistry for Lanthanides and Trivalent Actinides" in *Handbook on the Physics and Chemistry of Rare Earths'* Gschneidner, K. A.; Eyring, L.; Choppin, G.R.; Lander, G.H.; Elsevier: New York, **1994**, *18*, 197.

11. Mathur, J. N.; Murali, M.S.; Nash, K. L. *Solv. Extr. Ion Exch.* **2001**, *19*, 357 and references therein.

12. Nash, K. L.; Madic, C.; Mathur, J.N. *Actinide Separation Science and Technology* in *The Chemistry of the Actinide and Transactinide Elements*, Springer, Berlin, in Press, Ch 24.

13. Choppin, G. R.; Morgenstern, A. *J. Radioanal. Nucl. Chem.* **2000**, *243*, 45 and references therein.

14. Laidler, J. J.; Burris, L.; Collins, E. D.; Duguid, J.; Henry, R.N.; Hill, J.; Karell, E. J.; McDeavitt, S. M.; Thompson, M.; Williamson, M. A.; Willet, J. L. *Prog. Nucl. Energy* **2001**, *38*, 65.

15. Schulz, W. W.; Horwitz, E. P. *Sep. Sci. Tech.* **1988**, *23*, 1191.

16. Horwitz, E. P.; Chiarizia, R. *In Separation Techniques in Nuclear Waste Management, CRC Press*: New York, **1995**.

17. Horwitz, E. P.; Schultz, W. W. *Solvent Extraction in treatment Of Acidic High Level Liquid Waste, ACS Symposium Series 716*, **1999**.

18. Siddall, T. H. *J. Inorg. Nucl. Chem.* **1963**, *25*, 883.

19.   Siddall, T. H. *J. Inorg. Nucl. Chem.***1964**, *26*, 1991.

20.   Stewart, W. E.; and Siddall, T. H. *J. Inorg. Nucl. Chem.* **1968**, *30*, 1513.

21.   Stewart, W.E.; and Siddall, T.H. *J. Inorg. Nucl. Chem.* **1968**, *30*, 3281.

22.   Good, M. L; and Siddall, T. H. *J. Inorg. Nucl. Chem. Lett.* **1966**, *2*, 337.

23.   Stewart, W. E.; and Siddall, T. H. *J. Inorg. Nucl. Chem.* **1970**, *32*, 3599.

24.   Horwitz, E. P.; Kalina, D.G.; Diamond, H.; Vandegrift, G. F.; Schulz, W. W.
        *Solv. Extr. Ion. Exch.***1985**, *3*, 75.

25.   Horwitz, E. P.; Schulz, W. W.; The TRUEX Process: A Vital Tool for Disposal
        of U.S. Defense Nuclear Waste, New Separation Chemistry for Radioactive
        Waste and Other Specific Applications, Sponsored by the Commission of the
        European Communities and the Italian Commission for Nuclear and Alternative
        Energy Sources, Rome, Italy, May 16-18, **1990**.

26.   Horwitz, E. P.; Chiarizia, R. in *Separation Techniques in Nuclear Waste
        Management*, Carlson, T. E.; Chipman, N. A.; Wai, C. M., Eds., CRC Press, Boca
        Raton, FL, 3, **1993**.

27.   Mathur, J. N.; Murali, M. S.; Natarajan, P. R.; Badheka, L. P.; Aneroid, A.
        Talanta **1992**, *39*, 493.

28.   Nash, K. L.; Rickert, P. G. *Sep. Sci. Technol.* **1993**, *28*, 25.

29.   Mathur, J. N.; Nash, K. L. *Solvent Extr. Ion Exch.* **1998**, *16*, 1341.

30.   Bowen, S. M.; Duesler, E. N.; Paine, R.T.; Campana, C. F. *Inorg. Chim. Acta*
        1982, *59*, 53.

31.   Bowen, S. M.; Duesler, E. N.; Paine, R.T. *Inorg. Chim. Acta* **1982**, *61*, 155.

32.   Bowen, S. M.; Duesler, E. N.; Paine, R. T. *Inorg. Chem.* **1983**, *22*, 286.

33.   Jessup, J. J.; Duesler, E. N.; Paine, R. T. *Inorg. Chim. Acta* **1983**, *73*, 261.

34.   Bowen, S. M.; Duesler, E. N.; Paine, R.T. *Inorg. Chim. Acta* **1984**, *84*, 221.

35.   Bowen, S. M.; McCabe, D. J.; Duesler, E. N.; Paine, R.T. *Inorg. Chem.* **1985**, *24*, 1191.

36.   Caudle, L. J.; Duesler, E. N.; Paine, R. T. *Inorg. Chim. Acta* **1985**, *110*, 91.

37.   Caudle, L.J.; Duesler, E.N.; Paine, R.T. *Inorg. Chem.* **1985**, *24*, 4441.

38.   McCabe, D. J.; Duesler, E. N.; Paine, R.T. *Inorg. Chem.* **1985**, *24*, 4626.

39.   McCabe, D. J.; Bowen, S. M.; Paine, R.T. *Synthesis* **1986**, 320.

40.   McCabe, D.J.; Duesler, E.N.; Paine, R.T. *Inorg. Chem.* **1987**, *26*, 2300.

41.   McCabe, D. J.; Duesler, E. N.; Paine, R.T. *Inorg. Chim. Acta* **1988**, *147*, 265.

42.   McCabe, D. J.; Duesler, E. N.; Paine, R.T. *Inorg. Chem.* **1988**, *27*, 1220.

43.   Bowen, S. M.; Paine, R.T. *Inorg. Syn.* **1986**, *24*, 101.

44.   Conary, G. S.; Duesler, E. N.; Paine, R.T. *Inorg. Chim. Acta* **1988**, *145*, 149.

45.   McCabe, D. J.; Russell, A. A.; Karthikeyan, S.; Paine, R.T.; Ryan, R. R. *Inorg. Chem.* **1987**, *26*, 1230.

46.   Conary, G. S.; Russell, A. A.; Paine, R.T.; Ryan, R. R. *Inorg. Chem.* **1988**, *27*, 3242.

47.   Rapko, B. M.; Duesler, E. N.; Smith, P. H.; Paine, R.T.; Ryan, R.R. *Inorg. Chem.* **1993**, *32*, 2164.

48.   Engelhardt, U.; Rapko, B. M.; Duesler, E. N.; Frutos, D.; Paine, R.T. *Polyhedron* **1995**, *14*, 2361.

49.   Bond, E. M.; Englehardt, U.; Deere, T. P.; Rapko, B. M.; Paine, R.T.; FitzPatrick, J. R. *Solv. Extr. Ion Exch.* **1997**, *15*, 381.

50.   Bond, E. M.; Englehardt, U.; Deere, T. P.; Rapko, B. M.; Paine, R.T.; FitzPatrick, J. R. *Solv. Extr. Ion Exch.* **1998**, *16*, 967.

51.   Gan, X.; Duesler, E.N.; Paine, R.T. *Inorg. Chem.* **2001**, *40*, 4420.

52.   Nash, K. L.; Lavallette, C.; Borkowski, M.; Paine, R.T.; Gan, X. *Inorg. Chem.* **2002**, *41*, 5849.

53.   Bond, E. M.; Duesler, E. N.; Paine, R.T.; Nöth, H. *Polyhedron* **2000**, *19*, 2135.

54.   Bond, E. M.; Donhart, N.; Duesler, E. N.; Nöth, H.; Paine, R.T. *Inorg. Chem.* **2002**, *41*, 444.

55.   Gan, X.; Parveen, S.; Smith, W. L.; Duesler, E. N.; Paine, R.T. *Inorg. Chem.* **2000**, *39*, 4591.

56.   Braunstein, P.; and Naud, F. *Angew. Chem. Int. Ed.* **2001**, *40*, 680.

57.   Helmchen, G.; and Pfaltz, A. *Acc. Chem. Res.* **2000**, *33*, 336.

58.   Braunstein, P.; Clerc, G.; Morise, X.; Welter, R.; Montavon, G. *J. Chem. Soc. Dalton,* **2003,** 1601.

59.   Braunstein, P.; Fryzuk, M. D.; Dall, M. L.; Naud, F.; Rettig, S. J.; and Speiser, F. *J. Chem. Soc. Dalton Trans.* **2000**, 1067.

60.   Braunstein, P.; Speicer, F.; Saussine, L.; and Welter, R. *Organometallic* **2004**, *23,* 2613.

61.   Nishiyama, H.; Kondo, M.; Nakamura, T.; and Itohi, K. *Organometallics* **1991,** *10,* 500.

62.   Franco, D.; Gomez, M.; Jiménez, F.; Muller, G.; Rocamora, M.; Maestro, M. A.; and Mahia, J. *Organometallics* **2004,** *23,* 3197.

63.   Kniess, T.; Correia, J. D. G.; Domingos, A.; Palmer, E.; and Santos, I. *Inorg. Chem.* **2003,** *42,* 6130.

64.   Bhor, S.; Tse, M. K.; Klawonn, M.; Döbler, C.; Mägerlein, W.; and Beller, M. *Adv. Synth. Catal.* **2004,** *346,* 263.

65.   Tse, M. K.; Bhor, S.; Klawonn, M.; Anilkumar, G.; Jiao, H.; Spannenberg, A.; Döbler, C.; Mägerlein, W.; Hugl, H.; and Beller, M. *Chem. Eur. J.* **2006,** *12,* 1875.

66.   Nishiyama, H.; Itoh, Y.; Matsumoto, H.; Park, S. B.; Itoh, K. *J. Am. Chem. Soc.* **1994,** *116*, 2223.

67.   Paine, R. T.; Bond, E. M.; Parveen, S.; Donhart, N.; Duesler, E. N.; Smith, K. A.; and Nöth, H. *Inorg. Chem.* **2002,** *41(2),* 444.

68.   Tan, Y. C.; Gan, X. M.; Stanchfield, J. L.; Duesler, E. N.; and Paine, R. T. *Inorg. Chem.* **2001,** *40(12),* 2910.

69.   Meyers, A. I.; Gabel, R.; and Mihelich, E. D. *J. Org. Chem.* **1978,** *43(7),* 1372.

70.   Nelson, T. D.; and Meyers, A. I. *Tetrahedron Letters* **1994,** *35(20),* 3259.

71.   Meyers, A. I.; and Himmelsbach, R. J. *J. Am. Chem. Soc.* **1985,** *107,* 682.

72.   Franco, D.; Gómez, M.; Jiménez, F.; Muller, G.; Rocamora, M.; Maestro, M. A.; and Mahia, J. *Organometallics* **2004,** *23,* 3197.

73.   Gilbertson, S. R.; and Chang, C. T. *J. Org. Chem.* **1998,** *63,* 8424.

74.   Minami, T.; Isonaka, T.; Okada, Y.; and Ichikawa, J. *J. Org. Chem.* **1993,** *58,* 7009.

75.   Quin, L. D. *A Guide to Organophosphorus Chemistry; Wiley: New York* **2000.**

76.	Silverstein, R. M.; Bassler, G. C.; and Morrill, T.C. *Spectroscopic identification of organic compounds 5th edition* **1991,** pg 190, John Wiley and sons, Inc, New York.

77.	Whitaker, C. M.; Kott, K. L.; and McMahon, R. J. *J. Org. Chem.* **1995,** *60,* 3499.

Chapter 3

3.0 Synthesis and Coordination Chemistry of New Bifunctional Benzoxazole

Phosphine Oxide Ligands

3.1 INTRODUCTION

The instability of the oxazoline ring in acidic medium, led us to consider similar ring systems that are more stable. Benzoxazole, which is related to oxazoline, has been chosen in this case. It is appropriate to ask about the origin of this stability. Monocyclic planar compounds with $(4n + 2)$ p-π electrons, where $n = 0, 1, 2, 3$ etc, have shown exceptional stability. Such molecules are said to be "aromatic" due to π electron delocalization over the entire ring.[1, 2, 3] This concept of aromaticity can be extended as well to bicyclic compounds such as the benzoxazole molecule.

Figure 3.1 Molecular structure of benzoxazole
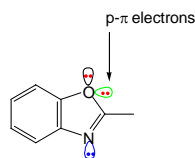
As shown in Figure 3.1, the contribution of two p-π electrons from the oxygen atom, make the total number of p-π electrons in the entire benzoxazole ring system to be 10, implying that it is aromatic and has increased stability. The remaining lone pairs of electrons on the oxygen and nitrogen atoms reside in the sp^2 ring framework and are not involved with the aromatic p-π electron system.

How does the aromatic nature influence the donor/ligation properties of benzoxazole relative to oxazoline? As mentioned in Chapter 2, no previous studies had

revealed coordination activity at the oxygen atom in oxazoline ligands and the new work described in Chapter 2 continued that trend.

Several studies have described the aromatic nature of other heterocyclic molecules[3, 4] such as pyrrole, thiophene and furan.
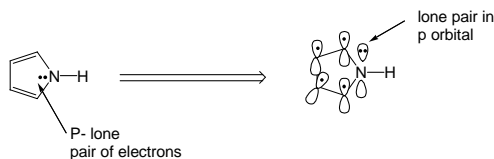
Pyrrole ring

In pyrrole, each of the four sp^2 – hybridized carbon atoms has a p-orbital perpendicular to the ring and each contributes one π electron. The nitrogen atom is also sp^2 – hybridized, and its lone pair of electrons occupies a p orbital. These provide a total number of six p-π electrons in the entire ring system, and this molecule is aromatic. The same applies to thiophene and furan.
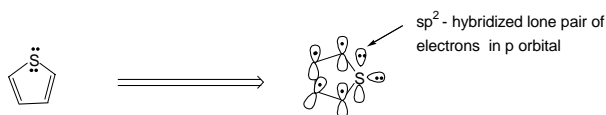
Thiophene ring
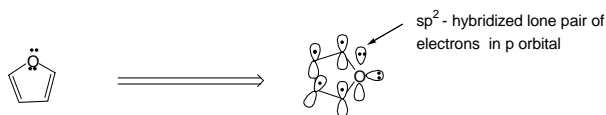
It follows that the aromatic nature of the benzoxazole ring results from the n = 2, 10 p-π electrons. As mentioned above the remaining lone pairs of electrons on the oxygen and nitrogen atoms are in the plane and are not involved in p-π electron delocalization.
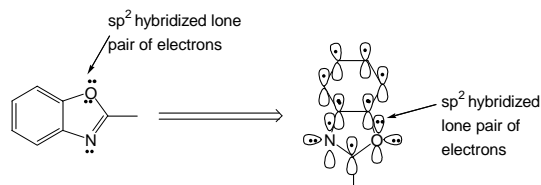
There is very little literature which describes the use of benzoxazole derivatives in coordination chemistry or separation of actinides and lanthanides.[5] Nevertheless, there is interest in the partitioning of minor actinide(III) ions and their transmutation products as part of a strategy for more efficient reprocessing of nuclear fuel,[6, 7] i.e., separation of Am(III) from Eu(III). Studies[5] have shown that polydentate nitrogen ligands, (Figure 3.2) can separate Am(III) from Ln(III).[8-11] Heterocyclic compounds such as pyridine, pyrazine, pyrimidine, 1,2,4-triazole, 1,2,4-triazine and 1,3,5-triazine (Figure 3.2), have been used in various combinations in separation of An(III). The extraction performance of these compounds was assumed to be influenced by the basic character on nitrogen atoms.[5]

Figure 3.2 Derivatives of nitrogen based heterocyclic compounds
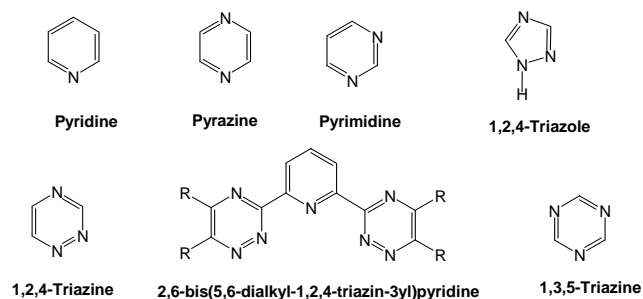
Very good Am(III)/Eu(III) separation factors (SF) have been obtained with either two weakly basic terminal 1,2,4-triazine or 1,2,4-triazole groups incorporated into a tridentate ligand.[12, 13] Both types of ligands were found to give Am(III)/Eu(III) separation factor values of 50-150 depending on the concentration of HNO_3 used during the extractions. As an example, it was found that 2,6-bis(5,6-dialkyl-1,2,4-triazin-3-yl)-

pyridines, offers very good extraction efficiency. However, these ligands undergo hydrolysis in acidic medium and upon exposure to radiation. This hinders their use in industrial separation processess.[14] Hence, other weakly basic extracting agents which are stable to hydrolysis and radiolysis were sought. For example, the tridentate ligand, 2,6-bis(benzimidazol-2-yl)-pyridine **22a** was synthesized by Burke, [15] and Drew and co-workers[5] synthesized examples of tridentate derivatives, **23** and **24** containing benzoxazole or benzothiazoles (Figure 3.3).

Figure 3.3 Tridentate ligands containing benzoxazole and benzothiazole fragments

22 (a) R, R', R"=H
(b) R, R'=H, R"=OH
(c) R, R'=Hexyl, R"=H
(d) R, R"=H, R'=Hexyl
(e) R, R'=H, R"=$OC_{12}H_{25}$

23 (a) R=H
(b) R'=OH
(c) R=$OC_{12}H_{25}$
(d) R=$OCH_2CH(C_{12}H_{25})(C_{10}H_{21})$

24 (a) R=OH
(b) R=$OC_{12}H_{25}$
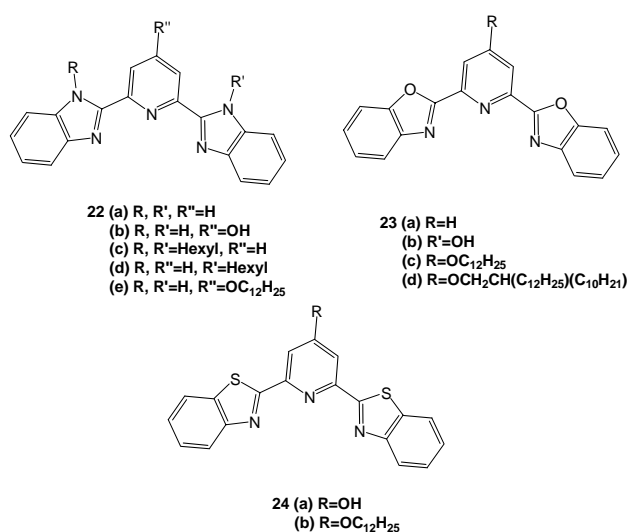
Studies[5] have shown that, benzoxazole based ligands (pKa -0.3) and benzothiazole (pKa 1.2) are less basic compared to benzimidazole (pKa 5.53). This property made benzoxazole and benzothiazole ligands good extractant of Am(III) from Eu(III) due to their ease of coordination prior to protonation, i.e., a weak base is not easily protonated by an acid as compared to a strong base.

Ligands **23-24** were synthesized adopting literature methods developed for the syntheses of examples of **22**.[15, 17] The precursors, compounds **22b, 23b** and **24a** required

for the synthesis of hydrophobic solvent extraction reagents were synthesized using the same methodology.[15, 17] The coupling reaction between these precursors and the hydrophobic chains was achieved after deprotonation of the hydroxyl groups with K_2CO_3 or NaH, followed by alkylation with 1-bromododecane/1-bromohexane to give hydrophobic derivatives, compounds **22c, 22e, 23c,** and **24b**. Solvent extraction experiments done using 1,1,2,2-tetrachloroethane as a solvent, showed the benzoxazole derivative **23c** to be the best extracting agent.[5] However, ligands **22e, 23c** and **24b** have poor solubility in hydrocarbon diluents, which is favored for solvent extraction. Subsequently, compound **23d**, a more hydrophobic version of **23c** was prepared with an attached 2-decyl-1-tetradecyl chain. Compound **23d** was directly synthesized from the reaction of 2-decyl-1-tetradecyl tosylate with **23b**.[5]

Ligand **23d** has good solubility in "hydrogenated tetra propene" (TPH) solvent and extraction was done at ligand concentrations of 0.02 M in TPH, against aqueous nitric acid solutions, 0.02-0.10 M. Using 0.02 M HNO_3, compound **23c** gave the largest separation factors Am(III)/Eu(III) in comparison to compounds **22** and **24**. For example **23c** gave separation factor Am(III)/Eu(III) 36, while other ligands gave 4-8. The good separation performance of **23c** was expected because benzoxazole derivatives have the lowest pKa (-0.3) which favor coordination of Ln(III)/An(III).[5]

The coordination chemistry of compounds **22-24** has also been studied. Initially, single crystals suitable for X-ray crystal structure determination with lanthanides were obtained with **23a**. Structures containing Nd, Pr and Er are isomorphous while complexes with Eu and Gd are different.

In all X-ray structures studied with ligands **22-24**, the complexes contain one ligand per metal bonded in a tridentate manner and three nitrates bonded in a bidentate manner to give a metal coordination number of 9. Several complexes containing **23a** also include two water molecules to give a total coordination number of 11 (Figure 3.4). Other complexes formed with Nd, Pr, and Er and **23a** contain one acetonitrile molecule to give a coordination number of 10 (Figure 3.5) and complexes of Eu, and Gd contain one water molecule, resulting in a coordination number of 10 (Figure 3.6). In all cases with **23,** the metal coordinates with the nitrogen atom of the oxazole ring rather than with the oxygen atom. This has been observed with a variety of transition metal complexes containing the oxazole and benzoxazole ligands.[5, 18-26] The same effect has also been observed with oxazoline ligand **19** reported in Chapter 2 (Figure 3.7) whereby only the nitrogen donor atom from the oxazoline fragment binds to Nd(III) and not oxygen.

Figure 3.4 The structure of La(23a)(NO$_3$)$_3$(H$_2$O) $_2$. Intramolecular hydrogen bonds are shown as dotted lines[5]

Figure 3.5 The structure of Nd(23a)(NO₃)₃(CH₃CN)[5]
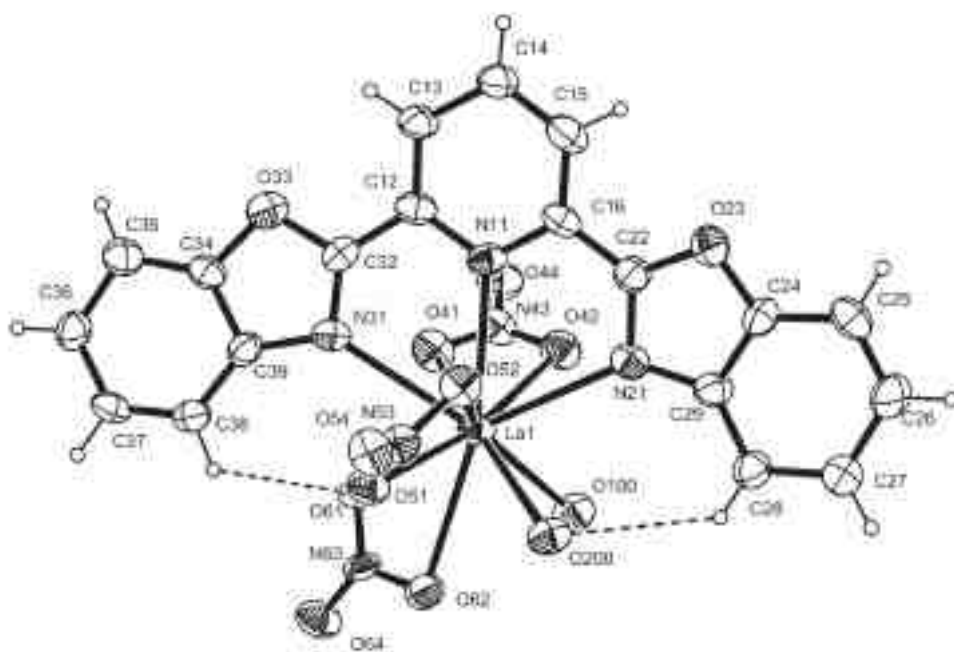
Figure 3.6 The structure of Gd(23a)(NO₃)₃(H₂O). Intramolecular hydrogen bonds are shown as dotted lines[5]
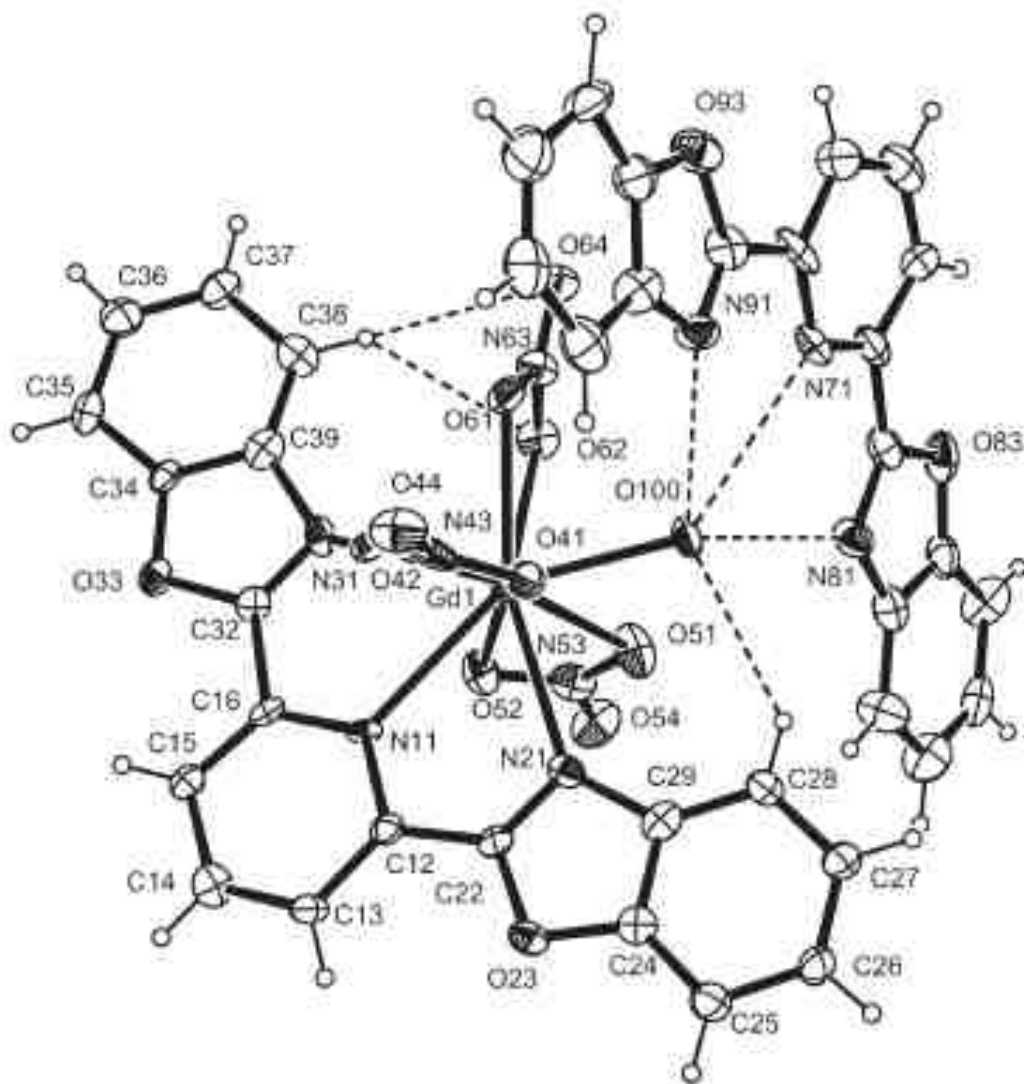
Figure 3.7 2-[(Diphenylphosphinoyl)methyl]-4,5-dihydro-oxazole, 19

19
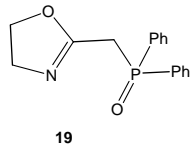
The structure and chemical similarities of benzoxazole and oxazoline suggest that 2-methyl-benzoxazole may undergo methyl deprotonation and substitution with phosphine or phosphine oxide groups. This would provide a stable backbone for new benzoxazole complexing ligands with hard/soft donors. The lone pair of electrons on the nitrogen atom of the benzoxazole would provide a suitable site for coordination as the case was observed with oxazoline ligand, **19** (Figure 3.7). A phosphine oxide donor group on the methylene spacer should result in a hard donor site that would provide a favorable environment for coordination with f-block elements (Figure 3.8).

Figure 3.8 Comparison of benzoxazole and oxazoline phosphine oxide derivatives

Benzoxazole   Oxazoline

25   **19**

R=Aromatic or alkyl substituents
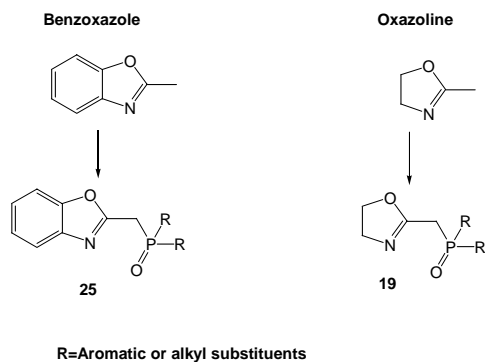
The synthesis of new ligands, with various substituents at the P=O, (Figure 3.9) is proposed. The aim in the current study is to explore the impact of varying electronic and steric modifications on the ligand in relation to the solubility of the ligand in hydrocarbon diluents and to study f-element coordination chemistry. The phosphine oxide group provides a suitable donor to bind hard f-element cations and the relatively "softer nitrogen" should facilitate hemilabile coordination to the Ln(III)/An(III). The

combination and proximity of these two different donor sites may lead to interesting hybrid ligands for f-element metals with possible applications as selective extractants to An(III) ions.

Figure 3.9 Proposed ligands for synthesis
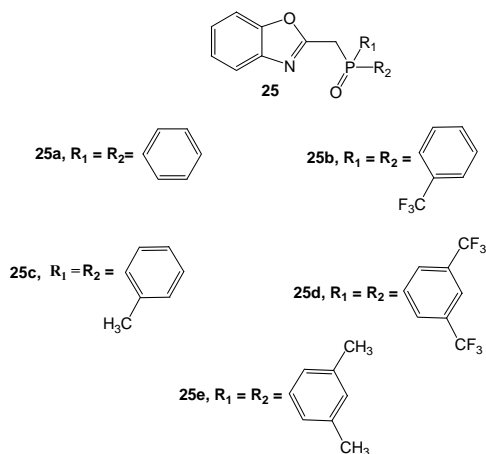
Ligands **25a, 25b, 25c, 25d,** and **25e** (Figure 3.9) have not been described in the literature and they can be viewed as variants of oxazoline ligands (Figure 3.7). Modifications made on the substituents on the phosphine oxide will enable us to explore their use as extractants as well as ligands with f-block element ions. One might also employ sterically larger groups on the phosphorus atom that might affect the overall structure of the complexes. Such steric modifications are illustrated with compounds **25d** and **25e**. The ligand set also contains variation in electronic effects as replacement of H with CH_3 (electron donating) and CF_3 (electron withdrawing) could alter the donor strength of the ligands.

3.2 STATEMENT OF PROBLEM

Hard P=O donor groups are expected to form strong coordinate interactions with Ln(III)/An(III) ions and the nitrogen (N) donor atom on the benzoxazole heterocyclic is expected to show a relatively weaker coordination to form hemilabile hybrid complexes.

The objective in this chapter is to synthesize several ligands based on benzoxazole which contain both a P=O and nitrogen (N) atom in the structure. It is expected that these families of ligands will act as hemilabile ligands and show good chelating behavior with Ln(III)/An(III).

Question: Can derivatives of benzoxazole be synthesized? If they can be, will they show stability in mineral acids compared to the oxazoline fragments?

3.3 EXPERIMENTAL

Three approaches have been examined for the synthesis of compound **25a**. The first is summarized in Scheme 7.

3.3.1 Synthesis of 2-[(diphenylphosphinoyl)methyl]-benzoxazole, 25a: Grignard Reagent

Scheme 7
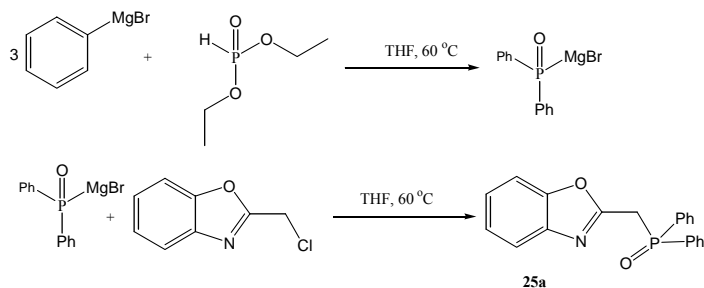
The pathway outlined in Scheme 7 has not been reported before, but similar reactions have been described.[16, 28-33, 40] A sample of phenyl magnesium bromide (30 ml, 2 M solution in THF, 20 mmol, 3 eq.) under nitrogen, was added dropwise to diethyl phosphite (1.0 ml, 6.5 mmol, 1 eq.) in dry THF (10 ml). The temperature of the solution rose during the addition, and the mixture was refluxed at 70 °C for 1 h, followed by addition of 2-chloromethylbenzoxazole (1.1 g, 6.5 mmol, 1 eq.) in dry THF (10 ml) at 23 °C. The reaction mixture was refluxed at 60 °C overnight, during which the color of

the mixture changed from yellow to black/brown or red/black. TLC analysis, using 5% MeOH/DCM, showed disappearance of the starting material, 2-chloromethylbenzoxazole. The THF was removed under vacuum. The workup was done by adding saturated aqueous solution of ammonium chloride (100 ml) to the residue, at room temperature and the resulting mixture was extracted with CHCl$_3$ (3 x 10 ml). Purification was done using column chromatography: silica gel, 70-230 mesh, 60Å, eluted with 5% MeOH/DCM. This resulted in pure yellow solid: Yield 2.1 g (96%), mp 160-161 $^{\circ}$C. Spectroscopic analyses were identical to the products obtained from the methods shown in Schemes 8 and 9.

3.3.2 One-pot synthesis of 2-[(diphenylphosphinoyl)methyl]-benzoxazole, 25a

Scheme 8
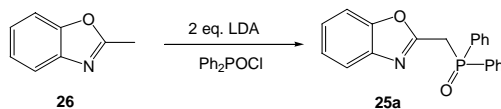
The general method of Minami *et al.*,[27] used for the synthesis of **25** (R = EtO), was adapted with modifications. Instead of using diethyl chlorophosphate, diphenylphosphinic chloride was used. To a dry THF (15 ml) solution of LDA (16 mmol, 2 eq.), generated in *situ* from diisopropylamine (2.2 ml, 16 mmol, 2 eq.) and BuLi (1.6 M in hexane, 10.2 ml, 16 mmol, 2 eq.), (-78 $^{\circ}$C, 10 min.) was added a solution of 2-methylbenzoxazole (1.1 g, 8 mmol, 1 eq.) in dry THF (10 ml). A yellow solution formed. The mixture was stirred (-78 $^{\circ}$C, 15 min.), then diphenylphosphinic chloride (1.5 ml, 8 mmol, 1 eq.) was added to the solution and the reaction mixture was stirred (1.5 h, -78 $^{\circ}$C). The reaction was quenched (-78 $^{\circ}$C) by addition of 1.2 M HCl (100 ml) and extracted with CHCl$_3$ (3 x 20 ml). The organic phase was washed with saturated brine solution (100 ml) and dried over Na$_2$SO$_4$. The solution was vacuum evaporated to give

2.9 g of the crude product. The crude product was purified using column chromatography: silica gel 70-230 mesh, 60Å, eluted with 100% CH_2Cl_2, followed by 2.5% $MeOH/CH_2Cl_2$, 5% $MeOH/CH_2Cl_2$ and finally 10% $MeOH/CH_2Cl_2$ to give a yellow solid: Yield 2.3 g (84%), mp 160-161 ^oC. This product was dried under vacuum for 1 day and crystallized from $CH_2Cl_2/MeOH$ mixture. White needles formed after evaporation of the solvent at room temperature, washed with hexane three times and left open to dry at room temperature for 2 days. Alternatively, crystallization was done from hot ethyl acetate to give yellow crystals. Further purification was done by washing crystals in CH_2Cl_2/hexane, filtered and the resulting white powder was dried under vacuum for 5 days to remove traces of ethyl acetate.

3.3.3 Two step synthesis of 2-[(diphenylphosphinoyl)methyl]-benzoxazole, 25a

Scheme 9
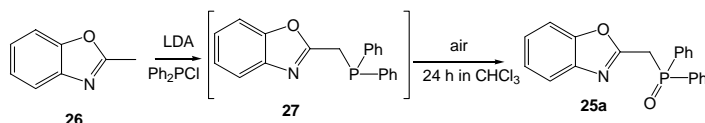
The general method of Minami *et al.*,[27] was adapted; however, in this case, diphenylphosphine chloride was used as summarized in Scheme 9. To a solution of LDA (32 mmol, 2 eq.), generated in *situ* from diisopropylamine (4.5 ml, 32 mmol, 2 eq.) and BuLi (1.6 M in hexane, 20.5 ml, 32 mmol, 2 eq.) in dry THF (15 ml), (-78 ^oC, 10 min.) was added a solution of 2-methylbenzoxazole (2.1 g, 16 mmol, 1 eq.) in dry THF (10 ml) (-78 ^oC). After stirring (-78 ^oC, 15 min.), diphenylphosphine chloride (3.3 ml, 17.6 mmol, 1.1 eq.) was added to the solution and the reaction mixture stirred (1.5 h, -78 ^oC). The reaction was quenched by addition of 1.2 M HCl (100 ml, -78 ^oC) and extracted with $CHCl_3$ (3 x 20 ml). The organic phase was washed with saturated brine solution (100 ml),

117

dried over Na_2SO_4 and left to oxidize by air for 24 h. The product was vacuum evaporated leaving 6.67 g of crude product. The crude product was purified using column chromatography: silica gel 70-230 mesh, 60Å, eluted with 100% CH_2Cl_2, followed by 2.5% MeOH/CH_2Cl_2 and 5% MeOH/CH_2Cl_2 to give a yellow solid: Yield 3.8 g (72%), mp 160-161 $^{\circ}$C. This was dried under vacuum for 3 days and crystallized from 5% MeOH, 95% CH_2Cl_2 solution. The solvent was left to evaporate slowly at room temperature giving white needles. Alternatively crystallization was done from hot ethyl acetate to give yellow crystals after several hours. This method gave lower yields and reduced purity compared to the method depicted in Schemes 7 and 8. Nevertheless, spectroscopic data are identical in all cases. The intermediate compound **27** was not isolated due to its ready oxidation into **25a** by air (oxygen) during the purification processes. Compound **25a** is soluble in $CHCl_3$, CH_2Cl_2, tetrachloroethane, CH_3OH, trifluoromethanesulfonyl-benzene (0.03 M) and is sparingly soluble in toluene and benzene.

Elemental Analysis from one-pot synthesis (Scheme 8)

Calculated for $C_{20}H_{16}NO_2P$ (FW=333.099 g/mole)   C, 72.07; H, 4.84; N, 4.20.

Found   C, 71.16; H, 4.85; N, 3.89.

Selected spectroscopic data for **25a** are summarized below and typical IR, ^{1}H NMR, ^{13}C{^{1}H} NMR and ^{31}P{^{1}H} NMR spectra are shown in Figures 3.10 – 3.15.

Infrared spectrum (KBr, cm^{-1}): 1610 ($v_{C=N}$), 1196 ($v_{P=O}$).

[1]H (250 MHz, 23 $^{\circ}$C, CDCl$_3$), δ (ppm): 4.1 (d, 2H, -CH_2-P=O, $^2J_{H-P}$ = 14.5 Hz), 7.2 (m, 2H, H-Ar), 7.3-7.5 (m, 8H, H-Ar), 7.7-7.8 (m, 4H, H-Ar).

^{13}C{^{1}H} **(62.9 MHz, 23 °C, CDCl$_3$), δ (ppm):** 33.0 (d, C$_1$, $^1J_{\text{C-P}}$ = 63.2 Hz), 110.6 (s), 119.7 (s), 124.3 (s), 124.9 (s), 128.7 (d, *ortho*-aryl, $^2J_{\text{C-P}}$ = 12.3 Hz), 131.1 (d, *meta*-aryl, $^3J_{\text{C-P}}$ = 9.7 Hz), 131.4 (d, *ipso*-aryl, $^1J_{\text{C-P}}$ = 103.1 Hz), 132.4 (d, $J_{\text{C-P}}$ = 2.4 Hz), 141.2 (s), 151.1 (s), C-Ar, 158.8 (d, C$_2$, $^2J_{\text{C-P}}$ = 8.8 Hz).

^{13}C{^{1}H} **(125.7 MHz, 23 °C, CDCl$_3$), δ (ppm):** 32.8 (d, C$_1$, $^1J_{\text{C-P}}$ = 64.8 Hz), 110.4 (s), 119.6 (s), 123.9 (s), 124.7 (s), 128.5 (d, *ortho*-aryl, $^2J_{\text{C-P}}$ = 12.5 Hz), 130.9 (d, *meta*-aryl, $^3J_{\text{C-P}}$ = 9.6 Hz), 131.3 (d, *ipso*-aryl, $^1J_{\text{C-P}}$ = 104.3 Hz), 132.1 (d, $J_{\text{C-P}}$ = 2.8 Hz), 141.0 (s), 150.9 (s), C-Ar, 158.6 (d, C$_2$, $^2J_{\text{C-P}}$ = 9.1 Hz).

^{13}C{^{1}H, ^{31}P} **(125.7 MHz, 23 °C, CDCl$_3$), δ (ppm):** 32.8 (s, C$_1$), 110.4 (s), 119.6 (s), 124.1 (s), 124.7 (s), 128.5 (s, *ortho*-aryl), 130.9 (s, *meta*-aryl), 131.3 (s, *ipso*-aryl), 132.2 (s), 141.0 (s), 150.9 (s), C-Ar, 158.6 (s, C$_2$).

^{31}P{^{1}H} **(101.3 MHz, 23 °C, CDCl$_3$), δ (ppm):** 27.7, -CH$_2$-P=O.

Mass spectrum (ESI) *m/e* **(fragment, relative intensity):** [M+H]$^+$ = 334.1003 and the calculated exact mass is 333.0919.

Figure 3.10 Infrared spectrum for 2-[(diphenylphosphinoyl)methyl]-benzoxazole, 25a
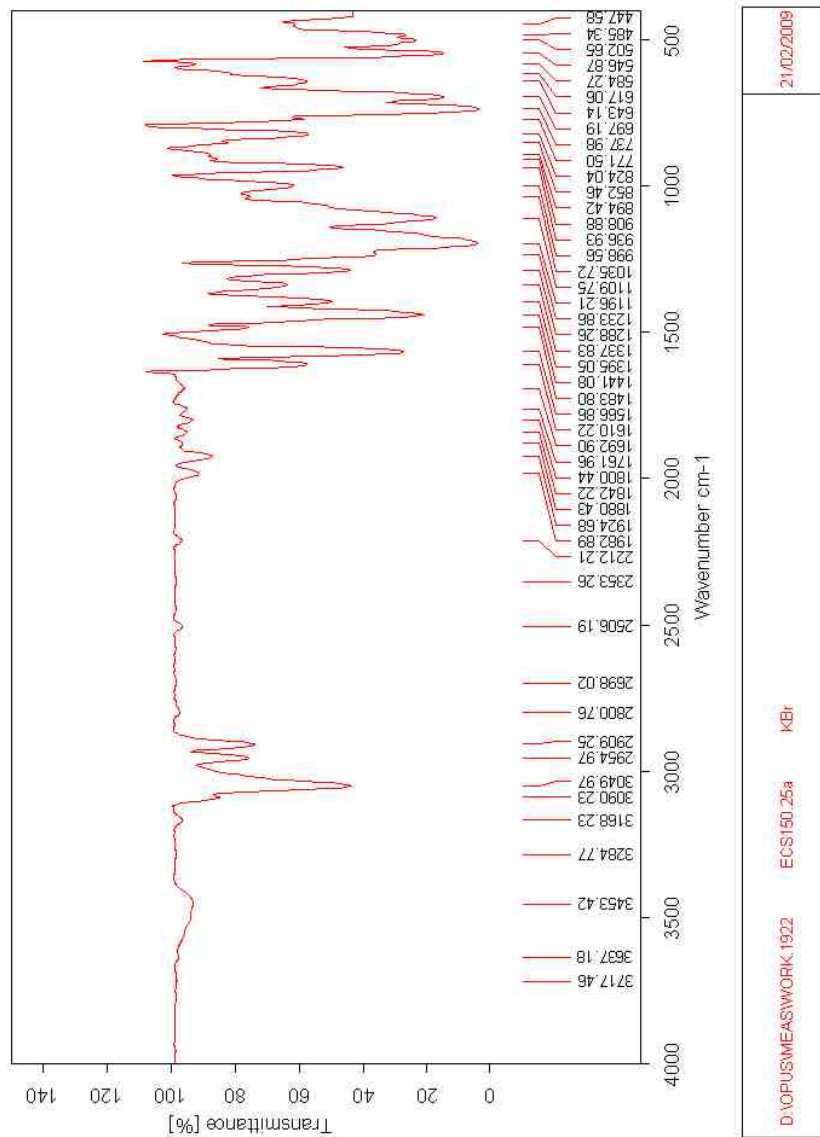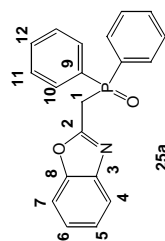
Figure 3.11 250 MHz ^{1}H NMR spectrum for 2-[(diphenylphosphinoyl)methyl]-benzoxazole, 25a
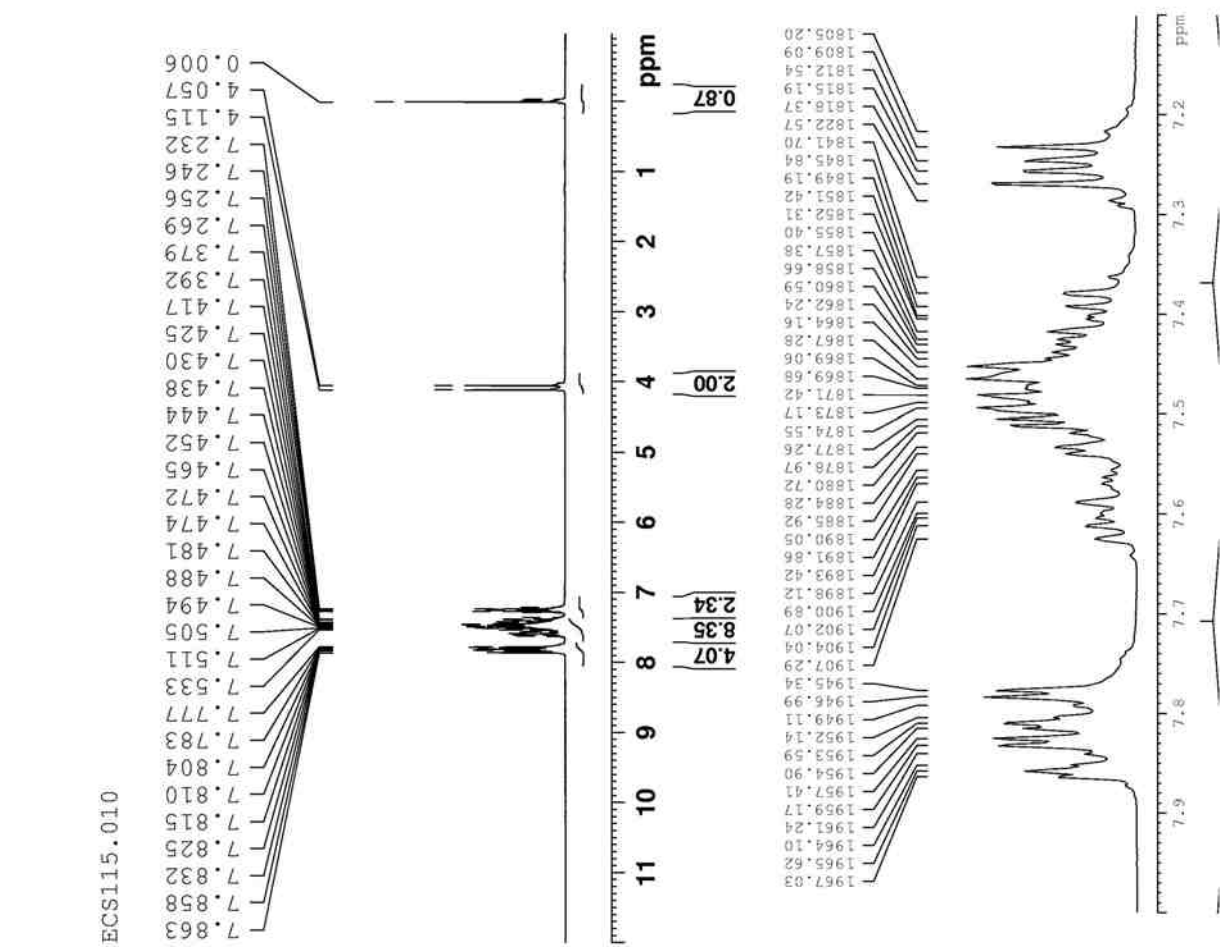
Figure 3.12 62.9 MHz ^{13}C{^{1}H} NMR spectrum for

2-[(diphenylphosphinoyl)methyl]-benzoxazole, 25a
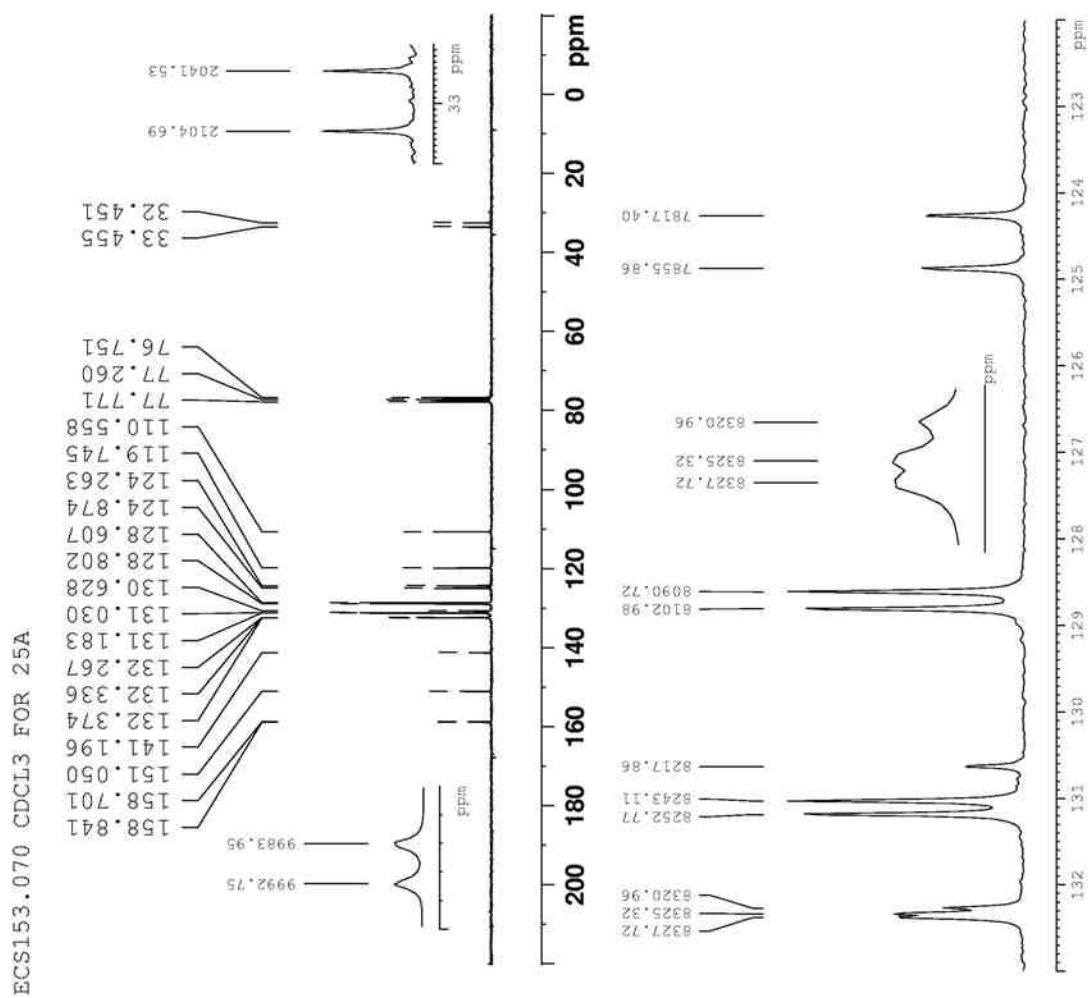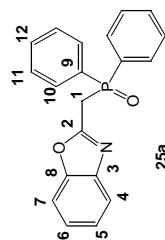
Figure 3.13 125.7 MHz $^{13}C\{^1H\}$ NMR spectrum for

2-[(diphenylphosphinoyl)methyl]-benzoxazole, 25a
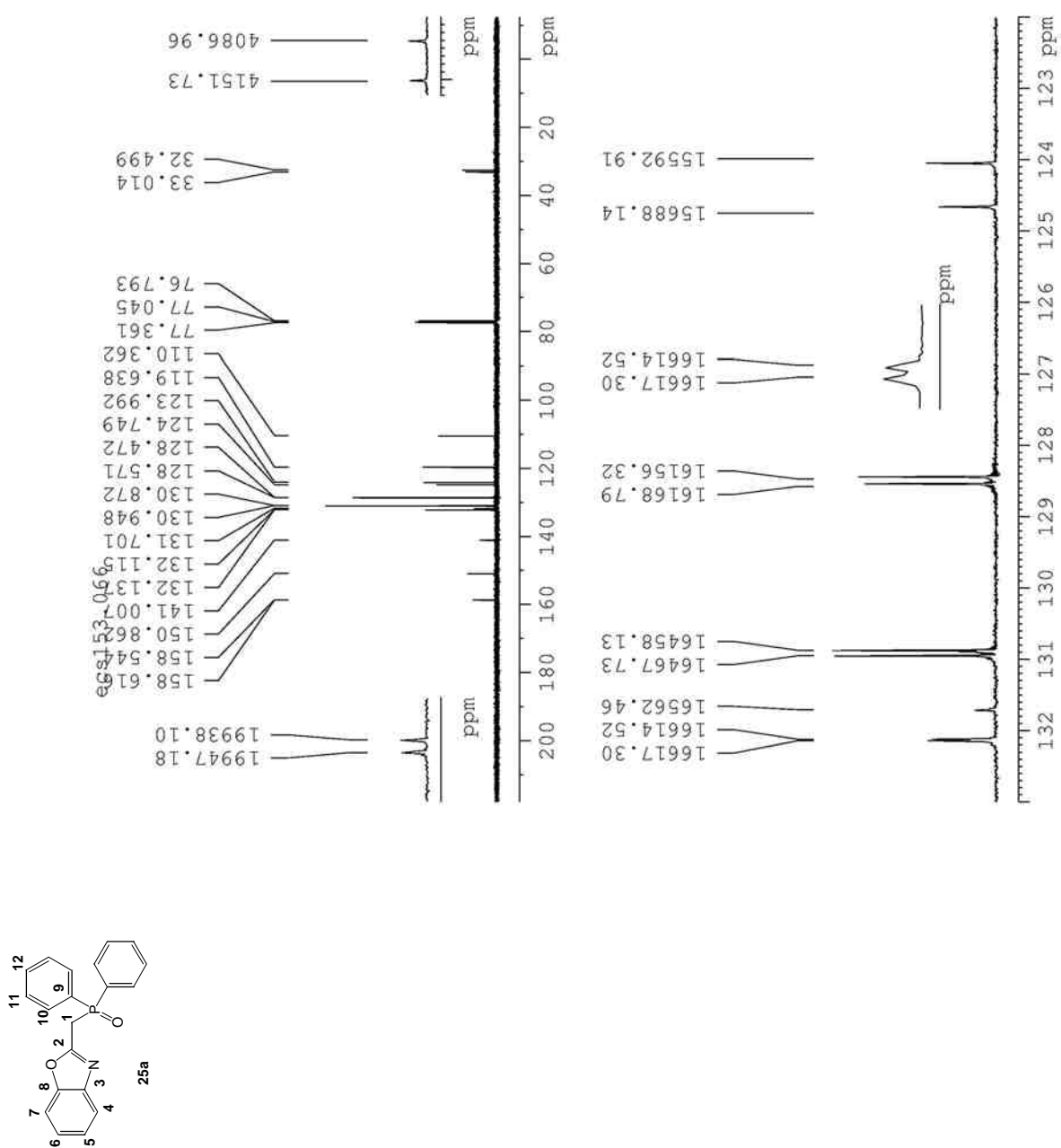
Figure 3.14 125.7 MHz ^{13}C{^{1}H, ^{31}P} NMR spectrum for

2-[(diphenylphosphinoyl)methyl]-benzoxazole, 25a
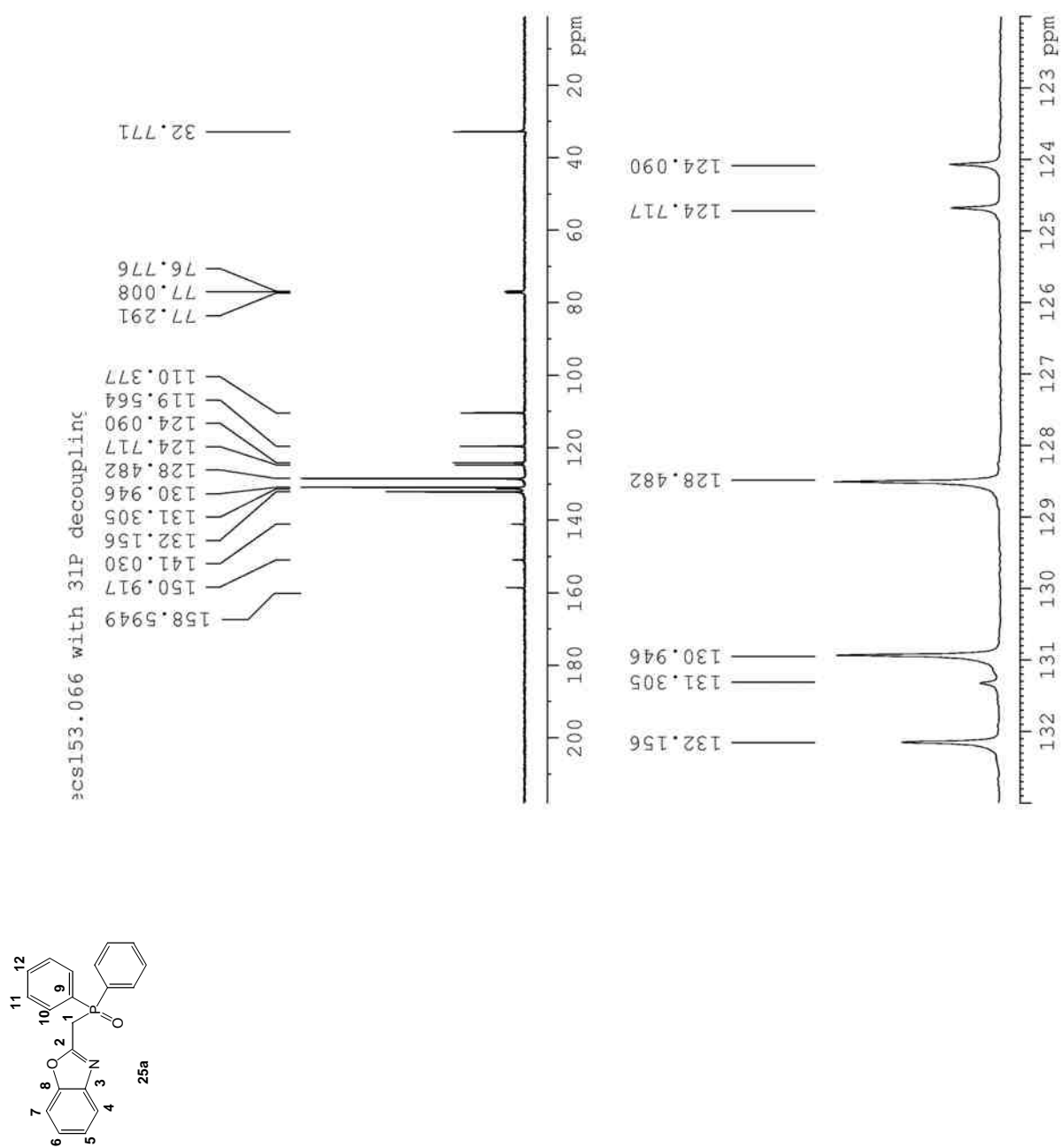
Figure 3.15 101.3 MHz ^{31}P{^{1}H} NMR spectrum for 2-[(diphenylphosphinoyl)methyl]-benzoxazole, 25a

27.750
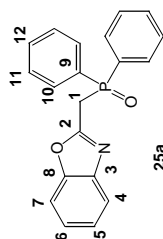
S115.011
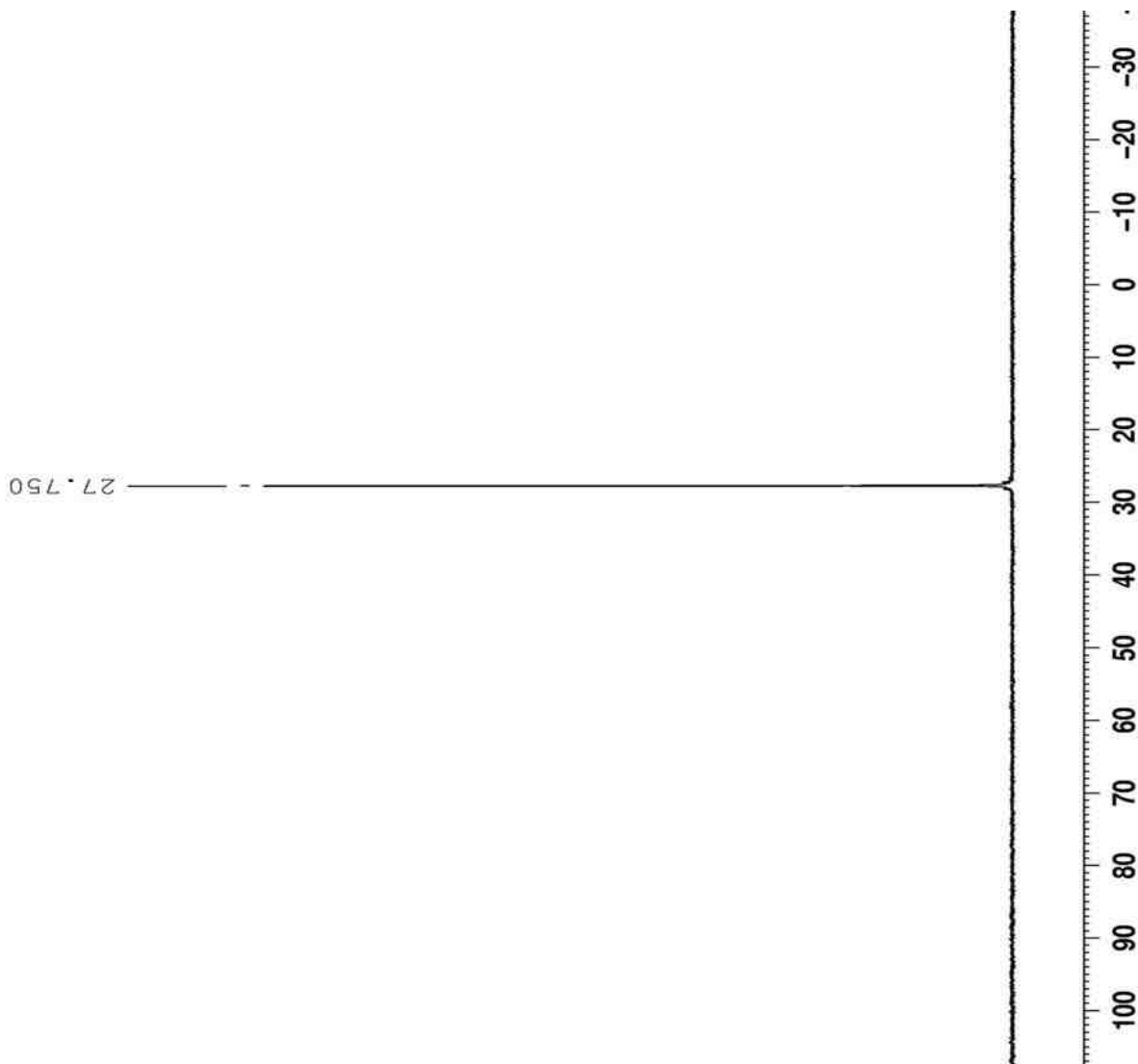
Single crystals suitable for X-ray diffraction were grown from CH_2Cl_2/MeOH solution. Slow evaporation at room temperature, after several days gave colorless crystals. The crystal structure determination for **25a** was completed. Crystal parameters are given in Table 3.1 and selected bond lengths are given in Table 3.2. The molecular structure is displayed in Figure 3.16.

Figure 3.16 Molecular structure and atom labeling scheme for single molecular unit of 2-[(diphenylphosphinoyl)methyl]-benzoxazole, 25a
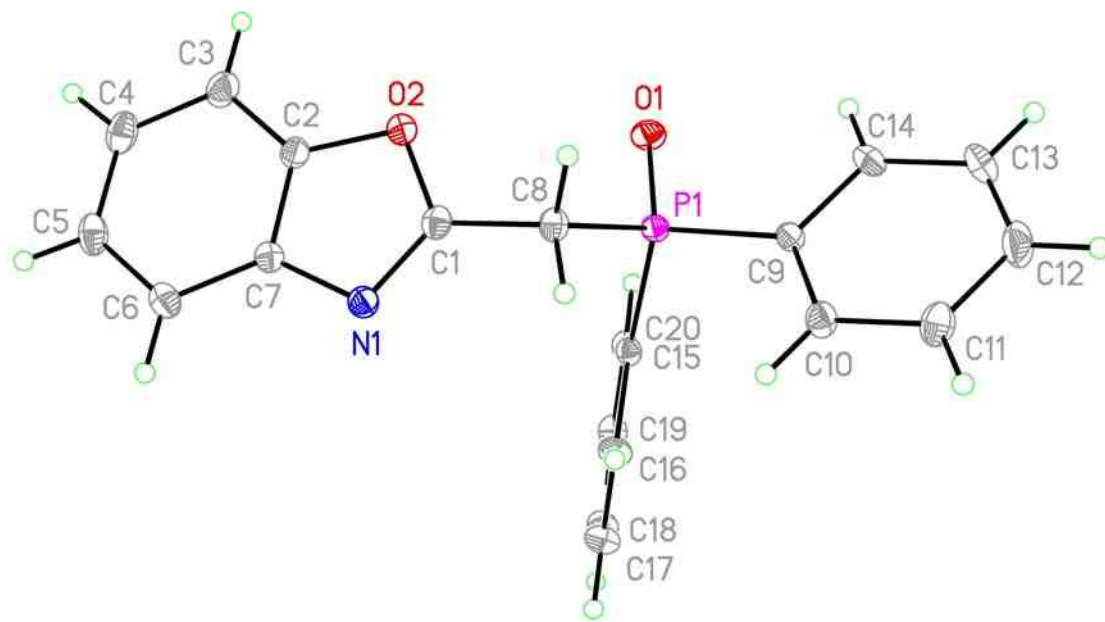
Table 3.1 Crystal parameters for 2-[(diphenylphosphinoyl)methyl]-benzoxazole, 25a

Empirical formula	$C_{20} H_{16} N O_2 P$
Formula weight	333.31
Temperature	223(2) K
Wavelength	0.71073 Å
Crystal system	Monoclinic
Space group	P2(1)/n
Unit cell dimensions	a = 8.7818(3) Å α= 90°.
	b = 18.4043(6) Å β= 109.015(2)°.
	c = 10.7928(3) Å γ = 90°.
Volume	1649.18(9) Å^3
Z	4
Density (calculated)	1.342 Mg/m^3
Absorption coefficient	0.178 mm^{-1}
F(000)	696
Crystal size	0.46 x 0.41 x 0.16 mm^3
Theta range for data collection	2.69 to 32.72°.
Index ranges	-13<=h<=13, -10<=k<=27, -16<=l<=16
Reflections collected	40488
Independent reflections	6066 [R(int) = 0.0225]
Completeness to theta = 32.72°	99.7 %
Absorption correction	Semi-empirical from equivalents
Max. and min. transmission	0.970 and 0.920

Refinement method	Full-matrix least-squares on F^2
Data / restraints / parameters	6066 / 0 / 217
Goodness-of-fit on F^2	1.027
Final R indices [I>2sigma (I)]	R1 = 0.0406, wR2 = 0.1149
R indices (all data)	R1 = 0.0495, wR2 = 0.1239
Largest diff. peak and hole	0.409 and -0.275 e.Å^{-3}

Table 3.2 Selected bond lengths [Å] for 2-[(diphenylphosphinoyl)methyl]-benzoxazole, 25a

P(1)-O(1)	1.4831(8)
P(1)-C(9)	1.7984(11)
P(1)-C(15)	1.8059(10)
P(1)-C(8)	1.8226(11)
O(2)-C(1)	1.3571(14)
O(2)-C(2)	1.3829(14)
N(1)-C(1)	1.2925(15)
N(1)-C(7)	1.3972(14)
C(1)-C(8)	1.4806(15)
C(2)-C(7)	1.3791(15)
C(2)-C(3)	1.3804(17)
C(3)-C(4)	1.383(2)
C(4)-C(5)	1.383(2)
C(1)-C(8)	1.4806(15)

3.3.4 Coordination Chemistry

The coordination chemistry of **25a** with several lanthanide ions was explored under a variety of conditions. Those that led to the isolation of well defined complexes are outlined here. For example, using methods described previously,[29-33] the combination of 3 equivalents of **25a** with $Yb(NO_3)_3 \cdot 5H_2O$ gave the chemistry described in Scheme 10 and in the following experimental protocol.

Scheme 10

25a
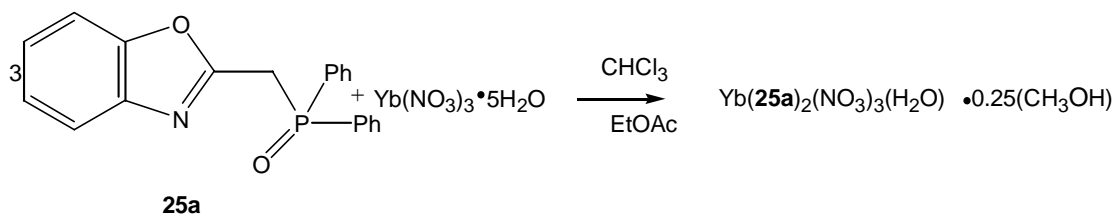
A sample of 2-[(diphenylphosphinoyl)methyl]-benzoxazole (0.2 g, 0.6 mmol, 3 eq.) in $CHCl_3$ (5 ml) was combined with $Yb(NO_3)_3 \cdot 5H_2O$ (0.08 g, 0.2 mmol, 1 eq.) in ethyl acetate (2 ml). The solution was stirred at 23 $^\circ$C for 12 h. The solution was left open to evaporate slowly for 5 days at room temperature. A yellow solid formed which was crystallized by dissolving in MeOH at room temperature followed by addition of hexane in excess. This solution was left open to evaporate for 5 days, leaving yellow crystals after evaporation. An infrared spectrum of the complex in KBr is shown in Figure 3.17 and is superimposed with a spectrum of the free ligand **25a**, in Figure 3.18. A diagnostic stretching vibration at 1159 cm^{-1} ($v_{P=O}$) appears and this is shifted down frequency from the corresponding vibrations in the free ligand: $\Delta v_{P=O} = 37$ cm^{-1}, mp > 250 $^\circ$C. Crystals were not soluble in chloroform; therefore chloroform was used in washing them (3 x 40 ml) to give pale yellow crystals suitable for X-ray diffraction studies. Single crystal X-ray diffraction analysis was completed. A view of the complex is shown in Figure 3.19.

Crystal parameters and selected bond lengths are summarized in Tables 3.3 and 3.4, respectively.

Elemental Analysis

Calculated for $C_{40.25}H_{35}N_5O_{14.25}P_2Yb$ C, 45.96; H, 3.32; N, 6.65.

Found   C, 47.90; H, 3.83; N, 5.79.

Figure 3.17 Infrared spectrum (KBr, cm^{-1}) for the complex

Yb(25a)$_2$(NO$_3$)$_3$(H$_2$O)•0.25(CH$_3$OH)
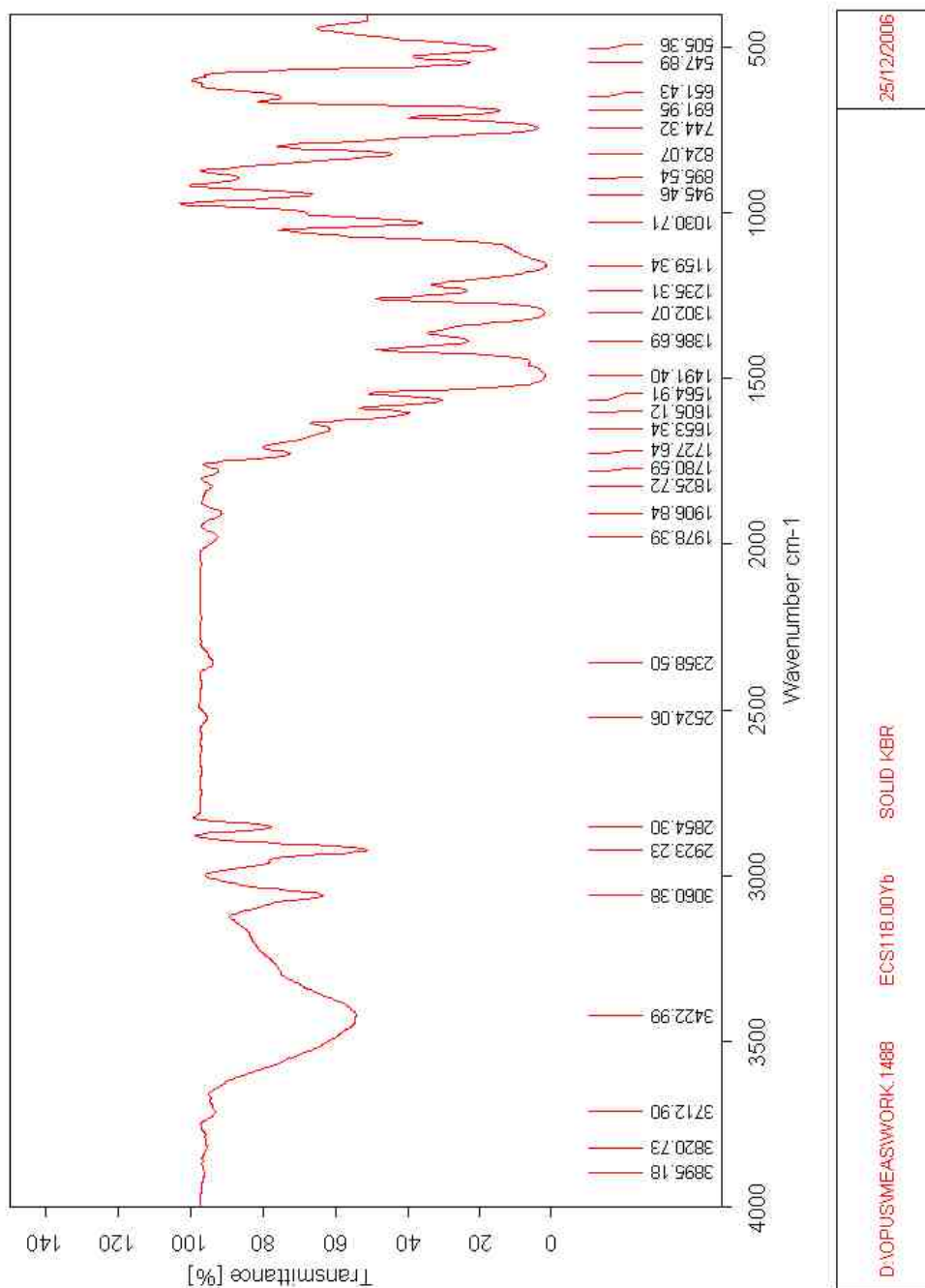
Figure 3.18 Infrared spectrum (KBr, cm^{-1}) for the

Yb(25a)$_2$(NO$_3$)$_3$(H$_2$O)•0.25(CH$_3$OH) superimposed with the free ligand, 25a
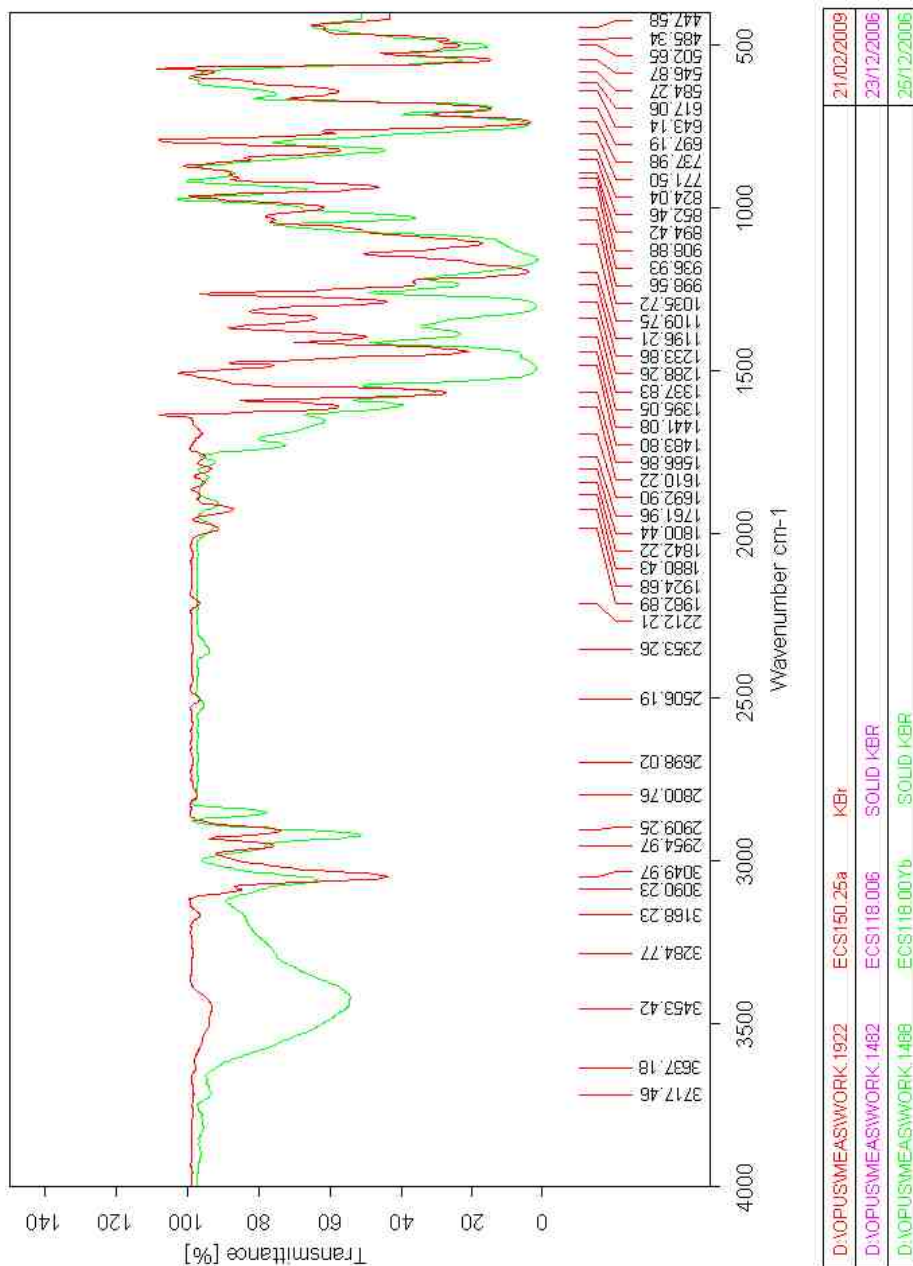
Figure 3.19 Molecular structure and atom labeling scheme for a single molecular unit, Yb(25a)$_2$(NO$_3$)$_3$(H$_2$O)•0.25(CH$_3$OH)
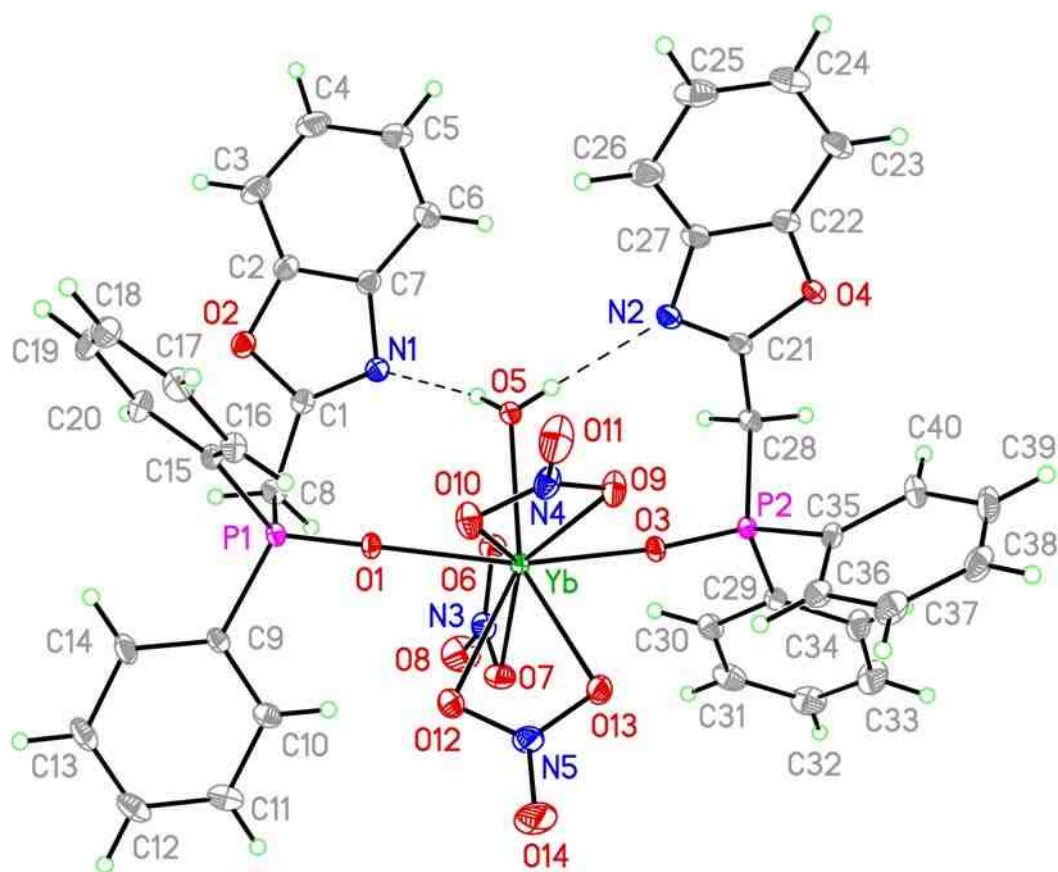
Table 3.3 Crystal parameters for Yb(25a)$_2$(NO$_3$)$_3$(H$_2$O)•0.25(CH$_3$OH)

Empirical formula	C$_{40.25}$H$_{35}$ N$_5$ O$_{14.25}$ P$_2$ Yb
Formula weight	1051.71
Temperature	223(2) K
Wavelength	0.71073 Å
Crystal system	Monoclinic
Space group	P2 (1)/n
Unit cell dimensions	a = 10.0465(8) Å α= 90°.
	b = 20.2381(16) Å β= 94.132(3)°.
	c = 21.2906(15) Å γ = 90°.
Volume	4317.6(6) Å^3
Z	4
Density (calculated)	1.618 Mg/m^3
Absorption coefficient	2.313 mm^{-1}
F(000)	2102
Crystal size	0.50 x 0.39 x 0.32 mm^3
Theta range for data collection	2.86 to 35.16°.
Index ranges	-15<=h<=16, -32<=k<=32, -34<=l<=34
Reflections collected	158885
Independent reflections	19173 [R(int) = 0.0317]
Completeness to theta = 35.16°	99.6 %
Absorption correction	Semi-empirical from equivalents
Max. and min. transmission	0.475 and 0.380

Refinement method	Full-matrix least-squares on F^2
Data / restraints / parameters	19173 / 0 / 577
Goodness-of-fit on F^2	0.930
Final R indices [I>2sigma (I)]	R1 = 0.0313, wR2 = 0.0749
R indices (all data)	R1 = 0.0399, wR2 = 0.0806
Largest diff. peak and hole	2.048 and -1.151 e.Å^{-3}

Table 3.4 Selected bond lengths [Å] for Yb(25a)$_2$(NO$_3$)$_3$(H$_2$O)•0.25(CH$_3$OH)

Yb-O(3)	2.2128(14)
Yb-O(1)	2.2272(14)
Yb-O(5)	2.2777(16)
Yb-O(13)	2.3641(18)
Yb-O(10)	2.3839(18)
Yb-O(7)	2.4106(18)
Yb-O(9)	2.4373(18)
Yb-O(12)	2.4490(19)
Yb-O(6)	2.5095(19)
Yb-H(5B)	2.72(3)
P(1)-O(1)	1.4913(15)
P(1)-C(15)	1.781(2)
P(1)-C(9)	1.793(2)
P(1)-C(8)	1.817(2)
P(2)-O(3)	1.4953(15)
P(2)-C(35)	1.782(2)

N(1)-C(1)   1.286(3)

N(1)-C(7)   1.402(3)

N(2)-C(21)   1.291(3)

N(2)-C(27)   1.407(3)

C(16)-C(17)   1.389(4)

The reaction in Scheme 10 was repeated using methanol as the solvent. The reaction mixture was stirred for 15 min., a yellow suspension formed, and further stirring was done for 2 h to complete the reaction. The resulting mixture was mixed with hexane in excess and left open to evaporate at room temperature for 2 days. A yellow oil formed that was vacuum dried for 2 days. The product was dissolved in chloroform to remove the uncomplexed ligand. A yellow suspension formed which was filtered and washed with hexane (3 x 20 ml). When the filtrate was left open for 2 days, brown crystals formed, which were filtered, washed with hexane, and left to dry on filter paper. Analysis of these crystals using X-ray crystallography showed similar results as the crystals in Figure 3.19 with the exception that hydrogen atoms in the coordinated water molecule were not located.

Scheme 11

25a
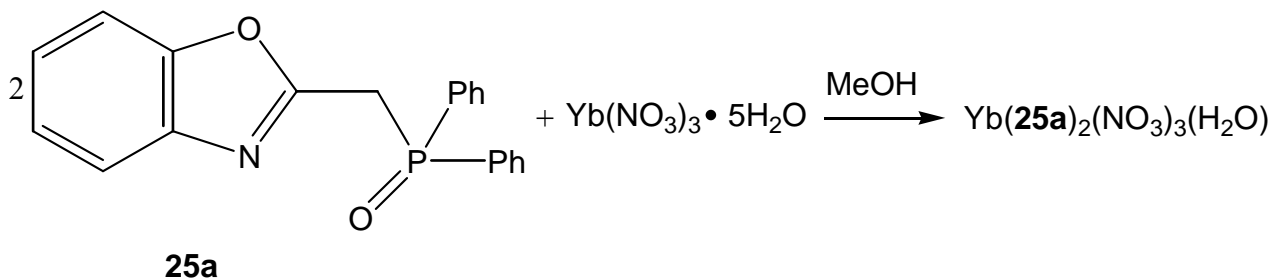
In another variation, a sample of 2-[(diphenylphosphinoyl)methyl]-benzoxazole (0.13 g, 0.40 mmol, 2 eq.) in MeOH (5 ml) was combined with $Yb(NO_3)_3 \cdot 5H_2O$ (0.08 g,

0.2 mmol, 1 eq.) in MeOH (2 ml) and the mixture was stirred (23 °C, 12 h) to give a yellow solution. The solution was left open to evaporate slowly for 5 days at room temperature. A yellow/brown solid formed which was crystallized from hot $CHCl_3$. The solution was filtered and treated with hexane and the solvent was allowed to slowly evaporate for 5 days, leaving yellow/brown crystals. The same reaction was done using a ratio of 1:1 ligand: metal. A yellow solution formed, which was left open to evaporate. After 5 days yellow/brown crystals formed. Single crystal X-ray diffraction analysis of both crystals showed two ligands are monodentate through P=O coordination while the nitrogen atoms form a hydrogen bond with the inner sphere water molecule, the same as Scheme 10.

Scheme 12

25a
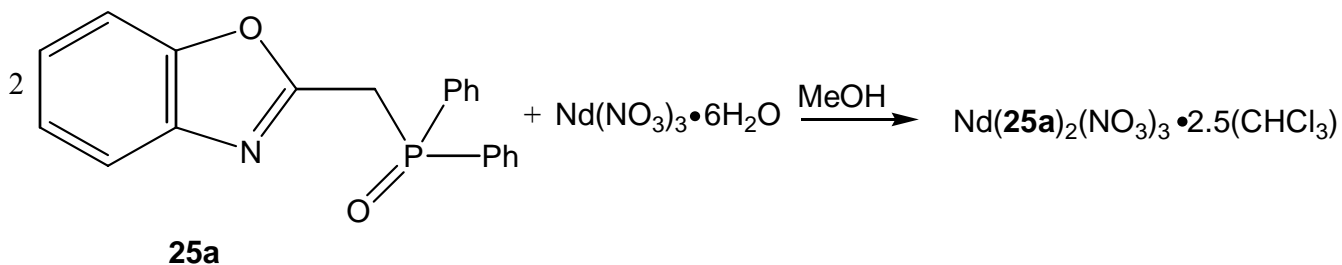
An additional variation with Nd(III) was also examined. A sample of 2-[(diphenylphosphinoyl)methyl]-benzoxazole (0.1 g, 0.30 mmol, 2 eq.) in MeOH (5 ml) was combined with $Nd(NO_3)_3•6H_2O$ (0.06 g, 0.15 mmol, 1 eq.) in MeOH (2 ml). The mixture was stirred for 12 h, to give a clear solution. The solution was left open to evaporate slowly for 4 days at room temperature. A white solid formed (0.25 g). The solid was crystallized from hot $CHCl_3$. The residue was removed by filtration. The hot filtrate was left capped for 7 days to give colorless crystals which were filtered and left to

dry at room temperature: Yield 0.15 g, (79%), assuming the composition **Nd(25a)$_2$(NO$_3$)$_3$•2.5(CHCl$_3$)**, mp > 250 ^{o}C.

Elemental Analysis

Calculated for C$_{42.5}$H$_{34.5}$Cl$_{7.5}$ N$_5$ O$_{13}$ P$_2$ Nd   C, 39.40; H, 2.66; N, 5.40.

Found   C, 42.33; H, 3.04; N, 6.21.

The infrared spectrum (KBr cm^{-1}) displays a band at 1155 ($\nu_{P=O}$) and this corresponds to peak shift of: $\Delta\nu_{P=O} = 41$cm^{-1} relative to free ligand. Typical spectra are shown in Figures 3.20 and 3.21. Single crystal X-ray crystallographic analysis shows two ligands coordinated with the Nd(III) and both are coordinated in a bidentate chelate mode through P=O, and nitrogen (N) donor centers. The complex shows a coordination number of 10 (Figure 3.22). Crystal parameters are displayed in Table 3.5 and selected bond lengths are summarized in Table 3.6. The same reaction was done using a 1:1 ligand: metal ratio. A clear solution was formed, which was left open to evaporate. After 5 days, a white solid formed. Efforts to crystallize the powder were unsuccessful.

Figure 3.20 Infrared spectrum (KBr, cm⁻¹) for

Nd(25a)$_2$(NO$_3$)$_3$•2.5(CHCl$_3$).
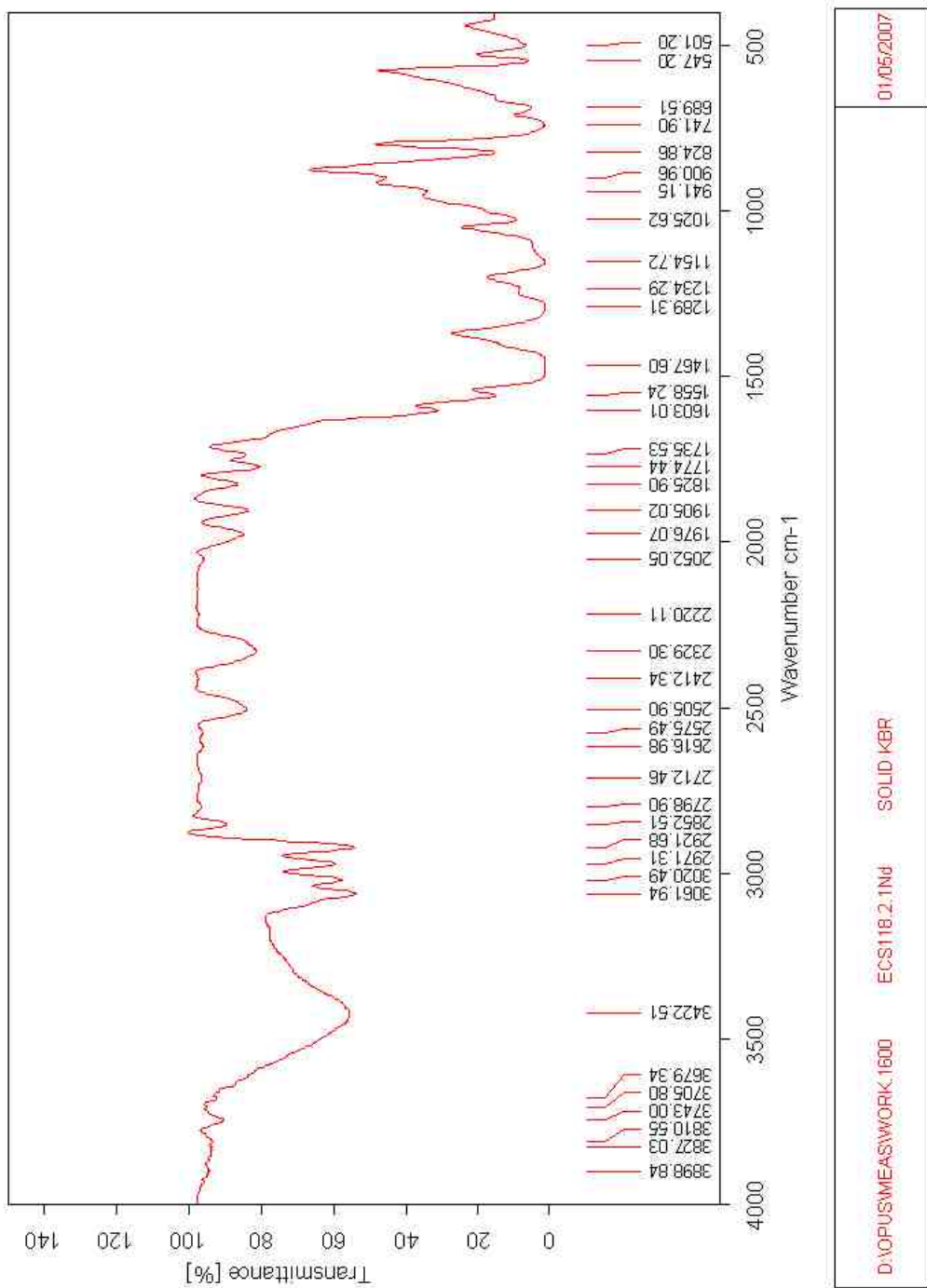
Figure 3.21 Infrared spectrum (KBr, cm^{-1}) for Nd(25a)$_2$(NO$_3$)$_3$•2.5(CHCl$_3$)

superimposed with a free ligand, 25a
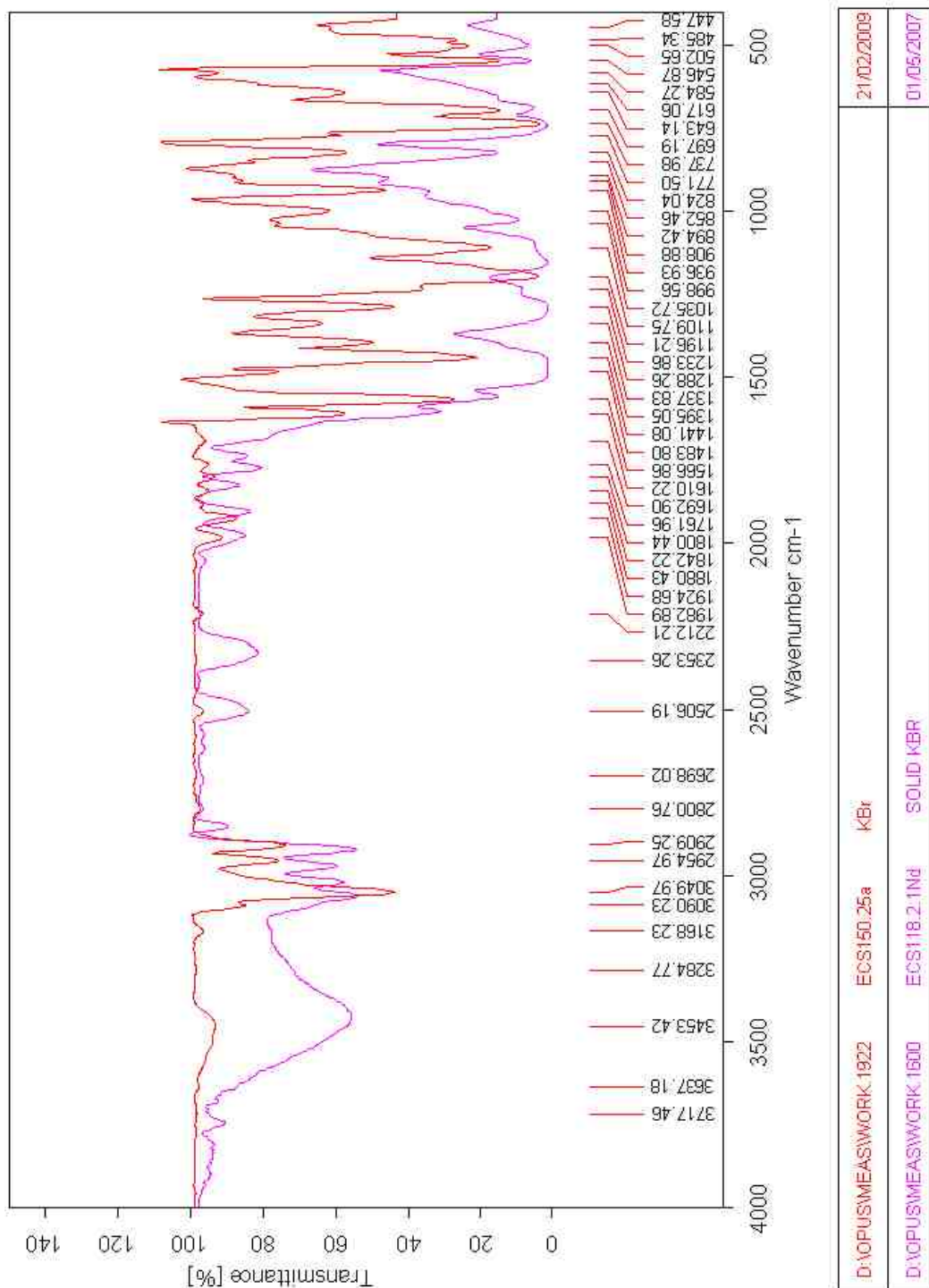
Figure 3.22 Molecular structure and atom labeling scheme for Nd(25a)$_2$(NO$_3$)$_3$ •2.5(CHCl$_3$).
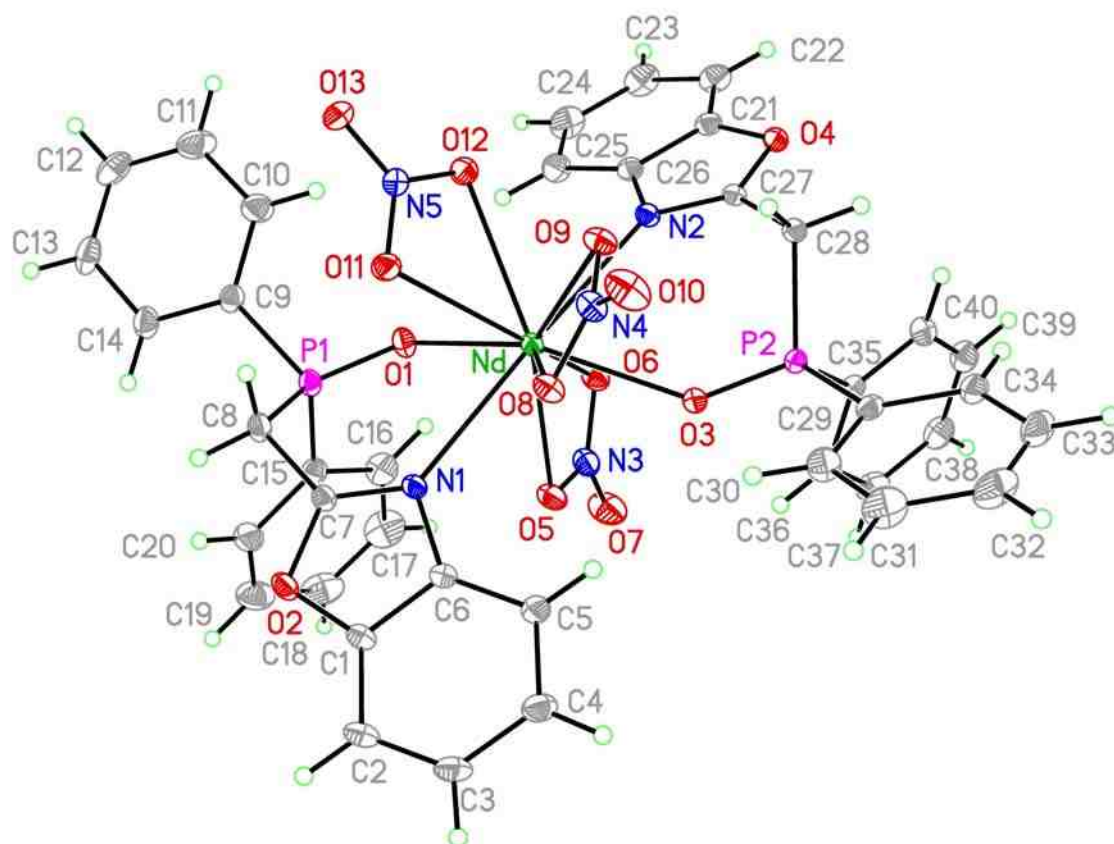
Table 3.5 Crystal parameters for Nd(25a)$_2$(NO$_3$)$_3$•2.5(CHCl$_3$).

Empirical formula	C$_{42.5}$ H$_{34.5}$ Cl$_{7.5}$ N$_5$ Nd O$_{13}$ P$_2$
Formula weight	1295.31
Temperature	223(2) K
Wavelength	0.71073 Å
Crystal system	Triclinic

Space group	P-1	
Unit cell dimensions	a = 13.1425(3) Å	α= 96.3680(10)°.
	b = 13.8228(3) Å	β= 110.695(2)°.
	c = 17.8614(5) Å	γ = 111.4380(10)°.
Volume	2715.91(11) Å^3	
Z	2	
Density (calculated)	1.584 Mg/m^3	
Absorption coefficient	1.446 mm^{-1}	
F(000)	1292	
Crystal size	0.299 x 0.260 x 0.092 mm^3	
Theta range for data collection	2.43 to 33.16°.	
Index ranges	-19<=h<=20, -21<=k<=21, -27<=l<=27	
Reflections collected	93947	
Independent reflections	20618 [R(int) = 0.0458]	
Completeness to theta = 33.16°	99.4 %	
Absorption correction	Semi-empirical from equivalents	
Max. and min. transmission	0.8759 and 0.6590	
Refinement method	Full-matrix least-squares on F^2	
Data / restraints / parameters	20618 / 0 / 712	
Goodness-of-fit on F^2	1.046	
Final R indices [I>2sigma (I)]	R1 = 0.0479, wR2 = 0.1437	
R indices (all data)	R1 = 0.0643, wR2 = 0.1566	
Largest diff. peak and hole	1.587 and -0.825 e.Å^{-3}	

Table 3.6 Selected bond lengths [Å] for Nd(25a)$_2$(NO$_3$)$_3$•2.5(CHCl$_3$)

Nd-O(1)	2.403(2)
Nd-O(3)	2.422(2)
Nd-O(5)	2.531(2)
Nd-O(6)	2.568(2)
Nd-O(11)	2.570(2)
Nd-O(9)	2.573(2)
Nd-O(8)	2.614(2)
Nd-O(12)	2.618(3)
Nd-N(1)	2.661(2)
Nd-N(2)	2.671(2)
P(1)-O(1)	1.501(2)
P(1)-C(9)	1.792(3)
P(1)-C(15)	1.793(4)
P(1)-C(8)	1.813(3)
O(2)-C(7)	1.361(4)
O(2)-C(1)	1.366(4)
N(1)-C(7)	1.288(4)
N(1)-C(6)	1.407(4)
C(1)-C(6)	1.382(4)
C(1)-C(2)	1.385(5)
C(2)-C(3)	1.375(6)

3.3.5 Synthesis of 2-[bis-(2-trifluoromethylphenyl)-phosphinoylmethyl]-benzoxazole, 25b

Scheme 13
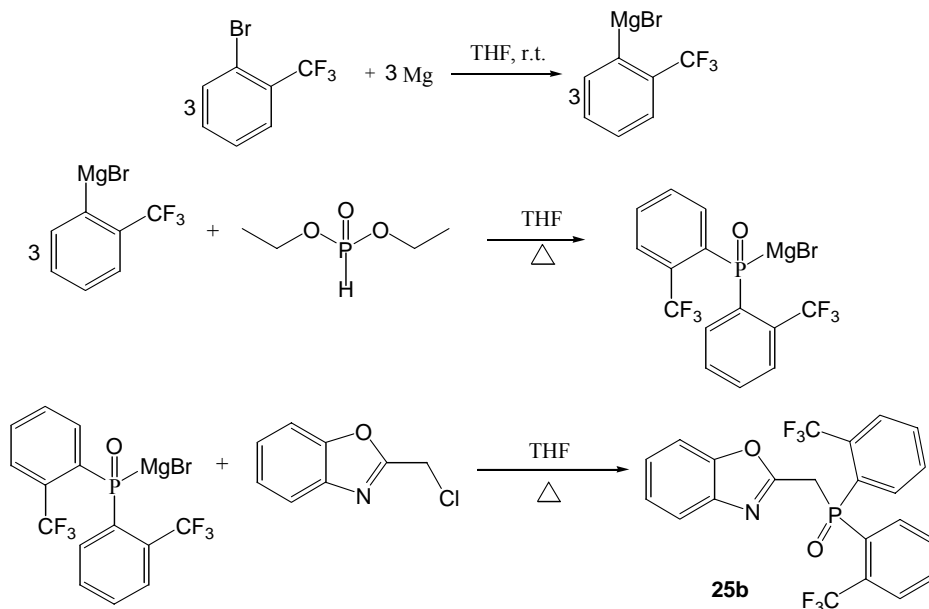
The reaction involves preparation of the required Grignard reagent using a method which has been reported in our group.[28-33, 40] Magnesium turnings (0.5 g, 20.5 mmol, 3 eq.) were placed in a 250 ml Schlenk vessel and the vessel was swept with dry nitrogen. Dry THF (10 ml) was added in the flask. A solution of 2-bromobenzotrifluoride (2.8 ml, 20.5 mmol, 3 eq.) in dry THF (10 ml) was added dropwise at 23 ^{o}C. The temperature of the reaction mixture rose. Stirring continued under reflux at 60 ^{o}C for 1 h to complete the reaction. Diethyl phosphite (1.0 ml, 7.5 mmol, 1 eq.) in dry THF (10 ml) was added drop wise to the Grignard reagent solution, (23 ^{o}C). The temperature rose during the addition, and the mixture was refluxed between 60-70 ^{o}C for an additional 1 h. The reaction mixture was then cooled to 23 ^{o}C and a solution of 2-chloromethylbenzoxazole, previously distilled under vacuum (1.3 g, 7.5 mmol, 1 eq.), in dry THF (10 ml) was added. The reaction was heated under reflux between 60 – 70 ^{o}C

overnight. The progress of the reaction was tested by TLC (95% CH$_2$Cl$_2$, 5% MeOH) and

this showed the absence of 2-chloromethylbenzoxazole. The solvent was removed under

reduced pressure, the residue was treated with saturated aqueous NH$_4$Cl solution (100 ml)

and then extracted with CHCl$_3$ (3 x 40 ml). The combined CHCl$_3$ extracts were dried

(Na$_2$SO$_4$) and then evaporated. The resulting orange solid was dried under vacuum for 2

days and purified by crystallization from ethyl acetate/hexane solution giving colorless

crystals: Yield 2.7 g, (74%), mp 140-141 $^{\circ}$C. Selected spectroscopic data for **25b** are

summarized here and typical spectra are displayed in Figures 3.23 – 3.28. Compound **25b**

is soluble in CHCl$_3$, CH$_2$Cl$_2$, Cl$_2$CH$_2$CH$_2$Cl$_2$, MeOH, trifluoromethanesulfonyl-benzene

(0.09 M) and EtOAc. Insoluble in hexane, pentane, toluene and benzene.

Elemental Analysis

Calculated for C$_{22}$ H$_{14}$F$_6$ N O$_2$ P (FW = 469.07 g/mole):   C, 56.30; H, 3.01; N, 2.98.

Found   C, 55.79; H, 2.89; N, 2.98.

Infrared spectrum (KBr, cm^{-1}): 1607 ($\nu_{C=N}$), 1125-1217 ($\nu_{P=O}$, ν_{C-F}).

^{1}H (250 MHz, 23 $^{\circ}$C, CDCl$_3$), δ (ppm): 4.3 (d, 2H, -CH$_2$-P=O, $^2J_{H-P}$ = 14.5 Hz), 7.2 (m,

2H, H-Ar), 7.3-7.4 (m, 1H, H-Ar), 7.5-7.6 (m, 5H, H-Ar), 7.7-7.8 (m, 2H, H-Ar), 8.2-8.3

(m, 2H, H-Ar).

^{13}C{^{1}H} (62.9 MHz, 23 $^{\circ}$C, CDCl$_3$), δ (ppm): 33.7 (d, C$_1$, $^1J_{C-P}$ = 69.4 Hz), 110.3 (s),

119.6 (s), 123.3 (qd, -CF$_3$, $^1J_{C-F}$ = 274.5 Hz, $^3J_{C-P}$ = 2.7 Hz), 124.2 (s), 124.9 (s), 127.6 (s),

130.5 (d, *ipso*-aryl, $^1J_{C-P}$ = 99.8 Hz), 131.4 (d, J_{C-P} = 11.9 Hz), 131.5 (qd, C$_{10}$, $^2J_{C-P}$ = 6.1

Hz, $^2J_{C-F}$ = 32.8 Hz), 132.3 (d, J_{C-P} = 1.5 Hz), 134.1 (d, J_{C-P} = 8.4 Hz), 140.9 (s), 150.9 (s),

C-Ar, 158.2 (d, C$_2$, $^2J_{C-P}$ = 9.2 Hz).

$^{13}C\{^1H\}$ **(125.7 MHz, 23 °C, CDCl$_3$), δ (ppm):** 34.0 (d, C$_1$, $^1J_{C-P}$ = 89.7 Hz), 110.4 (s),

119.7 (s), 123.4 (q, -CF$_3$, $^1J_{C-F}$ = 273.0 Hz), 124.2 (s), 124.9 (s), 127.6 (s), 130.6 (d, *ipso*-

aryl, $^1J_{C-P}$ = 99.3 Hz), 131.5 (d, J_{C-P} = 13.8 Hz), 131.8 (qd, C$_{10}$, $^2J_{C-P}$ = 6.5 Hz, $^2J_{C-F}$ = 33.5

Hz), 132.4 (s), 134.2 (d, J_{C-P} = 8.9 Hz), 141.0 (s), 150.9 (s), C-Ar, 158.3 (d, C$_2$, $^2J_{C-P}$ = 9.6

Hz).

$^{13}C\{^1H,\ ^{31}P\}$ **(125.7 MHz, 23 °C, CDCl$_3$), δ (ppm):** 33.9 (s, C$_1$), 110.3 (s), 119.4 (s),

123.3 (q, -CF$_3$, $^1J_{C-F}$ = 276.2 Hz), 124.1 (s), 124.8 (s), 127.5 (s), 130.5 (s, *ipso*-aryl),

131.3 (s), 131.6 (q, C$_{10}$, $^2J_{C-F}$ = 33.6 Hz), 132.2 (s), 134.0 (s), 140.8 (s), 150.7 (s), C-Ar,

158.1 (s, C$_2$).

$^{31}P\{^1H\}$ **(101.3 MHz, 23 °C, CDCl$_3$), δ (ppm):** 28.4, CH$_2$-P=O.

Mass spectrum (ESI) *m/e* **(fragment, relative intensity):** [M+H]$^+$ = 470.0743 and the

calculated exact mass is 469.0666.

Figure 3.23 IR spectrum for 2-[bis-(2-trifluoromethylphenyl)-phosphinoylmethyl]-benzoxazole, 25b
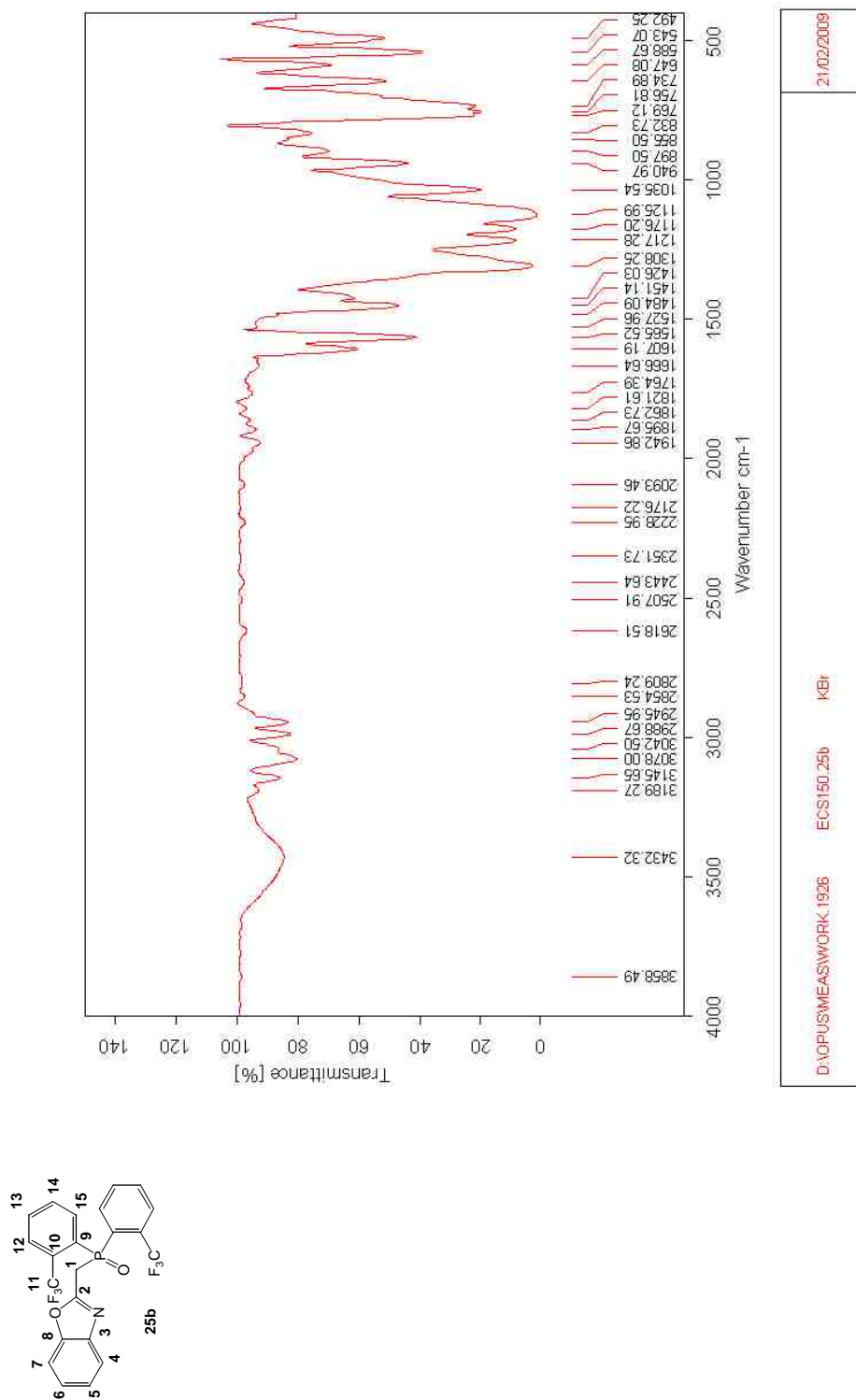
Figure 3.24 250 MHz ^{1}H NMR spectrum for 2-[bis-(2-trifluoromethylphenyl)

-phosphinoylmethyl]-benzoxazole, 25b
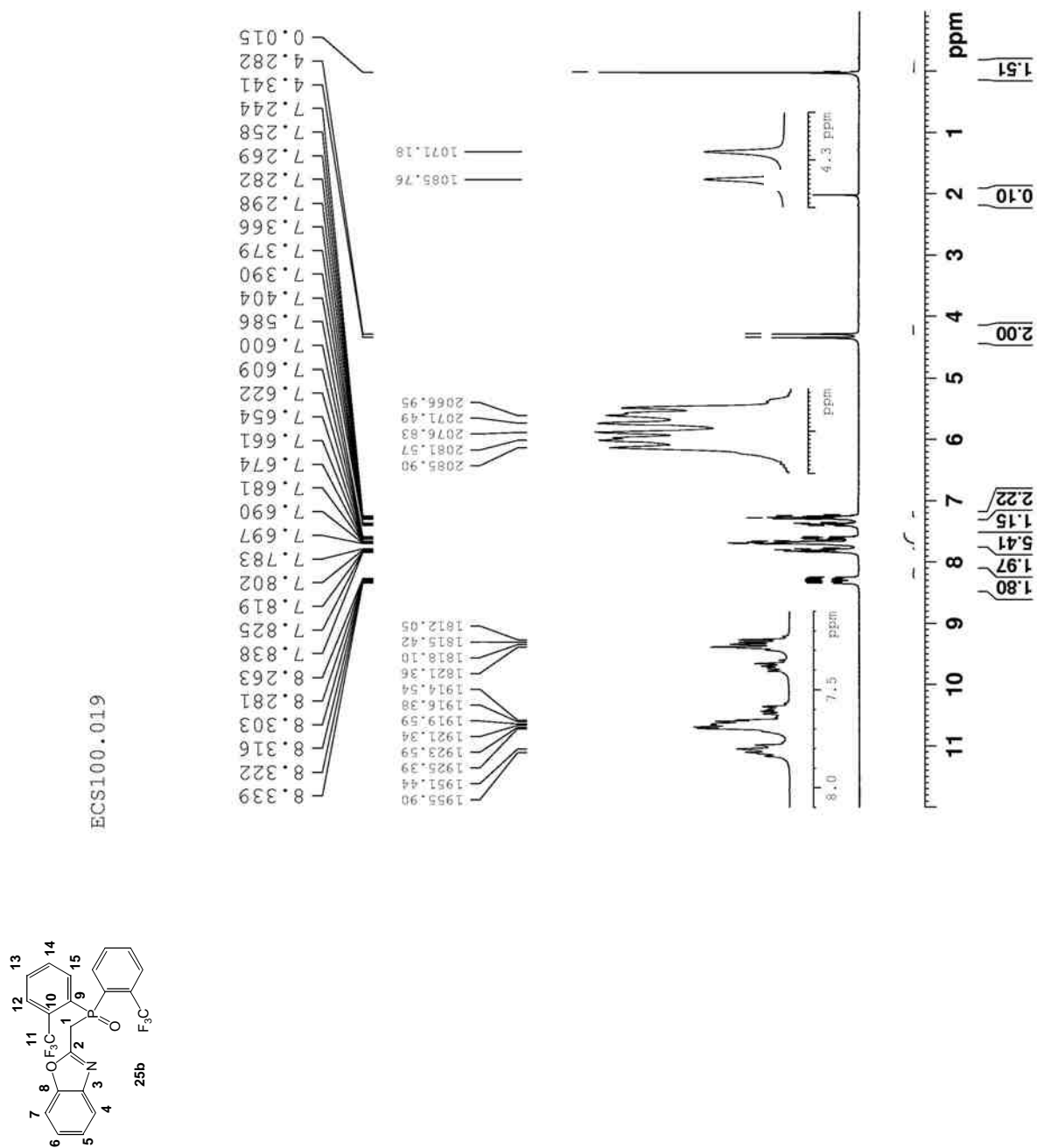
Figure 3.25 62.9 MHz $^{13}C\{^1H\}$ NMR spectrum for 2-[bis-(2-trifluoromethylphenyl)-phosphinoylmethyl]-benzoxazole, 25b
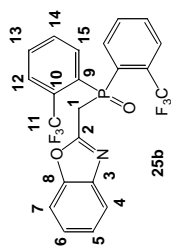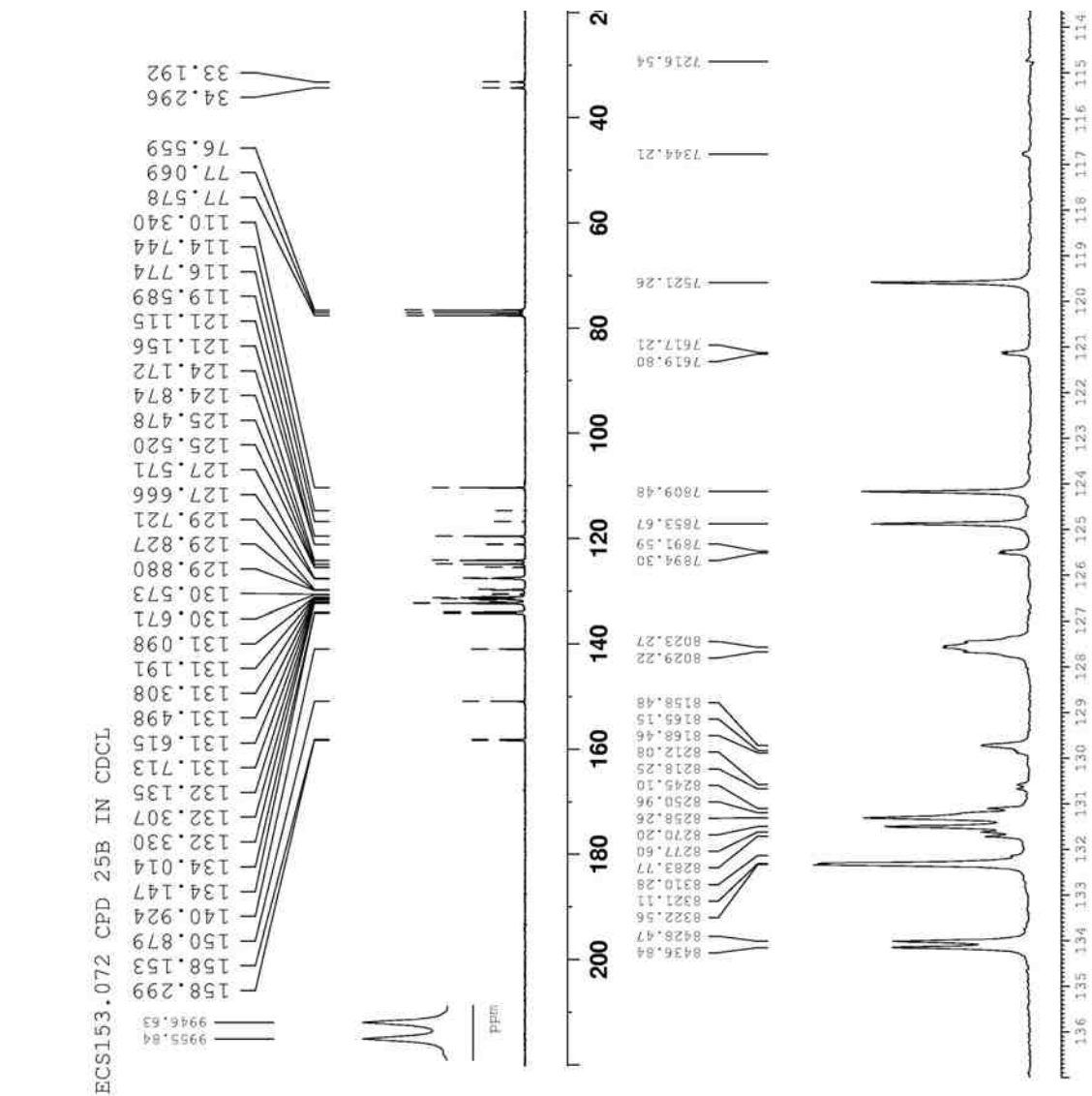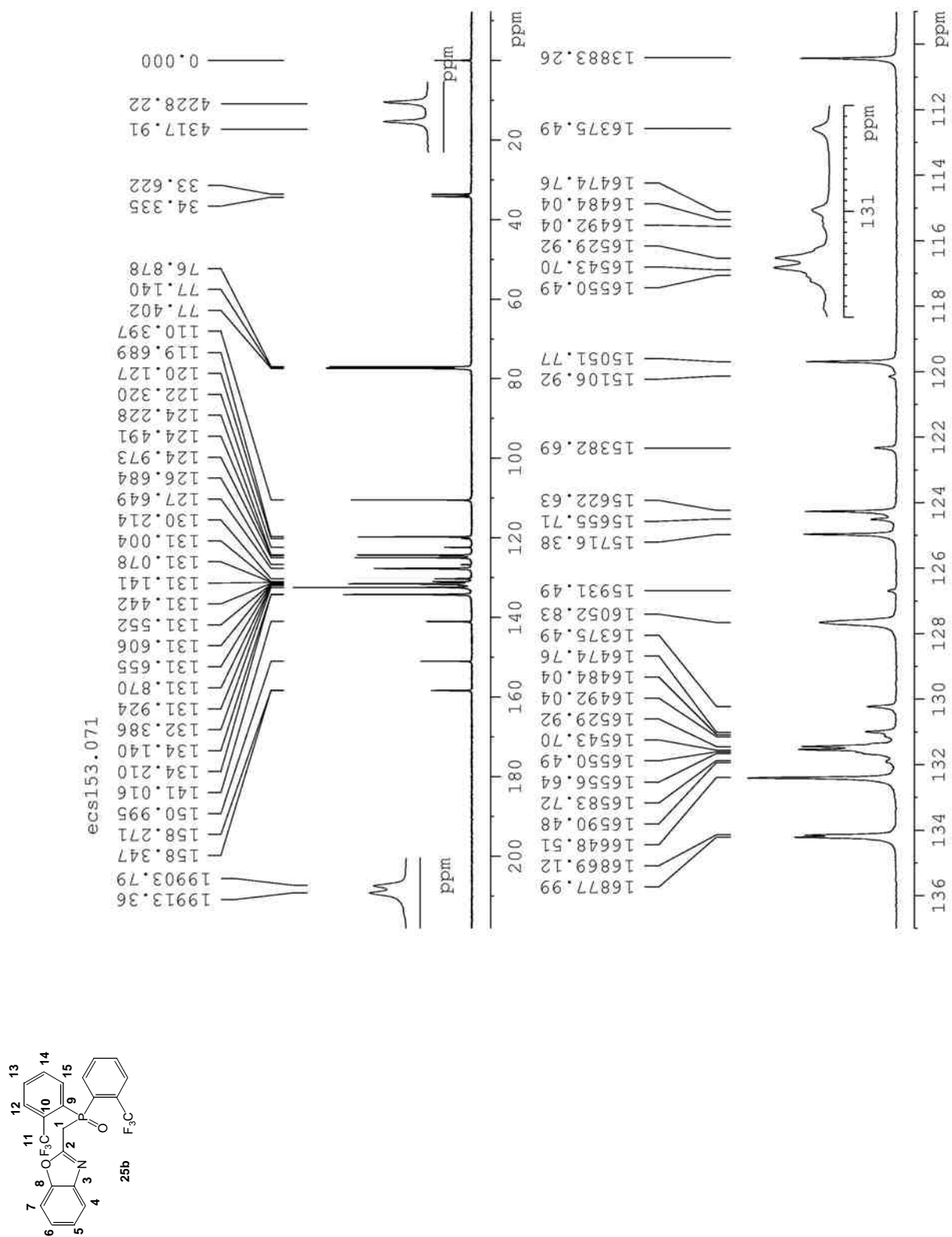
Figure 3.27 125.7 MHz ^{13}C{^{1}H, ^{31}P} NMR spectrum for 2-[bis-(2-trifluoromethylphenyl)-phosphinoylmethyl]-benzoxazole, 25b

151
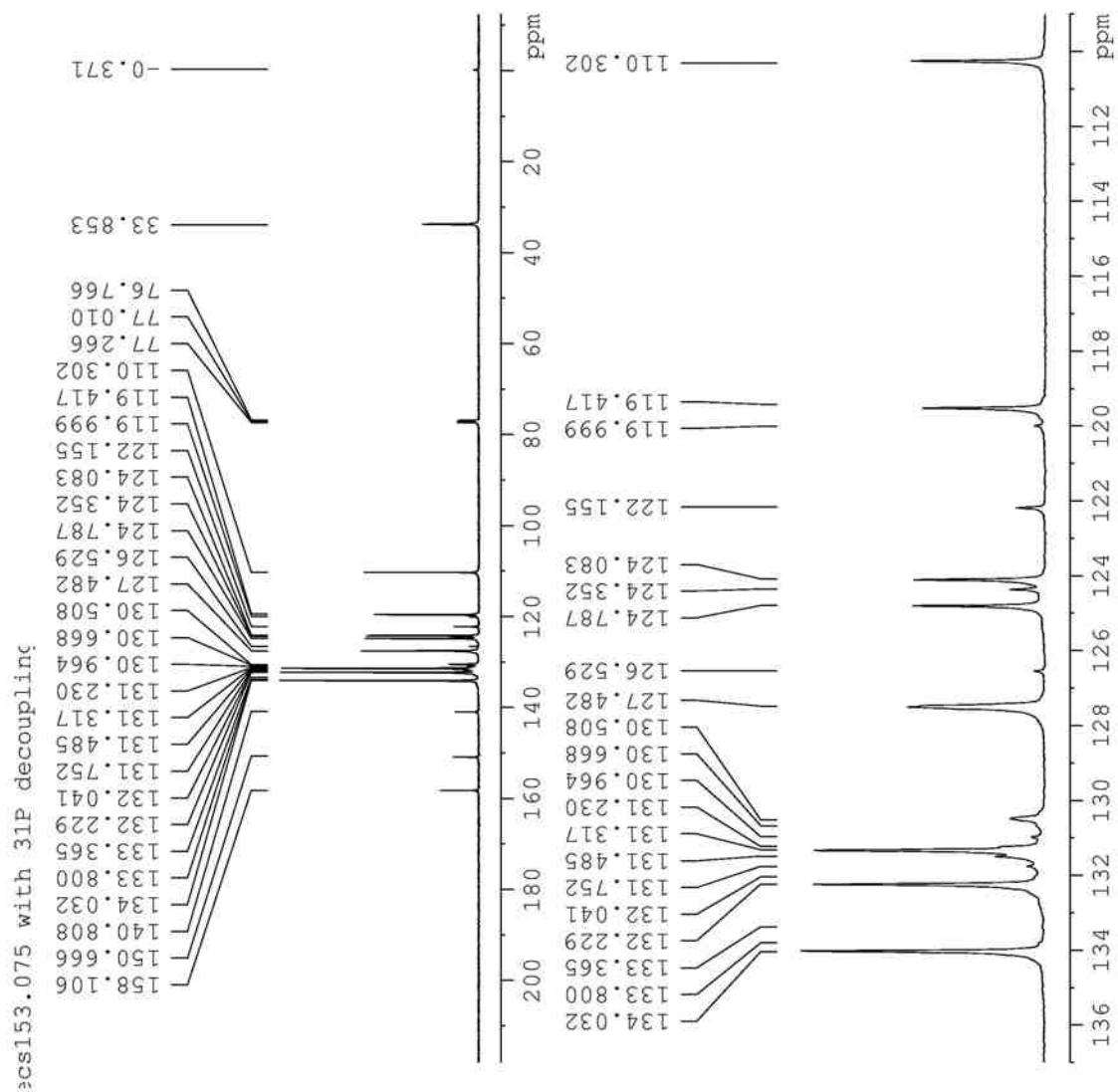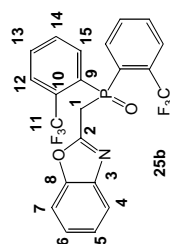
Figure 3.28 101.3 MHz ^{31}P{^{1}H} NMR spectrum for 2-[bis-(2-trifluoromethylphenyl)-phosphinoylmethyl]-benzoxazole, 25b

28.401

ECS100.020
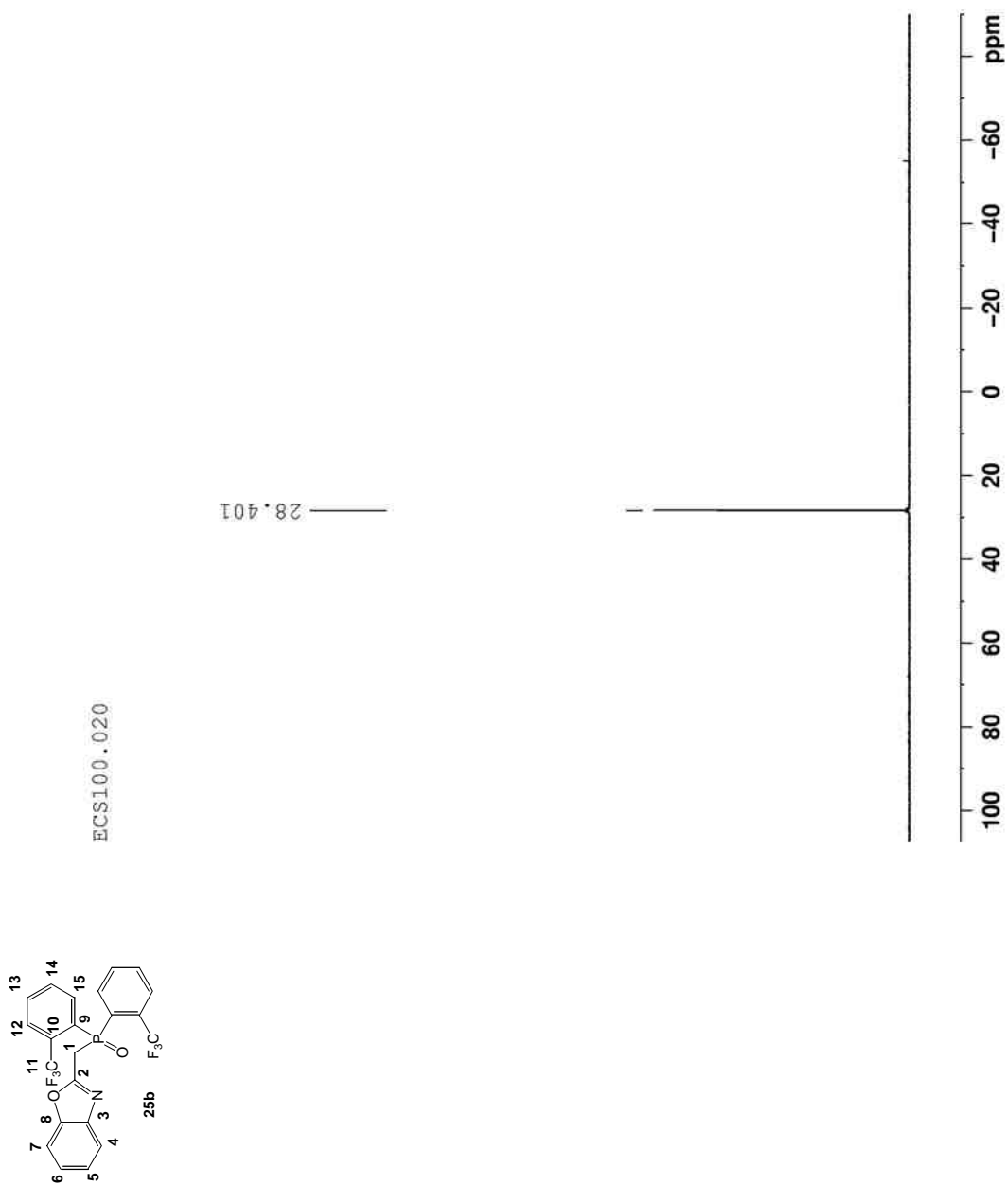
Single crystals suitable for X-ray diffraction were grown from ethyl acetate/hexane solution. Slow evaporation at room temperature, after several days gave colorless crystals. The crystal structure determination for **25b** was completed. Crystal parameters are given in Table 3.7 and selected bond lengths are given in Table 3.8. The molecular structure is displayed in Figure 3.29.

Figure 3.29 Molecular structure and atom labeling for 2-[bis-(2-trifluoromethylphenyl)-phosphinoylmethyl]-benzoxazole, 25b
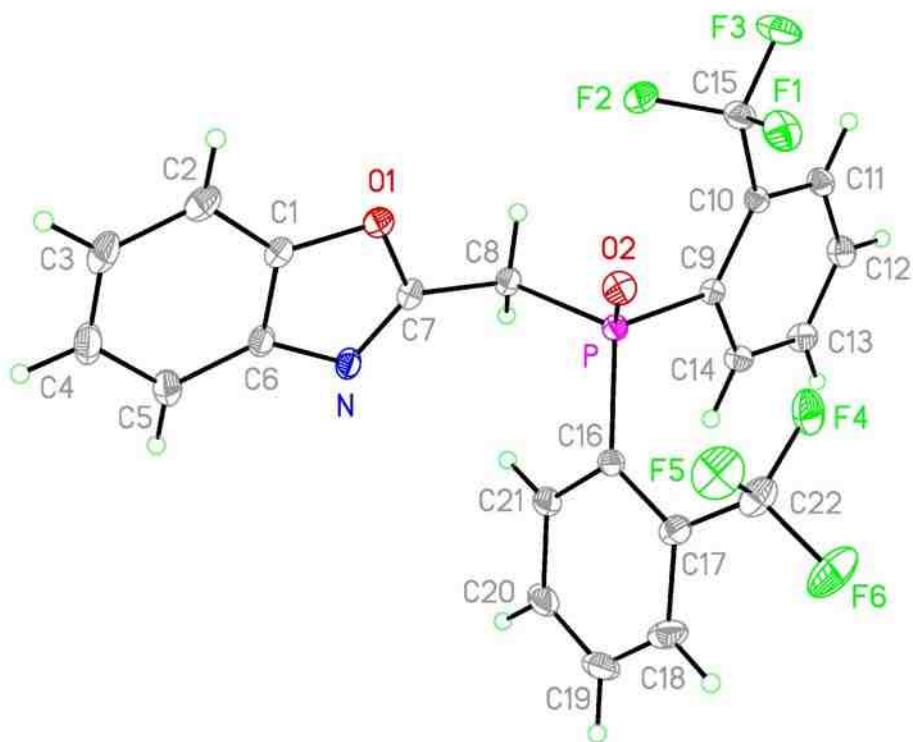
Table 3.7 Crystal parameters for 2-[bis-(2-trifluoromethylphenyl)-phosphinoylmethyl]-benzoxazole, 25b

Empirical formula	$C_{22} H_{14} F_6 N O_2 P$
Formula weight	469.31
Temperature	225(2) K
Wavelength	0.71073 Å
Crystal system	Monoclinic
Space group	P2(1)/n
Unit cell dimensions	a = 13.9184(7) Å $\quad$ α= 90°.
	b = 9.2015(5) Å $\quad$ β= 99.313(2)°.
	c = 15.9039(8) Å $\quad$ γ = 90°.
Volume	2009.97(18) Å³
Z	4
Density (calculated)	1.551 Mg/m³
Absorption coefficient	0.212 mm⁻¹
F(000)	952
Crystal size	0.41 x 0.39 x 0.25 mm³
Theta range for data collection	2.57 to 31.66°.
Index ranges	-20<=h<=20, -13<=k<=13, -22<=l<=23
Reflections collected	54342
Independent reflections	6777 [R(int) = 0.0196]
Completeness to theta = 31.66°	99.8 %
Absorption correction	Semi-empirical from equivalents

Max. and min. transmission	0.9460 and 0.9160
Refinement method	Full-matrix least-squares on F^2
Data / restraints / parameters	6777 / 0 / 289
Goodness-of-fit on F^2	1.049
Final R indices [I>2sigma(I)]	R1 = 0.0415, wR2 = 0.1194
R indices (all data)	R1 = 0.0507, wR2 = 0.1296
Largest diff. peak and hole	0.483 and -0.307 e.Å^{-3}

Table 3.8 Selected bond lengths [Å] for 2-[bis-(2-trifluoromethylphenyl)-phosphinoylmethyl]-benzoxazole, 25b

P-O(2)	1.4714(9)
P-C(16)	1.8170(13)
P-C(9)	1.8278(11)
P-C(8)	1.8304(13)
O(1)-C(7)	1.3521(16)
O(1)-C(1)	1.3838(17)
N-C(7)	1.2906(18)
N-C(6)	1.4004(17)
C(1)-C(6)	1.3788(19)
C(1)-C(2)	1.3814(19)
C(2)-C(3)	1.383(3)
C(3)-C(4)	1.387(3)
C(7)-C(8)	1.4823(18)

3.3.6 Coordination Chemistry

As with ligand **25a**, the coordination chemistry of **25b** was surveyed under a variety of conditions and selected results are described below.

Scheme 14

25b
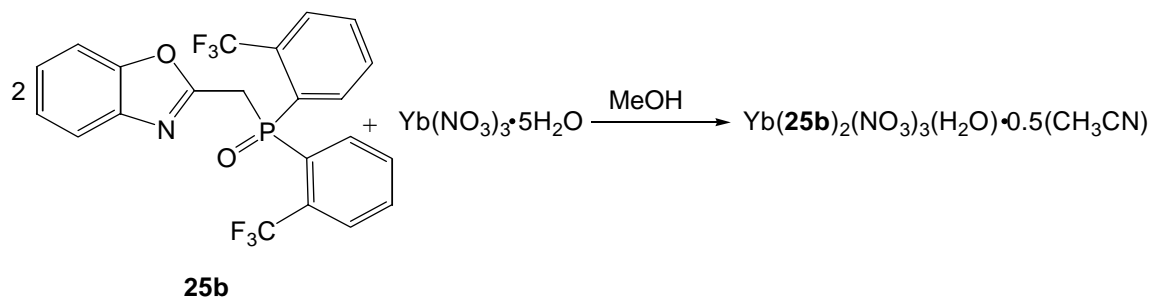
A sample of 2-[bis-(2-trifluoromethylphenyl)-phosphinoylmethyl]-benzoxazole (0.2 g, 0.43 mmol, 2 eq.) in MeOH (10 ml) was combined with Yb(NO$_3$)$_3$•5H$_2$O (0.1 g, 0.22 mmol, 1 eq.) in MeOH (2 ml). The mixture was stirred at 23 $^\circ$ C for 12 h. The solution was allowed to slowly evaporate at 23 $^\circ$ C. A white powder formed that was crystallized from CH$_3$CN to give colorless/pale yellow crystals: Yield 0.18 g, 64.3%, assuming the composition shown above (Scheme 14): mp > 250 $^\circ$ C.   An infrared spectrum (KBr cm^{-1}) is shown in Figure 3.30 and it is shown superimposed with the spectrum of free ligand **25b** in Figure 3.31. Infrared analysis did not show any significant peak shift for C=N toward low frequency and a peak shift of P=O band is in the range of 1125-1235 cm^{-1}. Single crystal X-ray crystallography was completed and crystal parameters are in Table 3.9 and selected bond lengths are summarized in Table 3.10. A view of the molecule is shown in Figure 3.32.

Elemental Analysis

Calculated for C$_{45}$H$_{31.50}$ F$_{12}$ N$_{5.50}$O$_{14}$P$_2$Yb   C, 40.44; H, 2.35; N, 5.76.

Found   C, 37.53; H, 2.63; N, 5.84.

Figure 3.30 IR spectrum for Yb(25b)$_2$(NO$_3$)$_3$(H$_2$O)•0.5(CH$_3$CN)
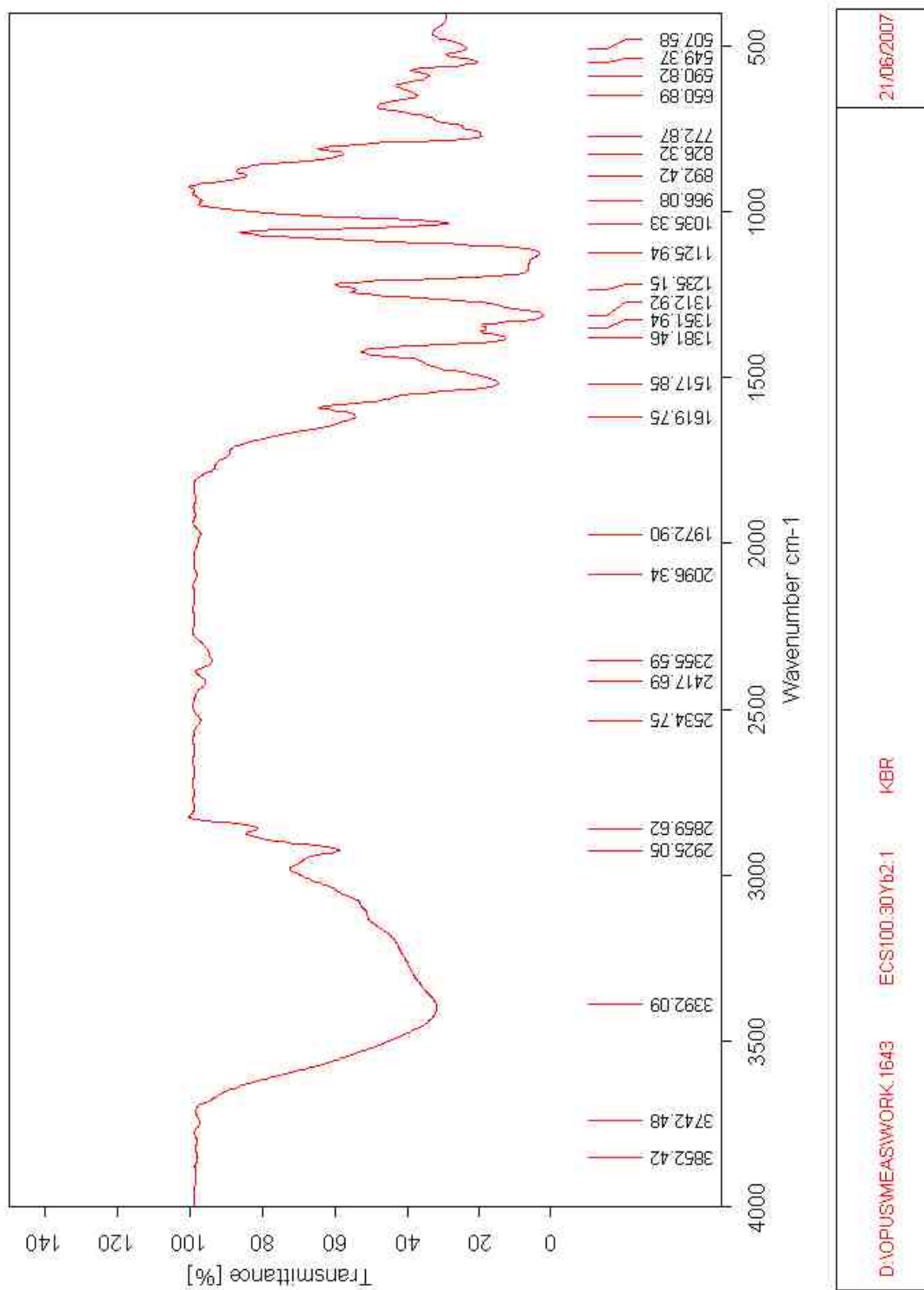
Figure 3.31 IR spectrum for Yb(25b)$_2$(NO$_3$)$_3$(H$_2$O)•0.5(CH$_3$CN) superimposed with free ligand, 25b
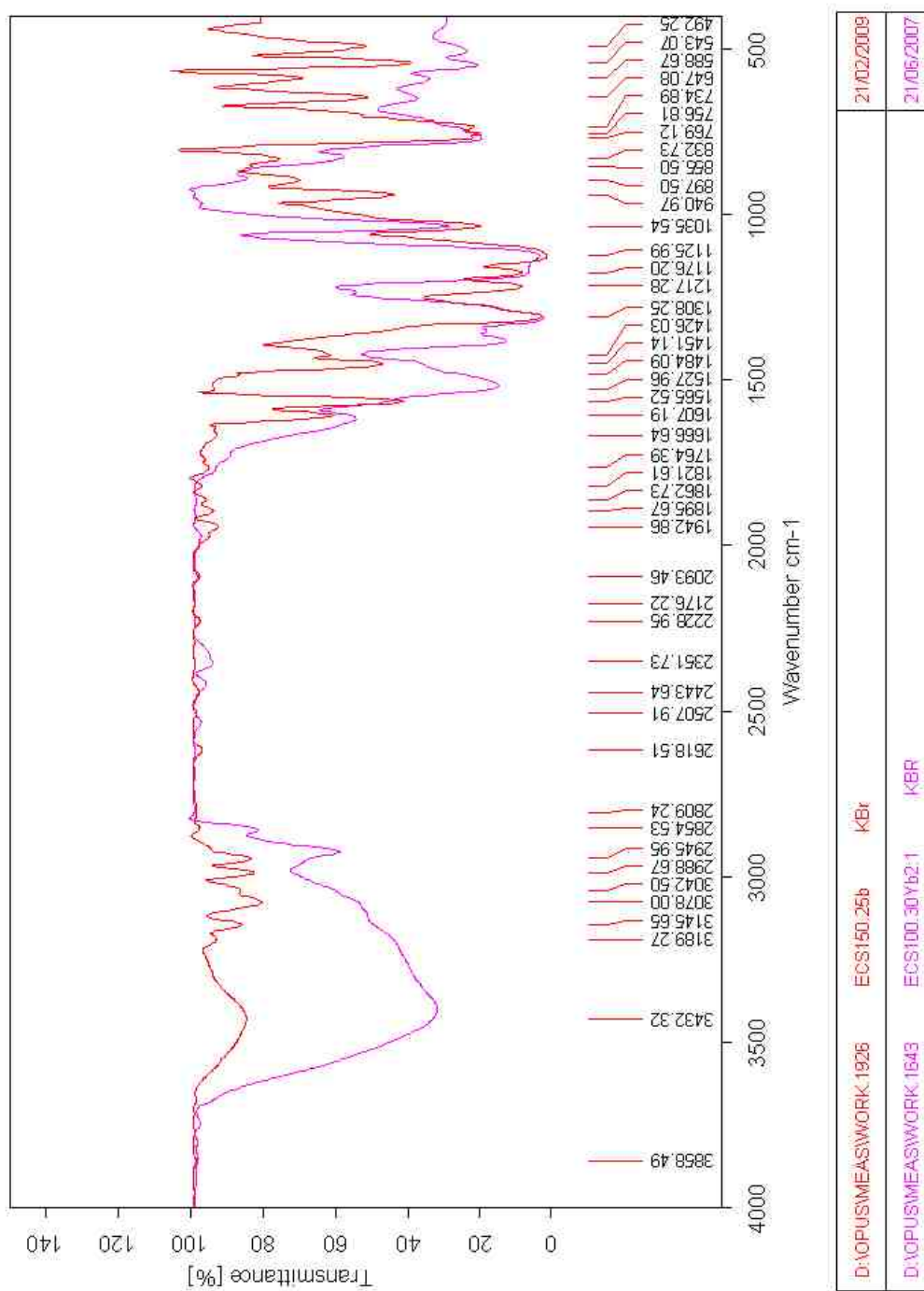
Figure 3.32 Molecular structure and atom labeling scheme for single molecular unit, Yb(25b)$_2$(NO$_3$)$_3$(H$_2$O)•0.5(CH$_3$CN)
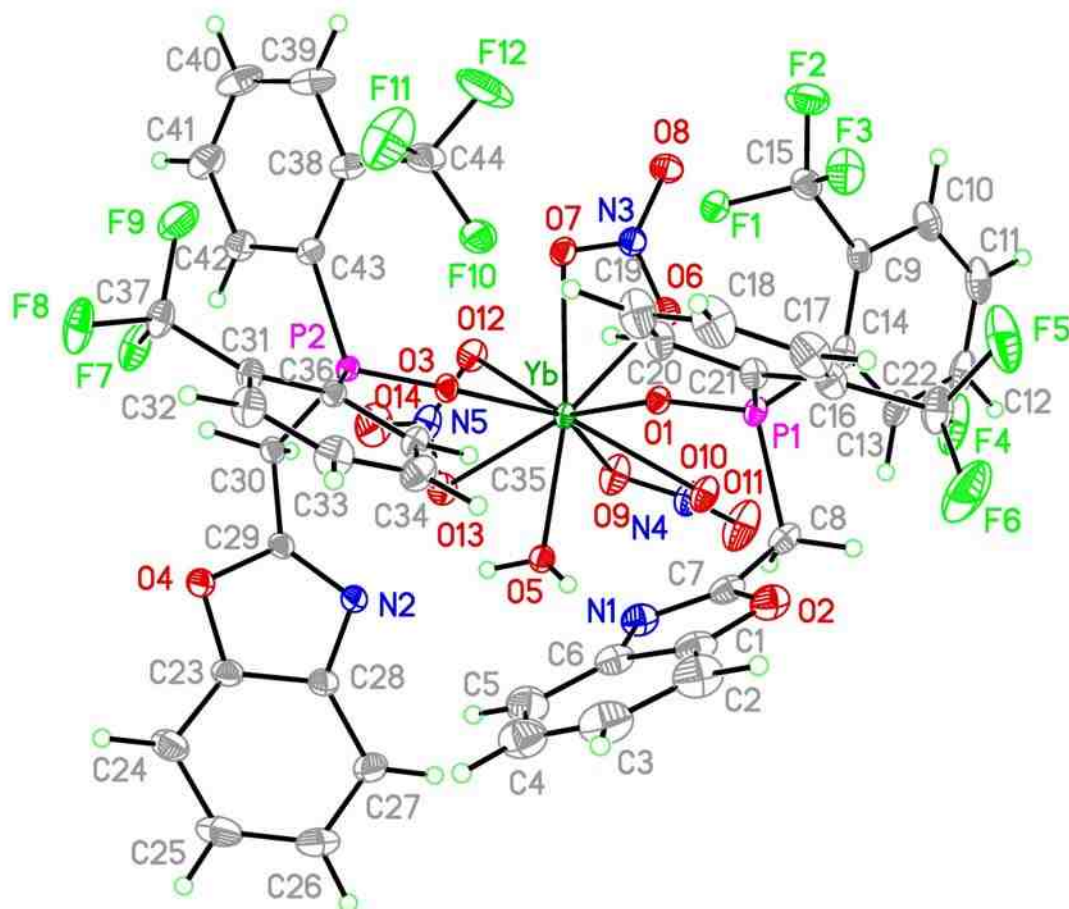
Table 3.9 Crystal parameters for Yb(25b)₂(NO₃)₃(H₂O)•0.5(CH₃CN)

Empirical formula	C_{45} $H_{31.50}$ F_{12} $N_{5.50}$ O_{14} P_2 Yb
Formula weight	1336.24
Temperature	225(2) K
Wavelength	0.71073 Å
Crystal system	Monoclinic
Space group	P2(1)/c
Unit cell dimensions	a = 11.8234(6) Å $\alpha = 90°$.
	b = 15.7990(8) Å $\beta = 92.062(2)°$.
	c = 26.8119(13) Å $\gamma = 90°$.
Volume	5005.2(4) $Å^3$
Z	4
Density (calculated)	1.773 Mg/m^3
Absorption coefficient	2.049 mm^{-1}
F(000)	2640
Crystal size	0.39 x 0.34 x 0.19 mm^3
Theta range for data collection	2.30 to 34.48°.
Index ranges	-18<=h<=18, -25<=k<=25, -42<=l<=42
Reflections collected	178785
Independent reflections	21100 [R(int) = 0.0263]
Completeness to theta = 34.48°	99.6 %
Absorption correction	Semi-empirical from equivalents
Max. and min. transmission	0.680 and 0.458

Refinement method	Full-matrix least-squares on F^2
Data / restraints / parameters	21100 / 1 / 731
Goodness-of-fit on F^2	1.081
Final R indices [I>2sigma(I)]	R1 = 0.0310, wR2 = 0.0723
R indices (all data)	R1 = 0.0472, wR2 = 0.0841
Largest diff. peak and hole	3.034 and -0.883 e.Å^{-3}

Table 3.10 Selected bond lengths [Å] for Yb(25b)$_2$(NO$_3$)$_3$(H$_2$O)•0.5(CH$_3$CN)

Yb-O(3)	2.2494(14)
Yb-O(1)	2.2691(14)
Yb-O(5)	2.3110(17)
Yb-O(6)	2.3541(18)
Yb-O(12)	2.3843(18)
Yb-O(9)	2.4306(19)
Yb-O(7)	2.4341(18)
Yb-O(10)	2.4359(18)
Yb-O(13)	2.4473(19)
P(1)-O(1)	1.4974(15)
P(1)-C(14)	1.811(2)
P(1)-C(21)	1.822(2)
P(1)-C(8)	1.833(3)
O(2)-C(7)	1.361(3)
O(2)-C(1)	1.371(4)
N(1)-C(7)	1.275(4)

N(1)-C(6)	1.413(4)
P(2)-O(3)	1.4940(15)
P(2)-C(43)	1.813(2)
P(2)-C(36)	1.820(2)
P(2)-C(30)	1.828(2)
N(2)-C(29)	1.290(3)
N(2)-C(28)	1.399(3)

Scheme 15

25b
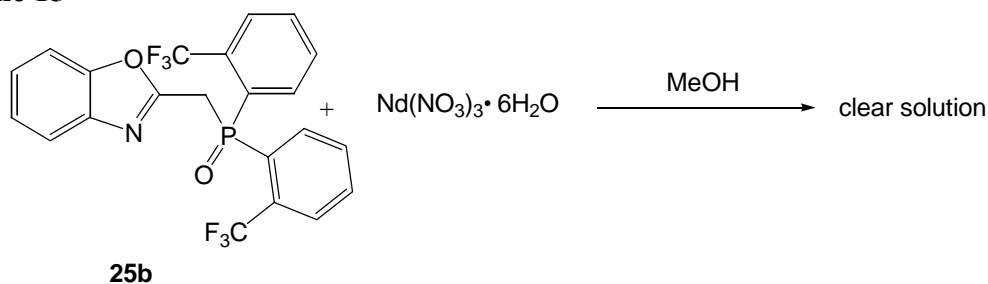
A sample of 2-[bis-(2-trifluoromethylphenyl)-phosphinoylmethyl]-benzoxazole

(0.2 g, 0.43 mmol, 1 eq.) in MeOH (10 ml) was combined with $Nd(NO_3)_3 \cdot 6H_2O$ (0.18 g,

0.43 mmol, 1eq.) in MeOH (5 ml). The mixture was stirred (12 h) to give a clear solution.

A white solid was formed after evaporation at room temperature. The mass of the solid

was 0.4 g. The powder was crystallized from hot dichloromethane to give pale yellow

crystals: Melting point 160-161 $^{\rm o}$C, i.e., the same as the mp for the free ligand. The

infrared spectrum (KBr cm^{-1}) did not indicate peak shifts for C=N. However, the P=O

peak shift appears in the range of 1126-1217 cm^{-1}. X-ray analysis of a crystal showed that

it is free ligand. Obviously no coordination with the Nd(III) occurred. Typical spectra are

shown in Figure 3.33 and 3.34.

Figure 3.33 IR spectrum for 2-[bis-(2-trifluoromethylphenyl)-phosphinoylmethyl]-benzoxazole, 25b + Nd(NO$_3$)$_3$•6H$_2$O
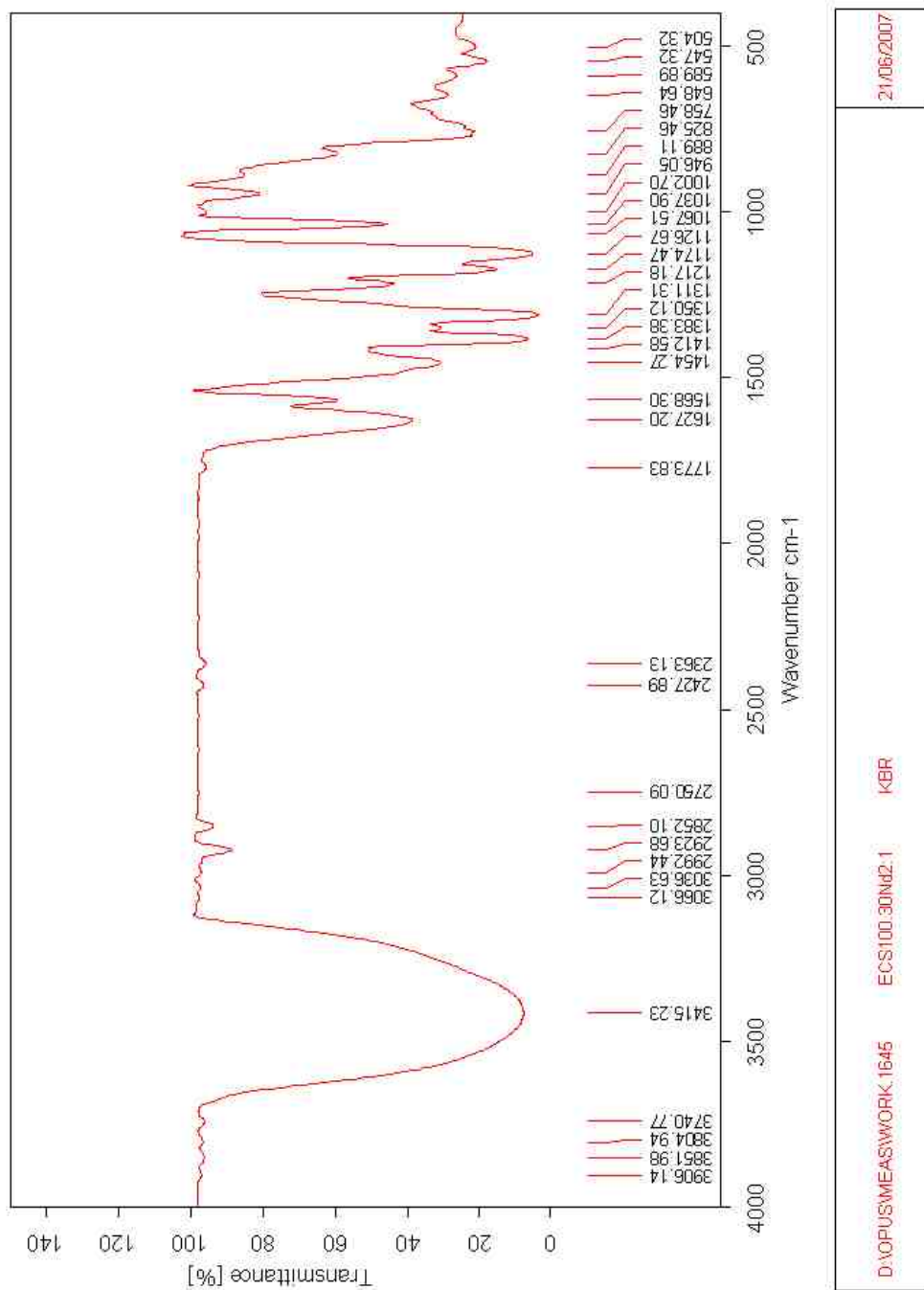
Figure 3.34 IR spectrum for 2-[bis-(2-trifluoromethylphenyl)-phosphinoylmethyl]-benzoxazole, 25b + Nd (NO$_3$)$_3$•6H$_2$O superimposed with the free ligand, 25b
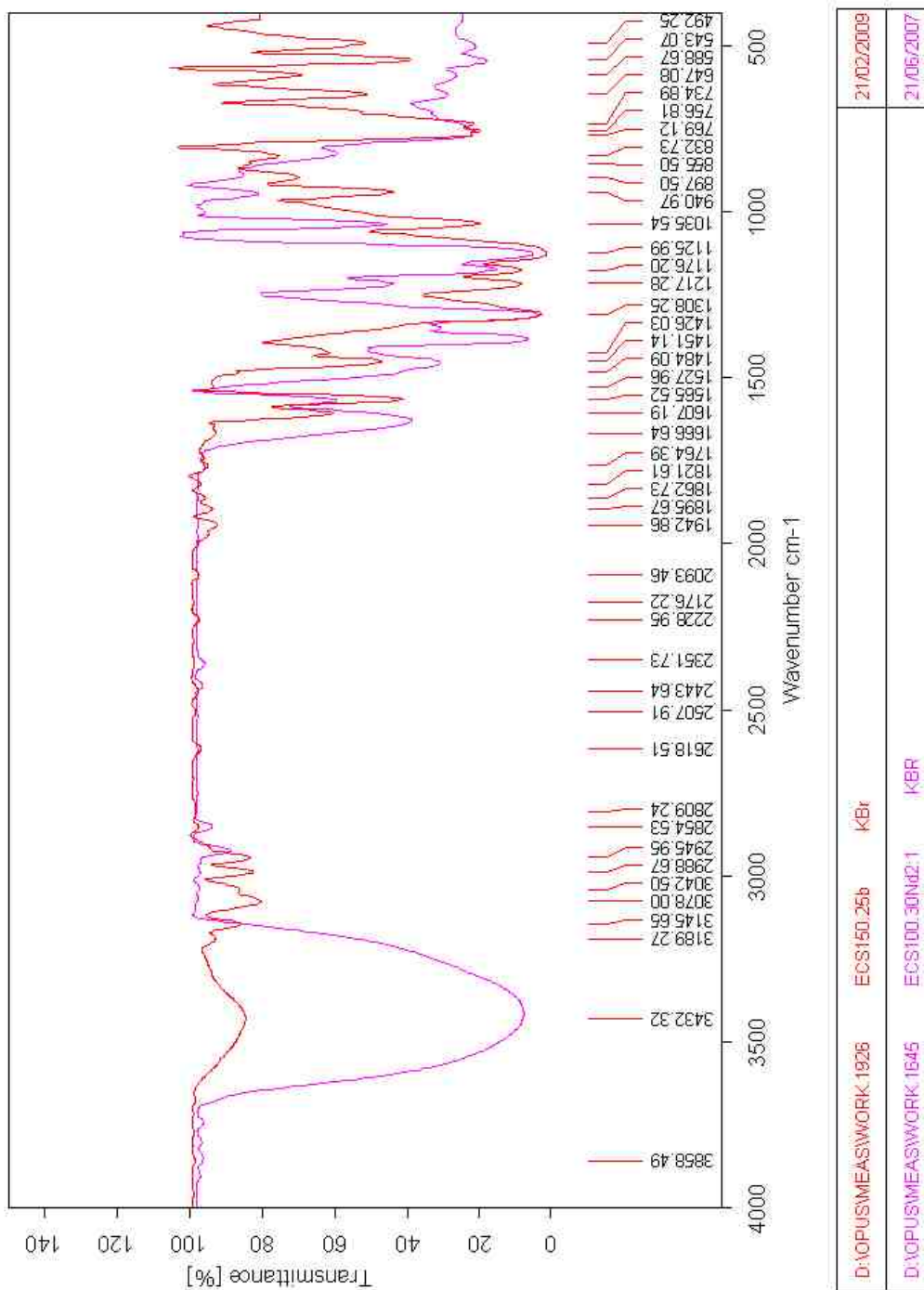
3.3.7 Synthesis of 2-(di-*o*-tolyl-phosphinoylmethyl)-benzoxazole, 25c

Scheme 16

25c
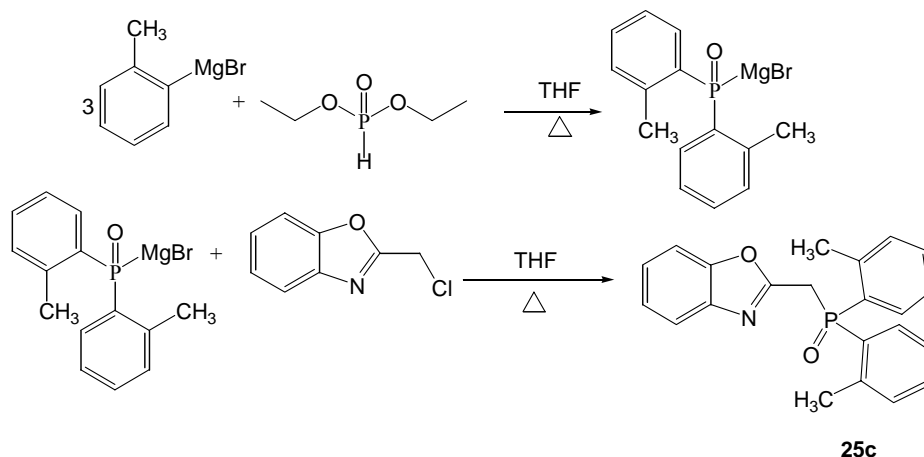
     This ligand was synthesized in order to compare its behavior against the –CF$_3$ analog compound **25b** (Scheme 13). A similar synthesis procedure[28-33, 40] was adapted with modifications as described below. A sample of *o*-tolylmagnesium bromide (6.5 ml, 2.0 M solution in Et$_2$O, 13.0 mmol, 3 eq.) was added to dry THF (15 ml) under dry nitrogen. To this solution was added dropwise a solution of diethyl phosphite (0.6 g, 4.4 mmol, 1 eq.) in dry THF (10 ml). The temperature rose during the addition. The mixture was refluxed (1 h, 70 °C), and 2-chloromethylbenzoxazole (0.7 g, 4.4 mmol, 1 eq.) in dry THF (10 ml) was added at 23 °C. This mixture was refluxed overnight (70 °C), volatiles were vacuum evaporated leaving a yellow solid. The yellow residue was treated with saturated aqueous NH$_4$Cl (100 ml) and extracted with CHCl$_3$ (3 x 20 ml). The combined CHCl$_3$ extracts were dried (Na$_2$SO$_4$) and vacuum evaporated. The resulting yellow residue was purified by column chromatography: silica gel 70-230 mesh, 60Å, eluted with 50% : 50% EtOAc: hexane, and finally 100% EtOAc to give a pale yellow oil: Yield 1.0 g (67%). The yellow oil was washed with a mixture of CH$_2$Cl$_2$/hexane, dried under vacuum for 2 days to give **25c** as a white solid, mp 161 – 162 °C.

Single crystals suitable for X-ray crystal structure determination were grown from a loosely capped solution of EtOAc/hexane/CH_2Cl_2 over two weeks that gave pale yellow crystals. A view of the molecule is displayed in Figure 3.41. Crystal parameters are given in Table 3.11 and selected bond lengths are given in Table 3.12. Compound **25c** is soluble in toluene, ethyl acetate, dichloromethane and methanol. Insoluble in hexane, pentane and *o*-xylene. For extraction, the solubility in toluene was found to be 0.0409 M and in trifluoromethanesulfonyl-benzene is 0.042 M.

Elemental Analysis

Calculated for $C_{22} H_{20} N O_2 P$ (FW= 361.12 g/mole): C, 73.12; H, 5.58; N, 3.88.

Found   C, 72.83; H, 5.66; N, 3.86.

Selected spectroscopic data are summarized here and typical spectra are displayed in Figures 3.35 – 3.40.

Infrared spectrum (KBr, cm^{-1}): 1603 ($\nu_{C=N}$), 1178 ($\nu_{P=O}$).

^{1}H (250MHz, 23 ^{o}C, CDCl$_3$), δ (ppm): 2.3 (s, 6H, -CH$_3$), 4.1 (d, 2H, -CH$_2$-P=O, $^2J_{H-P}$ = 14.2 Hz), 7.1-7.2 (m, 6H, H-Ar), 7.3 (m, 3H, H-Ar), 7.5 (m, 1H, H-Ar), 7.7-7.8 (d, 2H, H$_{15}$, $^3J_{H-P}$ = 13.8 Hz).

^{1}H (500 MHz, 23 ^{o}C, CDCl$_3$ ^{31}P coupled), δ (ppm): 2.4 (s, 6H, -CH$_3$), 4.2 (d, 2H, -CH$_2$-P=O, $^2J_{H-P}$ = 14.2 Hz), 7.2 (m, 6H, H-Ar), 7.3-7.4 (m, 3H, H-Ar), 7.5-7.6 (m, 1H, H-Ar), 7.7-7.8 (d, 2H, H$_{15}$, $^3J_{H-P}$ = 13.8 Hz).

^{1}H (500 MHz, 23 ^{o}C, CDCl$_3$ ^{31}P decoupled), δ (ppm): 2.4 (s, 6H, -CH$_3$), 4.2 (s, 2H, -CH$_2$-P=O), 7.1-7.2 (m, 5H, H-Ar), 7.3-7.4 (m, 3H, H-Ar), 7.5 (m, 1H, H-Ar), 7.7 (s, 2H, H$_{15}$).

$^{13}C\{^1H\}$ (62.9 MHz, 23 ^{o}C, CDCl$_3$): δ (ppm), 21.4 (d, C_{11}, $^3J_{C-P}$ = 4.3 Hz), 32.6 (d, C_1, $^1J_{C-P}$ = 63.0 Hz), 110.6 (s), 119.8 (s), 124.3 (s), 124.9 (s), 125.9 (d, *ortho*-aryl, $^2J_{C-P}$ = 12.5 Hz), 130.5 (d, *ipso*-aryl, $^1J_{C-P}$ = 100.3 Hz), 131.9 (d, J_{C-P} = 7.7 Hz), 132.1 (d, J_{C-P} = 7.3 Hz), 132.3 (d, J_{C-P} = 2.4 Hz), 141.3 (s), 142.2 (d, *meta*-aryl, $^3J_{C-P}$ = 9.0 Hz), 151.2 (s), C-Ar, 159.3 (d, C_2, $^2J_{C-P}$ = 8.5 Hz).

$^{13}C\{^1H\}$ (125.7 MHz, 23 ^{o}C, CDCl$_3$), δ (ppm): 21.0 (d, C_{11}, $^3J_{C-P}$ = 15.3 Hz), 32.3 (d, C_1, $^1J_{C-P}$ = 64.8 Hz), 110.4 (s), 119.5 (s), 123.9 (s), 124.6 (s), 125.6 (d, *ortho*-aryl, $^2J_{C-P}$ = 12.8 Hz), 130.2 (d, *ipso*-aryl, $^1J_{C-P}$ = 100.3 Hz), 131.6 (d, J_{C-P} = 11.8 Hz), 131.7 (d, J_{C-P} = 11.1 Hz), 132.0 (s), 141.0 (s), 141.9 (d, *meta*-aryl, $^3J_{C-P}$ = 9.7 Hz), 151.1 (s), C-Ar, 159.0 (d, C_2, $^2J_{C-P}$ = 8.5 Hz).

$^{13}C\{^1H, ^{31}P\}$ (125.7 MHz, 23 ^{o}C, CDCl$_3$), δ (ppm): 21.0 (s, C_{11}), 32.3 (s, C_1), 110.3 (s), 119.5 (s), 124.0 (s), 124.6 (s), 125.6 (s, *ortho*-aryl), 130.2 (s, *ipso*-aryl), 131.6 (s), 131.8 (s), 132.1 (s), 141.0 (s), 141.9 (s, *meta*-aryl), 150.9 (s), C-Ar, 159.0 (s, C_2).

$^{31}P\{^1H\}$ (101.3 MHz, 23 ^{o}C, CDCl$_3$): δ (ppm), 31.1, -CH$_2$-P=O.

Mass spectrum (ESI) *m/e* (fragment, relative intensity): [M+H$^+$] = 362.1304 and the calculated exact mass is 361.1232.

Figure 3.35 Infrared spectrum (KBr, cm^{-1}) for 2-(di-*o*-tolyl-phosphinoylmethyl)-benzoxazole, 25c

Figure 3.36(a) 250 MHz ^{1}H NMR spectrum for 2-(di-*o*-tolyl-phosphinoylmethyl)-benzoxazole, 25c
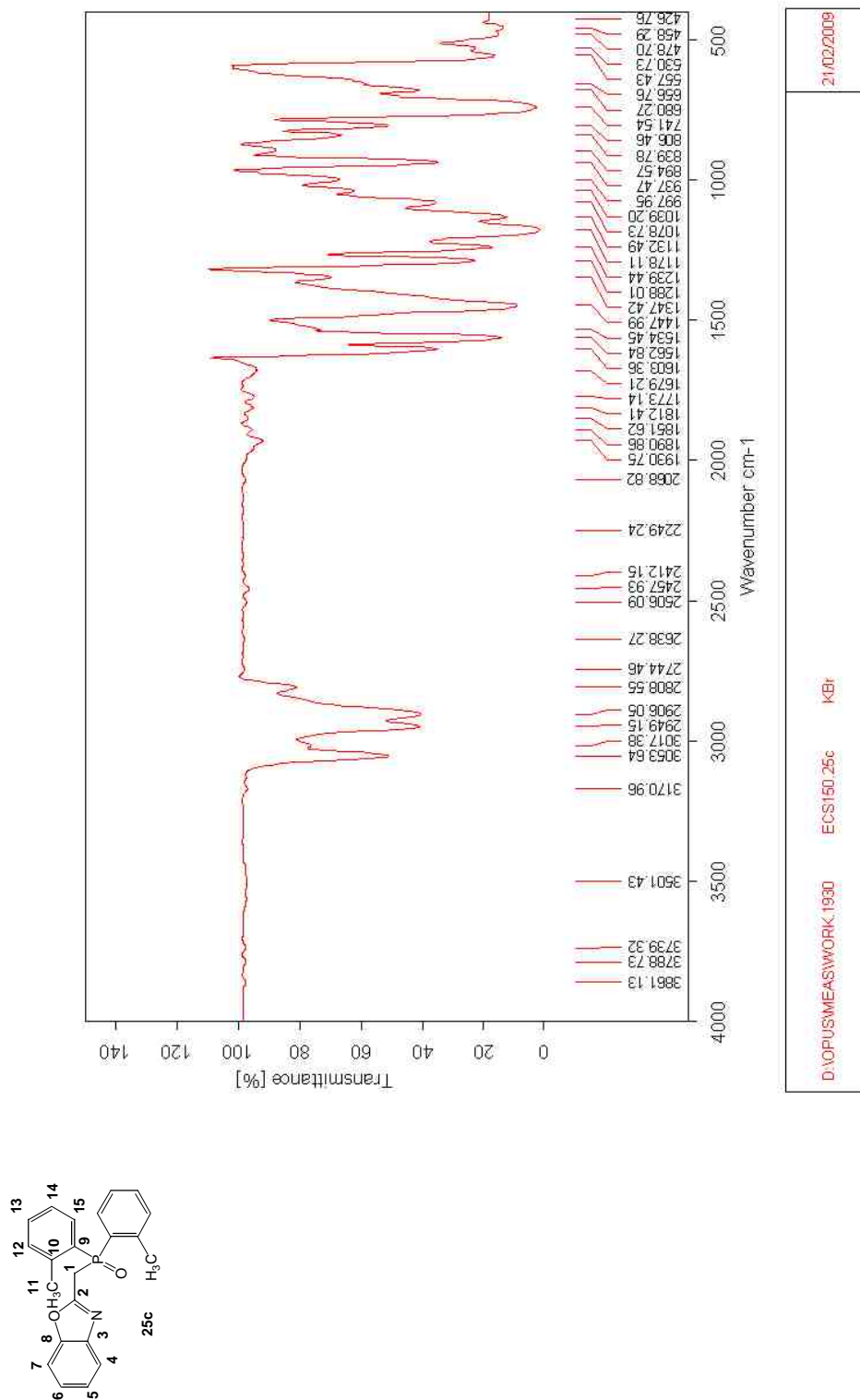
Figure 3.36(b) 500 MHz ^{1}H NMR spectrum for 2-(di-*o*-tolyl-phosphinoylmethyl)-benzoxazole, 25c with ^{31}P coupling

Figure 3.36(c) 500 MHz ^{1}H NMR spectrum for 2-(di-*o*-tolyl-phosphinoylmethyl)-benzoxazole, 25c with ^{31}P decoupling
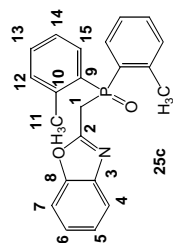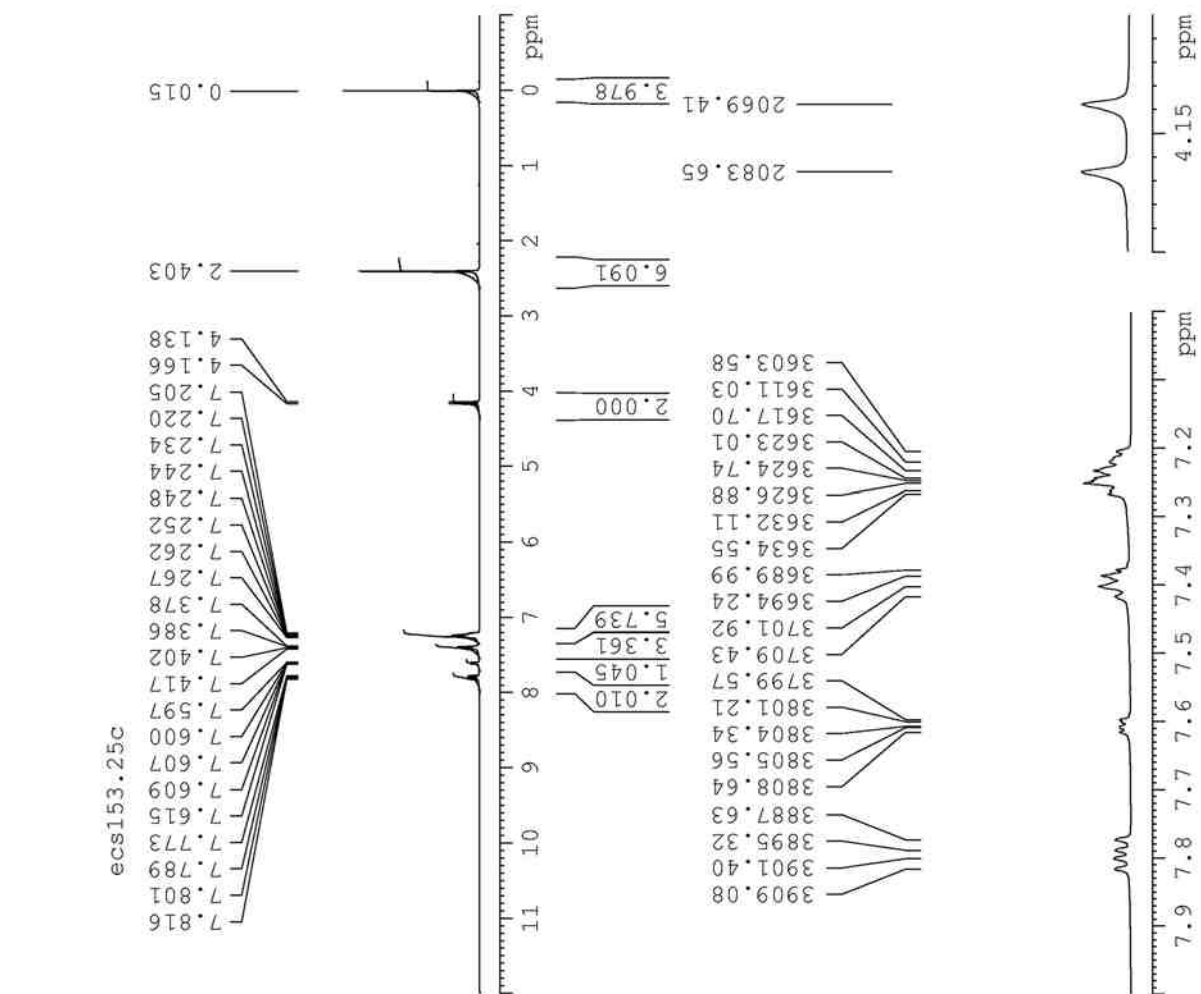
Figure 3.37 62.9 MHz $^{13}C\{^1H\}$ NMR spectrum for 2-(di-*o*-tolyl-phosphinoylmethyl)-benzoxazole, 25c
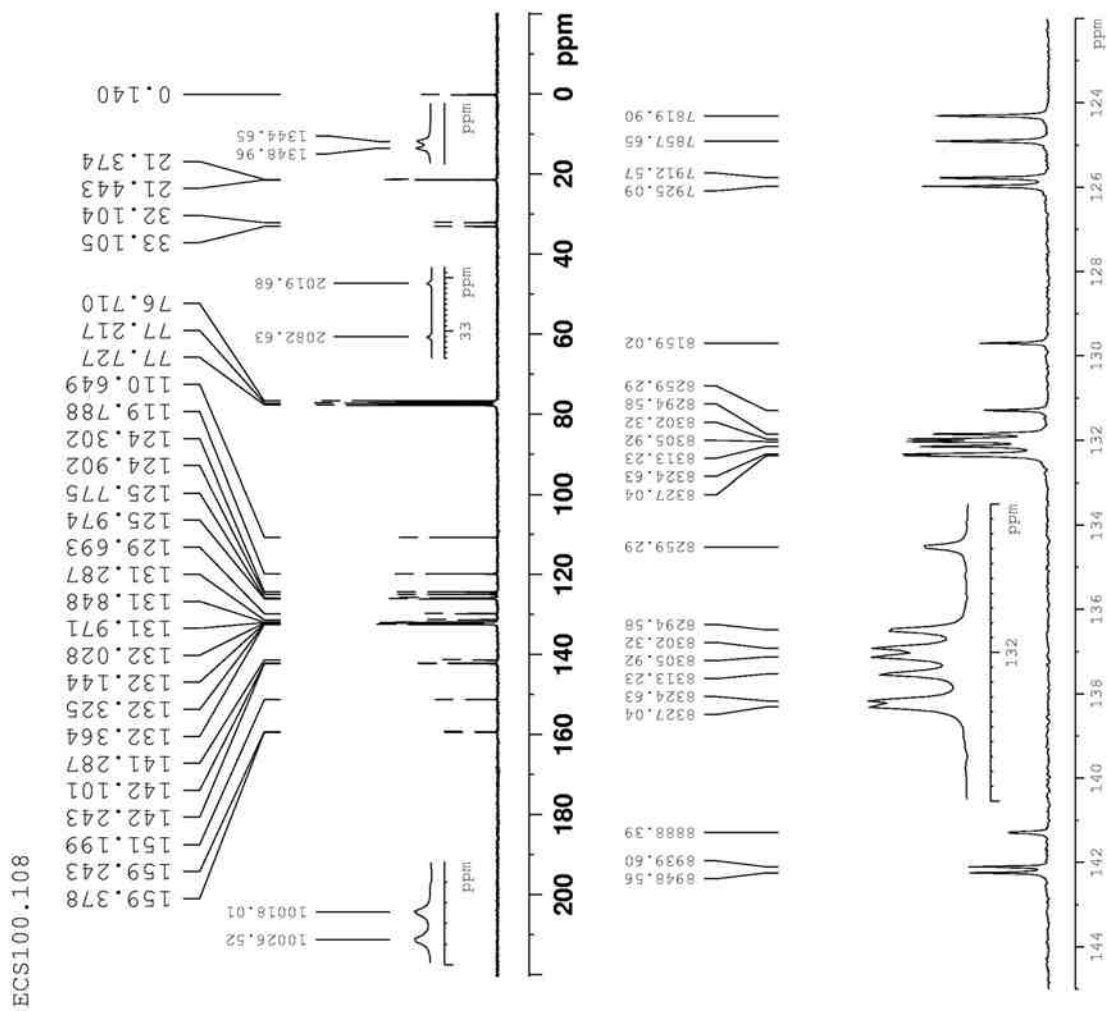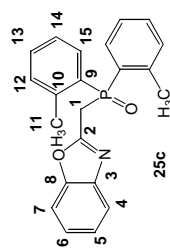
Figure 3.38 125.7 MHz ^{13}C{^{1}H} NMR spectrum for

2-(di-*o*-tolyl-phosphinoylmethyl)-benzoxazole, 25c

26635.05
26650.33
20.953
21.075
32.039
32.554

4029.20
4093.98

76.765
76.985
77.314
110.350
119.480
123.985
124.585
125.508
125.609
129.838
130.635
131.582
131.676
131.704
131.793
132.031
141.025
141.847
141.924
151.059
158.982
159.049

ecs153.068

155592.04
15667.54
15783.56
15796.33

16328.08
16428.41
16547.50
16559.31
16562.88
16574.02
16603.89

16547.50
16559.31
16562.88
16574.02

16603.89

132.0

17735.01
17838.31
17848.04

ppm
20
40
60
80
100
120
140
160
180
200

ppm
124
126
128
130
132
134
136
138
140
142
144

Figure 3.39 125.7 MHz ¹³C{¹H, ³¹P} NMR spectrum for

2-(di-*o*-tolyl-phosphinoylmethyl)-benzoxazole, 25c
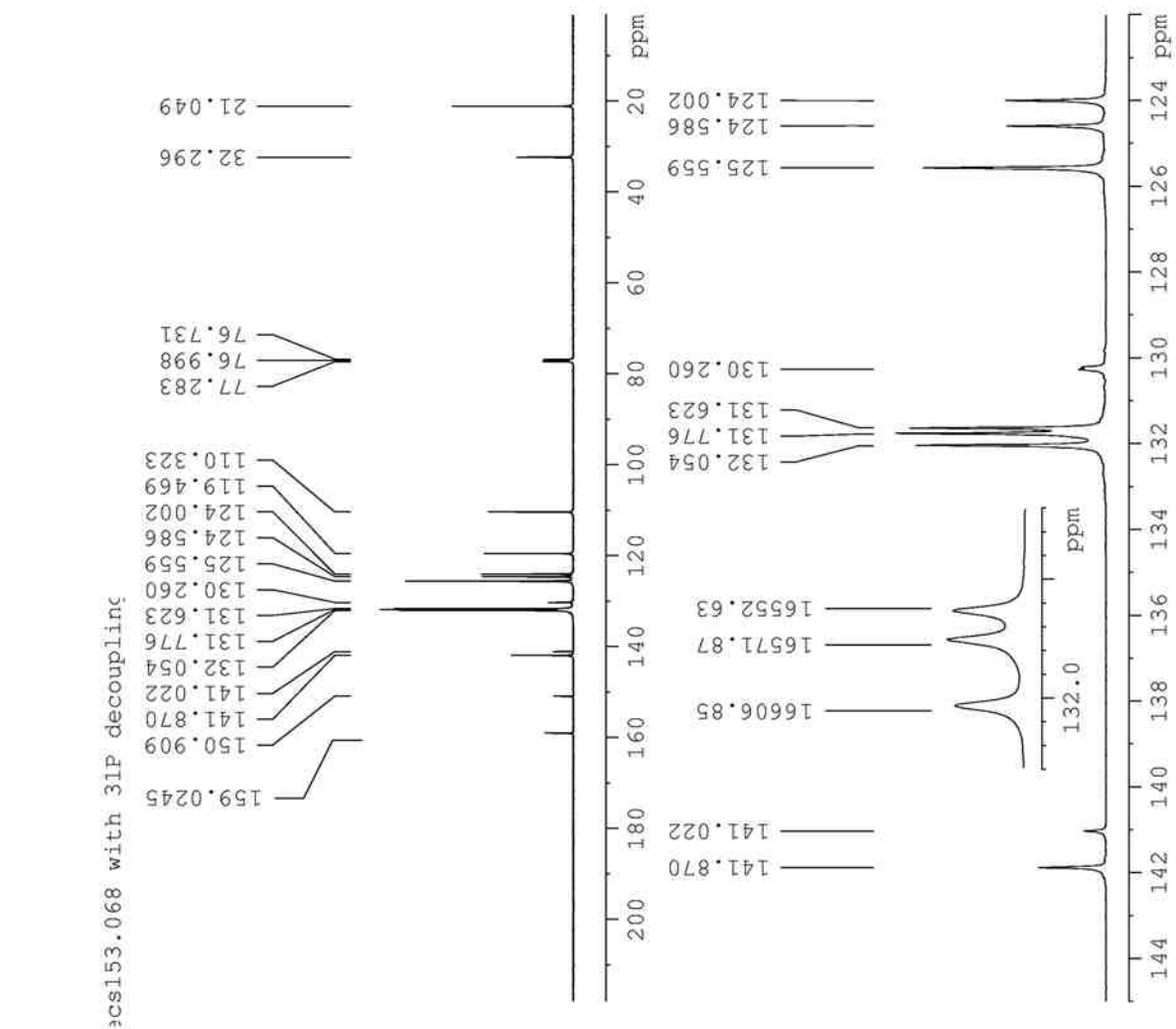
Figure 3.40 101.3 MHz ^{31}P{^{1}H} NMR spectrum for 2-(di-*o*-tolyl-phosphinoylmethyl)-benzoxazole, 25c
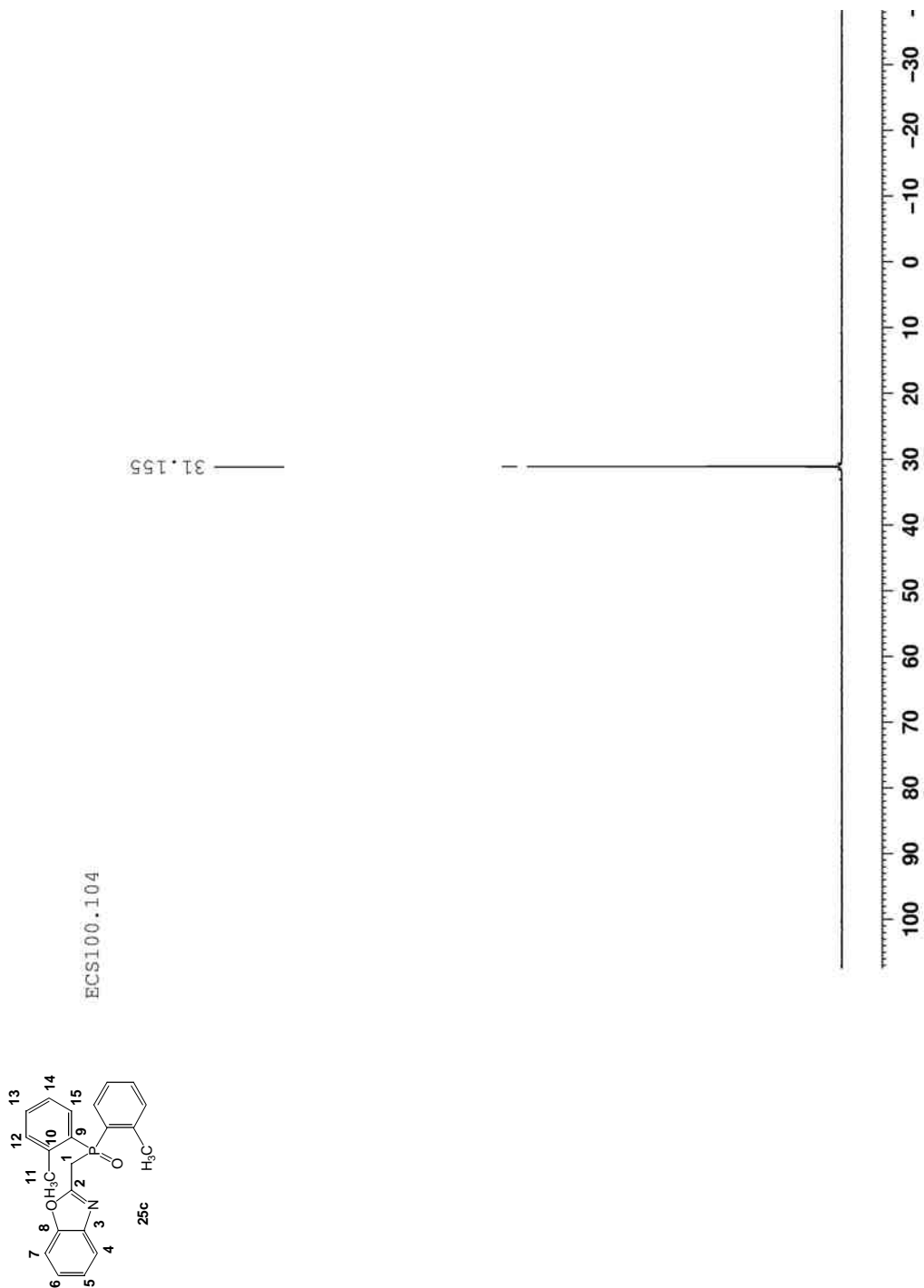
Figure 3.41 Molecular structure and atom labeling for single molecular unit, 2-(di-*o*-tolyl-phosphinoylmethyl)-benzoxazole, 25c
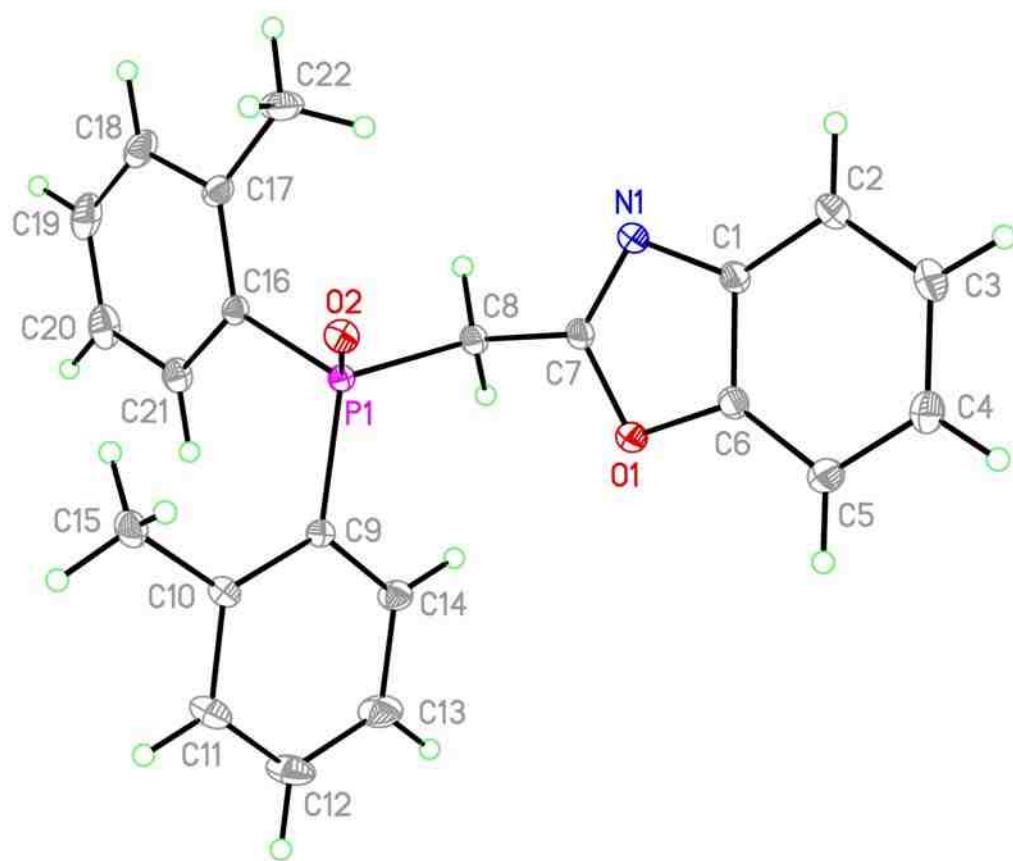
Table 3.11 Crystal parameters for 2-(di-*o*-tolyl-phosphinoylmethyl)-benzoxazole, 25c

Empirical formula	$C_{22} H_{20} N O_2 P$
Formula weight	361.36

Temperature	225(2) K	
Wavelength	0.71073 Å	
Crystal system	Monoclinic	
Space group	P2(1)/c	
Unit cell dimensions	a = 8.4150(5) Å	$\alpha = 90°$.
	b = 18.9817(11) Å	$\beta = 98.419(2)°$.
	c = 11.5290(6) Å	$\gamma = 90°$.
Volume	1821.69(18) Å^3	
Z	4	
Density (calculated)	1.318 Mg/m^3	
Absorption coefficient	0.167 mm^{-1}	
F(000)	760	
Crystal size	0.47 x 0.34 x 0.23 mm^3	
Theta range for data collection	2.45 to 32.15°.	
Index ranges	-12<=h<=12, -28<=k<=28, -17<=l<=17	
Reflections collected	74096	
Independent reflections	6263 [R(int) = 0.0243]	
Completeness to theta = 30.00°	100.0 %	
Absorption correction	Semi-empirical from equivalents	
Max. and min. transmission	0.9600 and 0.9200	
Refinement method	Full-matrix least-squares on F^2	
Data / restraints / parameters	6263 / 0 / 237	
Goodness-of-fit on F^2	1.087	

Final R indices [I>2sigma(I)]	R1 = 0.0384, wR2 = 0.1076
R indices (all data)	R1 = 0.0440, wR2 = 0.1141
Largest diff. peak and hole	0.455 and -0.212 e.$Å^{-3}$

Table 3.12 Selected bond lengths [Å] for 2-(di-*o*-tolyl-phosphinoylmethyl)-benzoxazole, 25c

P(1)-O(2)	1.4892(8)
P(1)-C(16)	1.8068(10)
P(1)-C(9)	1.8074(10)
P(1)-C(8)	1.8333(10)
O(1)-C(7)	1.3631(13)
O(1)-C(6)	1.3803(13)
N(1)-C(7)	1.2931(13)
N(1)-C(1)	1.3999(14)
C(1)-C(6)	1.3829(15)
C(1)-C(2)	1.3898(15)
C(2)-C(3)	1.3866(19)
C(3)-C(4)	1.3915(19)
C(4)-C(5)	1.3876(18)
C(5)-C(6)	1.3830(16)
C(7)-C(8)	1.4805(14)

3.3.8 Coordination Chemistry

As with ligand **25a** and **25b**, the coordination chemistry of **25c** was surveyed under a variety of conditions and selected results are described below.

Scheme 17

25c
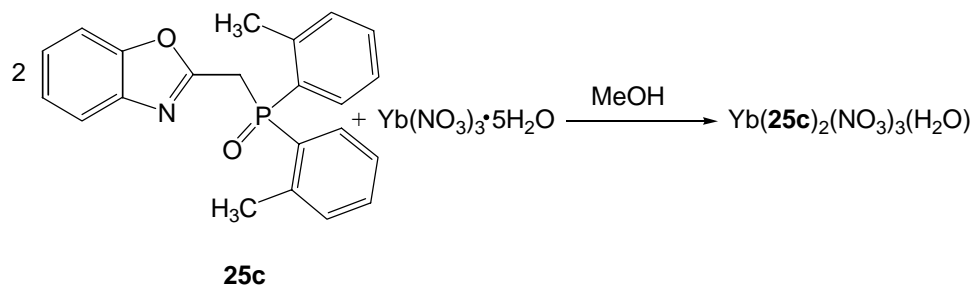
2-(Di-*o*-tolyl-phosphinoylmethyl)-benzoxazole (0.2 g, 0.55 mmol, 2 eq.) was dissolved in MeOH (10 ml). To this solution, $Yb(NO_3)_3 \cdot 5H_2O$ (0.12 g, 0.28 mmol, 1 eq.) dissolved in MeOH (2 ml) was added. The solution was stirred at 23 $^\circ$ C for 12 h. The mixture was left open to evaporate slowly for 4 days at room temperature. A pale yellow solid formed (0.37 g). The solid was crystallized from $CH_3CN/MeOH$ solution, capped for 7 days and later left open for 5 days. White crystals formed: Yield 0.26 g, (85.5%), assuming the composition **$Yb(25c)_2(NO_3)_3(H_2O)$**: mp 199-200 $^{\circ}$C. An X-ray crystal structure determination was completed. Crystal parameters are in Table 3.13 and selected bond lengths are summarized in Table 3.14. A view of molecule is shown in Figure 3.44. The infrared spectrum (KBr, cm^{-1}) displays a band at 1151 (ν_{PO}), and this corresponds to a peak shift of $\Delta\nu_{PO} = 27\ cm^{-1}$ relative to the free ligand. Typical spectra are shown in Figure 3.42 and 3.43.

Elemental Analysis

Calculated for $C_{44}H_{42}N_5YbO_{14}P_2$ C, 48.04; H, 3.81; N, 6.36.

Found   C, 44.73; H, 3.67; N, 6.38.

Figure 3.42 Infrared spectrum (KBr, cm^{-1}) for Yb(25c)$_2$(NO$_3$)$_3$(H$_2$O)
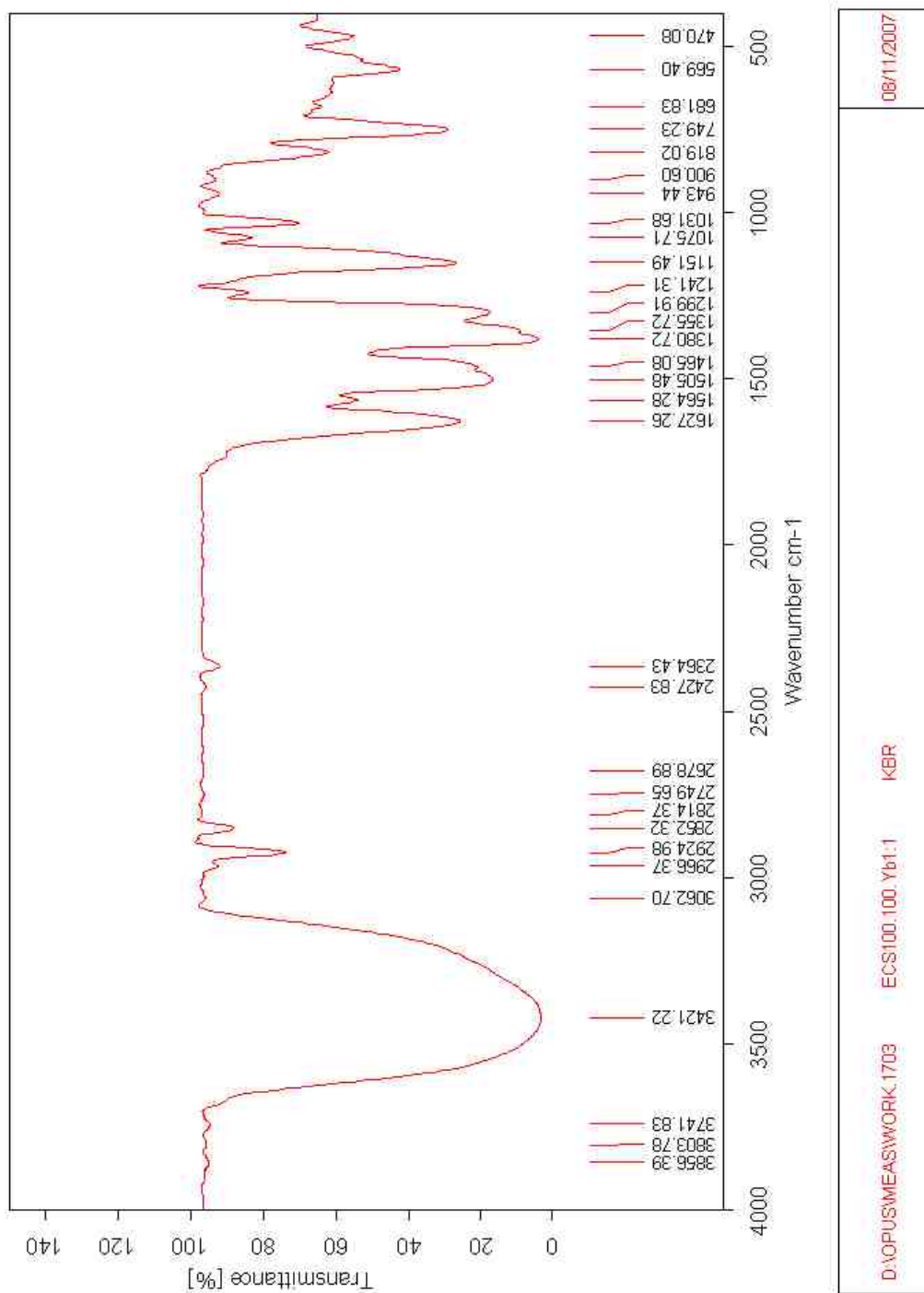
Figure 3.43 Infrared spectrum (KBr, cm^{-1}) for Yb(25c)$_2$(NO$_3$)$_3$(H$_2$O) complex superimposed with a free ligand, 25c
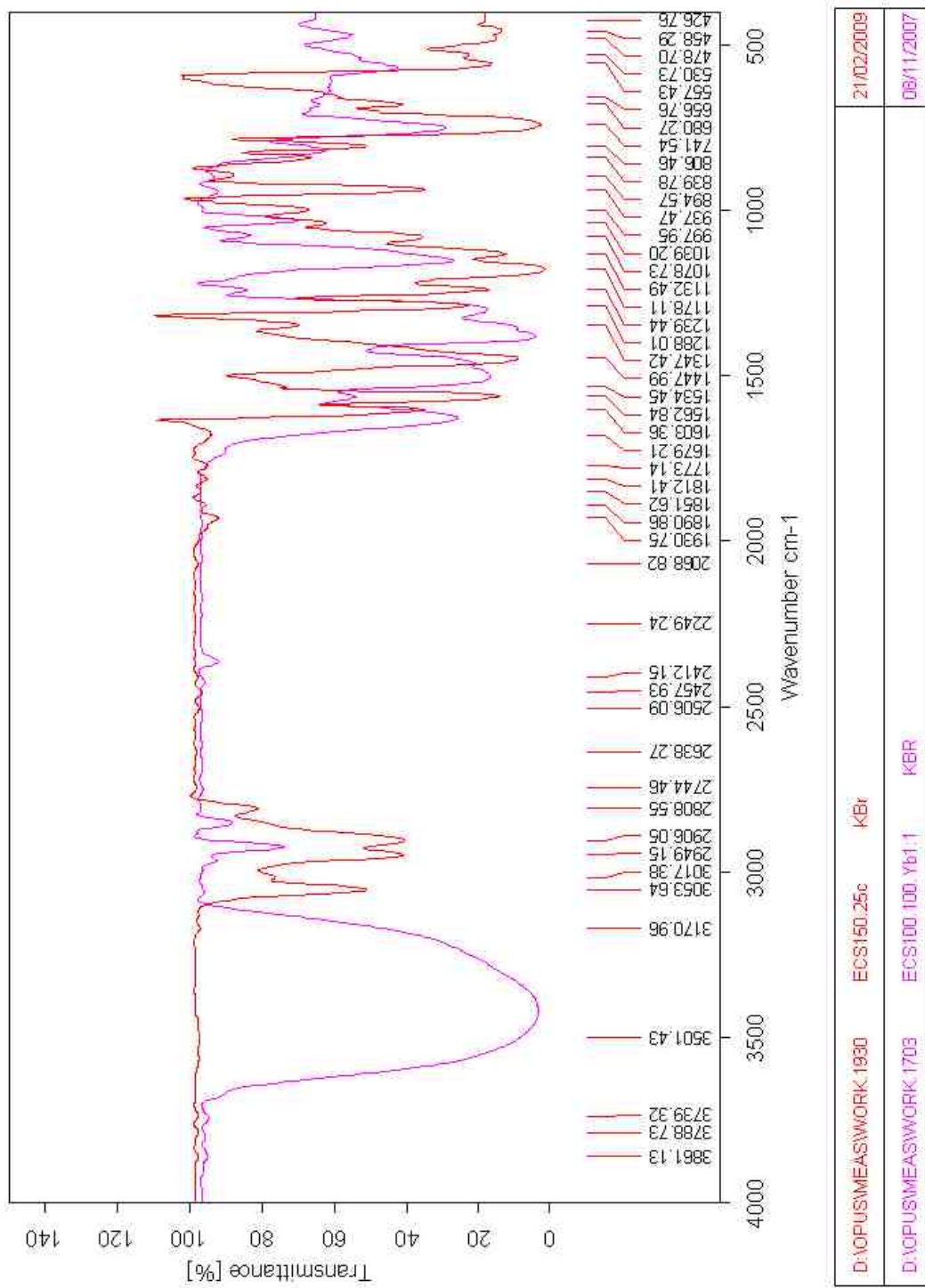
Figure 3.44 Molecular structure and atom labeling scheme for Yb(25c)$_2$(NO$_3$)$_3$(H$_2$O)
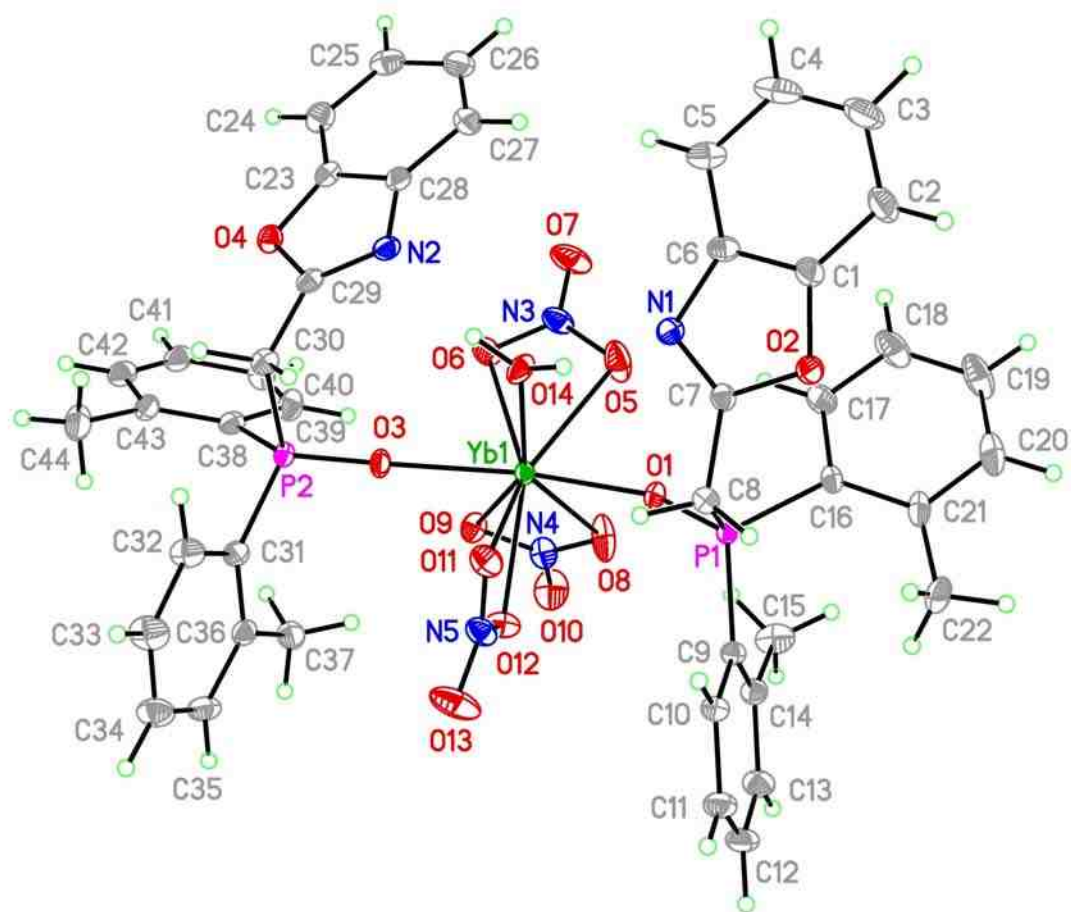
Table 3.13 Crystal parameters for Yb(25c)$_2$(NO$_3$)$_3$(H$_2$O)

Empirical formula	C$_{44}$ H$_{42}$ N$_5$ O$_{14}$ P$_2$ Yb
Formula weight	1099.81
Temperature	225(2) K
Wavelength	0.71073 Å
Crystal system	Orthorhombic
Space group	P2(1)2(1)2(1)
Unit cell dimensions	a = 10.6206(6) Å α= 90°.
	b = 11.6896(7) Å β= 90°.
	c = 37.538(2) Å γ = 90°.
Volume	4660.4(5) Å^3
Z	4
Density (calculated)	1.567 Mg/m^3
Absorption coefficient	2.146 mm^{-1}
F(000)	2212
Crystal size	0.46 x 0.25 x 0.14 mm^3
Theta range for data collection	2.65 to 33.96°.
Index ranges	-16<=h<=16, -18<=k<=18, -58<=l<=58
Reflections collected	183428
Independent reflections	18864 [R(int) = 0.0505]
Completeness to theta = 33.96°	99.5%
Absorption correction	Semi-empirical from equivalents
Max. and min. transmission	0.750 and 0.430

Refinement method	Full-matrix least-squares on F^2
Data / restraints / parameters	18864 / 0 / 587
Goodness-of-fit on F^2	1.005
Final R indices [I>2sigma(I)]	R1 = 0.0366, wR2 = 0.0829
R indices (all data)	R1 = 0.0415, wR2 = 0.0851
Largest diff. peak and hole	1.199 and -1.849 e.Å^{-3}

Table 3.14 Selected bond lengths [Å] for Yb(25c)$_2$(NO$_3$)$_3$(H$_2$O)

Yb(1)-O(1)	2.233(2)
Yb(1)-O(3)	2.234(2)
Yb(1)-O(14)	2.285(3)
Yb(1)-O(12)	2.369(3)
Yb(1)-O(8)	2.392(3)
Yb(1)-O(6)	2.411(3)
Yb(1)-O(9)	2.448(3)
Yb(1)-O(5)	2.453(3)
Yb(1)-O(11)	2.513(3)
P(1)-O(1)	1.494(2)
P(1)-C(9)	1.787(3)
P(1)-C(16)	1.799(3)
P(1)-C(8)	1.839(3)
P(2)-O(3)	1.495(2)
P(2)-C(38)	1.785(2)

Scheme 18

25c
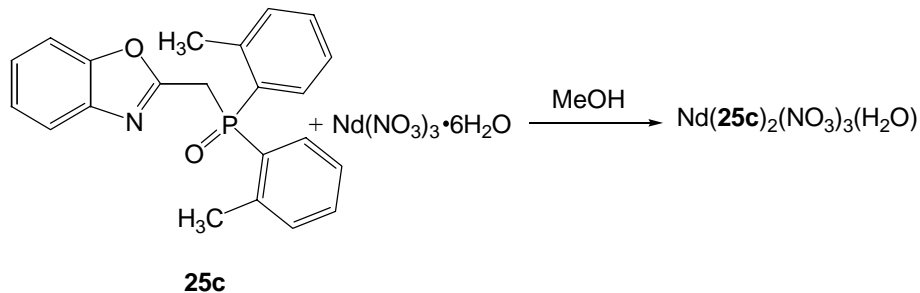
A sample of 2-(di-*o*-tolyl-phosphinoylmethyl)-benzoxazole (0.2 g, 0.55 mmol, 1 eq.) in MeOH (10 ml) was combined with $Nd(NO_3)_3 \cdot 6H_2O$ (0.24 g, 0.55 mmol, 1 eq.) in MeOH (5 ml). The solution was stirred (23 °C, 12 h) and allowed to slowly evaporate at room temperature. After several days, colorless crystals suitable for single crystal analysis were formed: Yield 0.38 g, (64.1%), assuming the composition **Nd(25c)$_2$(NO$_3$)$_3$(H$_2$O):** mp 198 – 200 °C. X-ray diffraction analysis was completed. A view of the complex is displayed in Figure 3.47. Crystal parameters are given in Table 3.15 and selected bond lengths are given in Table 3.16. The infrared spectrum (KBr cm^{-1}) shows a band at 1151 (ν_{PO}) that represents a coordination shift of $\Delta\nu_{P=O}$ = 27 cm^{-1} down frequency compared to the free ligand. Typical spectra are displayed in Figure 3.45 and 3.46 shows overlapping with the free ligand.

Elemental Analysis

Calculated for $C_{44}H_{42}N_5NdO_{14}P_2$ C, 49.34; H, 3.92; N, 6.53.

Found   C, 44.74; H, 3.63; N, 6.83.

Figure 3.45 Infrared spectrum (KBr, cm^{-1}) for Nd(25c)$_2$(NO$_3$)$_3$(H$_2$O)
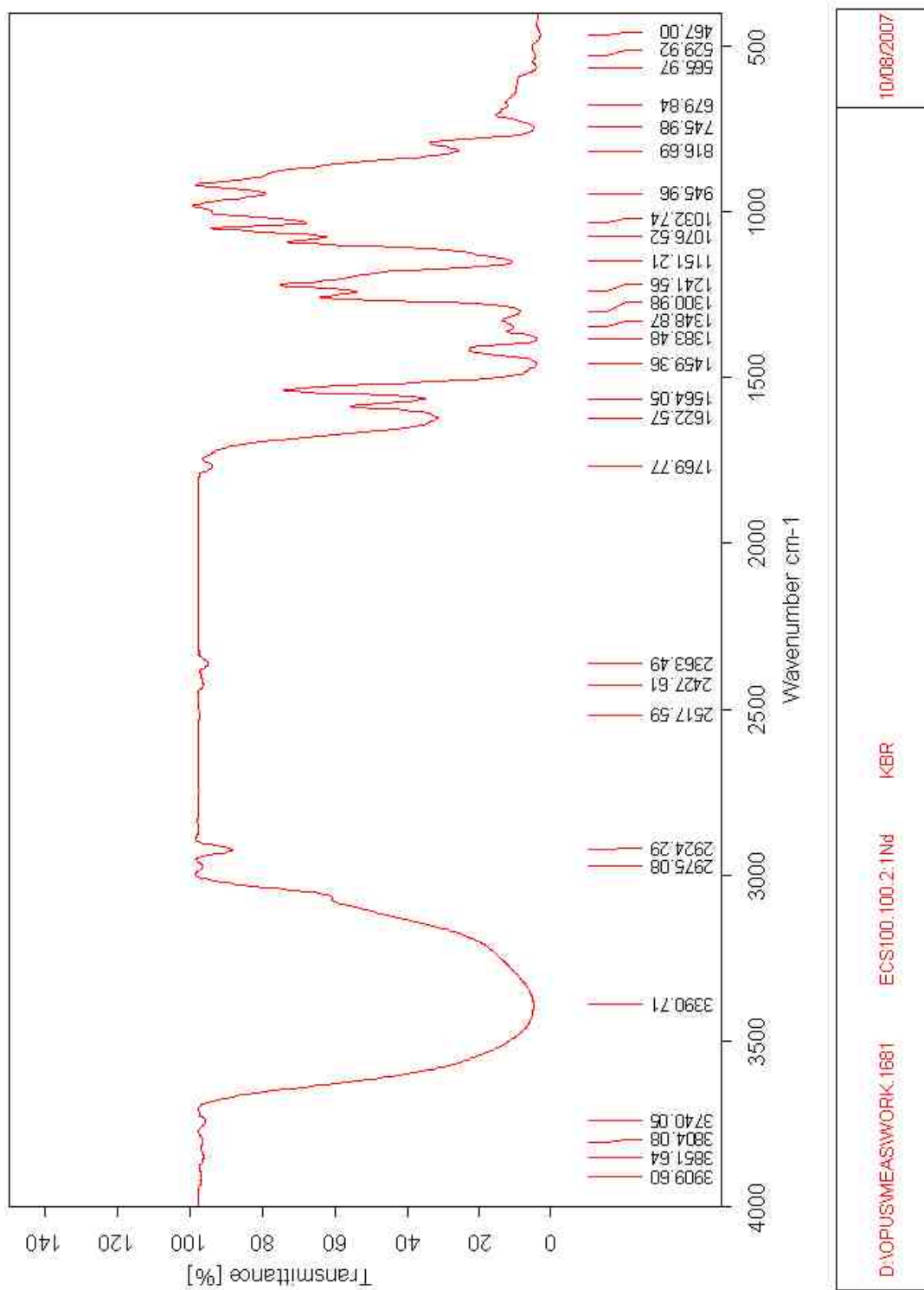
Figure 3.46 Infrared spectrum (KBr, cm^{-1}) for Nd(25c)$_2$(NO$_3$)$_3$(H$_2$O) superimposed with a free ligand, 25c
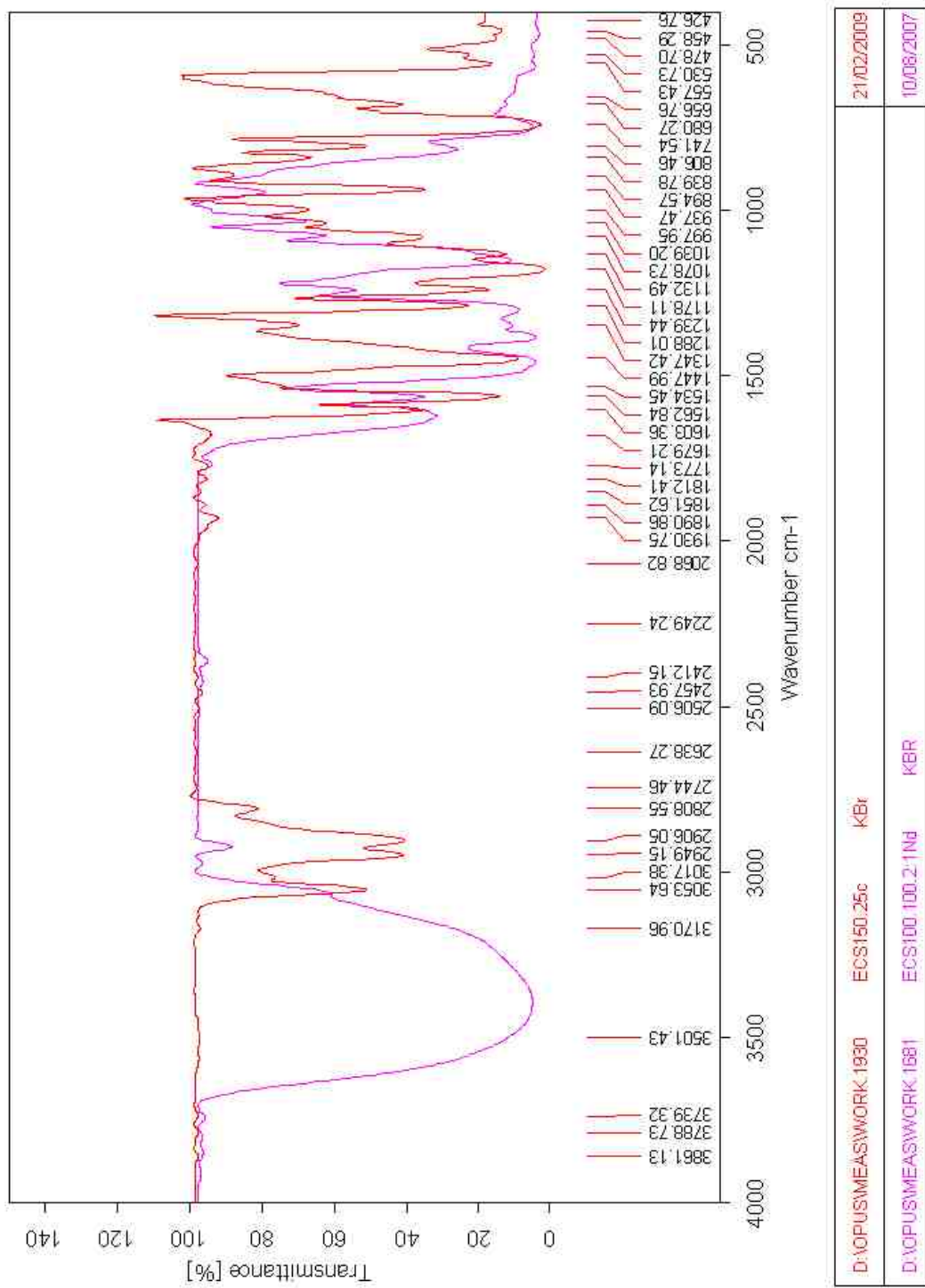
Figure 3.47 Molecular structure and atom labeling scheme for Nd(25c)$_2$(NO$_3$)$_3$(H$_2$O)
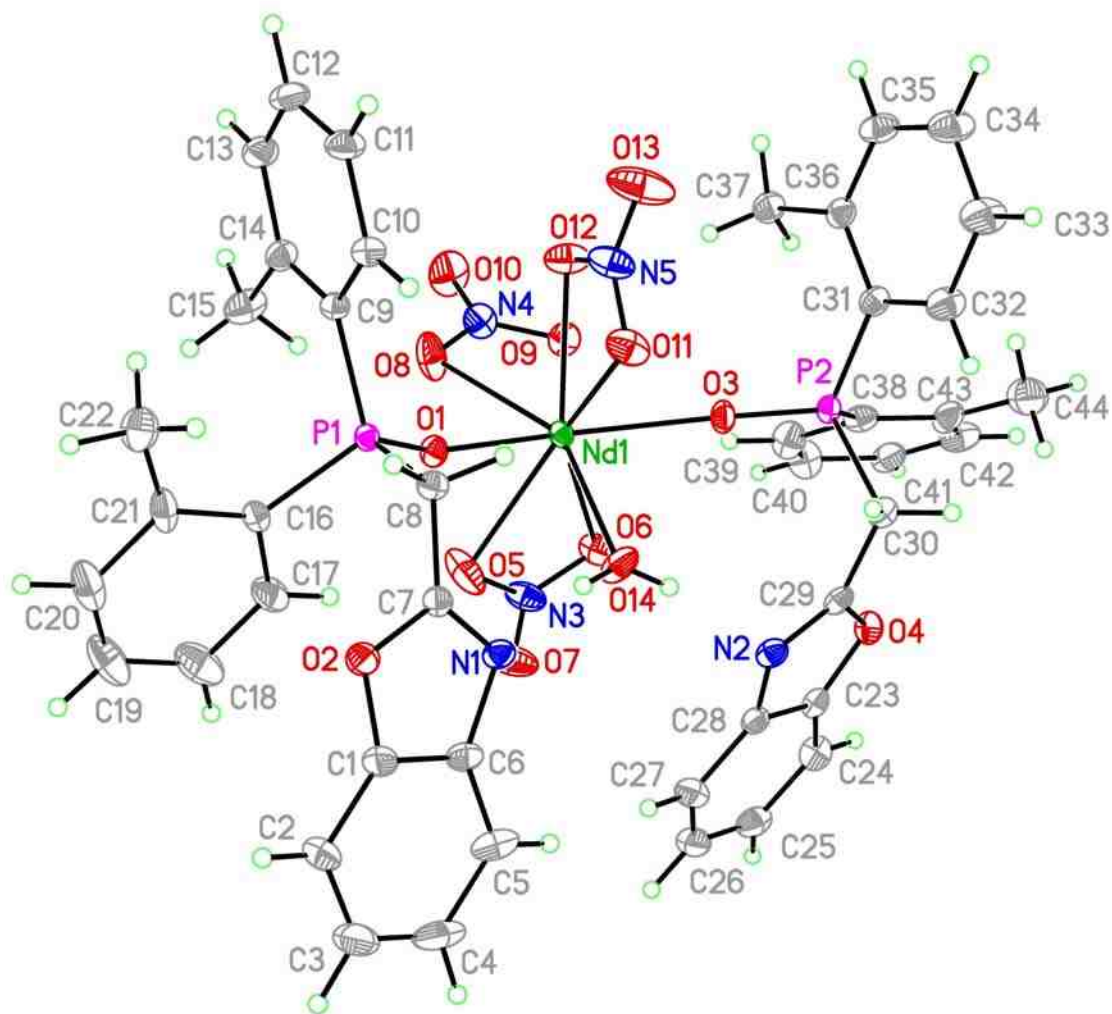
Table 3.15 Crystal parameters for Nd(25c)$_2$(NO$_3$)$_3$(H$_2$O)

Empirical formula	C$_{44}$ H$_{42}$ N$_5$ Nd O$_{14}$ P$_2$
Formula weight	1071.01
Temperature	225(2) K
Wavelength	0.71073 Å
Crystal system	Orthorhombic
Space group	P2(1)2(1)2(1)
Unit cell dimensions	a = 10.6978(13) Å α= 90°.
	b = 11.7144(14) Å β= 90°.
	c = 37.928(5) Å γ = 90°.
Volume	4753.1(10) Å^3
Z	4
Density (calculated)	1.497 Mg/m^3
Absorption coefficient	1.229 mm^{-1}
F(000)	2172
Crystal size	0.53 x 0.37 x 0.34 mm^3
Theta range for data collection	2.49 to 33.68°.
Index ranges	-15<=h<=16, -18<=k<=18, -58<=l<=58
Reflections collected	150752
Independent reflections	18473 [R(int) = 0.0441]
Completeness to theta = 31.00°	99.9 %
Absorption correction	Semi-empirical from equivalents
Max. and min. transmission	0.650 and 0.560

Refinement method	Full-matrix least-squares on F^2
Data / restraints / parameters	18473 / 0 / 587
Goodness-of-fit on F^2	1.148
Final R indices [I>2sigma(I)]	R1 = 0.0400, wR2 = 0.1004
R indices (all data)	R1 = 0.0431, wR2 = 0.1022
Absolute structure parameter	0.032(8)
Largest diff. peak and hole	1.517 and -1.628 e.$Å^{-3}$

Table 3.16 Selected bond lengths [Å] for Nd(25c)$_2$(NO$_3$)$_3$(H$_2$O)

Nd(1)-O(3)	2.350(2)
Nd(1)-O(1)	2.3531(19)
Nd(1)-O(14)	2.427(3)
Nd(1)-O(12)	2.500(3)
Nd(1)-O(8)	2.516(3)
Nd(1)-O(6)	2.538(3)
Nd(1)-O(5)	2.555(3)
Nd(1)-O(9)	2.556(3)
Nd(1)-O(11)	2.579(3)
P(1)-O(1)	1.498(2)
P(1)-C(9)	1.784(3)
P(1)-C(16)	1.804(3)
P(1)-C(8)	1.834(3)
P(2)-O(3)	1.504(2)
P(2)-C(38)	1.775(2)

3.3.9 Synthesis of 2-[bis-(3,5-bis-trifluoromethylphenyl)-phosphinoylmethyl]-benzoxazole, 25d

Scheme 19
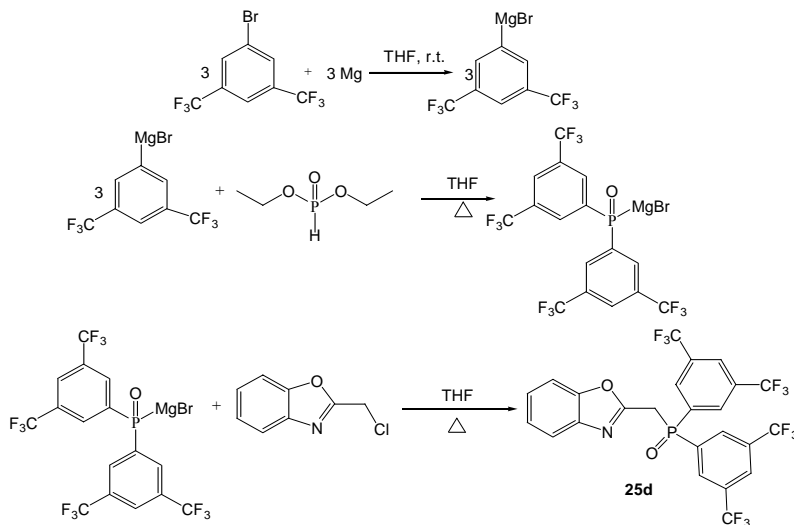
The reaction involves preparation of the required Grignard reagent using the method reported in the literature.[28-33, 40] Magnesium turnings (0.5 g, 20.5 mmol, 3 eq.) were placed in a 250 ml Schlenk vessel and the vessel was swept with dry nitrogen. Dry THF (10 ml) was added in the flask. A solution of 3,5-bis(trifluoromethyl)-bromobenzene (3.5 ml, 20.5 mmol, 3 eq.) in dry THF (10 ml) was added dropwise (23 ^{o}C). The temperature of the reaction mixture rose. Stirring was continued at room temperature for 1 h to complete the reaction. Diethyl phosphite (1.0 ml, 7.5 mmol, 1 eq.) in dry THF (10 ml) was added dropwise to the Grignard reagent solution and the temperature rose during the addition. The reaction mixture was heated under reflux between 50-60 ^{o}C for an additional 1 h. The reaction mixture was then cooled (23 ^{o}C) and a solution of 2-chloromethylbenzoxazole, (1.3 g, 7.5 mmol, 1 eq.) in THF (10 ml) was added. The reaction was heated under reflux between 50–60 ^{o}C overnight while monitoring by TLC: 100% CH$_2$Cl$_2$ showed the disappearance of

2-chloromethylbenzoxazole. The red black solution was vacuum evaporated to remove THF, the residue was treated with saturated aqueous NH_4Cl solution (100 ml), and extracted with $CHCl_3$ (3 x 40 ml). The combined $CHCl_3$ extracts were dried (Na_2SO_4) and evaporated. The resulting orange solid was dried under vacuum for 2 days and purified by crystallization from ethyl acetate/hexane solution that gave colorless crystals: Yield 2.6 g, (55%), mp 209 - 210 ^oC. Selected spectroscopic data for **25d** are summarized below and typical spectra are displayed in Figure 3.48 – 3.53. Compound **25d** is soluble in $CHCl_3$, CH_2Cl_2, $Cl_2CH_2CH_2Cl_2$, MeOH, trifluoromethanesulfonyl-benzene (0.038 M) and insoluble in hexane, pentane, toluene and benzene.

Elemental Analysis

Calculated for $C_{24} H_{12} F_{12} N O_2 P$ (FW= 605.04 g/mole): C, 47.62; H, 2.00; N, 2.31.

Found   C, 47.70; H, 2.05; N, 2.28.

Infrared spectrum (KBr, cm^{-1}): 1616 ($\nu_{C=N}$), 1140-1283 ($\nu_{P=O}$, ν_{C-F}).

^{1}H (250 MHz, 23 ^oC, CDCl$_3$), δ (ppm): 4.2 (d, 2H, -CH$_2$-P=O, $^2J_{H-P}$ = 16.2 Hz), 7.2 -7.3 (m, 3H, H-Ar), 7.6 (m, 1H, H-Ar), 8.1 (s, 2H, H$_{13}$), 8.4 (d, 4H, H$_{10}$, $^3J_{H-P}$ = 11.2 Hz).

^{1}H (500 MHz, 23 ^oC, CDCl$_3$ with ^{31}P coupling), δ (ppm): 4.3 (d, 2H, -CH$_2$-P=O, $^2J_{H-P}$ = 16.3 Hz), 7.2 -7.3 (m, 3H, H-Ar), 7.6 (m, 1H, H-Ar), 8.1 (s, 2H, H$_{13}$), 8.4 (d, 4H, H$_{10}$, $^3J_{H-P}$ = 11.8 Hz).

^{1}H (500 MHz, 23 ^oC, CDCl$_3$ with ^{31}P decoupling), δ (ppm): 4.3 (s, -CH$_2$-P=O), 7.2 -7.3 (m, 3H, H-Ar), 7.6 (m, 1H, H-Ar), 8.1 (s, 2H, H$_{13}$), 8.4 (s, 4H, H$_{10}$).

^{13}C{^{1}H} (62.9 MHz, 23 ^oC, CDCl$_3$): δ (ppm), 32.7 (d, C$_1$, $^1J_{C-P}$ = 67.3 Hz), 110.5 (s), 120.1 (s), 122.5 (q, –CF$_3$, $^1J_{C-F}$ = 273.6 Hz), 125.0 (s), 125.8 (s), 126.8 (s), 131.5 (d,

ortho-aryl, $^2J_{C-P}$ = 12.4 Hz), 132.6 (qd, *meta*-aryl, $^3J_{C-P}$ = 14.0 Hz, $^2J_{C-F}$ = 34.3 Hz), 133.5 (d, *ipso*-aryl, $^1J_{C-P}$ = 102.1 Hz), 140.7 (s), 150.8 (s), C-Ar, 156.5 (d, C_2, $^2J_{C-P}$ = 7.9 Hz).

$^{13}C\{^1H\}$ (125.7 MHz, 23 °C, CDCl$_3$), δ (ppm): 32.7 (d, C_1, $^1J_{C-P}$ = 67.6 Hz), 110.4 (s), 120.0 (s), 122.5 (q, –CF$_3$, $^1J_{C-F}$ = 273.5 Hz), 124.9 (s), 125.8 (s), 126.8 (s), 131.5 (d, *ortho*-aryl, $^2J_{C-P}$ = 8.4 Hz), 132.7 (qd, *meta*-aryl, $^3J_{C-P}$ = 12.4 Hz, $^2J_{C-F}$ = 34.6 Hz), 133.5 (d, *ipso*-aryl, $^1J_{C-P}$ = 102.3 Hz), 140.7 (s), 150.7 (s), C-Ar, 156.4 (d, C_2, $^2J_{C-P}$ = 7.7 Hz).

$^{13}C\{^1H, {}^{31}P\}$ (125.7 MHz, 23 °C, CDCl$_3$), δ (ppm): 29.7 (s, C_1), 110.4 (s), 120.1 (s), 122.5 (q, –CF$_3$, $^1J_{C-F}$ = 273.4 Hz), 125.1 (s), 125.7 (s), 126.8 (s), 131.5 (s, *ortho*-aryl), 132.7 (q, *meta*-aryl, $^2J_{C-F}$ = 34.2 Hz), 133.5 (d, *ipso*-aryl, J = 11.2 Hz), 140.7 (s), 150.8 (s), C-Ar, 156.5 (s, C_2).

$^{31}P\{^1H\}$ (101.3 MHz, 23 °C, CDCl$_3$): δ (ppm), 23.4, CH$_2$-P=O.

Mass spectrum (ESI) *m/e* (fragment, relative intensity): $[M+H]^+$ = 606.0496 and the calculated exact mass is 605.0414.

Figure 3.48 IR spectrum for 2-[bis-(3,5-bis-trifluoromethylphenyl)-

phosphinoylmethyl]-benzoxazole, 25d

Figure 3.49(a) 250 MHz ^{1}H NMR spectrum for 2-[bis-(3,5-bis-trifluoromethylphenyl)-phosphinoylmethyl]-benzoxazole, 25d

Figure 3.49(b) 500 MHz ^{1}H NMR spectrum for 2-[bis-(3,5-bis-trifluoromethylphenyl)-phosphinoylmethyl]-benzoxazole, 25d with ^{31}P coupling
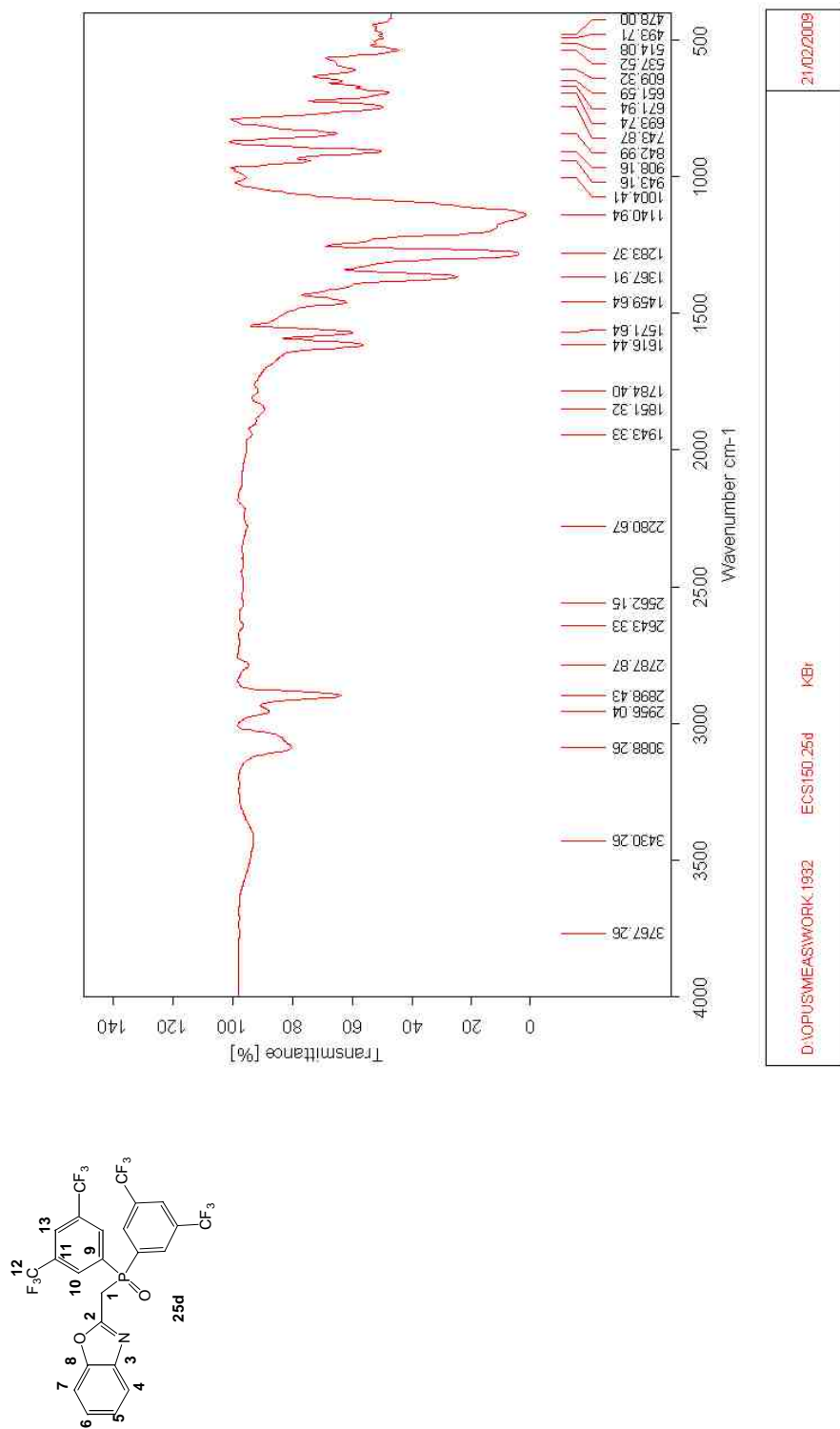
Figure 3.49(c) 500 MHz ^{1}H NMR spectrum for 2-[bis-(3,5-bis-trifluoromethylphenyl)-phosphinoylmethyl]-benzoxazole, 25d with ^{31}P decoupling
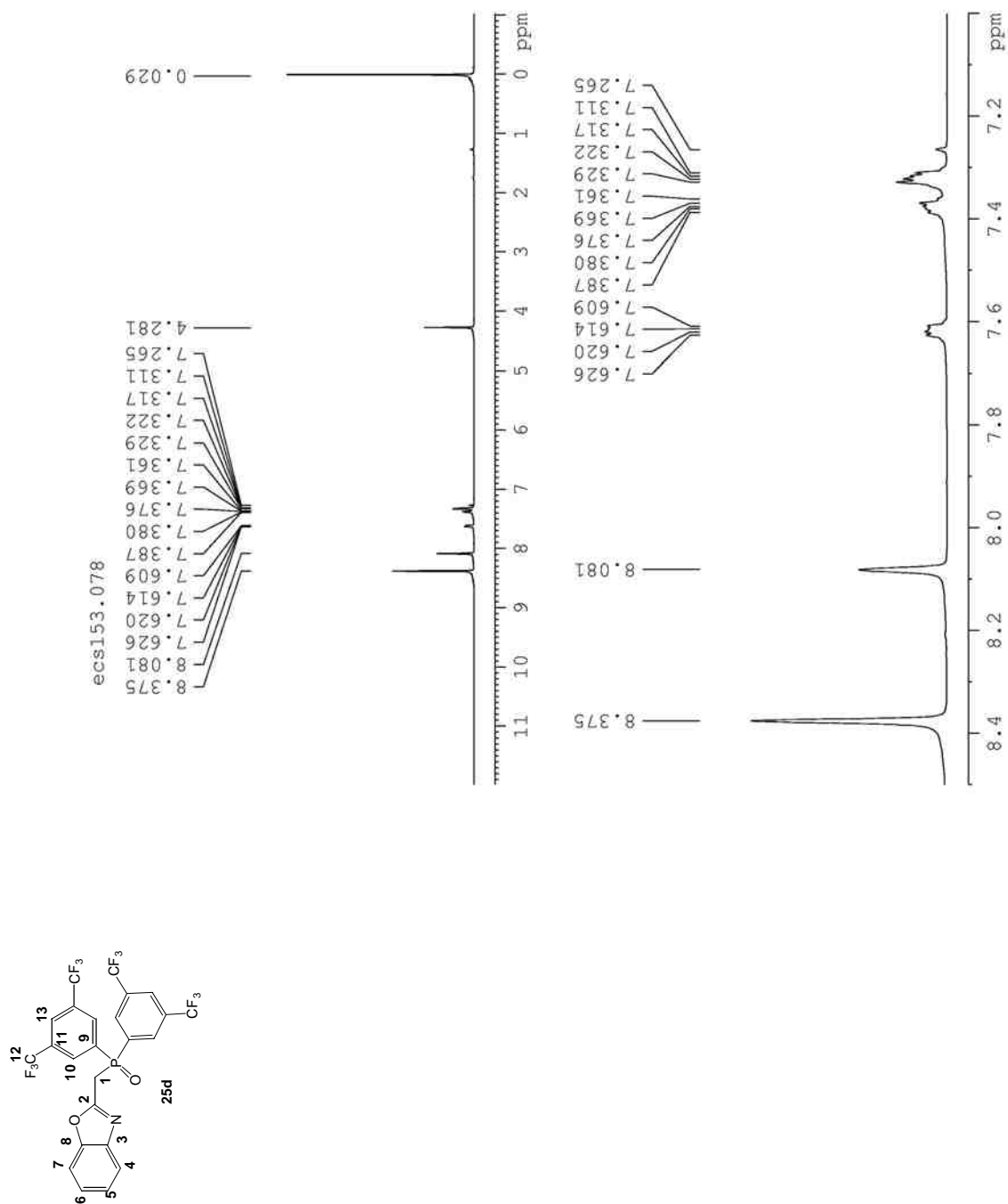
Figure 3.50 62.9 MHz $^{13}C\{^1H\}$ NMR spectrum for 2-[bis-(3,5-bis-trifluoromethylphenyl)-phosphinoylmethyl]-benzoxazole, 25d

ECS139.051
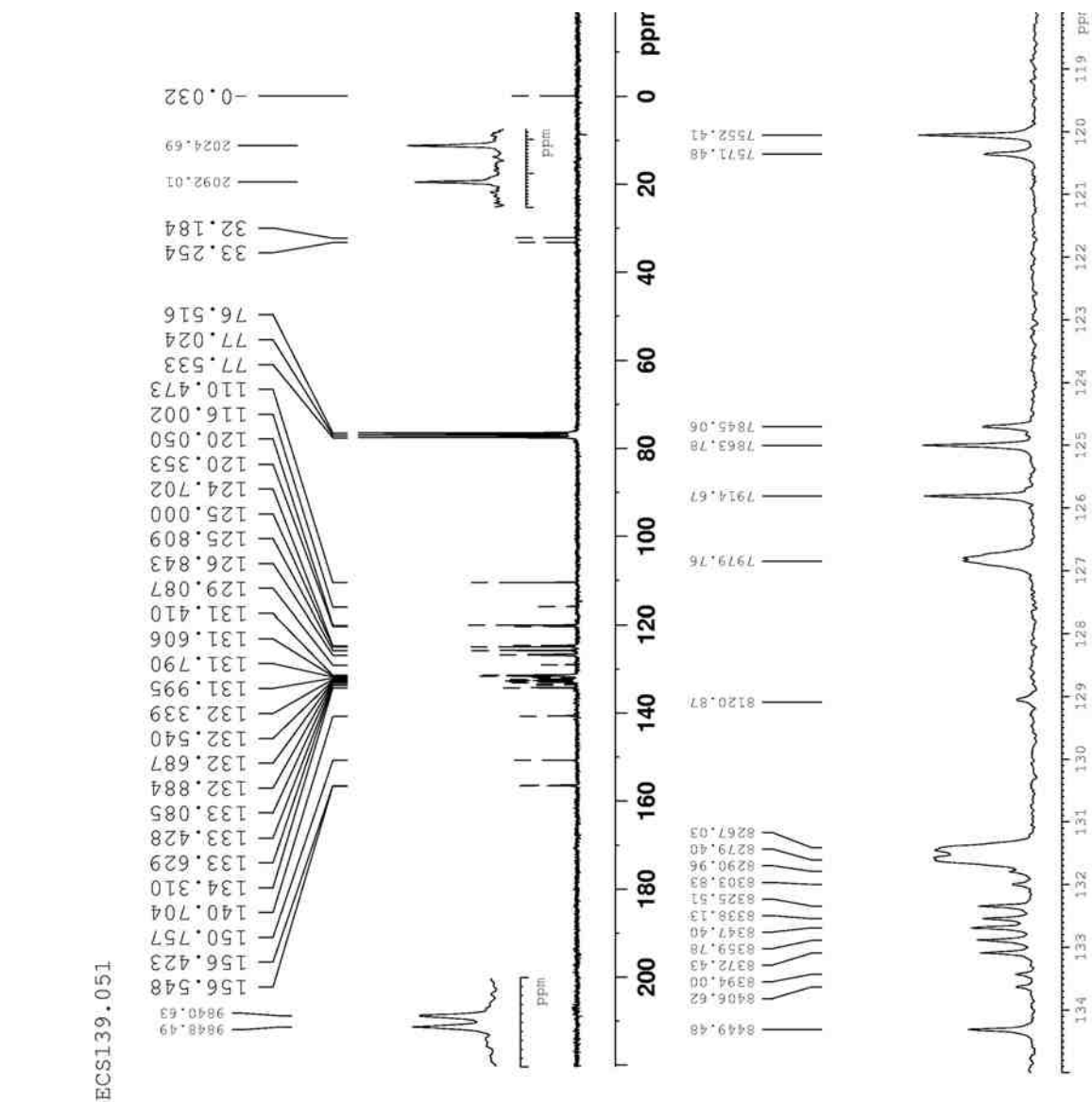
Figure 3.51 125.7 MHz ^{13}C{^{1}H} NMR spectrum for 2-[bis-(3,5-bis-trifluoromethylphenyl)-phosphinoylmethyl]-benzoxazole, 25d with ^{31}P coupling

ecs153.069 coupling C{31P}

4083.30
4150.85
32.469
33.007
76.698
76.950
77.202
110.440
119.225
120.025
121.398
123.573
124.288
124.983
125.793
126.789
127.553
128.863
131.422
131.488
131.694
132.230
132.331
132.518
132.617
132.792
132.890
133.062
133.159
133.875
140.668
150.731
156.415
156.476
19670.40
19678.13

14993.52
15094.05
15266.79
15540.25
15630.22
15717.60
15819.49
15944.70
16040.82
16205.55
16527.28
16535.69
16561.60
16628.95
16641.61
16665.22
16677.66
16699.60
16711.98
16733.62
16745.80
16835.87

ppm

Figure 3.52 125.7 MHz ^{13}C{^{1}H} NMR spectrum for 2-[bis-(3,5-bis-trifluoromethylphenyl)-phosphinoylmethyl]-benzoxazole, 25d with ^{31}P decoupling
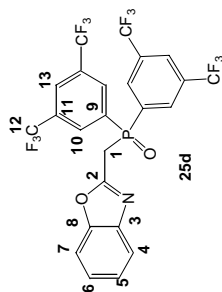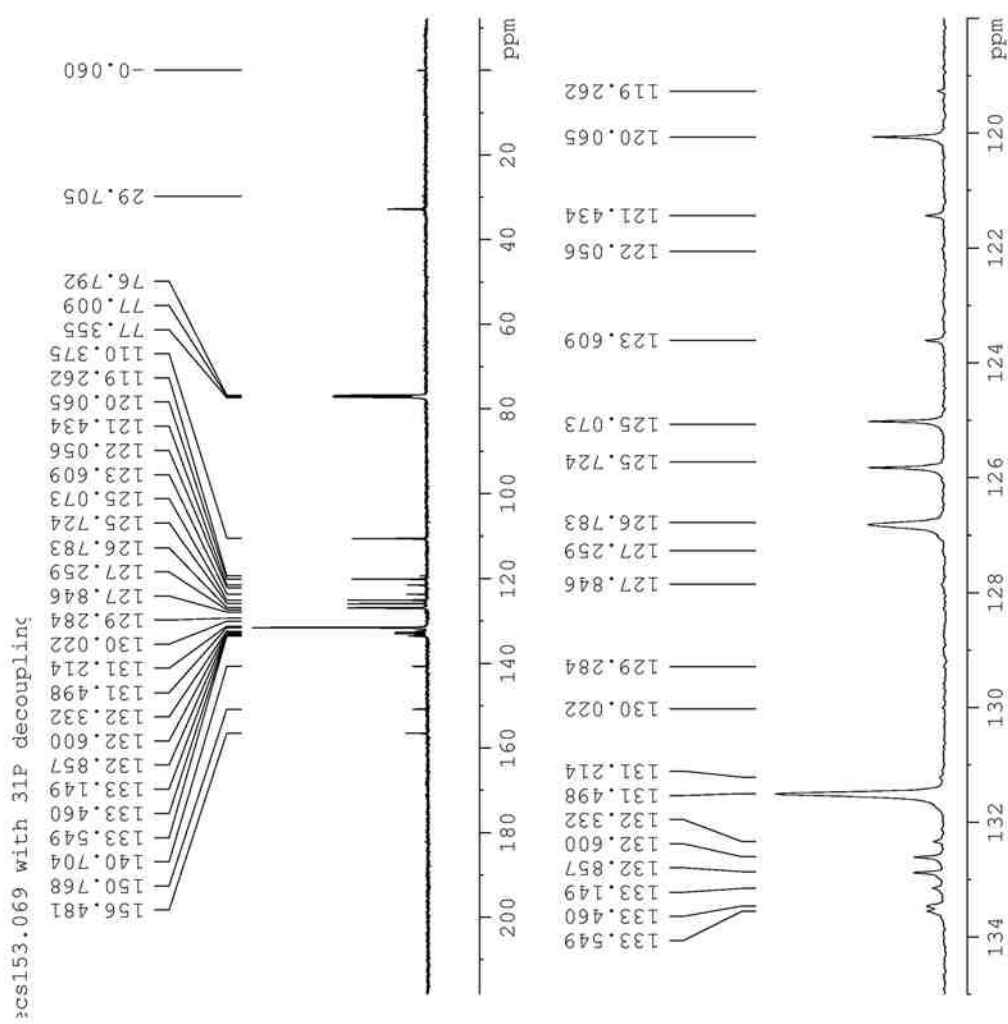
Figure 3.53 101.3 MHz ^{31}P{^{1}H} NMR spectrum for 2-[bis-(3,5-bis-trifluoromethylphenyl)-phosphinoylmethyl]-benzoxazole, 25d

ECS139.042

23.419
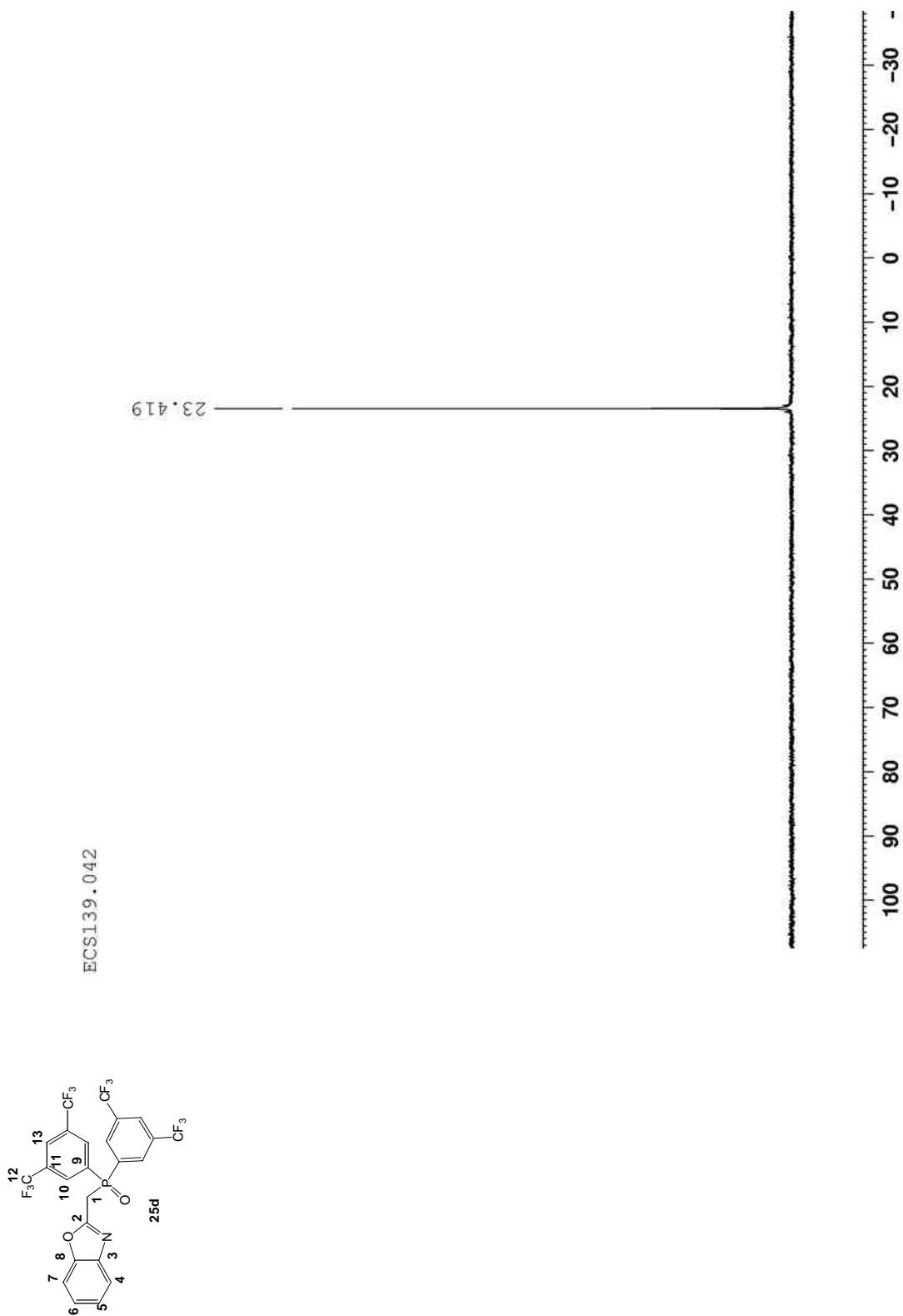
Single crystals suitable for X-ray crystal structure determination were grown from a solution of EtOAc/hexane that gave colorless crystals. A view of the molecule is displayed in Figure 3.54. Crystal parameters are given in Table 3.17 and selected bond lengths are given in Table 3.18.

Figure 3.54 Molecular structure and atom labeling scheme for 2-[bis-(3,5-bis-trifluoromethylphenyl)-phosphinoylmethyl]-benzoxazole, 25d
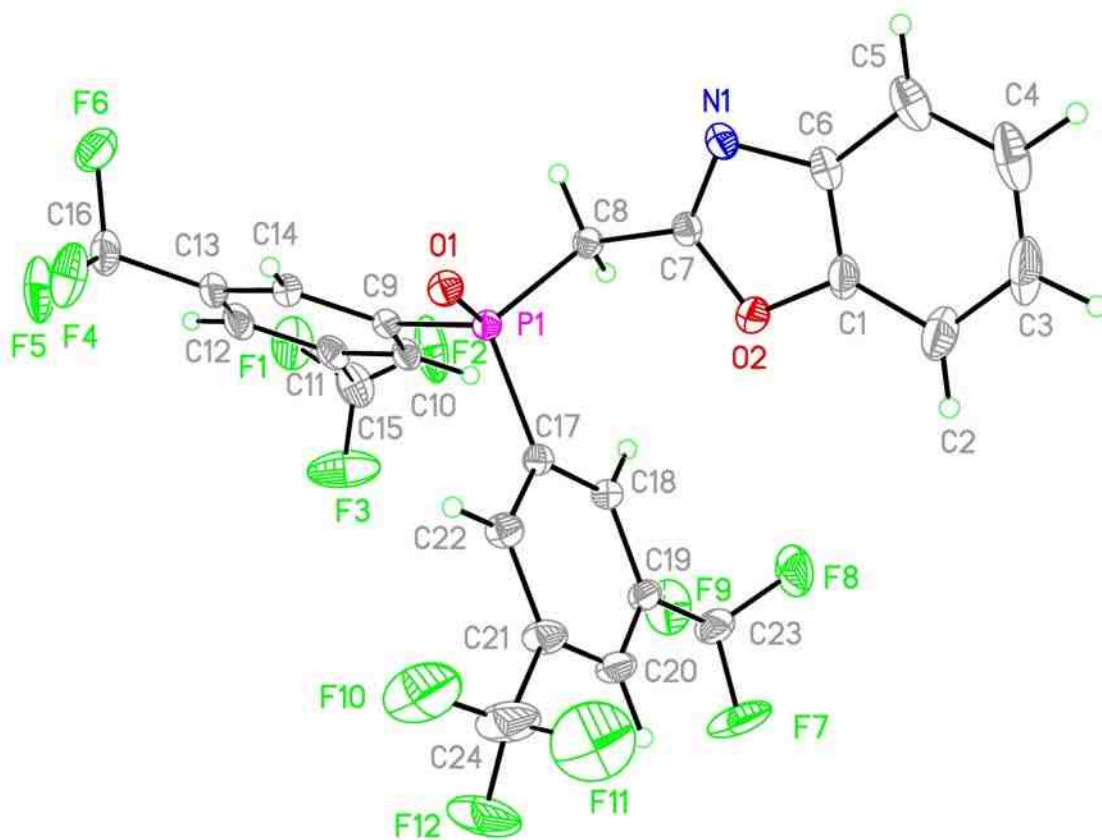
Table 3.17 Crystal parameters for 2-[bis-(3,5-bis-trifluoromethylphenyl)-phosphinoylmethyl]-benzoxazole, 25d

Empirical formula	$C_{24} H_{12} F_{12} N O_2 P$
Formula weight	606.32
Temperature	223(2) K
Wavelength	0.71073 Å
Crystal system	Rhombohedral, hexagonal axes
Space group	R-3
Unit cell dimensions	$a = 29.2229(19)$ Å $\quad \alpha = 90°$.
	$b = 29.2229(19)$ Å $\quad \beta = 90°$.
	$c = 15.5085(11)$ Å $\quad \gamma = 120°$.
Volume	11469.6(13) Å^3
Z	18
Density (calculated)	1.580 Mg/m^3
Absorption coefficient	0.219 mm^{-1}
F(000)	5446
Crystal size	0.57 x 0.46 x 0.21 mm^3
Theta range for data collection	2.75 to 31.05°.
Index ranges	-42<=h<=42, -42<=k<=41, -22<=l<=22
Reflections collected	94848
Independent reflections	8137 [R(int) = 0.0510]
Completeness to theta = 31.05°	99.6 %
Absorption correction	Semi-empirical from equivalents

Max. and min. transmission	0.95 and 0.88
Refinement method	Full-matrix least-squares on F^2
Data / restraints / parameters	8137 / 3 / 498
Goodness-of-fit on F^2	1.020
Final R indices [I>2sigma (I)]	R1 = 0.0450, wR2 = 0.1074
R indices (all data)	R1 = 0.0764, wR2 = 0.1287
Largest diff. peak and hole	0.290 and -0.284 e.Å^{-3}

Table 3.18 Selected bond lengths [Å] for 2-[bis-(3,5-bis-trifluoromethylphenyl)-phosphinoylmethyl]-benzoxazole, 25d

P(1)-O(1)	1.4817(11)
P(1)-C(17)	1.8025(14)
P(1)-C(9)	1.8048(14)
P(1)-C(8)	1.8099(15)
O(2)-C(7)	1.3538(19)
O(2)-C(1)	1.389(2)
N(1)-C(7)	1.286(2)
N(1)-C(6)	1.394(2)
C(7)-C(8)	1.476(2)
C(15)-F(1A)	1.179(8)
C(15)-F(3)	1.229(4)
C(15)-F(3A)	1.250(8)
C(15)-F(2)	1.290(4)
C(15)-F(1)	1.392(4)

C(15)-F(2A)	1.506(6)
C(16)-F(6A)	1.215(17)
C(16)-F(4A)	1.31(3)
C(16)-F(5A)	1.339(18)
C(23)-F(8A)	1.215(5)
C(23)-F(7)	1.273(6)
C(23)-F(8)	1.296(4)
C(23)-F(9A)	1.315(6)
C(23)-F(7A)	1.347(5)
C(23)-F(9)	1.386(6)
C(24)-F(10)	1.246(11)
C(24)-F(11A)	1.250(9)
C(24)-F(10A)	1.258(11)
C(24)-F(12)	1.291(9)
C(24)-F(11)	1.328(9)
C(24)-F(12A)	1.390(11)

3.3.10 Coordination Chemistry[31-33]

As with ligands **25a-25c**, the coordination chemistry of **25d** was surveyed under variety of conditions and selected results are described below.

Scheme 20
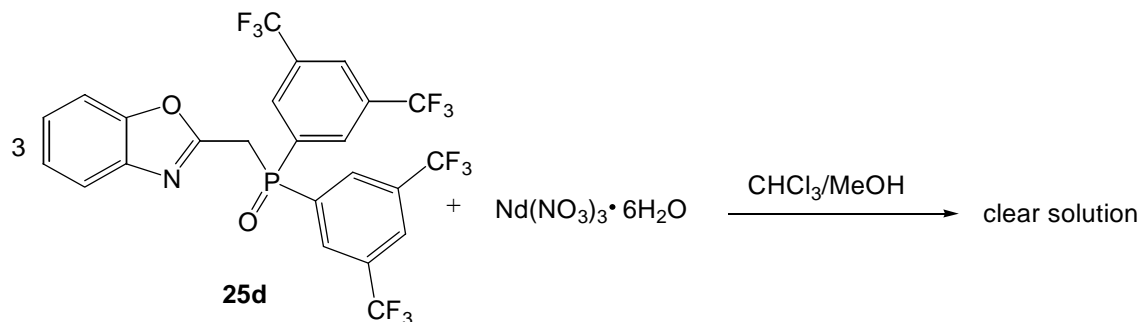
A sample of 2-[bis-(3,5-bis-trifluoromethylphenyl)-phosphinoylmethyl]-benzoxazole (0.2 g, 0.33 mmol, 3 eq.) in CHCl$_3$ (10 ml) was combined with Nd(NO$_3$)$_3$•6H$_2$O (0.05 g, 0.11 mmol, 1 eq.) in MeOH (2 ml). The mixture was stirred (23 $^{\circ}$C, 12 h) to give a clear solution. The solution was left open to evaporate slowly for 4 days at room temperature. A white solid formed (0.27 g) which was crystallized from CHCl$_3$/MeOH/hexane solution, loosely capped for 3 days. White crystals were isolated: 0.18 g, mp 206-208 $^{\circ}$C. Single crystal X-ray diffraction analysis indicated that the crystal was free ligand. Apparently no coordination complex formed.

Scheme 21
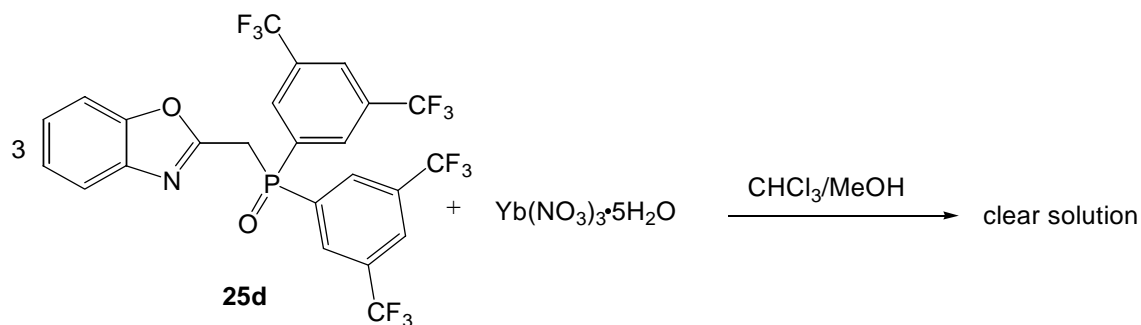
A sample of 2-[bis-(3,5-bis-trifluoromethylphenyl)-phosphinoylmethyl]-benzoxazole (0.2 g, 0.33 mmol, 3 eq.) in CHCl$_3$ (10 ml) was combined with Yb(NO$_3$)$_3$•5H$_2$O (0.05 g, 0.11 mmol, 1 eq.) in MeOH (2 ml), stirred (23 °C, 12 h). A clear solution formed. The solution was left open at room temperature to evaporate slowly for 4 days. A white solid (0.3 g) deposited that was crystallized from CHCl$_3$/MeOH/hexane solution, loosely capped for 3 days: Yield 0.19 g, mp 208-212 °C. Infrared analysis showed no peak shifts and X-ray crystallographic analysis gave a crystal structure for the pure ligand i.e., no coordination with Yb(III) observed.

Scheme 22
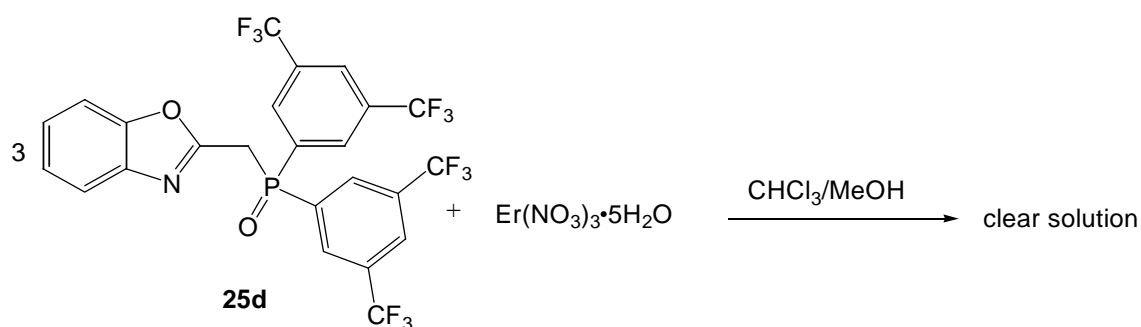
A sample of 2-[bis-(3,5-bis-trifluoromethylphenyl)-phosphinoylmethyl]-benzoxazole (0.3 g, 0.5 mmol, 3 eq.) in CHCl$_3$ (10 ml) was combined with Er(NO$_3$)$_3$•5H$_2$O (0.08 g, 0.17 mmol, 1 eq.) in MeOH (2 ml). The solution was stirred for 12 h, at room temperature to give a clear solution. The solution was left open to evaporate slowly for 4 days at room temperature. A white solid was formed (0.41 g) which was crystallized from a mixture of CHCl$_3$, MeOH and hexane solution, loosely capped for 3 days, giving white crystals: Yield 0.27 g, mp 207-212 °C. Infrared analysis showed no significant peak shifts. X-ray crystallography showed that the solid was free ligand.

Scheme 23
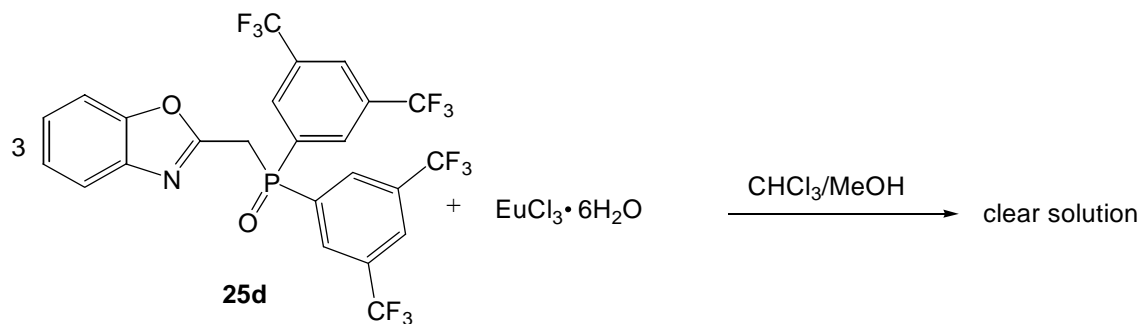
A sample of 2-[bis-(3,5-bis-trifluoromethylphenyl)-phosphinoylmethyl]-benzoxazole (0.2 g, 0.33 mmol, 3 eq.) in CHCl$_3$ (10 ml) was combined with EuCl$_3$•6H$_2$O (0.04 g, 0.11 mmol, 1 eq.) in MeOH (2 ml) and the mixture was stirred for 12 h, to give a clear solution. The solution was left open to evaporate slowly for 4 days at room temperature. A white solid formed (0.26 g) which was crystallized from a mixture of CHCl$_3$, MeOH and hexane, loosely capped for 3 days, leaving white crystals: Yield 0.17 g, mp 206-210 °C. Infrared analysis showed no significant peak shifts. X-ray crystallographic analysis showed uncoordinated ligand.

3.3.11 Synthesis of 2-[bis-(3,5-dimethyl-phenyl)-phosphinoylmethyl]-benzoxazole, 25e

Scheme 24

25e
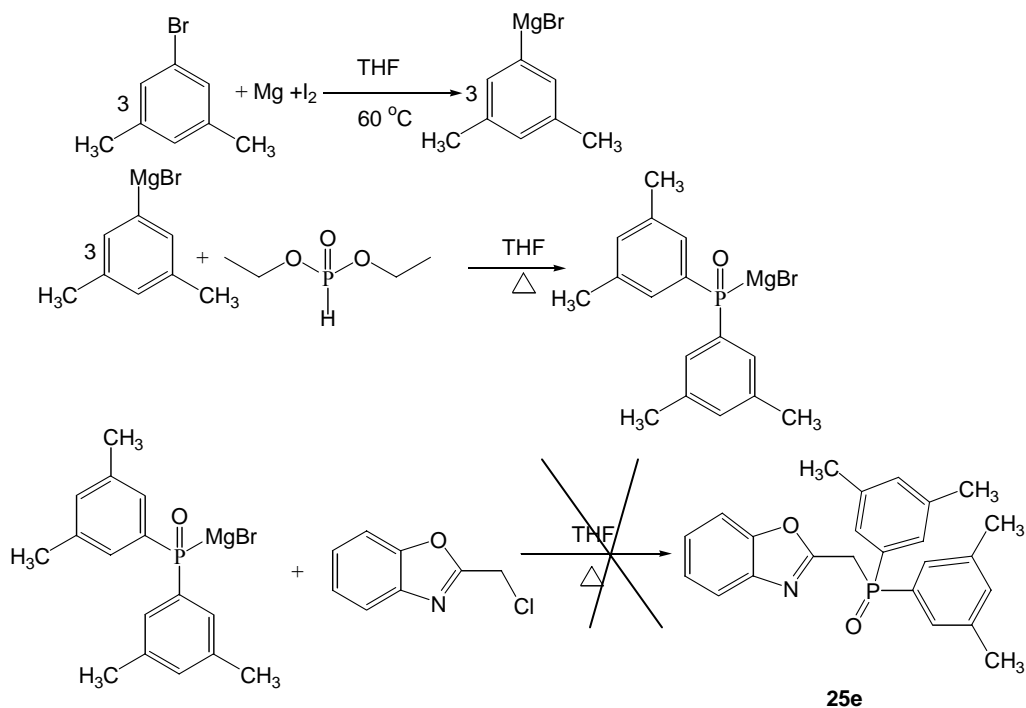
The literature method used in the synthesis of compounds **25a-25d** was adapted for an attempted preparation of **25e**.[28-33, 40] A 250 ml flask fitted with reflux condenser, swept with nitrogen and charged with magnesium turnings (0.40 g, 15 mmol, 3 eq.) and several pieces of iodine. The solid mixture was heated briefly with a sand bath until purple vapor from the iodine appeared. A solution of 1-bromo-3,5-dimethylbenzene (2.8 g, 15 mmol, 3 eq.) in dry THF (20 ml) was prepared in a nitrogen atmosphere and transferred to the reaction flask. An aliquot (5 ml) of solution was added to the magnesium turnings (23 $^{\circ}$C) and this mixture was warmed using a sand bath to initiate the reaction. Once started the additional THF solution was added dropwise at a rate that enabled continuous reflux. After the addition was complete, the mixture was refluxed for

an additional 1 h of which the Grignard reagent formed turned to a gray/black color. After cooling the mixture to room temperature, a solution containing diethyl phosphite (0.6 g, 4.4 mol, 1 eq.) in dry THF (10 ml) was added dropwise. The temperature of the mixture rose during the addition and the final mixture was refluxed for 1 h, oil bath temperature 60 $^{\circ}$C. A solution of 2-chloromethylbenzoxazole (0.8 g, 4.4 mol, 1 eq.) in dry THF (10 ml) was prepared and transferred to the Grignard reagent using a syringe at room temperature, 23 $^{\circ}$C. The reagent changed to a yellow color immediately. The resulting mixture was refluxed for an additional 12 h (overnight), during which the color changed to yellow/brown. The solvent was then removed under reduced pressure. The resulting yellow residue (solid) was treated with saturated aqueous NH_4Cl solution (100 ml) and the mixture extracted with $CHCl_3$ (3 x 50 ml). The combined $CHCl_3$ fractions were washed with water (100 ml) and dried (Na_2SO_4). Evaporation of the $CHCl_3$ extract, under reduced pressure, gave a crude product as a yellow oil. The oil was purified by column chromatography: silica gel 70-230 mesh, 60Å, eluted with 20% ethyl acetate: 80% hexane. Spectroscopic analysis and mass spectrometry showed that the expected product was not formed.

3.4 RESULTS AND DISCUSSION

3.4.1 Strategies for the syntheses of 25a

The initial target ligand **25a** was prepared using three approaches that are summarized in Schemes 7-9. The method described in Scheme 7 that employs a Grignard reagent appears to be best due to higher yield (96%) as compared to other methods outlined in Schemes 8 (84%) and 9 (72%).

Scheme 7
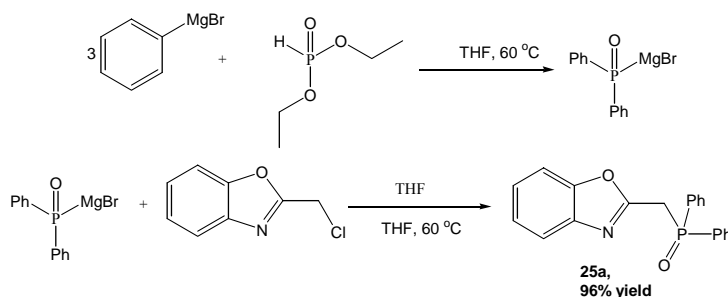
In addition, the Grignard method is more easily used to synthesize other derivatives. For example, compounds **25b-25e** have been synthesized using this method. All precursors used in Scheme 7 are commercially available, except 2-chloromethylbenzoxazole which was synthesized using the method developed by Kosaka and co-workers,[34] and the procedure is described in the appendix.

One step substitution synthesis of **25a** using chlorodiphenyl phosphine oxide (Scheme 8) gave a product with good purity in 84% yield and the sample for elemental analysis was obtained from this method. This is a good route for synthesis of **25a**, but not for the other derivatives since the precursor phosphine oxides are not commercially available.

Scheme 8

26 → (LDA, Ph₂POCl) → **25a, 84% yield**
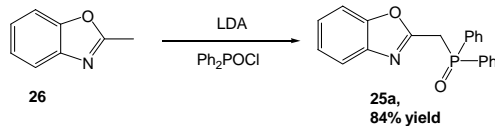
Compound **25a** was also synthesized in a two step process adapting the method developed by Minami and co-workers.[27] In this reaction chlorodiphenylphosphine was used[27] (Scheme 9). Deprotonation of 2-methylbenzoxazole **26** with LDA facilitates the substitution reaction. The workup was done as described in the experimental part to give the target molecule in 72% yield. The lower yield and purity of **25a** may result from the sluggish air oxidation. Previous work has shown that the oxidation of phosphine compounds to phosphine oxides by exposure to oxygen leads to the formation of several side products and therefore low yield and purity.[45] Attempts to purify the intermediate compound **27** were unsuccessful due to its ready oxidation when exposed in air. The synthetic summary of **25a** is shown in Table 3.19

Scheme 9

26 → (LDA, Ph₂PCl) → [**27**] → (air, 24 h in CHCl₃) → **25a, 72% yield**
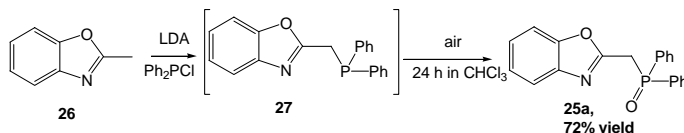
Table 3.19 Summary for the synthesis of compound 25a

Scheme	Method	% yields	Purity	Advantage	Disadvantage
1	Using Grignard reagent	96	Moderate	High yield and structural modification can be made	Expensive and air/water sensitive
2	Direct synthesis	84	Good	Short and high purity	Difficult to introduce structural modification
3	Two step synthesis	72	Moderate	Cheap	Lower purity and instability of the intermediate phosphine to air (O_2)

3.4.2 Studies of the influence of the base on synthesis of 25a

An attempt was made to use BuLi instead of LDA for deprotonation of **26** as described for the synthesis of compound **19** (Chapter 2).[18]
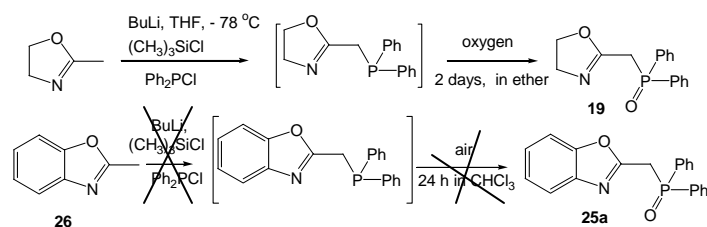
The target molecule **25a** was not obtained. An infrared spectrum from the product mixture revealed that the heterocycle was destroyed as evidenced by the lack of the typical band for C=N, which appears in the range of 1600 to 1690 cm^{-1}. This reaction was repeated without using (CH$_3$)$_3$SiCl. The target molecule was not obtained, and the products remain unidentified. When BuLi was used in the direct synthesis of **25a** (Scheme 8), using Ph$_2$P(O)Cl, with and without (CH$_3$)$_3$SiCl, compound **25a** was not formed. The disruption of the heterocycle suggests that benzoxazole may be unstable in BuLi solution.
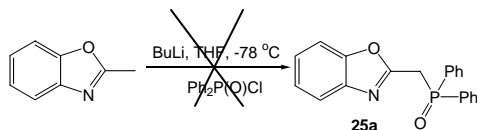
The Minami approach for the synthesis of **25** (R= OEt) calls for the use of two equivalents of LDA in combination with one equivalent of 2-methylbenzoxazole.[27] To test the need for excess LDA, the reaction was also run with 1 equivalent of LDA. This resulted in a reduced yield (41%). This indicates that excess LDA is required for the deprotonation. Since LDA is prepared in *situ* probably its formation is not complete and therefore a need for excess BuLi and diisopropylamine.

Table 3.20 Summary for various strategies used in the synthesis of 25a
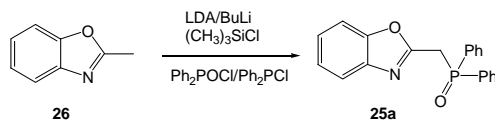
Reagent	With (CH₃)₃SiCl		Without (CH₃)₃SiCl	
	LDA (2 eq.)	BuLi (2 eq.)	LDA (2 eq.)	BuLi (2 eq.)
Ph₂P(O)Cl	**25a** was not formed	**25a** was not formed	84%	**25a** was not formed
Ph₂PCl	**25a** was not formed	**25a** formed as minor product	72%	**25a** was not formed

Compound **25a** was purified using column chromatography on silica gel with MeOH/CH₂Cl₂ as eluant in different ratios as described in the experimental part **(Section 3.3.1-3.3.3).** Compound **25a** is initially isolated as a yellow solid but when washed with CH₂Cl₂/hexane a white powder is obtained. Crystallization was accomplished either from MeOH/CH₂Cl₂ or hot EtOAc solution to give colorless and yellow crystals, respectively that were suitable for single crystal X-ray diffraction analysis.

3.4.3 Spectroscopic analyses for compounds 25a
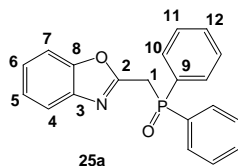
Elemental analysis for compound **25a** shows good agreement between the calculated and the experimental data. High resolution mass spectrometry (HRMS) for compound **25a** shows an intense peak corresponding to [M+H⁺] ion at 334.1003 which provides additional confirmation of the composition.

From an IR spectrum of **25a**, the $\nu_{P=O}$ band is assigned to a strong band at 1196 cm^{-1}. This falls in the same range as other phosphine oxide ligands developed in our group with –CH$_2$-P=O connectivity.[28-33, 41-42] Further, the assignment can be compared to the $\nu_{P=O}$ band for the oxazoline ligand, **19** (Figure 3.7) that displays a band at 1188 cm^{-1} and Ph$_3$P=O: with $\nu_{P=O}$ band at 1195 cm^{-1} reported in the literature.[46] A strong absorption band at 1610 cm^{-1} can be assigned to $\nu_{C=N}$. This value is comparable to 1611 cm^{-1} ($\nu_{C=N}$) observed in 2-chloromethylbenzoxazole, compound **35**, (reported in the appendix, page 287) a precursor used for the synthesis of **25a** (Scheme 7). This data is also comparable to other benzoxazole compounds previously reported in the literature[27, 50-54] that show the $\nu_{C=N}$ band in the range of 1610 – 1632 cm^{-1}. The analogous oxazoline, **19** (Figure 3.7) has an absorption band at 1659 cm^{-1} ($\nu_{C=N}$). The higher value for $\nu_{C=N}$ in the oxazoline may result from the absence of p-π delocalized electrons as in benzoxazole compounds.

Figure 3.7 2-chloromethylbenzoxazole and 2-[(diphenylphosphinoyl)methyl]-4,5-dihydro-oxazole
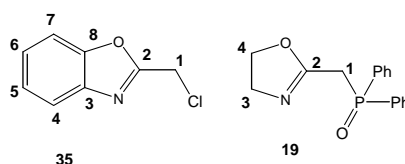
The NMR spectra are in agreement with the reported structure of **25a**. A singlet at 27.7 ppm is seen in the ^{31}P{^{1}H} NMR spectrum which can be compared to the oxazoline ligand, **19** (Figure 3.7) that appears at 28.1 ppm. When these values are compared to shifts for NOPO, **28** (R = Ph), 31.7 ppm and NOPOPO, **29** (R = Ph) 31.3 ppm, the latter are shifted to slightly lower field.[43] This may be attributed to a N-O deshielding effect on the P=O function.

Figure 3.55 NOPO and NOPOPO ligands

NOPO

28

NOPOPO

29
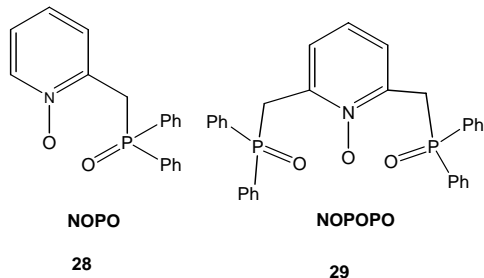
In the ^{1}H NMR for compound **25a**, the methylene proton resonance (C$_1$) appears at 4.1 ppm, as a doublet, $^2J_{\text{H-P}}$ = 14.5 Hz. This can be compared against the values in **19**, 3.4 ppm, (doublet, $^2J_{\text{H-P}}$ = 14.6 Hz) and in the precursor compound **35**, 4.7 ppm (singlet). The resonance for **35** is more deshielded due to the presence of chlorine, which is a strongly electron withdrawing substituent. The methylene protons appear at 4.1 ppm, (doublet, $^2J_{\text{H-P}}$ = 14.5 Hz) in NOPO, **28** and at 4.1 ppm (doublet, $^2J_{\text{H-P}}$ = 13.8 Hz) in NOPOPO, **29**. [43] The doublet results from coupling to the adjacent P=O functional group. The aromatic protons for compound **25a** show multiplet resonances between 7.2–7.8 ppm. These data can be compared to the aromatic resonances of the oxazoline, **19** and the precursor **35** (Figure 3.7) which appear in the ranges of 7.4 -7.8 ppm and 7.2 -7.7 ppm, respectively (appendix, page 287). The ^{1}H NMR spectrum for **35** reported in a patent[47] indicates aromatic resonances in the range of 7.3-7.7 ppm.

In the ^{13}C{^{1}H} NMR spectrum, the C$_1$ resonance for **25a** appears at 33.0 ppm (doublet, $^1J_{\text{C-P}}$ = 63.2 Hz). This is similar to data for the oxazoline, **19** 32.5 ppm (doublet, $^1J_{\text{C-P}}$ = 64.2 Hz), NOPO, **28** 30.7 ppm (doublet, $^1J_{\text{C-P}}$ = 66 Hz) and NOPOPO, **29** 31.4 ppm (doublet, $^1J_{\text{C-P}}$ = 67 Hz). In **35,** the methylene resonance appears at 36.2 ppm (singlet). The aromatic carbons for **25a** show resonances in the region 110.6-151.1 ppm. These can be compared with aromatic resonances observed in **35** that appear in the range

110.6 -150.8 ppm (appendix page 287). As with compound **19** (Chapter 2), splitting of several aromatic carbon resonances was observed in compound **25a** due to coupling with the ^{31}P nucleus (Figure 3.12). In order to confirm this coupling a triple resonance ^{13}C{^{1}H, ^{31}P} NMR experiment was obtained at 125.7 MHz. The ^{13}C{^{1}H} spectrum (Figure 3.13) and ^{13}C{^{1}H, ^{31}P} spectrum (Figure 3.14) are compared in Figure 3.56(a). A comparison expanded for clarity (Figures 3.56(b). The aromatic carbons in the ^{13}C{^{1}H} spectrum show doublet resonances at 128.5, 130.9, 131.3 and 132.1 ppm with $^{2}J_{\text{C-P}}$ =12.5 Hz, $^{3}J_{\text{C-P}}$ = 9.6 Hz, $^{1}J_{\text{C-P}}$ = 104.3 Hz and $J_{\text{C-P}}$ = 2.8 Hz respectively. These become singlets following ^{31}P decoupling. Resonances and magnitude of $J_{\text{C-P}}$ couplings in 25**a** is comparable with arylphosphine oxide compounds reported in the literature.[60]

Table 3.21 Comparative chemical shifts and coupling constants of the phenyl aromatic carbons for compounds 25a and 19

Compound 25a	Compound 19
128.5 ppm, (doublet), *ortho*-carbon, $^{2}J_{\text{C-P}}$ = 12.5 Hz	128.9 ppm, (doublet), *ortho*-carbon, $^{2}J_{\text{C-P}}$ = 12.2 Hz
130.9 ppm, (doublet), *meta*-carbon, $^{3}J_{\text{C-P}}$ = 9.6 Hz	131.5 ppm, (doublet), *meta*-carbon, $^{3}J_{\text{C-P}}$ = 9.7 Hz
131.3 ppm, (doublet), *ipso*-carbon, $^{1}J_{\text{C-P}}$ = 104.3 Hz	132.4 ppm, (doublet), *ipso*-carbon, $^{1}J_{\text{C-P}}$ = 100.9 Hz
132.1 ppm, (doublet), $J_{\text{C-P}}$ = 2.8 Hz	132.5 ppm, (doublet), $J_{\text{C-P}}$ = 2.5 Hz

The $^{13}C\{^1H\}$ NMR data for compound **25a** and **19** are compared in Table 3.21. The magnitudes of the C-P coupling constants indicate short and long range C-P coupling. The resonance at 132.5 ppm, (doublet), J_{C-P} = 2.5 Hz for compound **19** and 132.1 ppm, (doublet), J_{C-P} = 2.8 Hz for **25a** may be *para*-carbons. The *ipso, ortho* and *meta*-carbons in **25a** are also comparable to **19** (Table 3.21). The resonance for C_2 in **25a** recorded at 62.9 MHz appears at 158.8 ppm (doublet) with $^2J_{C-P}$ = 8.8 Hz and the $^{13}C\{^1H\}$ NMR done with 125.7 MHz (Figure 3.13) indicates resonance at 158.6 ppm (doublet, C_2, $^2J_{C-P}$ = 9.1 Hz). This compares with data for **19**: 161.4 ppm (doublet, $^2J_{C-P}$ = 7.4 Hz). The $^{13}C\{^1H\}$ NMR spectrum shows 10 C-aromatic resonances instead of the expected 18 C contained in the molecule perhaps due to overlapping of several resonances. In $^{13}C\{^1H\}$ NMR experiment done with 125.7 MHz spectrometer with ^{31}P coupled (Figure 3.13) and $^{13}C\{^1H, ^{31}P\}$ (Figure 3.14) indicates also 10- aromatic carbon resonances.

Figure 3.56(a) 125.7 MHz $^{13}C\{^{1}H\}$ NMR spectrum and $^{13}C\{^{1}H, ^{31}P\}$ for 25a

$^{13}C\{^{1}H\}$ (^{31}P coupled)

$^{13}C\{^{1}H, ^{31}P\}$
(^{31}P decoupled)
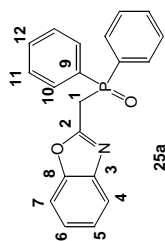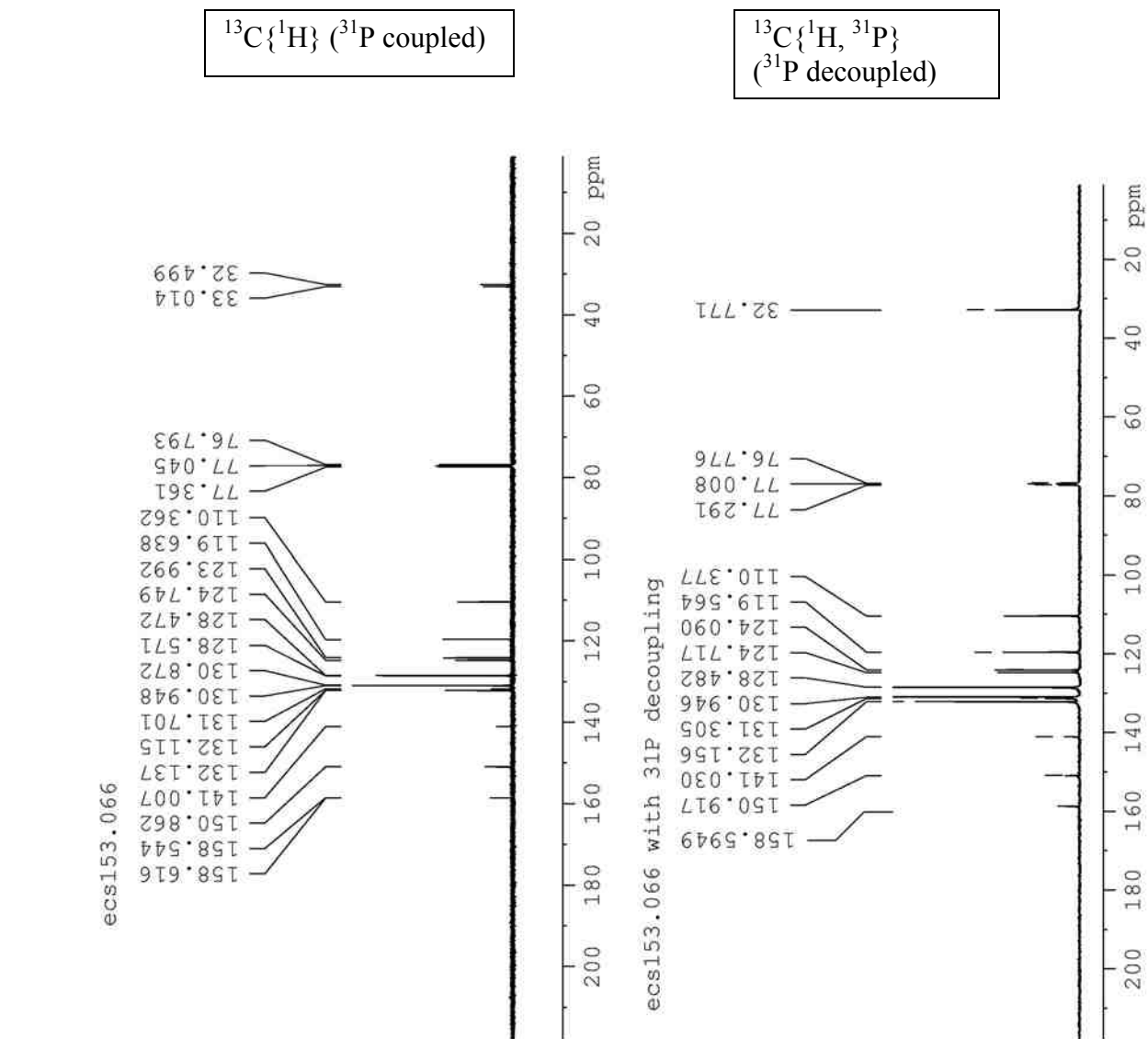
Figure 3.56(b) Expansion of 125.7 MHz ^{13}C{^{1}H} NMR spectrum and ^{13}C{^{1}H, ^{31}P} for 25a
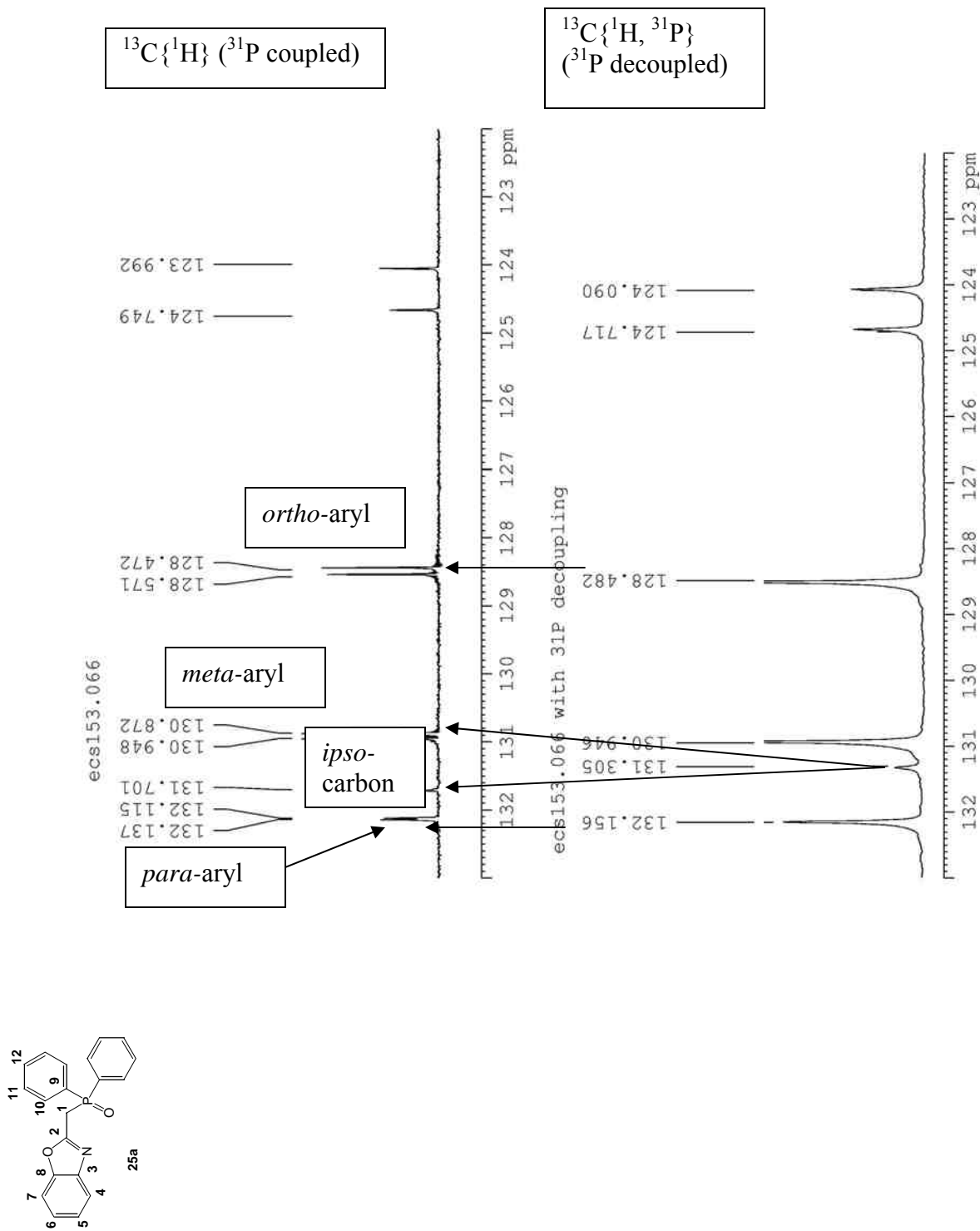
Figure 3.56(b) is also compared with $^{13}C\{^1H\}$ NMR spectrum recorded at 62.9 MHz and this indicate a decrease in peak separation for the spectra recorded at 125.7 MHz, signifies that the *ipso*-carbon is ^{31}P coupled. Only the ^{31}P coupled resonances are shown.

Figure 3.56(c) 125.7 MHz $^{13}C\{^1H\}$ and $^{13}C\{^1H, ^{31}P\}$ NMR spectra compared with 62.9 MHz $^{13}C\{^1H\}$ NMR spectrum for 25a

62.9 MHz $^{13}C\{^1H\}$ (^{31}P coupled)

125.7 MHz $^{13}C\{^1H\}$ (^{31}P coupled)

125.7 MHz $^{13}C\{^1H, ^{31}P\}$ (^{31}P decoupled)

ortho-aryl

meta-aryl

ipso-carbon

para-aryl
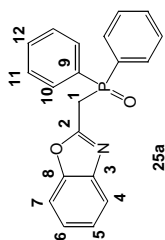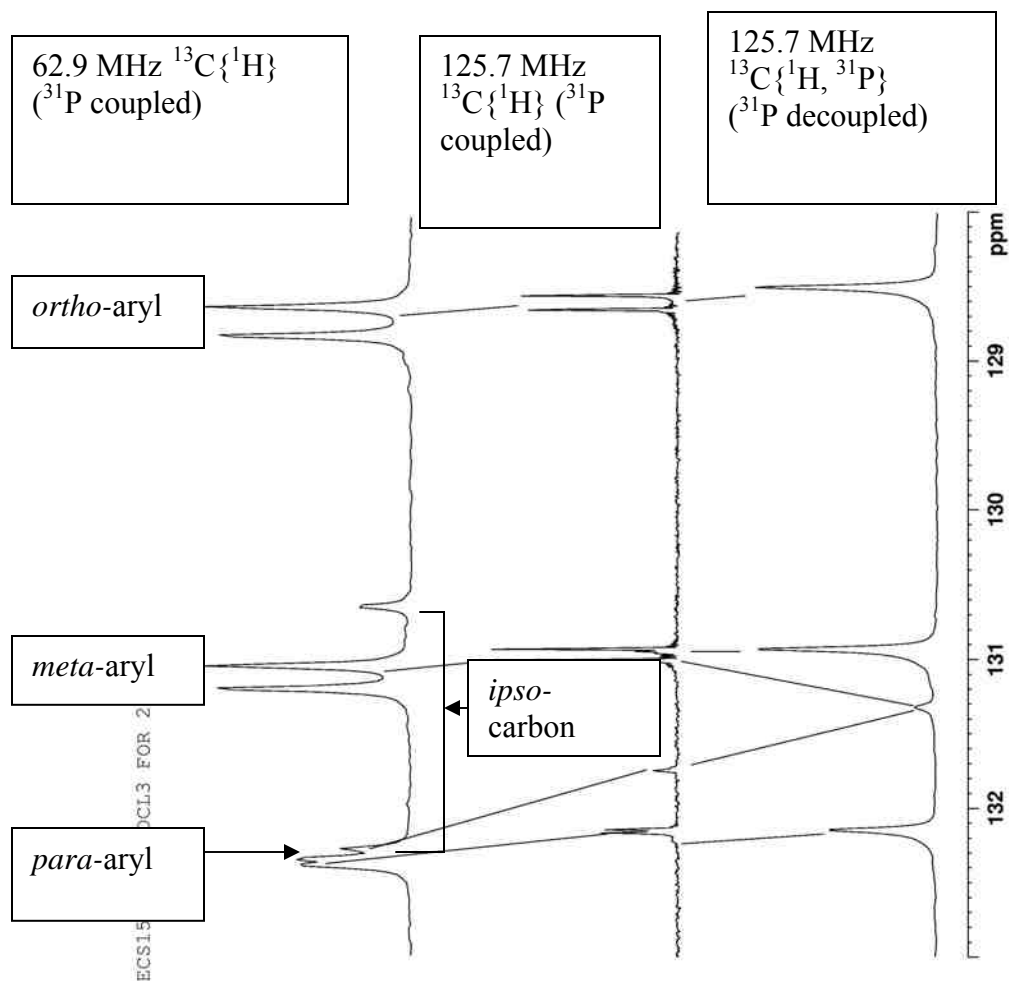
3.4.4 X-ray crystallographic analyses for compound 25a

The molecular structure of **25a** is displayed in Figure 3.16, and selected bond lengths are listed in Table 3.2. Comparisons of several bond lengths for the oxazoline, **19** (Figure 3.7) and **25a** are shown in Table 3.22. The intra-ring distances O(2)-C(1) and N(1)-C(1) are shorter in compound **19** (Figure 3.7) as a result of the greater electron localization.

Table 3.22 Comparison of bond lengths between, 19 (Figure 3.7) and 25a

Type of bond	Oxazoline, 19 (Figure 3.7)	Compound 25a
P(1)-O(1)	1.4865(8)	1.4831(8)
O(2)-C(1)	1.3443(15)	1.3571(14)
N(1)-C(1)	1.2528(17)	1.2925(15)

A view of the crystal packing suggests that there are several weak intermolecular interactions that are responsible for ordering in the lattice. Hydrogen bonding contributes to ordering; however, in this case all H-atoms are bonded to carbon atoms. A view of intermolecular C-H-------O=P approaches is shown in Figure 3.57 and these distances fall in a range 2.26 Å-2.57 Å. Usually hydrogen bonds that involve C-H as a donor are said to be very weak. The plane calculation indicates that the P=O group is oriented by 59.2^{o} from the plane bonded to nitrogen donor atom. This means that the two donor atoms are not in the same plane.

Figure 3.57 H-bonding within crystal structure of compound 25a
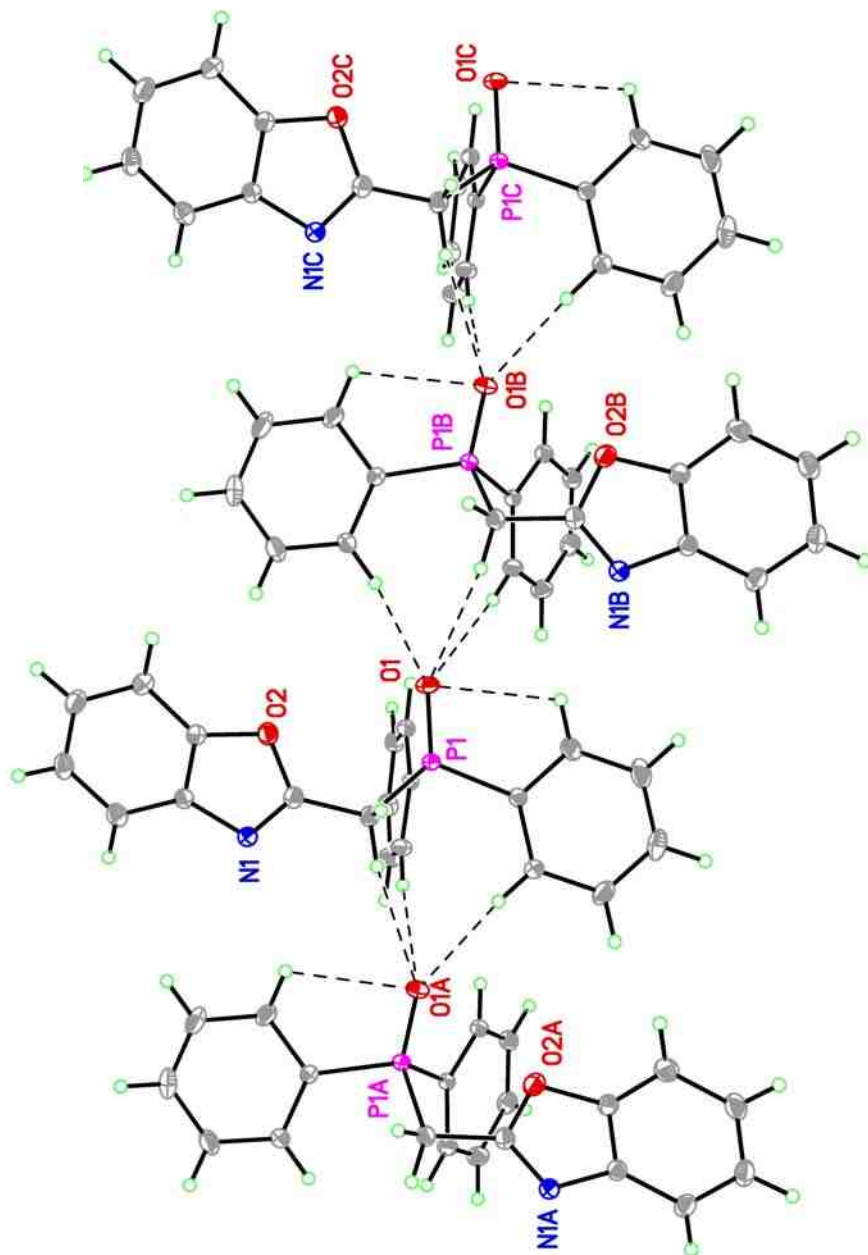
3.4.5 Architectural modification of compound 25a

Compound **25a** is soluble in CHCl$_3$, CH$_2$Cl$_2$, Cl$_2$CH$_2$CH$_2$Cl$_2$, CH$_3$OH and sparingly soluble in toluene and benzene. Since this compound is insoluble in hydrocarbon diluents it may not be suitable for practical solvent extraction applications that employ hydrocarbon or other radiation stable diluents such as FS-13. Therefore, we decided to synthesize derivatives of **25a** that may be soluble in hydrocarbon/FS-13 solvents while retaining the same donor atoms (P=O and N). Compounds **25b-25e** were synthesized using appropriate Grignard reagents.
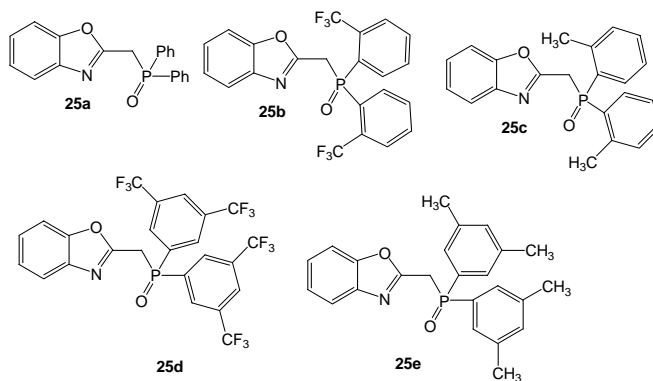
Compounds **25b-25e** have not been previously reported.

3.4.6 Synthesis of compound 25b

Compound **25b** was obtained in 74% yield as shown in Scheme 13. The Grignard reagent was prepared using commercially available 2-bromobenzotrifloride adapting methods which have been developed in our group and others.[28-33, 40] The organo-Grignard reagent was treated with diethyl phosphite to give the required phosphono-Grignard reagent. Substitution with phosphono-Grignard reagent on 2-chloromethylbenzoxazole, **35,** gave compound **25b** as an orange solid that was recrystallized leaving colorless crystals in 74% yield.

25b   35
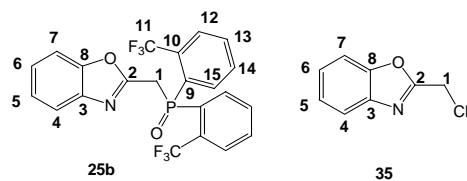
3.4.7 Spectroscopic analyses of compound 25b

The elemental analysis is consistent with the proposed formulation and an intense peak, *m/e* 470.0743 corresponding to [M+H$^+$] is seen in the ESI mass spectrum. An IR spectrum for **25b** shows strong bands at 1607 cm^{-1} and 1125-1217 cm^{-1}. These are tentatively assigned to $\nu_{C=N}$ and $\nu_{P=O}$, respectively, and both are shifted down-frequency from the bands in **25a** which appear at 1610 cm^{-1} ($\nu_{C=N}$) and 1196 cm^{-1} ($\nu_{P=O}$). The $\nu_{C=N}$ band can be compared to the value in 2-chloromethylbenzoxazole, **35**, (reported in the appendix, page 287), 1611 cm^{-1} and other benzoxazole molecules reported in the literature.[50-54] However, the assignment of the $\nu_{P=O}$ is not certain due to the presence of –CF$_3$ group within the molecule that also shows band in the same range.[55]

Compound **25b** shows a single ^{31}P{^{1}H} NMR resonance at 28.4 ppm which is slightly downfield from the shift in **25a**. Both ^{1}H and ^{13}C{^{1}H} NMR data show consistency with 2-chloromethylbenzoxazole, **35.** The methylene protons on C$_2$, appear at 4.3 ppm (doublet, $^2J_{H-P}$ = 14.5 Hz), and compound **35**: 4.7 ppm (singlet). These data can be compared with similar resonance for **25a** that appears at 4.1 ppm (doublet), $^2J_{C-P}$ = 14.5 Hz. Resonances observed between 7.2-8.3 ppm (multiplet) are assigned to aromatic protons for **25b** and in compound **35** all aromatic protons appear as a multiplet in the range of 7.2 -7.7 ppm. Resonances observed between 8.2-8.3 ppm with an integration ratio of 2H, may be assigned to the aromatic protons adjacent to the –CF$_3$ substituents. The aromatic protons for **25a** show multiplet resonances between 7.2 – 7.8 ppm.

The $^{13}C\{^1H\}$ NMR spectrum contains a doublet at 33.7 ppm with $^1J_{C\text{-}P} = 69.4$ Hz assigned to the phosphorus coupled C_1 atom. The $^{13}C\{^1H\}$ NMR resonance for the C_1 in **25a** appears at 33.0 ppm with $^1J_{C\text{-}P} = 63.2$ Hz. Apparently the CF_3 group does not strongly affect the carbon chemical shift of C_1 but the small downfield shift and small increase in $^1J_{C\text{-}P}$ are consistent with electron withdrawal by CF_3. The aromatic carbon resonances appear between 110.3-150.9 ppm for **25b.** These data are comparable to the aromatic carbon resonances in **25a** which appear at 110.6 -151.1 ppm, and the aromatic resonances for **35** appear in the range of 110.6 -150.8 ppm (singlet). In addition, the -CF_3 resonances in $^{13}C\{^1H\}$ NMR spectrum appear at 123.3 ppm (quartet), with $^1J_{C\text{-}F} =$ 274.5 Hz for **25b**. These data are comparable to the literature[56-59] data that reported the $^{13}C\{^1H\}$ NMR for -CF_3 resonances in the range of 122 – 125 ppm (quartet), with $^1J_{C\text{-}F}$ ranges from 272 – 276 Hz. The splitting of aromatic carbon resonances is also observed in compound **25b** due to coupling with ^{31}P nucleus (Figure 3.25). The carbon-13 NMR experiments done at 125.7 MHz as $^{13}C\{^1H\}$ (Figure 3.26) and $^{13}C\{^1H, \,^{31}P\}$ (Figure 3.27) assist in the assignment of observed couplings. A comparison between Figure 3.26 and 3.27 is shown on Figure 3.58a-c. The aromatic carbons show doublet at 130.6 ppm, with $^1J_{C\text{-}P} = 99.3$ Hz assigned to *ipso*-carbon, and a quartet of doublets appear at 131.8 ppm, with $^2J_{C\text{-}P} = 6.5$ Hz, $^2J_{C\text{-}F} = 33.5$ Hz is assigned to the *ortho*-carbon bonded to CF_3 group. Studies[57, 58] have also shown that, the C-CF_3 resonances appear as quartet of doublets in the range of 132.4-133.6 ppm, with $^2J_{C\text{-}P} = 5.4$ Hz and $^2J_{C\text{-}F} = 33$ Hz

Resonances that appear at 131.5 ppm (doublet), with $J_{C\text{-}P} = 13.8$ Hz and 134.2 ppm (doublet), $J_{C\text{-}P} = 8.9$ Hz may be assigned to C_{15} and C_{14} respectively. Multiple splitting of the C_{10} in **25b** is due to $^2J_{C\text{-}F}$ coupling with –CF_3 group. In the $^{13}C\{^1H\}$ NMR

spectrum if all carbon atoms are magnetically inequivalent 18 C-aryl resonances are expected along with C_1, C_2 and two $-CF_3$ groups. In both the 62.9 and 125.7 MHz $^{13}C\{^1H\}$ 12-carbon resonances are observed that are consistent with expected number of magnetically inequivalent aromatic carbons. The resonance for C_2 appears at 158.2 ppm (doublet, $^2J_{C-P}$ = 9.2 Hz) for **25b** which is comparable to C_2 resonance for **25a** that appears at 158.8 ppm (doublet, $^2J_{C-P}$ = 8.8 Hz).

Figure 3.58(a) 125.7 MHz $^{13}C\{^1H\}$ NMR spectrum compared with the $^{13}C\{^1H,\ ^{31}P\}$ for 25b

$^{13}C\{^1H\}$ (^{31}P coupled)

$^{13}C\{^1H,\ ^{31}P\}$ (^{31}P decoupled)
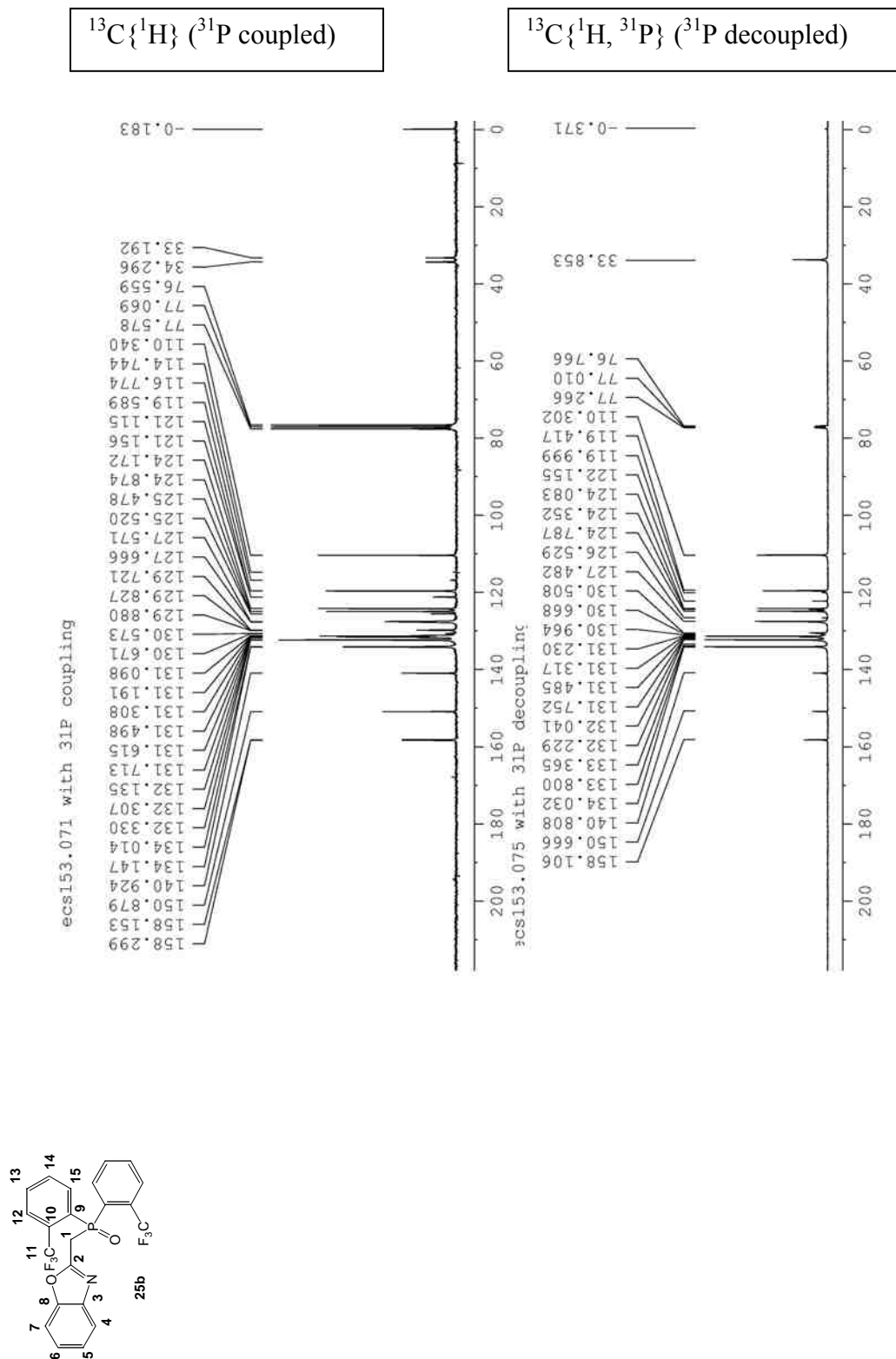
Figure 3.58(b) Expansion of 125.7 MHz ^{13}C{^{1}H} NMR spectrum compared with the ^{13}C{^{1}H, ^{31}P} for 25b

^{13}C{^{1}H} (^{31}P coupled)

^{13}C{^{1}H, ^{31}P} (^{31}P decoupled)
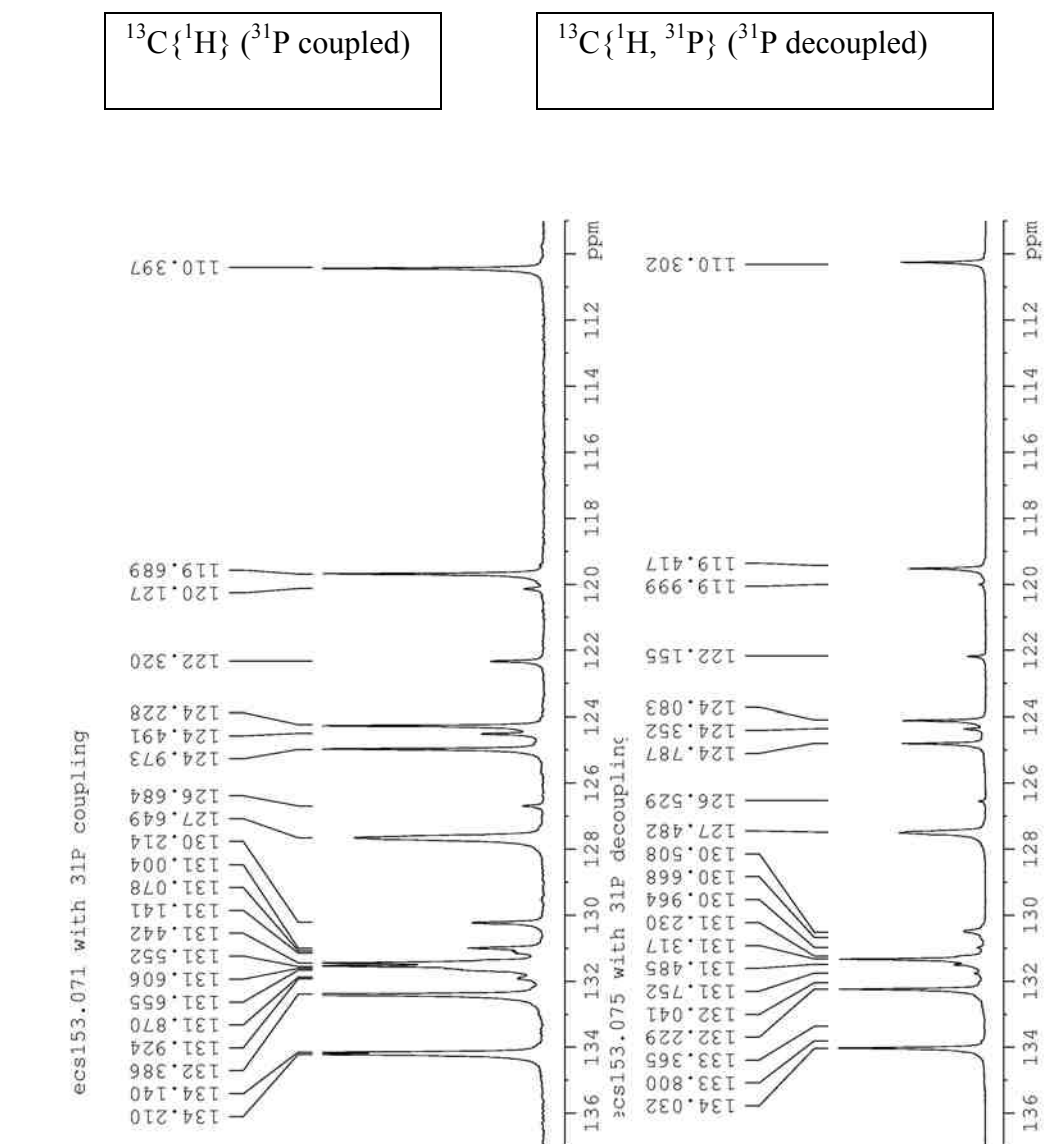
Figure 3.58(c) Expansion of 125.7 MHz ^{13}C{^{1}H} NMR spectrum compared with the

^{13}C{^{1}H, ^{31}P} for 25b

^{13}C{^{1}H}
(^{31}P coupled)

^{13}C{^{1}H, ^{31}P}
(^{31}P decoupled)

ipso-carbon

ortho-aryl
C-CF$_3$

meta-aryl
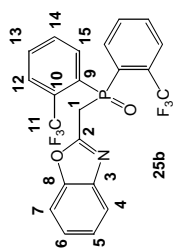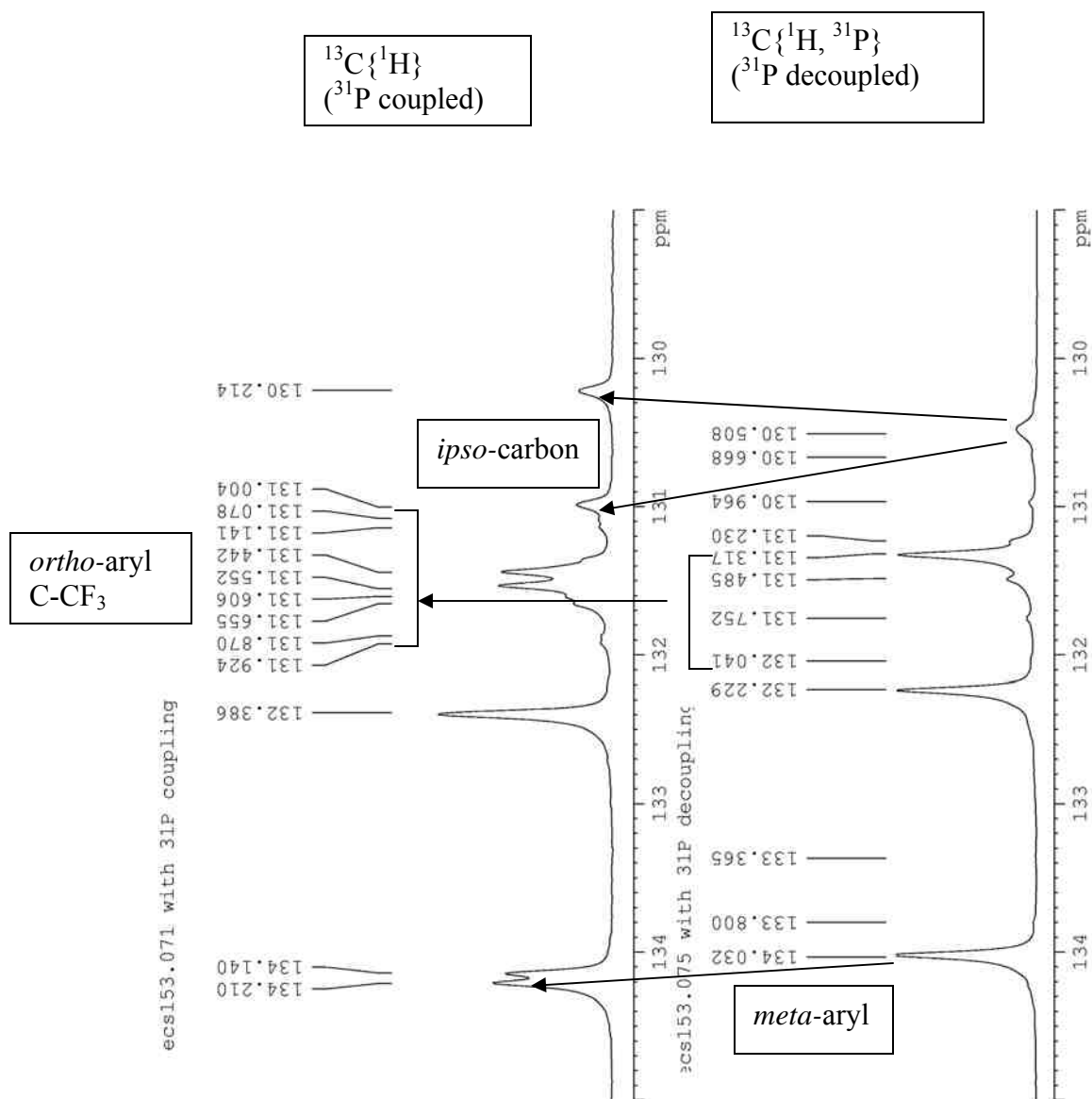
3.4.8 X-ray crystallographic analyses of compound 25b

The crystal and molecular structure of **25b** was determined by single crystal X-ray diffraction methods. No solvent molecules were observed in the crystal lattice. In this structure the torsion angle between P=O plane and nitrogen (N) is 65.4^o. The reason for this orientation rests with N electron pair/P=O bond dipole repulsion. Previous studies[44] show that the presence of –CF$_3$ substituents in a molecule has both electronic as well as steric impacts on the phenyl ring resulting from interaction between π-orbitals of the phenyl ring and π-antibonding orbitals (π^*) of -CF$_3$ which causes electron charge displacement from the benzene ring to the π^*-orbitals belonging to –CF$_3$ substituent. It has been noted that the –CF$_3$ has a strong inductive attraction to neighboring electrons also.[44]

3.4.9 Synthesis of compound 25c

Another new compound which was synthesized using the Grignard method is compound **25c**. Commercially available *o*-tolylmagnesium bromide (3 equivalents) was combined with diethyl phosphite (1 equivalent) to form the required phosphono Grignard reagent. Substitution of this reagent on 2-chloromethylbenzoxazole (1 equivalent) gave the target molecule **25c** in 67% yield. The workup and purification of the crude product has been described in the experimental part (Scheme 16).

3.4.10 Spectroscopic analyses of compound 25c

Elemental CHN analyses agree with the theoretical value for **25c**. The mass spectrum shows an intense peak corresponding to [M+H$^+$] at 362.1304 *m/e* consistent with the proposed composition of **25c**.
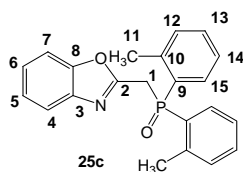
The IR spectrum of **25c**, displays bands at $\nu_{C=N}$ = 1603 cm^{-1} and $\nu_{P=O}$ =1178 cm^{-1}. This data can be compared against $\nu_{C=N}$ = 1610 cm^{-1} in similar molecules reported by Minami and co-workers,[27] and other benzoxazole molecules reported in the literature.[50-54] The assignment of $\nu_{P=O}$ = 1178 cm^{-1} in compound **25c** is down frequency shifted compared to $\nu_{P=O}$ for **25a** (1196 cm^{-1}). The presence of electron donating CH$_3$ at *ortho* position weakens the P=O bond probably due to electron repulsion between P=O and the phenyl ring.

The NMR data for **25c** are consistent with the proposed structure. A singlet at 31.1 ppm is seen in the ^{31}P{^{1}H} NMR spectrum for **25c.** This resonance is comparable with **25a** which appears at 27.7 ppm and **25b**, 28.4 ppm. In the ^{1}H NMR for **25c,** the methylene protons on C$_1$ show a resonance at 4.1 ppm (doublet, $^{2}J_{\text{H-P}}$ = 14.2 Hz), this can be compared to similar resonances observed in **25a**, 4.1 ppm (doublet, $^{2}J_{\text{H-P}}$ = 14.5 Hz), **25b**, 4.3 ppm (doublet, $^{2}J_{\text{H-P}}$ = 14.5 Hz) and compound **35**, 4.7 ppm (singlet). A resonance appears at 2.3 ppm (singlet) with an integration of 6H corresponds to the aryl –CH$_3$ protons. Resonances observed in the range 7.1-7.8 ppm with a total integration of 12H are assigned to the aromatic protons, and in compound **35** all aromatic protons appear as multiplet in the range of 7.2 -7.7 ppm. The aromatic protons for **25a** and **25b** appear as multiplet in the ranges of 7.2 – 7.8 ppm and 7.2 – 8.3 ppm respectively. In addition, splitting of aromatic proton resonances in **25c** between 7.7-7.8 ppm is a result of coupling with ^{31}P nucleus. A ^{1}H NMR experiment recorded on 500 MHz with ^{31}P coupling and ^{31}P decoupling confirmed that these resonances become a singlet (Figure

3.36b and 3.36c). A comparison between the two spectra is displayed on Figure 3.59a and

b.

Figure 3.59(a) 500 MHz ^{1}H NMR spectrum with ^{31}P coupling compared with ^{31}P

decoupling for 25c
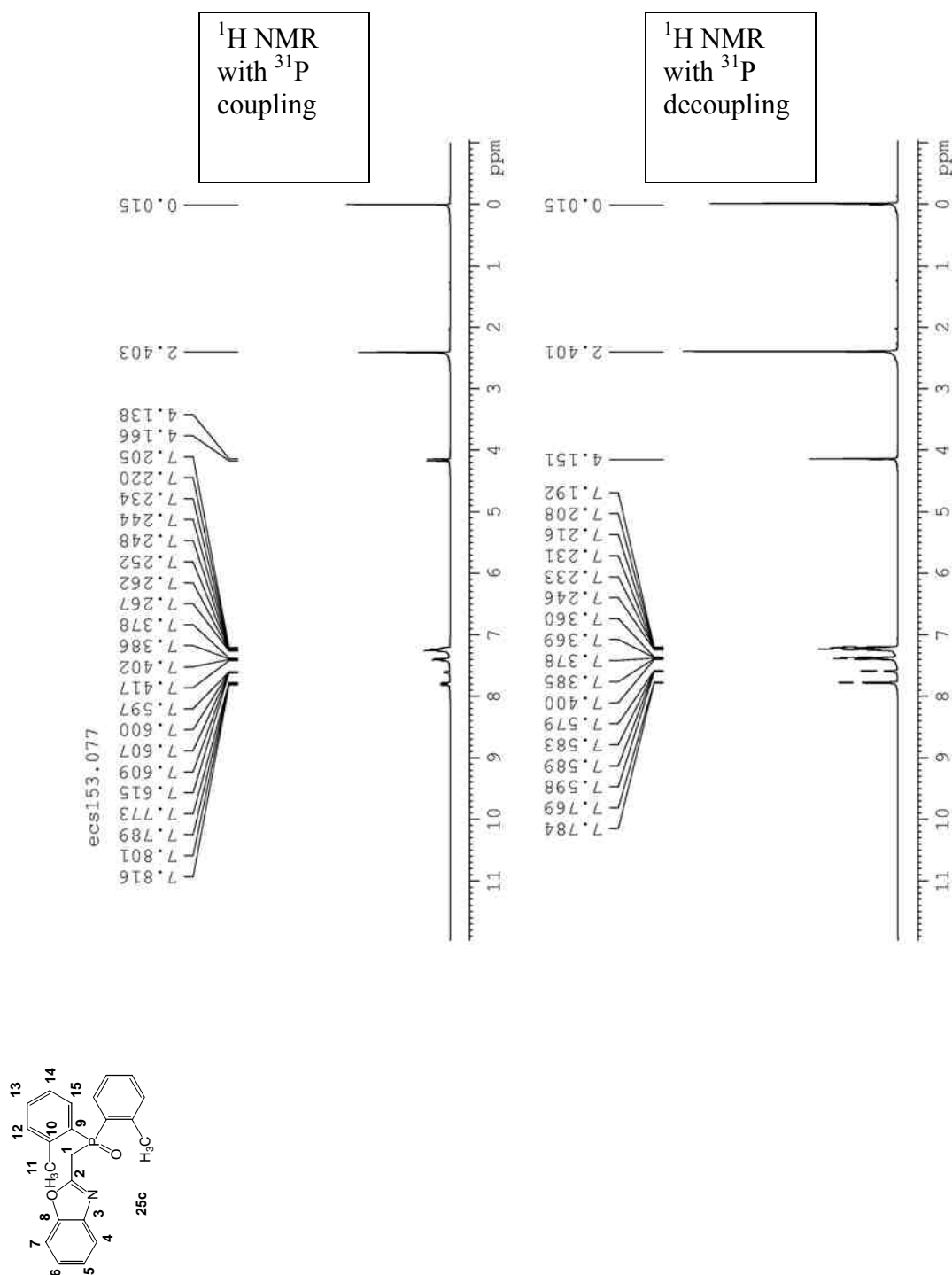
Figure 3.59(b) Expansion of Figure 3.59(a)

¹H NMR with ³¹P coupling

7.205
7.220
7.234
7.244
7.248
7.252
7.262
7.267
7.378
7.386
7.402
7.417

7.597
7.600
7.607
7.609
7.615

ecs153.077

7.773
7.789
7.801
7.816

doublet

¹H NMR with ³¹P decoupling

7.192
7.208
7.216
7.231
7.233
7.246

7.360
7.369
7.378
7.385
7.400

7.579
7.583
7.589
7.598

7.769
7.784

singlet
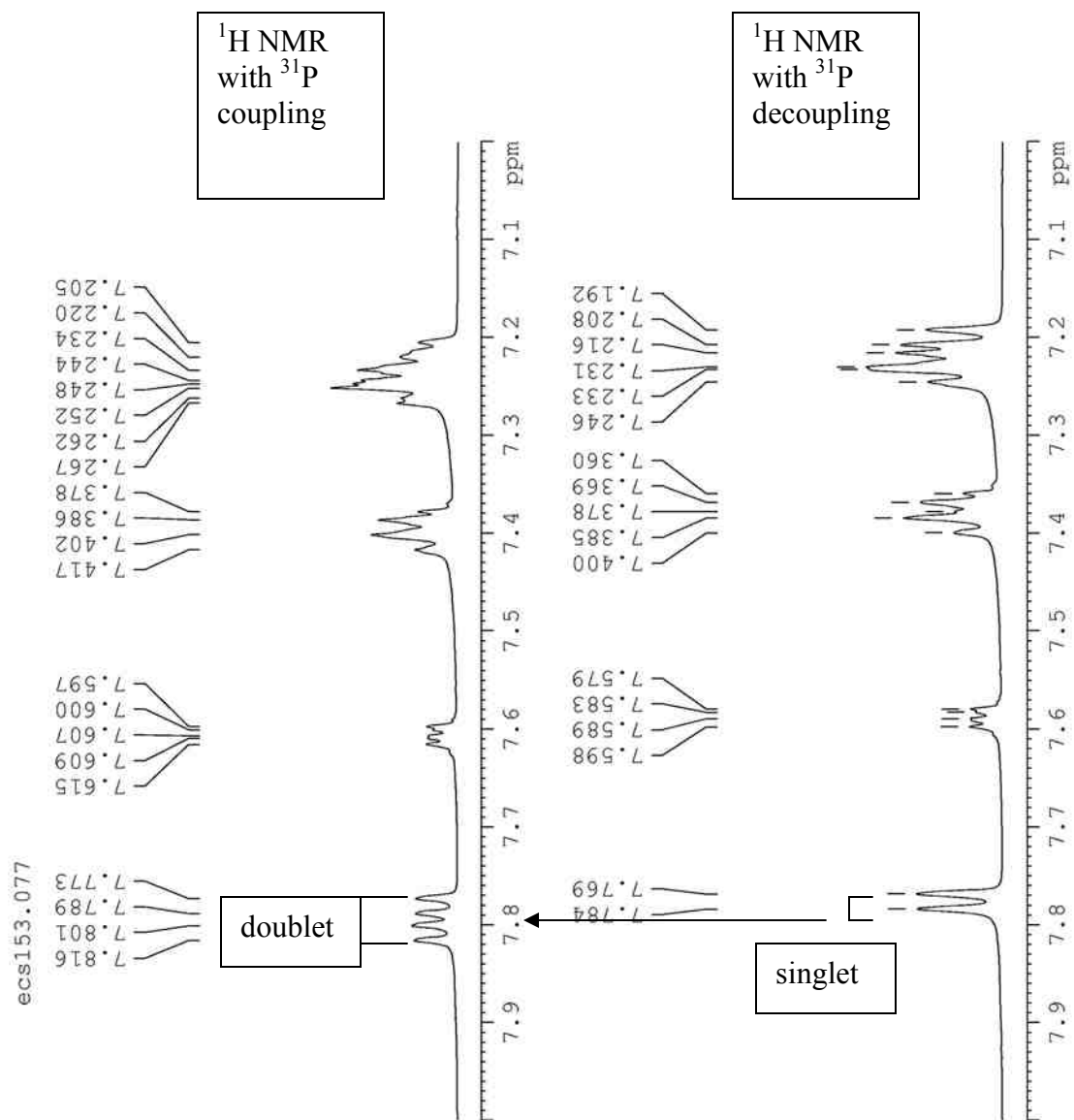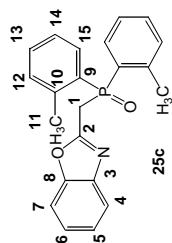
In the $^{13}C\{^1H\}$ NMR spectrum, the C_1 resonance appears at 32.6 ppm (doublet, $^1J_{C-P}$ = 63.0 Hz), similar resonances for **25a** is 33.0 ppm (doublet, $^1J_{C-P}$ = 63.2 Hz) and **25b** is 33.7 ppm (doublet, $^1J_{C-P}$ = 69.4 Hz). A resonance at 21.4 ppm (doublets), $^3J_{C-P}$ = 4.3 Hz is assigned to CH_3-Ph. The doublet is due to long range C-P coupling. The aromatic carbon resonances appear between 110.6-151.2 ppm. These data are comparable to the $^{13}C\{^1H\}$ NMR spectrum for **25a, 25b** and **35.** Coupling of aromatic carbons in **25c** with ^{31}P is observed (Figure 3.37). The $^{13}C\{^1H\}$ NMR spectrum was repeated at 125.7 MHz with and without ^{31}P coupling (Figure 3.38 and Figure 3.39). A comparison between Figure 3.38 and 3.39 is shown in Figure 3.60(a) and its expansion is made for clarity (Figure 3.60(b)-(c)).

Figure 3.60(a) 125.7 MHz ^{13}C{^{1}H} NMR spectrum compared with ^{13}C{^{1}H, ^{31}P} for 25c

^{13}C{^{1}H}
(^{31}P coupled)

^{13}C{^{1}H, ^{31}P}
(^{31}P decoupled)

meta-aryl
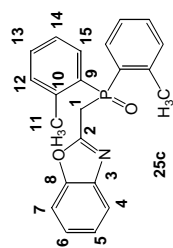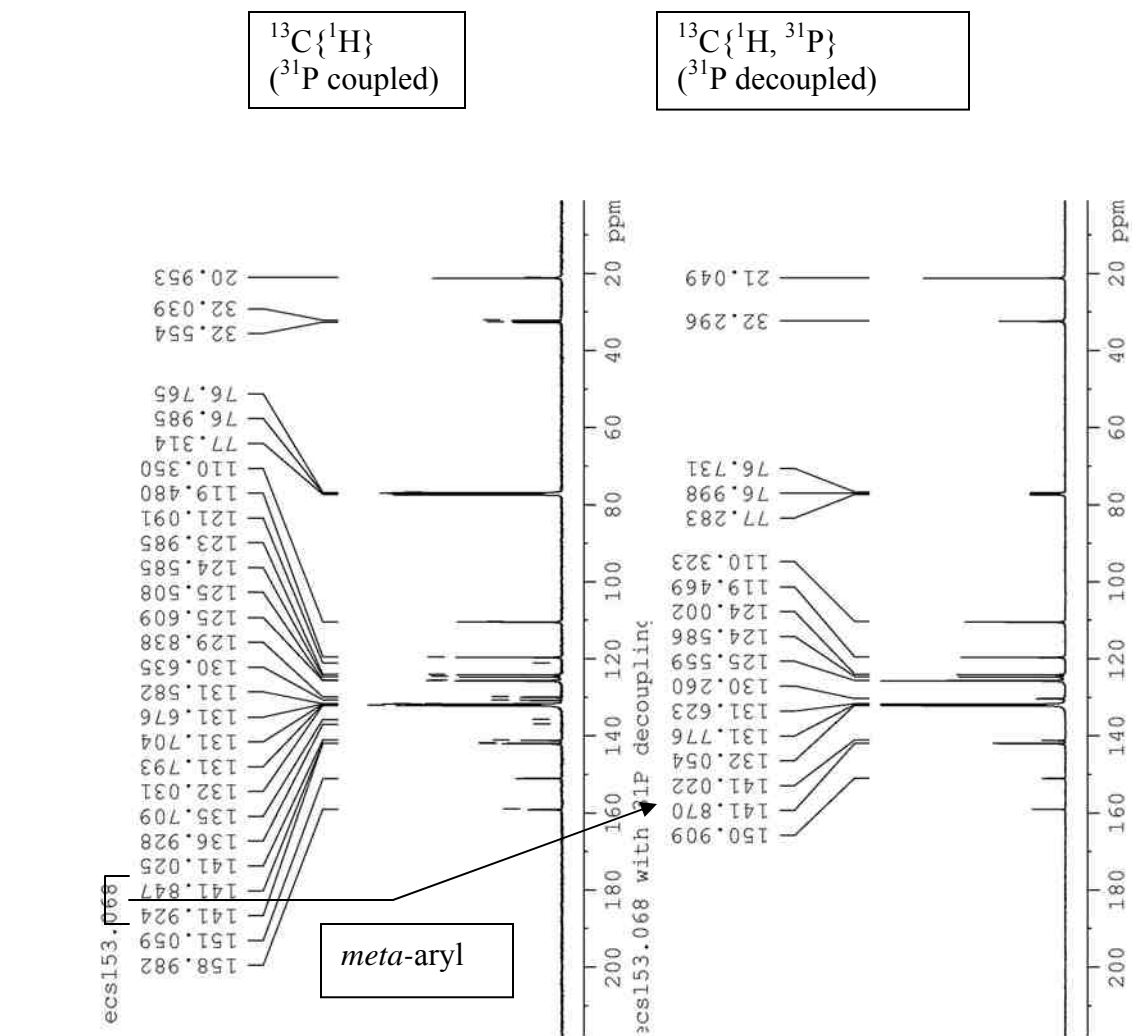
Figure 3.60(b) Expansion of 125.7 MHz ^{13}C{^{1}H} NMR spectrum compared with ^{13}C{^{1}H, ^{31}P} for 25c
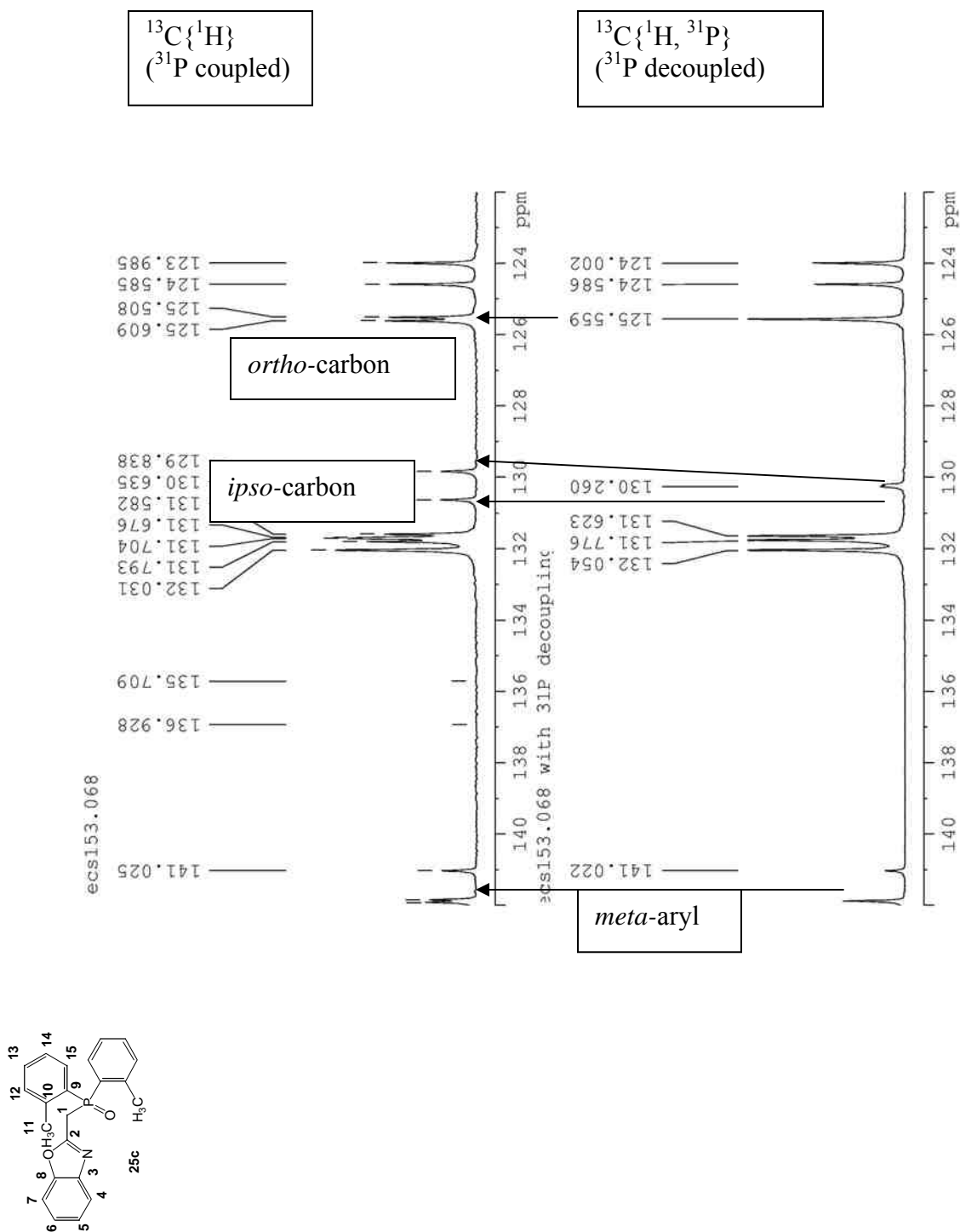
Figure 3.60(c) Expansion of 125.7 MHz ^{13}C{^{1}H} NMR spectrum compared with ^{13}C{^{1}H, ^{31}P} for 25c
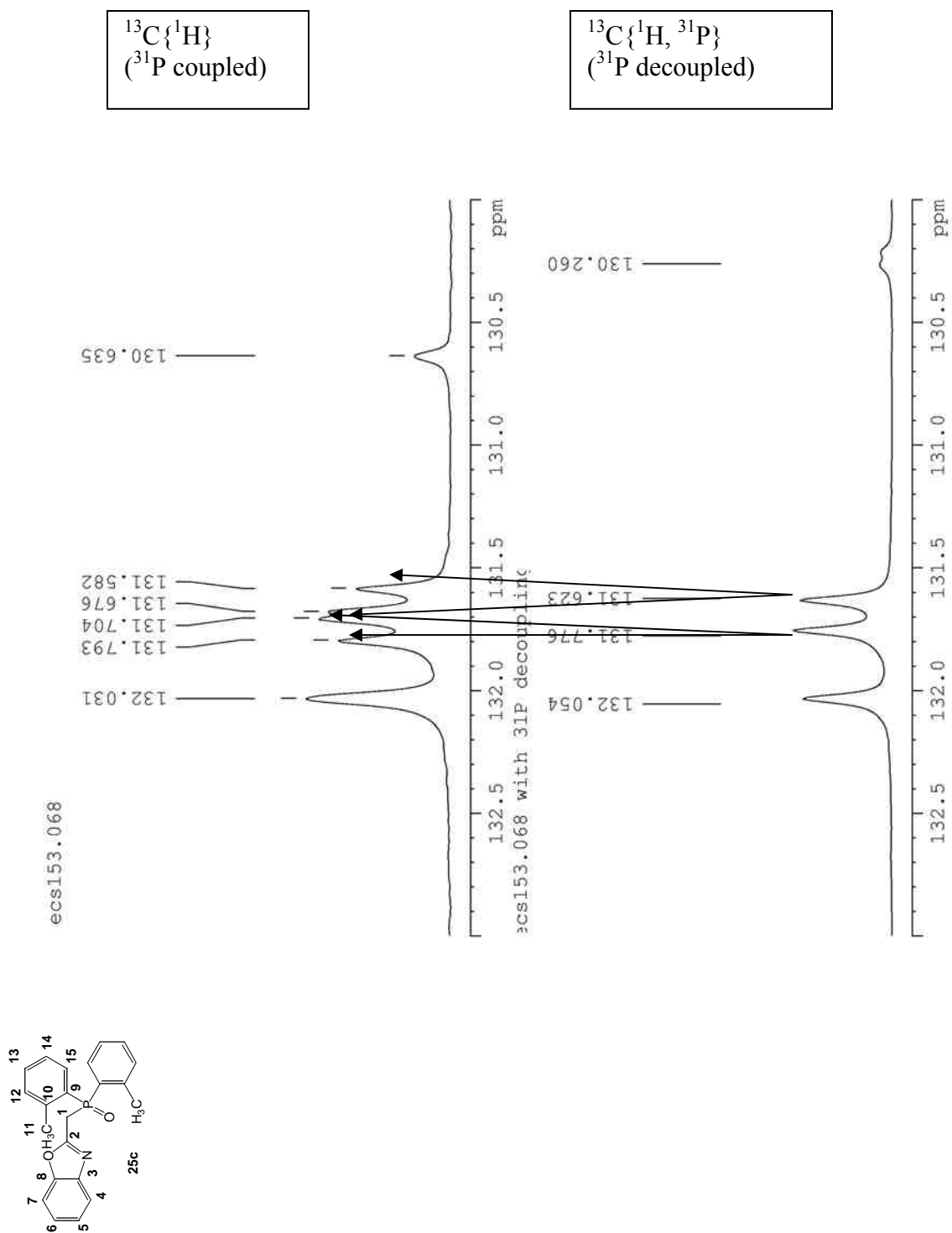
The $^{13}C\{^1H\}$ resonance at 125.6 ppm, (doublet), is assigned to the *ortho*-carbon, with $^2J_{C-P}$ = 12.8 Hz. This resonance is shifted to high field compared to the related resonance in **25a** which appears at 128.5 ppm as a doublet, with $^2J_{C-P}$ = 12.5 Hz. The shift may reflect the presence of electron denoting substituent (-CH$_3$) at the *ortho* position increases the electron density in **25c** compared to the unsubstituted phenyl in **25a**. The doublet resonance at 130.2 ppm with $^1J_{C-P}$ = 100.3 Hz is assigned to *ipso*-carbon. This data is also shifted to high field when compared to similar resonance for **25a** that appears at 131.3 ppm (doublet) with $^1J_{C-P}$ = 104.3 Hz. Further coupling in **25c** appears at 131.6 ppm, J_{C-P} = 11.8 Hz and 131.7 ppm, J_{C-P} = 11.1 Hz may be C$_{12}$ and C$_{15}$ respectively. A doublet resonance appears at 141.9 ppm, J_{C-P} = 9.7 Hz probably is the *meta*-carbon. In the $^{13}C\{^1H\}$ NMR spectrum recorded at 62.9 MHz, 18 C-aromatic resonances are expected to appear, but only 12 C resonances are resolved. The 125.7 MHz $^{13}C\{^1H\}$ NMR spectrum shows the same number of aromatic carbon resonances which is consistent with the expected number of magnetically inequivalent aromatic carbons in **25c**. The resonance for C$_2$ appears at 159.3 ppm (doublet, $^2J_{C-P}$ = 8.5 Hz) at 62.9 MHz that is comparable to 159.0 ppm (doublet, $^2J_{C-P}$ = 8.5 Hz) at 125.7 MHz.

3.4.11 X-ray crystallographic analyses of compound 25c

Compound **25c** was crystallized from ethyl acetate/hexane/dichlomethane solution to give pale yellow crystals. The molecular structure of **25c** was determined by single crystal X-ray diffraction analysis (Figure 3.41). Crystal parameters and selected bond lengths are summarized in Table 3.11 and 3.12.

Table 3.23 Comparison of related bond lengths for crystal structures 25a, 25b and 25c ligands

25a 25b 25c
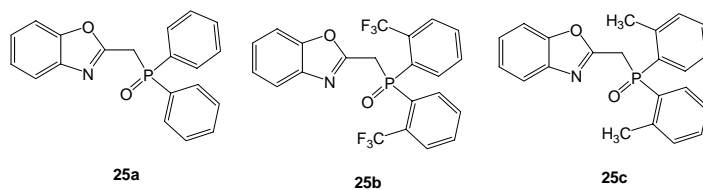
Bond length (Å)	Compound 25a	Compound 25b	Compound 25c
P-O	1.4831(8)	1.4714(9)	1.4892(8)
P-C	1.8226(11)	1.8304(13)	1.8333(10)
N-C	1.2925(15)	1.2906(18)	1.2931(13)
O-C	1.3571(14)	1.3521(16)	1.3631(13)
C-P	1.8059(10)	1.8170(13)	1.8068(10)
C-P	1.7984(11)	1.8278(11)	1.8074(10)
C-CH$_2$	1.4806(15)	1.4823(18)	1.4805(14)

The P=O bond lengths for **25a** (1.4831(8)Å and **25c** (1.4892(8)Å are comparable but relatively, longer compared to similar P=O bond length in **25b** (1.4714(9)Å. The presence of the electron withdrawing CF$_3$ group probably reduces the electron density on the aryl-P=O bond, hence strengthen the P=O bond. The P-C, N-C, O-C and C-CH$_2$ bond

lengths in **25a**, **25b** and **25c** are essentially identical. However, both the C-P bond lengths are slightly different within the same structure and compound **25b** shows longer C-P bond length than **25a** and **25c** and these data is shown in Table 3.23. In addition the torsion angle between the plane bonded to P=O and nitrogen donor atoms is 88.8°, in **25a** is 59.2°. The reason to this variation may be the electron donating CH_3 increases the electron density within the molecule such that the repulsion between the lone pair of electrons on nitrogen and P=O unit becomes more pronounced.

3.4.12 Synthesis of compound 25d

The new compound **25d** was synthesized using the Grignard reagent method used to prepare **25a-25c**.[28-33, 40] (Scheme 19).
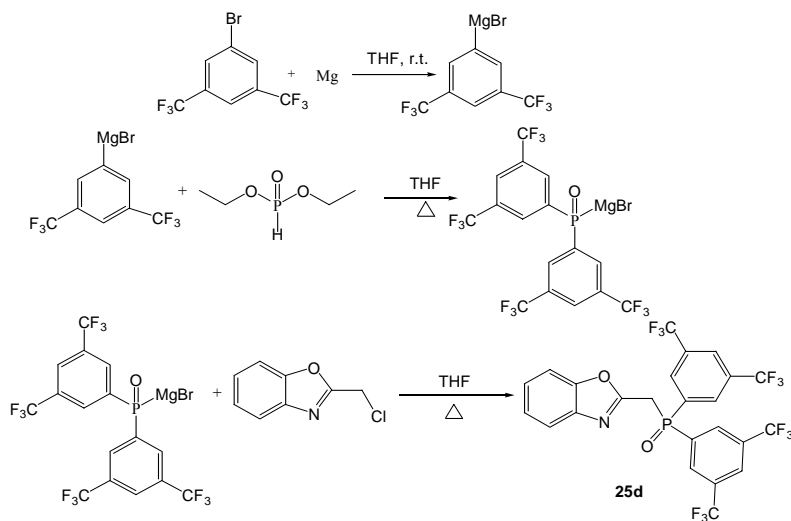
The Grignard reagent was prepared from the combination of magnesium turnings (3 eq.) with commercially available 3,5-bis(trifluoromethyl)-bromobenzene (3 eq.) in dry THF. The resulting solution was converted to the relevant phosphono Grignard reagent by dropwise addition of diethyl phosphite. Substitution with 2-chloromethylbenzoxazole afforded compound **25d** in 55% yield. The workup and purification of the crude product have been described in the experimental part.

3.4.13 Spectroscopic analyses of compound 25d

The elemental analyses found are consistent with the calculated data indicating that **25d** is obtained in pure condition. The mass spectrum shows an intense peak corresponding to [M+H$^+$] at 606.0496 *m/e* which is consistent with the composition of compound **25d**.
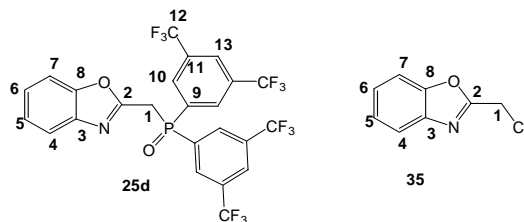
The IR spectrum of compound **25d**, displays bands at $\nu_{C=N}$ = 1616 cm^{-1} and $\nu_{P=O}$ (1140-1283 cm^{-1}). The $\nu_{C=N}$ band for **25d** slightly compares to $\nu_{C=N}$ band for **25a** ($\nu_{C=N}$ = 1610 cm^{-1}), and **35** ($\nu_{C=N}$ = 1611 cm^{-1}). The band at 1616 cm^{-1} for **25d** closely compares with the $\nu_{C=N}$ =1610 cm^{-1} for similar molecules reported by Minami and co-workers[27] and other related benzoxazole compounds reported in the literature,[50-54] that show bands in the range of 1610 – 1632 cm^{-1}. Compounds **25b** ($\nu_{C=N}$ = 1607 cm^{-1}) and **25c** ($\nu_{C=N}$ = 1603 cm^{-1}) have the lowest IR $\nu_{C=N}$ bands compared to **25d** and **25a**. However, the assignment of $\nu_{P=O}$ in compound **25d** is not perfect due to –CF$_3$ group that shows band in the same range.[55]

The ^{31}P{^{1}H} NMR spectrum shows a singlet at 23.4 ppm which is shifted upfield compared to **25a** (27.7 ppm), **25b** (28.4 ppm) and **25c** (31.1 ppm). The reason to this may be the presence of two electrons withdrawing –CF$_3$ groups at the *meta* position in **25d** compared to one CF$_3$ in **25b**.

The ^{1}H NMR for compound **25d** displays a resonance at 4.2 ppm (doublet, $^2J_{\text{H-P}}$ = 16.2 Hz) that is assigned to the methylene protons on C$_1$. These data are comparable to

the resonance for methylene protons on C_1 for **25b** that appears at 4.3 ppm (doublet, $^2J_{H-P}$ = 14.5 Hz). Resonances observed between 7.2-8.3 ppm with an integration of 10H are assigned to aromatic protons and in **25b** the aromatic protons appears between 7.2 – 8.3 ppm. The resonance at 8.4 ppm (doublet, J = 11.2 Hz) with an integration ratio of 4H are assigned to the aromatic protons adjacent to P=O group that lead to $^3J_{H-P}$ = 11.2 Hz. This data is also comparable to literature[59] resonance for similar protons that appear at 7.8 ppm with $^3J_{H-P}$ = 12.2 Hz. In order to confirm the J_{H-P} coupling in **25d,** a ^1H NMR experiment was repeated on 500 MHz with and without ^{31}P coupling (Figure 3.49b-c) and these show that the doublet resonance that appears at 8.4 ppm is reduced into singlet after ^{31}P decoupling. The comparison between Figure 3.49b and 3.49c is shown on Figure 3.61a-b.

Figure 3.61(a) 500 MHz ^{1}H NMR spectrum with ^{31}P coupling compared with ^{31}P decoupling for 25d
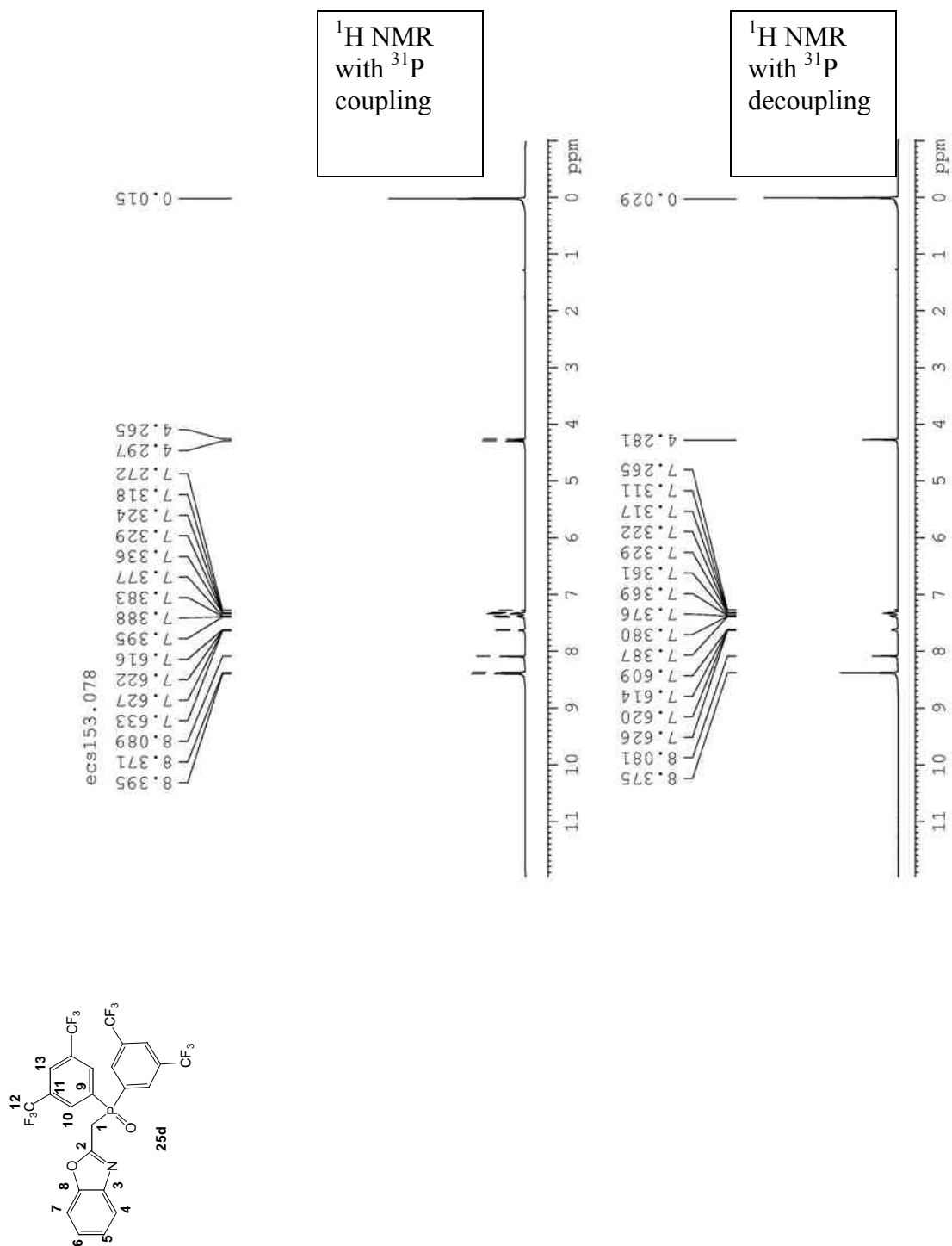
Figure 3.61(b) Expansion of Figure 3.61(a)
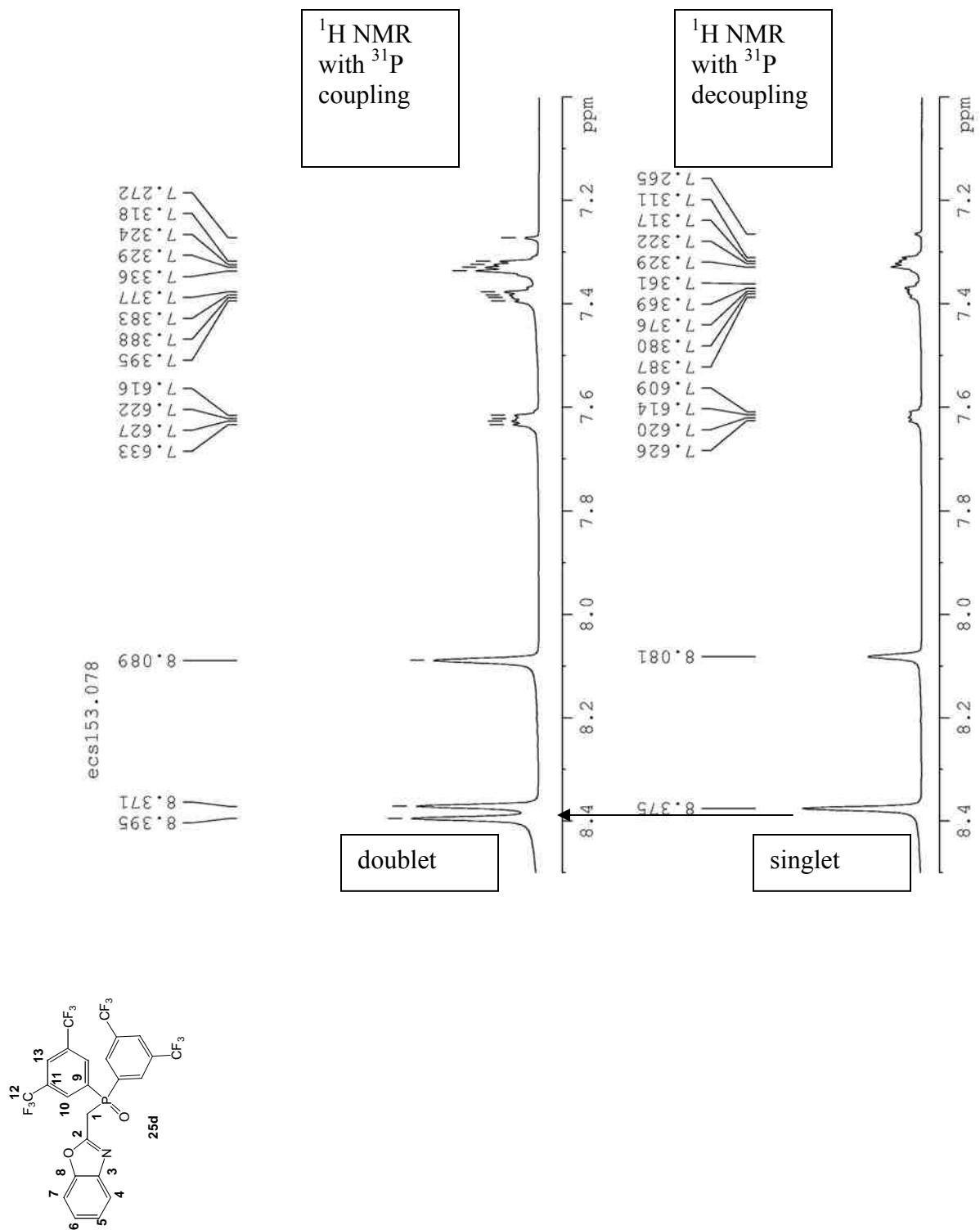
The aromatic proton resonances for **25d** and **25b** are slightly downfield shifted compared to the aromatic protons for **25a** and **25c** that appear in the range of 7.2 − 7.8 ppm, probably due to the electron withdrawing CF_3 group in **25b** and **25d**.

In the $^{13}C\{^1H\}$ NMR spectrum, the C_1 resonance appears at 32.7 ppm (doublet, $^1J_{C-P} = 67.3$ Hz). This data is comparable to similar resonance for C_1 in **25b** that appears at 33.7 ppm (doublet, $^1J_{C-P} = 69.4$ Hz). The aromatic carbon resonances for **25d** appear in the range of 110.5-150.8 ppm and in **25b** is 110.3 − 150.9 ppm. The resonance at 122.5 ppm (quartet), with $^1J_{C-F} = 273.6$ Hz is assigned to $-CF_3$ group and similar $^{13}C\{^1H\}$ resonance for $-CF_3$ in **25b** appears at 123.3 ppm (quartet, $^1J_{C-F} = 274.5$ Hz). These data is comparable to similar resonances reported in the literature[56-59] that appear in the range of 122 − 125 ppm as a quartet with coupling constants ranges from 272 − 276 Hz. In addition, further splitting of three aromatic carbon resonances was observed in **25d** due to coupling with ^{31}P and CF_3 group (Figure 3.50). The $^{13}C\{^1H\}$ NMR spectrum was also recorded at 125.7 MHz with and without ^{31}P coupling (Figure 3.51 and Figure 3.52) in order to confirm the ^{31}P coupling. The comparison between Figure 3.51 and 3.52 is displayed in Figure 3.62a and its expansion in Figure 3.62b and 3.62c.

Figure 3.62(a) 125.7 MHz $^{13}C\{^1H\}$ NMR spectrum compared with $^{13}C\{^1H, ^{31}P\}$ for 25d

$^{13}C\{^1H\}$
(^{31}P coupled)

$^{13}C\{^1H, ^{31}P\}$
(^{31}P decoupled)

ppm

ppm

-0.094

-0.060

32.469
33.007

29.705

76.698
76.950
77.202
110.440
119.225
120.025
121.398
123.573
124.288
124.983
125.793
126.789
127.553
128.863
131.422
131.488
131.694
132.230
132.331
132.518
132.617
132.792
132.890
133.062
133.159
133.875
140.668
150.731
156.415
156.476

76.792
77.009
77.355
110.375
119.262
120.065
121.434
122.056
123.609
125.073
125.724
126.783
127.259
127.846
129.284
130.022
131.214
131.498
132.332
132.600
132.857
133.149
133.460
133.549
140.704
150.768
156.481

ecs153.069 with 31P coupling

ecs153.069 with 31P decoupling

25d

Figure 3.62(b) Expansion of 125.7 MHz ^{13}C{^{1}H} NMR spectrum compared with ^{13}C{^{1}H, ^{31}P} for 25d

^{13}C{^{1}H} (^{31}P coupled)

^{13}C{^{1}H, ^{31}P}
(^{31}P decoupled)

Left spectrum (^{13}C{^{1}H} ^{31}P coupled), ppm:

119.225
120.025
121.398
123.573
124.288
124.983
125.793
126.789
127.553
128.863
131.422
131.488
131.694
132.230
132.331
132.518
132.617
132.792
132.890
133.062
133.159
133.875

ecs153.069 with 31P coupling

Right spectrum (^{13}C{^{1}H, ^{31}P} ^{31}P decoupled), ppm:

119.262
120.065
121.434
122.056
123.609
125.073
125.724
126.783
127.259
127.846
129.284
130.022
131.214
131.498
132.332
132.600
132.857
133.149
133.460
133.549

ecs153.069 with 31P decoupling

25d

Figure 3.62(c) Expansion of 125.7 MHz ^{13}C{^{1}H} NMR spectrum compared with ^{13}C{^{1}H, ^{31}P} for 25d
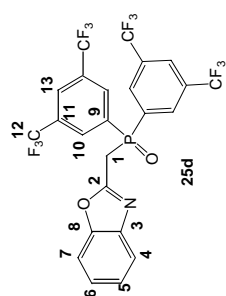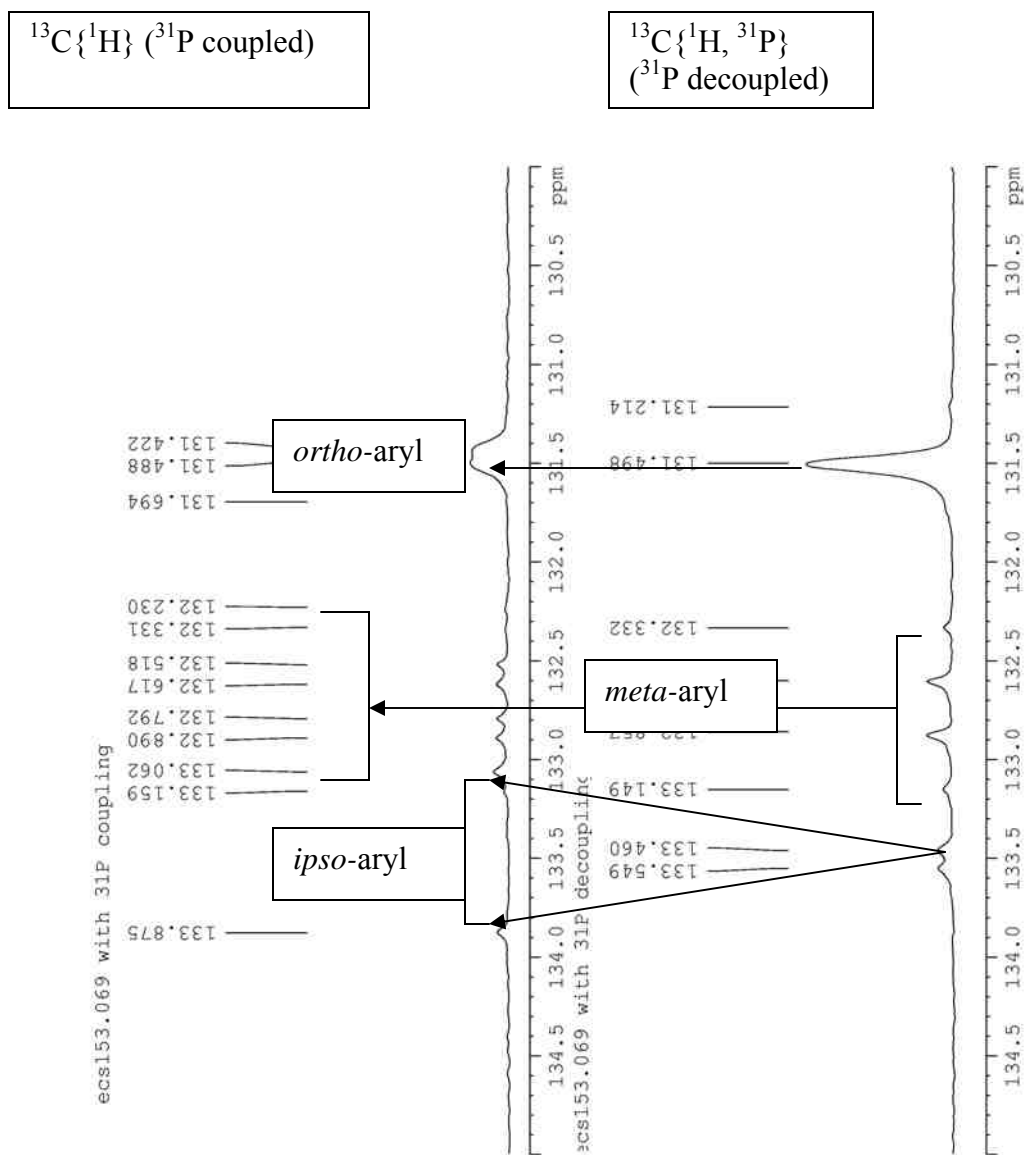
The aromatic carbons show $^{13}C\{^1H\}$ resonances at 131.5 ppm (doublets), with $^2J_{C-P}$ = 8.4 Hz, 132.7 ppm quartet of doublets, with $^3J_{C-P}$ = 12.4 Hz, $^2J_{C-F}$ = 34.6 Hz and 133.5 ppm (doublet), with $^1J_{C-P}$ = 102.3 Hz, are assigned to *ortho*, *meta* and *ipso*-carbons respectively (Figure 3.62c). The comparison of data for **25d** and **25b** is summarized in Table 3.24.

Table 3.24 Comparative chemical shifts and coupling constants of aromatic carbons for compound 25d and 25b

Compound 25d	Compound 25b
131.5 ppm, (doublet), *ortho*-carbon, $^2J_{C-P}$ = 8.4 Hz	131.8 ppm, (quartet of doublet), *ortho*-carbon, $^2J_{C-P}$ = 6.5 Hz, $^2J_{C-F}$ = 33.5 Hz
132.7 ppm, (quartet of doublet), *meta*-carbon, $^3J_{C-P}$ = 12.4 Hz and $^2J_{C-F}$ = 34.6 Hz	131.5 ppm, (doublet), *meta*-carbon, $^3J_{C-P}$ = 13.8 Hz
133.5 ppm, (doublet), *ipso*-carbon, $^1J_{C-P}$ = 102.3 Hz	130.6 ppm, (doublet), *ipso*-carbon, $^1J_{C-P}$ = 99.3 Hz

The chemical shifts for **25d** with two $-CF_3$ at *meta* position and **25b** with single $-CF_3$ at *ortho* position are slightly comparable. For example, the coupling constants for *ipso*-carbon in **25d** (102.3 Hz) is in the same range to similar C-P coupling in **25b** (99.3 Hz), and the resonance for *meta* carbon on **25d** (132.7 ppm) is slightly downfield shifted compared to **25b** (131.5 ppm) due to bonding with electron withdrawing CF_3 group in **25d**. There is a close correlation between $^2J_{C-F}$ =34.6 Hz in **25d** and $^2J_{C-F}$ =33.5 Hz for **25b**.

In the $^{13}C\{^1H\}$ NMR spectrum 18 C-aromatic and 4 x CF_3 (which appear in the same range) resonances are expected to appear for compound **25d**, but only 10-C resonances appear (Figure 3.50) suggesting overlapping of several resonances. The same number of resonances are also observed when $^{13}C\{^1H\}$ NMR was repeated using 125.7 MHz (Figure 3.51). The resonance for C_2 appears at 156.5 ppm (doublet, C_2, $^2J_{C-P} = 7.9$ Hz) and similar resonance in **25b** is 158.2 ppm (doublet, C_2, $^2J_{C-P} = 9.2$ Hz)

3.4.14 X-ray crystallographic analyses for compound 25d

Compound **25d** was crystallized from ethyl acetate/hexane solution. The molecular structure of **25d** was determined by single crystal X-ray diffraction analysis (Figure 3.54). Crystal parameters and selected bond lengths are summarized in Table 3.17 and 3.18. The comparison of selected bond lengths between **25d** and analogous compounds reported in this Chapter are displayed in Table 3.25 and this indicates that, the corresponding bond lengths are essentially identical.

Table 3.25 Selected bond lengths for 25a-25d ligands

Bond	25a, Ph	25b, *ortho*-CF$_3$	25c, *ortho*-CH$_3$	25d, *meta*-(CF$_3$)$_2$
P(1)-O(1)	1.4831(8)	1.4714(9)	1.4892(8)	1.4817(11)
O(2)-C(1)	1.3571(14)	1.3521(16)	1.3631(13)	1.3538(19)
N(1)-C(1)	1.2925(15)	1.2906(18)	1.2931(13)	1.286(2)

However, a slight variation in bond lengths is observed. For example, compound **25c** with an electron donating CH_3 at the *ortho* position appear to increase the P=O, O-C and C=N bond lengths compared to **25a**, **25b** and **25d**. On the other hand the electron withdrawing CF_3 at the ortho position decreases the P=O and O-C bond lengths in **25b**

compared to two CF_3 in **25d**, the reason to this may be due to the distance between the

P=O bond and the CF_3 at *meta* position is longer than at the *ortho* position in **25b**.

Compound **25a** without a substituent on the phenyl ring appears to have longer bond

lengths compared to **25b** and **25d**. The plane calculation indicates that the torsion angle

between the P=O and N donor atoms is 99.3^o for **25d**. This data is slightly comparable to

the similar angles observed in **25c** (88.8^o) followed with **25b** (65.4^o) and **25a** (59.2^o).

These data indicate that the introduction of a substituent on the phenyl ring significantly

impact the torsion angle and this may also affect the coordination behavior of the ligand.

A tabular summary of selected spectroscopic data for **25a-25d** is provided in Table 3.26

for comparison.

Table 3.26 Spectroscopic data for compounds 25a-25d

Ligand	IR (cm^{-1})		^{1}HNMR (ppm)	$^2J_{H-P}$ (Hz)	$^{13}C\{^1H\}$ NMR (ppm)	$^1J_{C-P}$ (Hz)	$^{31}P\{^1H\}$ NMR(ppm)
	C=N	P=O	$-CH_2-P=O$		$-CH_2P=O$		$-CH_2P=O$
25a	1610	1196	4.1, doublet	14.5	33.0, doublet	63.2	27.7
25b	1607	1125-1217	4.3, doublet	14.5	33.7, doublet	69.4	28.4
25c	1603	1178	4.1, doublet	14.2	32.6, doublet	63.0	31.1
25d	1616	1140-1283	4.2, doublet	16.2	32.7, doublet	67.3	23.4

The variation of $v_{C=N}$ in the IR spectrum is in the order of **25c** < **25b** < **25a** < **25d**. This

signify that the CF_3 group has the tendency of strengthening the C=N bond (**25d**) while

the electron donating weakens the C=N bond as observed in **25c**. The variation of the

$v_{C=N}$ increases with the number of substituents. This is seen in **25b** with one CF_3 group

and **25d** with the two CF_3 group having the highest $\nu_{C=N}$. This behavior is also seen in the ^{1}H NMR data in **25d** that shows the highest $^2J_{H\text{-}P}$ = 16.2 Hz (Table 3.26). However this trend is reversed in $^{13}C\{^1H\}$ NMR, although resonances for **25a-25d** appear in the same range but the $^1J_{C\text{-}P}$ = 69.4 Hz in **25b** with one CF_3 on the *ortho* position and $^1J_{C\text{-}P}$ = 67.3 in **25d** with two CF_3 on *meta* position. This indicates that the position of the substituent determines the magnitude of the coupling constant in NMR data. The $^{31}P\{^1H\}$ NMR for **25d** shows resonance at 23.4 ppm, **25b** (28.4 ppm), **25a** (27.7 ppm) and **25c** (31.1 ppm). This is an interesting result as it is expected that compounds with an electron withdrawing effect (**25d and 25b**) will have their resonances shifted to low field but this is not observed in this study. The reason to this observation may be apart from the inductive effect of substituents, other factors may apply like directing effect of the substituents and the steric hindrance.

3.4.15 Attempted synthesis of compound 25e

When the Grignard approach was applied for the synthesis of **25e** (Scheme 24) the target molecule was not obtained. Mass spectrometry of the crude product suggests the formation of the target molecule as a minor product but the major product appears to be compound **25g**. Attempts to isolate and purify **25e** and **25g** were unsuccessful.

Scheme 24

25e

25g
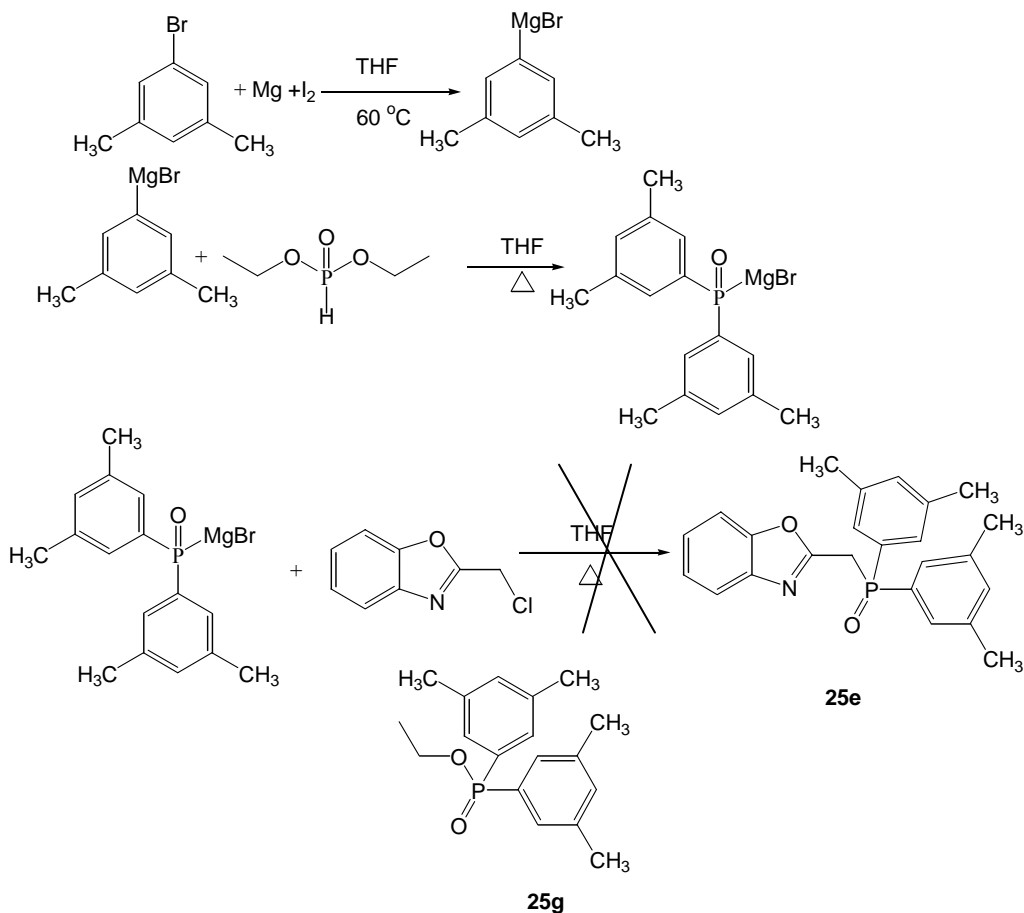
3.4.16 Coordination chemistry for compound 25a with Yb(NO$_3$)$_3$•5H$_2$O

Coordination chemistry of **25a** was attempted by combining the ligand with Pr(NO$_3$)$_3$•5H$_2$O, Nd(NO$_3$)$_3$•6H$_2$O, Er(NO$_3$)$_3$•5H$_2$O and Yb(NO$_3$)$_3$•5H$_2$O starting with a ratio of 3:1 ligand:lanthanide. Only Yb(III) produced crystals under this condition. After slow recrystallization from chloroform/hexane or methanol/hexane at room temperature, pale yellow crystals suitable for X-ray analysis were obtained. The infrared spectrum of the complex shows down-frequency shift of $v_{P=O}$ band compared to the free ligand: $\Delta v_{P=O}$ = 37 cm^{-1}. The IR $v_{C=N}$ peak shift is not observed. Single crystal X-ray diffraction analysis showed two ligands coordinated to Yb(III) in monodentate fashion via the phosphine oxide groups (Figure 3.19) with an overall inner coordination sphere

composition of **Yb(25a)₂(NO₃)₃(H₂O).** There is also 0.25 CH_3OH molecule in the outer

sphere. Crystal parameters and selected bond lengths are shown in Tables 3.3 and 3.4.

The crystal structure of the complex shows that the torsion angle between the plane

bonded to P=O and N donor atoms in both ligands is 62.1° and 60.0° respectively. When

this data is compared to the torsion angle of the free ligand that is 59.2° indicates that the

complex formation has no significant change on the P=O and N donor atoms signifying

that the coordination chemistry with lanthanide(III) is thermodynamically favored.

Table 3.27 Selected bond lengths between 25a and Yb(25a)₂(NO₃)₃(H₂O) complex.

Type of bond	Free ligand, 25a	Complex, Yb(25a)₂(NO₃)₃(H₂O)
P(1)-O(1)	1.4831(8)	1.4913(15)
P(2)-O(3)	-	1.4953(15)
C(1)-N(1)	1.2925(15)	1.286(3)
C(21)-N(2)	-	1.291(3)
C(1)-O(2)	1.3571(14)	1.362(3)
C(21)-O(4)	-	1.359(2)

The P-O bonds are longer in the complexed ligand than in the free ligand

consistent with a coordination of the P=O. The Yb(III) is also coordinated to three

bidentate nitrate ions and a water molecule. The water hydrogens form hydrogen bonds

with the nitrogen atom in each **25a** ligand, with bond lengths O(5)-H….N(1) 1.98(4)Å

and O(5)-H….N(2) 2.06(3)Å respectively. The CN = 9 coordination polyhedron formed

by the oxygen atoms bonded to Yb(III) approximates a capped square antiprism (Figure 3.63).

Figure 3.63 Coordination polyhedron of Yb
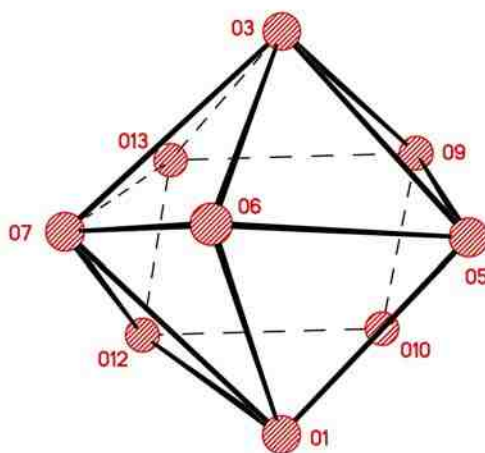
When a 2:1 and 1:1 ligand:metal reaction ratios were employed the same complex with $Yb(NO_3)_3 \cdot 5H_2O$ was obtained. An attempt to effect bidentate chelation for this ligand on Yb (III) was made by dissolving the complex in methanol followed by dropwise addition of this solution into boiling tetrachloroethane (boiling point 147 $^{\circ}$C). This was done in an effort to displace the water molecule. The solution was concentrated to remove the solvent. Attempts to recrystallize this product using $CHCl_3$/hexane, MeOH/hexane and other solvent combinations ($CHCl_3$/MeOH, DMF, MeOH,

MeOH/CH$_2$Cl$_2$ and Cl$_2$CH$_2$CH$_2$Cl$_2$) gave a yellow powder. This suggests that, the stabilization of the complex by hydrogen bonding is important in crystal formation. The source of the molecule of water may be the salt Yb(NO$_3$)$_3$•5H$_2$O or from the solvent of crystallization.

3.4.17 Coordination chemistry for compound 25a with Nd(NO$_3$)$_3$•6H$_2$O

Combination of 2-[(diphenylphosphinoyl)methyl]-benzoxazole, **25a** with Nd(NO$_3$)$_3$•6H$_2$O in MeOH at a ratio of 2:1 gave a clear solution. After evaporation of this solution a white powder formed. Crystallization of this powder from hot CHCl$_3$ gave small crystals after slow evaporation of the solvent at room temperature. The infrared spectrum of the complex shows down-frequency shift $v_{P=O}$ band compared to the free ligand: $\Delta v_{P=O}$ = 41 cm^{-1}. Single crystal X-ray diffraction analysis showed two ligands coordinated to Nd(III) in bidentate fashion, via the phosphine oxide groups as well as the nitrogen (Figure 3.22) with an overall composition of **Nd(25a)$_2$(NO$_3$)$_3$•2.5(CHCl$_3$)**. The crystal structure of the complex shows that the torsion angle between the plane bonded to P=O and N donor atoms in both ligands is 126.5^o and 122.3^o respectively. When these data are compared to the torsion angle of the free ligand that is 59.2^o indicates that the bidentate coordination has a significant change on the orientation of P=O and nitrogen donor centers, signifying that the coordination chemistry with lanthanide(III) is not thermodynamically favored.

All three nitrates are bidentate coordinated. The coordination number of Nd(III) is 10. Bidentate coordination may be due to the lager ionic radius of Nd(III), 0.995Å compared to Yb(III), 0.858Å.[48] Although the C=N bonds to Nd(III), but there is no significant peak shift in the IR spectrum for C=N. Selected bond lengths are compared in

Table 3.28. The longer M-O bond length is largely a result of the larger ionic radius for Nd(III) and probably bidentate coordination. The Yb-O bond length is shorter than Nd-O, this indicates that regardless of the shorter ionic radius of Yb(III) but monodentate coordination results in a more stronger bonding.

Table 3.28 Comparison of bond lengths for Yb(25a)$_2$(NO$_3$)$_3$(H$_2$O) and Nd(25a)$_2$(NO$_3$)$_3$•2.5(CHCl$_3$)

Type of bond	Bond length (Å) Yb(25a)$_2$(NO$_3$)$_3$(H$_2$O) Coordination Number 9	Bond length (Å) Nd(25a)$_2$(NO$_3$)$_3$•2.5(CHCl$_3$) Coordination number 10
M-O(1)	2.2272(14)	2.403(2)
M-O(3)	2.2128(14)	2.422(2)
M-(N1)	-	2.661(2)
M-N(2)	-	2.671(2)

In addition, the Nd-O bond lengths are shorter than Nd-N probably as a result of the relatively softer donor character of the ring N atom compared to P=O leading to weaker coordination of the N donor atom.

In the Nd(III) complex, there are 2.5 outer sphere CHCl$_3$ molecules, one of which has disordered chlorine (Figure 3.64). The disorder at C42 has two sets of chlorine atoms each with 50% occupancy. The C43 is occupied by half of a CHCl$_3$ lead to 2.5(CHCl$_3$) solvent molecules in the outer sphere of the complex (Figure 3.64).

Figure 3.64 Outer sphere CHCl$_3$ solvent disorder in Nd(25a)$_2$(NO$_3$)$_3$•2.5(CHCl$_3$)
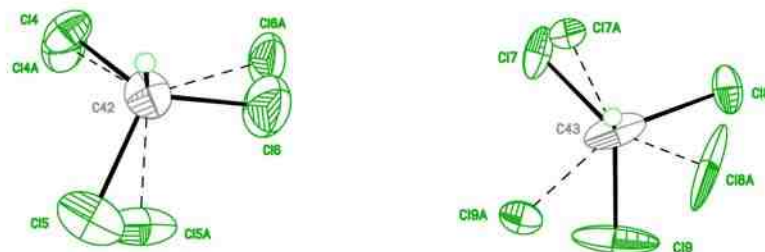
The ten vertex coordination polyhedron about Nd is distorted from ideal. It can be described as a cubicosahedron. There are 3 combinations of capped pentagons opposite rectangles. The best plane through the distorted rectangles was chosen as the base: N1-O1-O5-O6 (Figure 3.65).

Figure 3.65 Coordination polyhedron about Nd in Nd(25a)$_2$(NO$_3$)$_3$•2.5(CHCl$_3$)
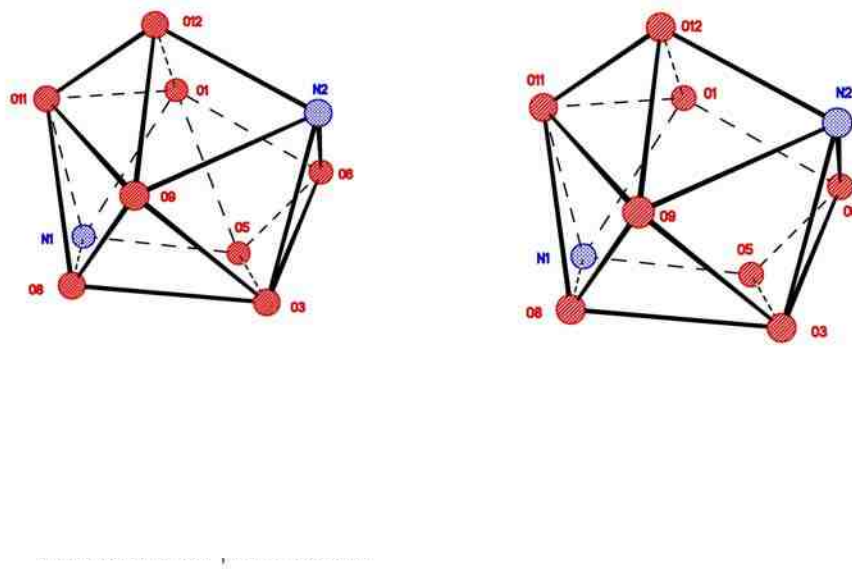
3.4.18 Coordination chemistry for compound 25b with Yb(NO$_3$)$_3$•5H$_2$O

A coordination complex of **25b** was formed by combining the ligand with Yb(NO$_3$)$_3$•5H$_2$O at a ratio of 2:1 in methanol. The solution was stirred (12 h) and allowed to slowly evaporate at room temperature. After several days a white powder formed. Crystallization of the white powder from CH$_3$CN gave crystals suitable for single crystal X-ray diffraction analysis. The infrared spectrum for the complex did not reveal significant peak shifts when compared to the free ligand. This is probably because of overlapping between the infrared bands of P=O and –CF$_3$ that makes mode assignment

difficult. The –CF$_3$ group IR bands appear between 1140 cm^{-1} – 1250 cm^{-1} [44, 55] and 1120 cm^{-1} – 1350 cm^{-1}. [49] The CF$_3$ vibrations therefore obscure the expected band shift region. The crystal structure determination for the complex shows two ligands coordinated to Yb(III) in a monodentate fashion via P=O, oxygen atoms with an overall complex composition of **Yb(25b)$_2$(NO$_3$)$_3$(H$_2$O)•0.5CH$_3$CN** (Figure 3.32). Crystal parameters and selected bond lengths are shown in Table 3.9 and 3.10. In addition, three nitrates are bidentate bonded to Yb(III) and one water molecule oxygen is bonded to the central metal. The two hydrogen atoms from water form hydrogen bonds with the nitrogen atom from each ligand. The coordination number of Yb(III) is 9.

The X-ray crystal structure also shows a disordered half CH$_3$CN solvent molecule (Figure 3.66). There are 4 Yb(III) complexes and 2 solvent molecules in the unit cell. The solvent molecule adapts 2 orientations with equal occupancy. The coordination polyhedron about Yb(III) is a distorted monocapped square anti-prism (Figure 3.67).

The crystal structure of the complex shows that the torsion angle between the plane bonded to P=O and N donor atoms in both ligands is 70.4^o and 65.2^o respectively. When these data are compared to the torsion angle of the free ligand that is 65.4^o indicates that the complex formation has no significant change on the P=O and N donor atoms signifying that the coordination chemistry with lanthanide(III) can be thermodynamically favored.

Figure 3.66 Disorder of CH₃CN group, only ordered part 1 with thermal ellipsoids at 10%
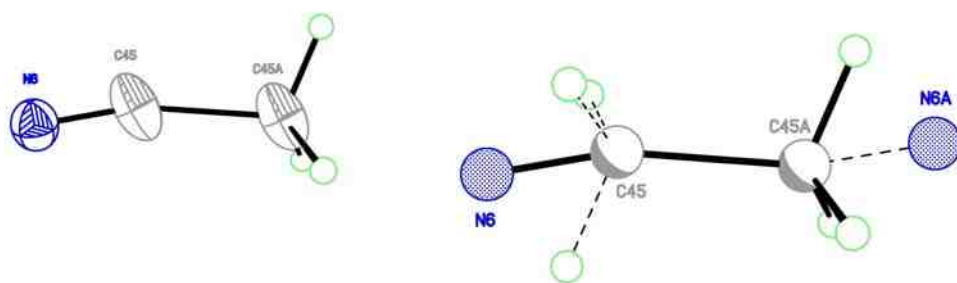
Figure 3.67 Coordination polyhedron of Yb(III)
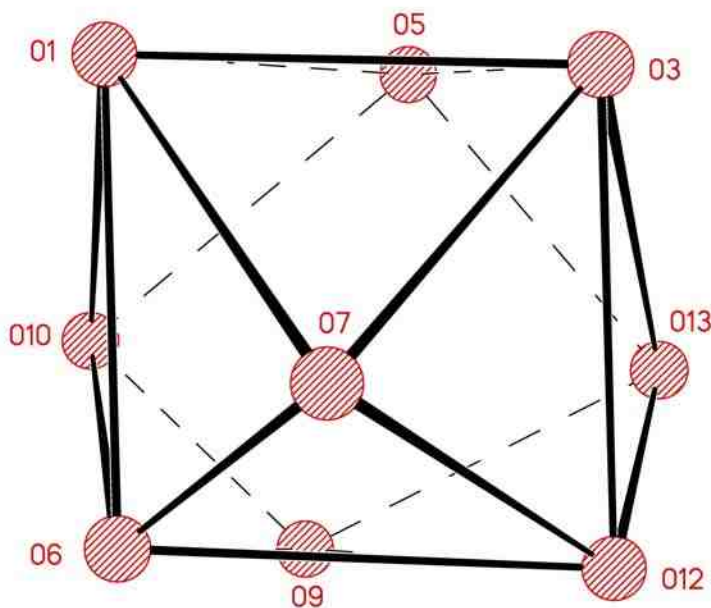
Comparison of bond lengths (Table 3.29) between **Yb(25a)$_2$(NO$_3$)$_3$(H$_2$O)** and **Yb(25b)$_2$(NO$_3$)$_3$(H$_2$O)** show that the Yb-O bond lengths are shorter with **25a** than **25b.** This may result from electron withdrawal by the CF$_3$ groups making the P=O donor group less basic toward Yb(III). The P(1)-O(1), P(2)-O(2), N(1)-C(7) and N(2)-C(29) bond lengths are comparable in both complexes.

Table 3.29 Comparison of bond lengths between $Yb(25a)_2(NO_3)_3(H_2O)$ and $Yb(25b)_2(NO_3)_3(H_2O)$ complexes

Bond lengths	$Yb(25a)_2(NO_3)_3(H_2O)$	$Yb(25b)_2(NO_3)_3(H_2O)$
Yb-O(1)	2.2272(14)	2.2691(14)
Yb-O(3)	2.2128(14)	2.2494(14)
P(1)-O(1)	1.4913(15)	1.4974(15)
P(2)-O(2)	1.4953(15)	1.4940(15)
N(1)-C(7)	1.286(3)	1.275(4)
N(2)-C(29)	1.291(3)	1.290(3)

3.4.19 Coordination chemistry for compound 25c with $Yb(NO_3)_3 \bullet 5H_2O$

A coordination complex of **25c** was formed by the combination with $Yb(NO_3)_3 \bullet 5H_2O$ in a ratio of 2:1 in MeOH. A pale yellow solution formed after stirring (12 h). The solution was allowed to evaporate slowly at room temperature leaving a pale yellow solid which was crystallized from CH_3CN/MeOH solution. After slow evaporation of solvent at room temperature white crystals formed. The infrared spectrum of the free ligand compared to the complex represents coordination shift: $\Delta v_{P=O} = 27$ cm^{-1}. Single crystal X-ray diffraction analysis shows two ligands coordinated to Yb(III) via the P=O oxygen donor atoms (Figure 3.44). Crystal parameters and selected bond lengths are shown in Table 3.13 and 3.14. Both ligands are monodentate on the Yb(III) and one water molecule oxygen is monodentate bonded to Yb(III) and the two water hydrogen atoms form a hydrogen bond with nitrogen atom lone pairs from both ligands. Three nitrates bond to Yb(III) with bidentate coordination. The coordination

number of Yb(III) is 9 with an overall complex composition of **Yb(25c)$_2$(NO$_3$)$_3$(H$_2$O)**.

The coordination polyhedron about Yb1 is a mono-capped square antiprism (Figure 3.68). In addition the crystal structure of the complex shows that the torsion angle between the plane bonded to P=O and N donor atoms in both ligands are 111.3° and 79.7° respectively. When these data are compared to the torsion angle of the free ligand that is 88.8° indicates that the complex formation has a significant change on the P=O and N donor atoms on one of the coordinating ligands signifying that the two ligands are not equally bonded.

Figure 3.68 Coordination polyhedron for the Yb(25c)$_2$(NO$_3$)$_3$(H$_2$O).
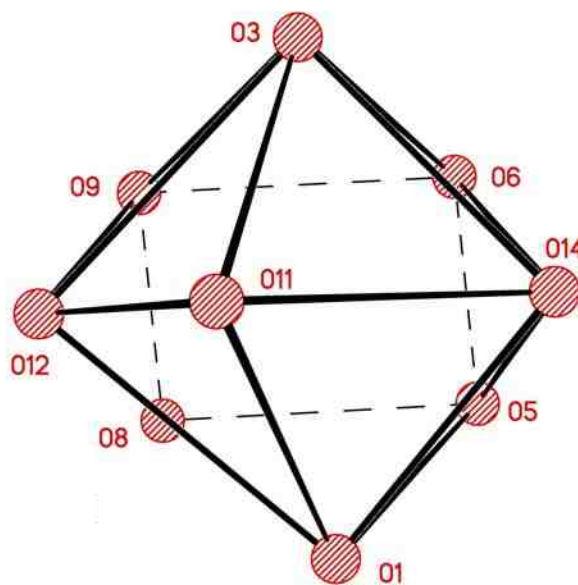
Table 3.30 Comparison of bond lengths for ytterbium complexes formed with 25a, 25b and 25c ligands

Bond lengths	Yb(25a)$_2$(NO$_3$)$_3$(H$_2$O) -Ph	Yb(25b)$_2$(NO$_3$)$_3$(H$_2$O) -CF$_3$	Yb(25c)$_2$(NO$_3$)$_3$(H$_2$O) -CH$_3$
Yb-O(1)	2.2272(14)	2.2691(14)	2.233(2)
Yb-O(3)	2.2128(14)	2.2494(14)	2.234(2)
P(1)-O(1)	1.4913(15)	1.4974(15)	1.494(2)
P(2)-O(3)	1.4953(15)	1.4940(15)	1.495(2)
N(1)-C(7)	1.286(3)	1.275(4)	1.279(4)
N(2)-C(29)	1.291(3)	1.290(3)	1.290(5)

Several bond lengths for the three Yb(III) complexes are summarized in Table 3.30. Clearly, the **Yb(25c)$_2$(NO$_3$)$_3$(H$_2$O)** complex is most comparable with **Yb(25a)$_2$(NO$_3$)$_3$(H$_2$O)** complex which is consistent with the similar expected donor strengths for **25a** and **25c**. The P(1)-O(1), P(2)-O(3), N(1)-C(7) and N(2)-C(29) within the ligands are comparable to each other.

Electron displacement
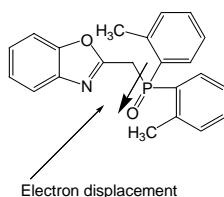
3.4.20 Coordination chemistry for compound 25c with Nd(NO$_3$)$_3$•6H$_2$O

Similar coordination occurred between **25c** with Nd(NO$_3$)$_3$•6H$_2$O in MeOH where a clear solution was formed. Significant down frequency peak shifts were observed in the IR spectrum corresponding to: $\Delta v_{P=O}$ = 27 cm^{-1}. When this solution was allowed to

evaporate slowly at room temperature, crystals suitable for single crystal diffraction were formed. The overall composition of the complex is **Nd(25c)$_2$(NO$_3$)$_3$(H$_2$O)** identical to the one formed with Yb(III). A view of the complex is displayed in Figure 3.47. Crystal parameters and selected bond lengths are shown in Table 3.15 and 3.16. The crystal structure of the complex shows that the torsion angle between the plane bonded to P=O and N donor atoms in both ligands are 110.9° and 80.3° respectively. When these data are compared to the torsion angle of the free ligand that is 88.8° indicates that the complex formation is identical to that formed with Yb(III) above and the reason to this may be due to monodentate coordination in both cases.

The coordination polyhedron about Nd1 is a nine coordinate mono-capped square antiprism (Figure 3.69).

Figure 3.69 Coordination polyhedron for Nd(25c)$_2$(NO$_3$)$_3$(H$_2$O)
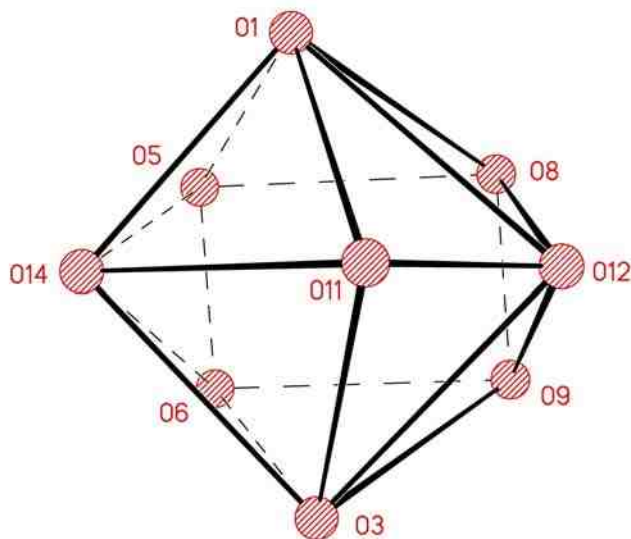
Table 3.31 Comparison of bond lengths between Yb(25c)$_2$(NO$_3$)$_3$(H$_2$O) and Nd(25c)$_2$(NO$_3$)$_3$(H$_2$O) complexes

Bond length	Yb(25c)$_2$(NO$_3$)$_3$(H$_2$O)	Nd(25c)$_2$(NO$_3$)$_3$(H$_2$O)
M-O(1)	2.233(2)	2.3531(19)
M-O(3)	2.234(2)	2.350(2)
P(1)-O(1)	1.494(2)	1.498(2)
P(2)-O(3)	1.495(2)	1.504(2)

A comparison between Yb(III) and Nd(III) bond lengths show that, the Yb-O bond length is less than Nd-O. This is partly attributed to smaller ionic radius for Yb(III), 0.858 Å and Nd(III), 0.995Å.[48] In addition a M-O bonding strength can be deduced from the bond length since a shorter bond is expected to be more stronger compared to a longer bond i.e. Yb(III) having a smaller ionic radius bonds more strongly to **25c** compared to Nd(III) with larger ionic radius. There is a close correlation between the bond lengths for P(1)-O(1) and P(2)-O(3) in both complexes.

3.4.21 Coordination chemistry for 25d with Ln(NO$_3$)$_3$•xH$_2$O

The coordination chemistry examined with Nd(NO$_3$)$_3$•6H$_2$O, Yb(NO$_3$)$_3$•5H$_2$O, Er(NO$_3$)$_3$•5H$_2$O and Eu(NO$_3$)$_3$•6H$_2$O resulted into no coordination complexes. The analysis of crystals obtained from this combination using X-ray diffraction indicated uncoordinated ligand, **25d**.

3.5 CONCLUSION

In this chapter the syntheses of substituted benzoxazole ligands **25a-25e** were developed. Since these compounds are new, characterization using mass spectrometry, elemental analysis (CHN), IR, ^{1}H, ^{13}C, and ^{31}P NMR spectroscopy were done.

The initial objective in this study was to develop a stable ligand containing a softer donor (N) and a harder donor P=O compared to those already developed ligands in our group. [43] This was achieved through substitution of the Ph$_2$P(O)- group on 2-methylbenzoxazole at the methyl position. The newly synthesized benzoxazole ligands **25a-25d** were found to be stable in 1.2 M HCl. The introduction of electron denoting substituent (-CH$_3$) increases the solubility of the ligand in hydrocarbon diluents. For example compound **25c** with CH$_3$ substituent is soluble in toluene (0.0409 M) and trifluoromethanesulfonyl-benzene (0.0419 M). On the other hand the electron withdrawing substituents (-CF$_3$) appear to decrease the solubility of the ligand in hydrocarbons. Compound **25b,** having one CF$_3$ at *ortho* position, is insoluble in toluene and benzene, but soluble in trifluoromethanesulfonyl-benzene (0.0914 M) and **25d** with two CF$_3$ groups is insoluble in hydrocarbon diluents but soluble in trifluoromethanesulfonyl-benzene (0.0376 M).

Interesting results were obtained in IR data for $\nu_{C=N}$ absorption bands and other spectroscopic data (Table 3.32). By varying the substituent on the phenyl rings there was a gradual change in the IR absorption frequencies in the order **25d** > **25a** > **25d** > **25c**. The two CF$_3$ in **25d** appear to strengthen the C=N bond which is electron withdrawing substituent. At the same time the electron donating CH$_3$ in **25c** weakens the C=N bond and this probably is due to high electron density that lead to the repulsion with C=N

bonding electrons. Nevertheless, this trend is not observed with other X-ray and spectroscopic data and this may indicate that these changes are not significant or are not consistent with other measurements.

Table 3.32 Comparison of spectroscopic data and bond lengths for C=N in compounds 25a-25d

Ligand		$\nu_{C=N}$ (cm^{-1})	Bond length (C=N) (Å)	^{13}C{^{1}H} NMR (ppm)
25a	Ph	1610	1.2925(15)	158.8
25b	CF$_3$	1607	1.2906(18)	158.2
25c	CH$_3$	1603	1.2931(13)	159.3
25d	2x CF$_3$	1616	1.286(2)	156.5

The coordination chemistry between Nd(III) and Yb(III) ions with these compounds was examined. Crystal structures for isolated complexes show similar monodentate P=O-M coordination. However, compound **25a** with Nd(III) shows the ligand bonded in bidentate fashion via P=O donor as well as N donor group.

In compound **25a,** the P=O donor is strongly bonded to Nd(III) compared to N donor atom. This can be deduced from the bond lengths for Nd-O=P (2.403(2)Å and 2.422(2)Å respectively), while the Nd-N are 2.661(2)Å and 2.671(2)Å. The presence of one molecule of water in the inner sphere of the Yb(III) complexes was important in crystal formation. When this water was removed, recrystallization of the complex was not successful. Compounds **25b** and **25c** show monodentate coordination to lanthanide(III) ions.

3.6 REFERENCES

1. C:\Documents and Settings\Owner.YOUR-D674E4A0BA\Desktop\Aromatic Compounds and Aromaticity.mht

2. Solomon's 6th Edition; Chapter 14 p 614 – 654; Chapter 15 p 655 – 703 (Reactions).

3. McMurry, J. *Organic Chemistry, 5th edition,* **2000,** Cornell University, Brooks/Cole, Thomson Learning.

4. Domene, C.; Jenneskenes, L. W.; and Fowler, P. W. *Tetrahedron Letters* **2005,** *46,* 4077.

5. Drew, M. G. B.; Hill, C.; Hudson, M. J.; Iveson, P. B.; Madic, C.; Vaillant, L.; and Youngs G. A. *New J. Chem.* **2004,** *28, 462.*

6. Mathur, J. M.; Murali, M. S.; and Nash, K. L. *Ion Exch. Solvent Extr.* **2001,** 357.

7. Madic, C.; Lecomte, M.; Baron, P.; and Bouillis, B. *C. R. Physique* **2002,** *3,* 797.

8. Cordier, P. Y.; Hill, C.; Baron, P.; Madic, C.; Hudson, M. J.; and Liljenzin, J. O. *J. Alloys Comp.* **1998,** *271,* 738.

9. Hagstrom, I.; Spjuth, L.; Enarsson, Å.; Liljenzin, J. O.; Skalberg, M.; Hudson, M. J.; Iveson, P. B.; Madic, C.; Cordier, P. Y.; Hill, C.; and Francois, N. *Ion Exch. Solvent Extr.* **1999**, *17*, 21.

10. Drew, M. G. B.; Iveson, P. B.; Hudson, M. J.; Liljenzin, J. O.; Spijuth, L.; Cordier, P. Y.; Enarsson, A.; Hill, C.; and Madic, C. *J. Chem. Soc. Dalton Trans.* **2000,** 821.

11. Boubals, N.; Drew, M. G. B.; Hill, C.; Hudson, M. J.; Iveson, P. B.; Madic, C.; Russell, M. L.; and Youngs, T. G. A. *J. Chem. Soc. Dalton Trans.* **2002,** 55.

12. Kolaric, Z.; Mullich, U.; and Gassner, F. *Ion Exch. Solvent Extr.* **1999,** *17,* 23.

13. Kolaric, Z.; Mullich, U.; and Gassner, F. *Ion Exch. Solvent Extr.* **1999,** *17,* 1155.

14. Madic, C.; Hudson, M. J.; Lilnjenzin, J. O.; Glatz, J. P.; Nannicini, R.; Facchin, A.; Kolaric, Z.; and Odoj, R. *New Partitioning Techniques for Minor Actinides* **2000,** EUR 19149EN.

15. Addison, A. W.; and Burke, P. J. *Heterocyclic Chem.* **1981,** *18,* 803.

16. Nash, K. L.; Lavallette, C.; Borkowski, M.; Paine, R. T.; and Gan, X. *Inorg. Chem.* **2002,** *41(22),* 5849.

17. Froidevaux, P.; Harrowfield, J. M.; and Sobolev, A. N. *Inorg. Chem.* **2000,** *39,* 4678.

18. Braunstein, P.; Fryzuk, M. D.; Dall, M. L.; Naud, F.; Rettig, S. J.; and Speiser, F. *J. Chem. Soc. Dalton Trans.* **2000**, 1067.

19. Braunstein, P.; Speicer, F.; Saussine, L.; and Welter, R. *Organometallics* **2004**, *23,* 2613.

20. Nishiyama, H.; Kondo, M.; Nakamura, T.; and Itohi, K. *Organometallics* **1991,** *10,* 500.

21. Franco, D.; Gomez, M.; Jiménez, F.; Muller, G.; Rocamora, M.; Maestro, M. A.; and Mahia, J. *Organometallics* **2004,** *23,* 3197.

22. Kniess, T.; Correia, J. D. G.; Domingos, A.; Palmer, E.; and Santos, I. *Inorg. Chem.* **2003,** *42,* 6130.

23. Bhor, S.; Tse, M. K.; Klawonn, M.; Döbler, C.; Mägerlein, W.; and Beller, M. *Adv. Synth. Catal.* **2004,** *346,* 263.

24. Tse, M. K.; Bhor, S.; Klawonn, M.; Anilkumar, G.; Jiao, H.; Spannenberg, A.; Döbler, C.; Mägerlein, W.; Hugl, H.; and Beller, M. *Chem. Eur. J.* **2006,** *12,* 1875.

25. Nishiyama, H.; Itoh, Y.; Matsumoto, H.; Park, S. B.; Itoh, K. *J. Am. Chem. Soc.***1994,** *116*, 2223.

26. Helmchen, G.; and Pfaltz, A. *Acc. Chem. Res.* **2000,** *33,* 336.

27. Minami, T.; Isonaka, T.; Okada, Y.; and Ichikawa, J. *J. Org. Chem.* **1993,** *58,* 7009.

28. Gan, X. M.; Duesler, E. N.; and Paine, R. T. *Inorg. Chem.* **2001,** *40,* 4420.

29. Tan, Y. C.; Gan, X. M.; Stanchfield, J. L.; Duesler, E. N.; and Paine, R. T. *Inorg. Chem.* **2001,** *40,* 2910.

30. Gan, M. X.; Parveen, S.; Smith, L. Y.; Duesler, E. N.; and Paine, R. T. *Inorg. Chem*. **2000**, *39(20),* 4591.

31. Gan, X. M.; Duesler, E. N.; and Paine, R. T. *Inorg. Chem*. **2001**, *40*, 4420.

32. Bond, E. M.; Duesla, E. N.; Paine, R. T.; and Nöth, H. *Polyhedron* **2000,** *19,* 2135.

33. Paine, R. T.; Bond, E. M.; Parveen, S.; Donhart, N.; Duesler, E.; Smith, K. A.; and Nöth, H. *Inorg. Chem.* **2002,** *41(2),* 444.

34. Kosaka, T.; and Wayabashi, T. *Heterocycles* **1995,** *41(3),* 477.

35. Cava, M. P.; Lakshmikantham, M. V.; and Mitchell, M. J. *J. Org. Chem.* **1969,** *34(9),* 2666.

36. Schramm, G.; Grötsch, H.; and Pollmann, W. *Angew. Chem. Internat. Edit.* **1962,** *1(1),* 1.

37. Burkhardt, G.; Klein, M. P.; and Calvin, M. *Structure of the so called "Ethyl Metaphosphate." * **1964,** 591.

38. Pollmann, W.; and Schramm, G. *Biochim. Biophys. Acta* **1964,** *80,* 1.

39. Albert, L.; Casalnuovo, T. V.; Rajan, B.; Timothy, A. A.; and Timothy, H. W. *J. Am. Chem. Soc.* **1994,** *116,* 9869.

40. McKinstry, L.; and Livinghouse, T. *Tetrahedron* **1994,** *50(21),* 6145.

41. Ungelhardit, U; Rapko, B. M.; Duesler, E. N.; Frutos, D.; Paine, R. T.; and Smith, P. H. *Polyhedron* **1995,** *14(17-18),* 2361.

42. Douce, L.; Charbonniere, L.; Cesario, M.; and Ziessel, R. *New J. Chem.* **2001,** *25,* 1024.

43. Rapko, B. M.; Duesler, E. N.; Smith, P. H.; Paine, R. T.; and Ryan, R. R. *Inorg. Chem.* **1993,** *32,* 2164.

44. Poleshchuk, O, Kh.; Korobeinicheva, I. K.; Fugaeva, O. M.; and Furin, G. G. *Russian Journal of Organic Chemistry* **2003**, *39(11),* 1603.

45. Quin, L. D. *A Guide to Organophosphorus Chemistry; Wiley: New York* **2000.**

46. Deakin, L.; Levason, W.; Popham, M. C.; Reid, G.; and Webster, M. *J. Chem. Soc. Dalton Trans.* **2000,** 2439.

47. United States Patent: 5084463.

48. Cotton, F. A.; and Wilkinson, G. F. R. S. *Advanced Inorganic Chemistry,* A Comprehensive Text, 3rd edition **1972**, Interscience Publishers, A division of John Wiley and Sons, New York pg 1057.

49. Silverstein, R. M.; Bassler, G. C.; and Morrill, T.C. *Spectroscopic identification of organic compounds 5th edition* **1991,** pg 130, John Wiley and sons, Inc, New York.

50. Xu, X.; and Zhang; Y. *Synthetic communications* **2003,** *33(20),* 3559.

51. Forgues-Fery, S.; and Paillous, N. *J. Org. Chem.* **1986,** *51(5),* 672.

52. Bayh, O.; Awad, H.; Mongin, F.; Hoarau, C.; Bischoff, L.; Trcourt, F.; Quguiner, G.; Marsais, F.; Blanco, F.; Abarca, B.; and Ballesteros, R. *J. Org. Chem.* **2005,** *70(13),* 5190.

53. Padwa, A.; Austin, D. J.; Precedo, L.; and Zhi, L. *J. Org. Chem.* **1993,** *58(5),* 1144.

54. Shimada, T.; and Yamamoto, Y. *Supporting information: Carbon-carbon bond cleavage of diynes through the hydroamination with transition metal-catalysts-* Department of Chemistry, Graduate School of Science, Tohoku University Sendai 980-8578, Japan.

55. Eapen, K. C.; and Tamborski, C. *Journal of Fluorine Chemistry* **1980,** *15,* 239.

56. Goodson, F. E.; Hauck, S. I.; and Hartwig, J. F. *J. Am. Chem. Soc.* **1999,** *121(33),* 7527.

57. Casey, C. P.; Paulsen, E. L.; Beuttenmueller, E. W.; Proft, B. R.; Matter, B. A.; and Powell, D. R. *J. Am. Chem. Soc.* **1999,** *121(1),* 63.

58. Howell, J. A. S.; Fey, N.; Lovatt, J. D.; Yates, P. C.; McArdle, P.; Cunningham, D. Sadeh, E. Gottlieb, H. E.; Goldschmidt, Z.; Hursthouse, M. B.; and Light, M. E. *J. Chem. Soc., Dalton Trans.,* **1999,** 3015.

59. Frew, J. J. R.; Clarke, M. L.; Mayer, U.; Rensburg, H. V.; and Tooze, R. P. *Communication, Dalton Transactions* **2008,** 1976 with its supplementary material (ESI).

60. Whitaker, C. M.; Kott, K. L.; and McMahon, R. J. *J. Org. Chem.* **1995,** *60,* 3499.

Chapter 4

4.0 Syntheses and Coordination Summary

In this chapter, a summary of the development of new oxazoline and benzoxazole derivatives functionalized with a hard P=O donor group is provided. The new compounds include **19** and **25a-25d**.
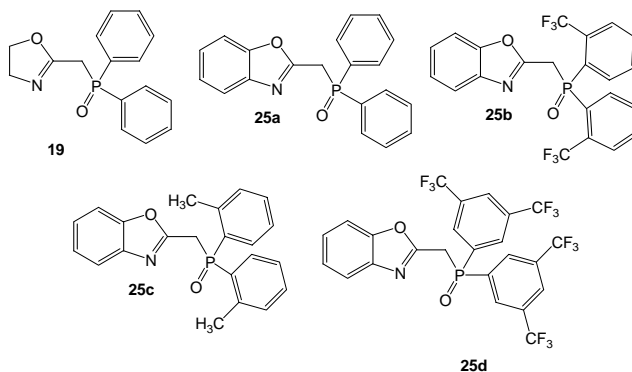
4.1 Synthesis and coordination chemistry of oxazoline-based ligands, 19

The initial objective in this study was to synthesize new oxazoline-based ligands such as illustrated by **19** via oxidation of the phosphine **18**. The synthesis of **18** had been reported in the literature as indicated in Scheme 5 (Chapter 2).

Scheme 5
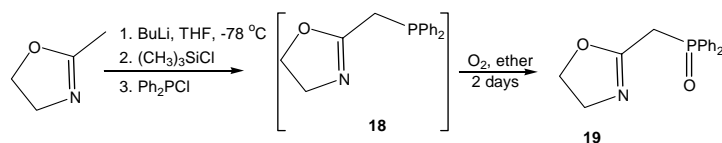
Following synthesis of **19** the goal was to explore the coordination chemistry of the ligand with hard f-block metal ions, i.e., Ln^{3+} ions. It was expected that the hard P=O donor group would form strong coordinate bonds to Ln^{3+}. On the other hand, it was not clear whether **19** would act as a bidentate chelate ligand through either heterocyclic ring N or O-atom lone pair donation. Lastly it was of interest to assess the potential for **19** to act as an extractant for Ln^{3+} ions. The chemistry reported in Chapter 2 has shown that

compound **19** can be efficiently prepared and the ligand forms stable complexes with Ln(III) ions. Although only a few examples could be fully characterized by crystallographic methods, it is clear that **19** can act as either a monodentate P=O bonded ligand or a P=O, N bonded ligand. The observations suggested that the ligand may behave as a hemilabile ligand in solution with Ln(III) ions. This encourages considerations of **19** for extraction studies, but unfortunately the ligand undergoes reactions in acidic aqueous solutions. Therefore, no further effort was given to the preparation of additional examples of **19**.

4.2 Syntheses and coordination chemistry of benzoxazole-based ligands, 25

It was initially thought that the next target should be the oxazole derivative shown here since this would be the aromatic analog of **19**. A preliminary examination of the
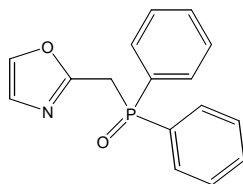
literature did not appear to be encouraging; therefore, attention was directed to the synthesis of the benzoxazole derivative **25**.
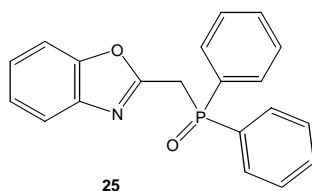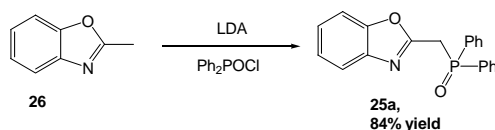
Here, the same donor environment would be provided as in the oxazoline ligand **19**. The benzoxazole might also be expected to be easily purified and crystallized thereby facilitating characterization by spectroscopic and X-ray diffraction methods. Three

strategies were developed to synthesize **25a** (R=Ph) as summarized in Schemes 7-9 (Chapter 3).
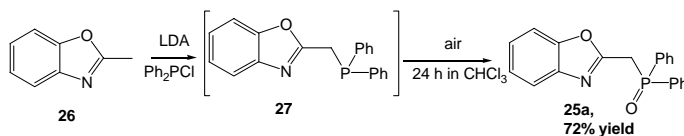
Scheme 7
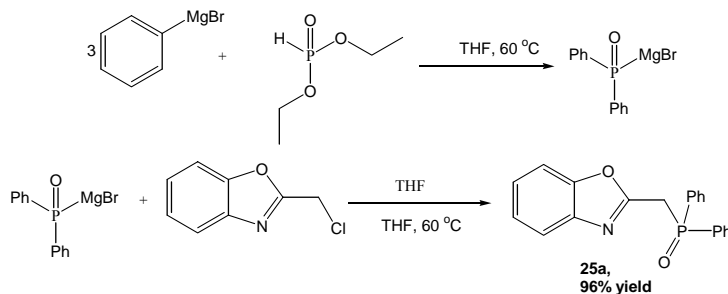
Scheme 8

Scheme 9

As described in detail in Chapter 3, each route is relatively efficient. The choice of one route over another depends mostly on the availability and cost of starting materials. The route in Scheme 7 probably is the most adaptable to a wide range of R groups on phosphorus.
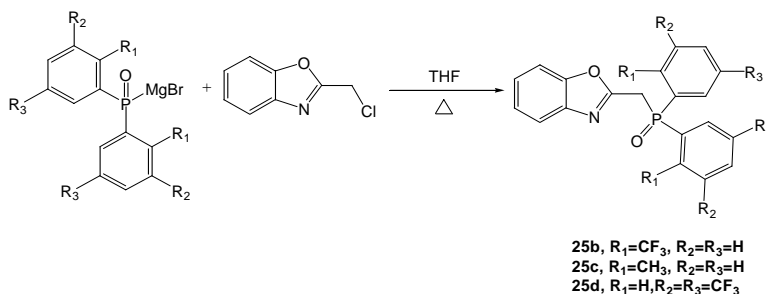
As with **19**, the coordination chemistry of **25a** was examined with several $Ln(NO_3)_3 \cdot xH_2O$, but in this study only $Yb(NO_3)_3 \cdot 5H_2O$ and $Nd(NO_3)_3 \cdot 6H_2O$ produced crystalline complexes suitable for X-ray diffraction studies. In the isolated 2:1 complexes monodentate P=O and bidentate P=O, N coordination conditions were found with **25a**.

Compound **25a** is stable in 1.2 M HCl but insoluble in hydrocarbon diluents that

are commonly used in separation of Ln(III)/An(III) ions. However, **25a** is soluble in trifluoromethanesulfonyl-benzene (FS-13), a solvent that has been recommended for separation of Ln(III)/An(III) ions. This observation led to the development of benzoxazole derivatives that incorporate one or two CF_3 substituents, **25b** and **25d**. It was anticipated that the new compounds having CF_3 on the aryl rings would be more soluble in FS-13 than **25a** without CF_3 substituents. A comparative molecule with the electron donating substituent CH_3, **25c**, was also prepared.

A general synthetic approach shown in Scheme 25 was developed and used to prepare these derivatives. The method involved the preparation of suitable Grignard reagents with relevant substituents on R_1, R_2 and R_3, and compounds **25b**, **25c** and **25d** were obtained with reasonable yields.

Scheme 25

25b, R_1=CF_3, R_2=R_3=H
25c, R_1=CH_3, R_2=R_3=H
25d, R_1=H, R_2=R_3=CF_3

The coordination chemistry with these ligands was examined with Ln(III) ions. No crystalline complexes were obtained with **25d** but the others formed crystalline complexes with either Yb(III) and/or Nd(III). For example, **25b** formed a complex with Yb(III) with a 2:1 ligand:metal stoichiometry, and the ligand bonds in a monodentate mode via the P=O only. This complex was identical to the complex formed with **25a**. Ligand **25c** formed complexes with both Yb(III) and Nd(III) that were similar to each other, Figures 3.32, 3.44 and 3.47 (Chapter 3).

Compound **25b** with one CF_3 substituent was found to be two times more soluble in FS-13 than **25c.** In addition, the ligand is stable in 1.2 M HCl and it displays favorable coordination behavior to Ln(III) ions. This suggests the possible use of **25b** in practical separations of Ln(III)/An(III) and the appropriate characterization of extraction performance will be undertaken in separate collaborative studies.

.

APPENDIX

Experimental

General Procedures. The organic reagents used in the syntheses were purchased from Aldrich Chemical Co., and organic solvents were obtained from Burdick & Jackson and dried by standard procedures. The lanthanide nitrate salts were purchased from Aldrich. All reactions were performed in oven-dried glassware under a dry nitrogen gas atmosphere. Anhydrous solvents and liquids were obtained by distillation from the indicated reagents: diethyl ether ($LiAlH_4$), THF ($LiAlH_4$), distilled from benzophenone/sodium mixture, benzene ($LiAlH_4$), acetone (K_2CO_3), chloroform (dried by shaking with water to remove ethanol, then kept over $CaCl_2$ and stirred with P_4O_{10}, followed with distillation under nitrogen), several reagents were distilled under nitrogen and stored over 4Å molecular sieves and used without further purification. Solid ligands synthesized were dried over $Na_2SO_4/MgSO_4$ and crystallized. All solid ligands isolated as solid were shown to be pure by ^1H NMR, ^{13}C NMR obtained from Bruker FX-250 spectrometer using $(CH_3)_4Si$ and ^{31}P NMR (85% H_3PO_4 as shift standards). Elemental analyses determination using the CE-440 elemental analyzer was done from Galbraith Laboratories. Infrared spectra were recorded on a BRUCKER TENSOR27-BI016203, OPUS-serial 422448097 instrument. Column chromatographic separations were performed by using silica gel 70-230 mesh, 60Å eluted with different solvent systems. Melting points were taken on a Thomas-Hoover Uni-Melt capillary melting point apparatus and reported uncorrected. ^1H NMR spectra were recorded by using $CDCl_3$ and DMSO solutions at 250 MHz, ^{13}C and DEPT-135 NMR spectra were recorded in $CDCl_3$. Chemical shifts are reported in ppm relative to $CDCl_3$ at 7.24 ppm or TMS 0 ppm for

proton NMR and 77.0 ppm or 0 ppm for ^{13}C NMR. ^{1}H NMR data are reported as follows: chemical shift, multiplicity (s = singlet, d = doublet, t = triplet, q = quartet, m = multiplet, br = broad), integration and coupling constant (*J* in Hz). High resolution mass spectra (HRMS) were obtained at UNM Waters LCT Premier TOF, mass spectrometry facility, Albuquerque, New Mexico. All downfield shifts from the reference were designated as +δ.

Synthesis of 2-chloromethylbenzoxazole, 35

This is a two step synthesis involves the preparation of N-(2-hydroxyphenyl) chloroacetoamide and polyphosphate ester precursors as described in Schemes 26 and 28.

Scheme 26

Synthesis of N-(2-hydroxyphenyl)chloroacetoamide, 31
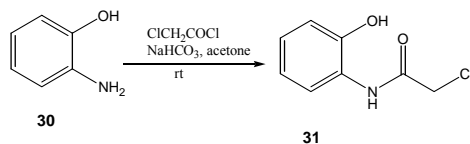
The method reported by Kosaka and co-workers[34] was adopted without modifications. To a stirred suspension of 2-aminophenol (2.0 g, 18.8 mmol, 1 eq.) and NaHCO$_3$ (3.2 g, 37.6 mmol, 2 eq.) in anhydrous acetone (30 ml) (dried by shaking with anhydrous K$_2$CO$_3$ and left to stand for 24 h, followed by distillation) under nitrogen atmosphere, was added, dropwise, chloroacetyl chloride (1.5 ml, 19.7 mmol, 1 eq.). The reaction mixture was stirred for 2 h at room temperature; the precipitate was separated by suction and washed with acetone. The combined filtrate was concentrated under vacuum and the residue was crystallized from hot ethyl acetate to give the product as a gray powder. Yield: 2.6 g (76%), mp 130-132 ^{o}C. This product was used in the subsequent reaction (Scheme 28) without further purification.

Selected spectroscopic data for N-(2-hydroxyphenyl)chloroacetoamide are summarized here.

Infrared spectrum (KBr, cm^{-1}): 1684 (s, $\nu_{C=O}$), 3434 ($\nu_{OH/NH}$)

^{1}H (250MHz, 23 ^{o}C, DMSO), δ (ppm): 4.2 (s, 2H, -CH$_2$-Cl), 6.7-6.8 (m, 1H, H-Ar), 6.9 (m, 2H, H-Ar), 8.0 (d, 1H, H-Ar, $^3J_{H-H}$ = 7.9 Hz), 9.1 (s, 1H, NH), 9.5 (s, 1H, OH)

^{13}C{^{1}H} (62.9 MHz, 23 ^{o}C, DMSO), δ (ppm): 41.4 (s, –CH$_2$-Cl), 113.9 (s), 117.9 (s), 118.8 (s), 123.4 (s), (4C, C-Ar), 124.1 (s, C-NH), 145.4 (s, C-OH), 162.6 (s, C=O).

Mass spectrum (ESI) *m/e* (fragment, relative intensity): [M+H]$^+$ = 186.0343 and the calculated exact mass is 185.0244.

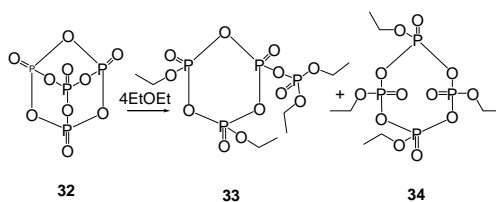These data can be compared with data from the literature.[34]

Yield: 74%, mp 139-140.5 ^{o}C.

Infrared spectrum (KBr, cm^{-1}): 1656 (s, $\nu_{C=O}$).

^{1}H (CDCl$_3$), δ (ppm): 4.27 (s, 2H), 6.85-7.10 (m, 2H), 7.10-7.35 (m, 2H), 7.85 (br s, 1H), 8.55 (br s, 1H).

**Synthesis of polyphosphate ester (ethyl polyphosphate)**

Scheme 27

Phosphorus pentoxide (37.5 g) was added to a solution of anhydrous ether (75 ml) distilled under LiAlH$_4$ and alcohol free chloroform (37.5 ml), dried by shaking with water to remove ethanol, then kept over CaCl$_2$ and stirred with P$_4$O$_{10}$, followed with distillation under nitrogen. The reaction mixture was refluxed at 70 ^{o}C under dry nitrogen

for 4 days (reflux for 24 h gave a clear solution) and the resulting clear solution was decanted from a small amount of residue. The solution was concentrated to colorless syrup in a rotary evaporator; residual traces of solvent were removed by heating the syrup for 36 h at 40 °C using a sand bath under vacuum. The mass of the product was 60.6 g. This reagent was used directly without further purification (Scheme 28).

**Synthesis of 2-chloromethylbenzoxazole, 35**

Scheme 28
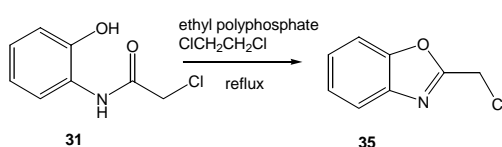
CAUTION: 2-Chloromethylbenzoxazole is an aggressive skin and eye irritant as well as bronchial irritation. Therefore handling of this reagent and its solutions should be done in a well ventilated hood, with double gloves because it diffuses through the membrane of gloves.

To a solution of ethyl polyphosphate (30.0 g) in dry 1, 2-dicholoroethane (60 ml) under nitrogen atmosphere was added, portion wise N-(2-hydroxyphenyl) chloroacetoamide (2.6 g, 13.5 mmol), the mixture was heated to reflux for 2 h. After cooling to room temperature, the mixture was diluted with CH_2Cl_2 (50 ml), washed with water, dried over $MgSO_4$, and concentrated under vacuum. The residue was purified by column chromatography: silica gel, 70-230 mesh, 60 Å, eluted with 100% CH_2Cl_2, gave pale yellow oil, which was purified by vacuum distillation to give 2-chloromethylbenzoxazole as colorless oil. Yield: 1.4 g (62%). When ethyl polyphosphate was used in excess (i.e., 1.3 eq.), no unreacted starting material was observed.

Selected spectroscopic data for 2-chloromethylbenzoxazole are summarized here and typical IR, ^{1}H NMR, and ^{13}C NMR are shown in Figure 3.70-3.72.
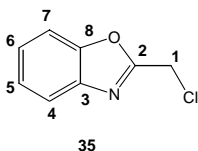
Infrared spectrum (KBr, cm^{-1}): 1611 (s, $\nu_{C=N}$).

^{1}H (250MHz, 23 ^{o}C, CDCl$_3$), δ (ppm): 4.7 (s, 2H, -CH$_2$-Cl), 7.2-7.3 (m, 2H, H-Ar), 7.4 (m, 1H, H-Ar), 7.6-7.7 (m, 1H, H-Ar).

Literature[47] reported only ^{1}H NMR data:

^{1}H (CDCl$_3$), δ (ppm): 4.76 (s, 2H, -CH$_2$-Cl), 7.38 (m, 2H, H-Ar), 7.56 (m, 1H, H-Ar), 7.73 (m, 1H, H-Ar).

^{13}C{^{1}H} (62.9 MHz, 23 ^{o}C, CDCl$_3$), δ (ppm): 36.2 (s, C$_1$), 110.6 (s), 120.2 (s), 124.5 (s), 125.6 (s), 140.6 (s), 150.8 (s), C-Ar, 160.5 (s, C$_2$).

Mass spectrum (ESI) *m/e* (fragment, relative intensity): [M+H]$^+$ = 168.0202 and the calculated exact mass is 167.0138.

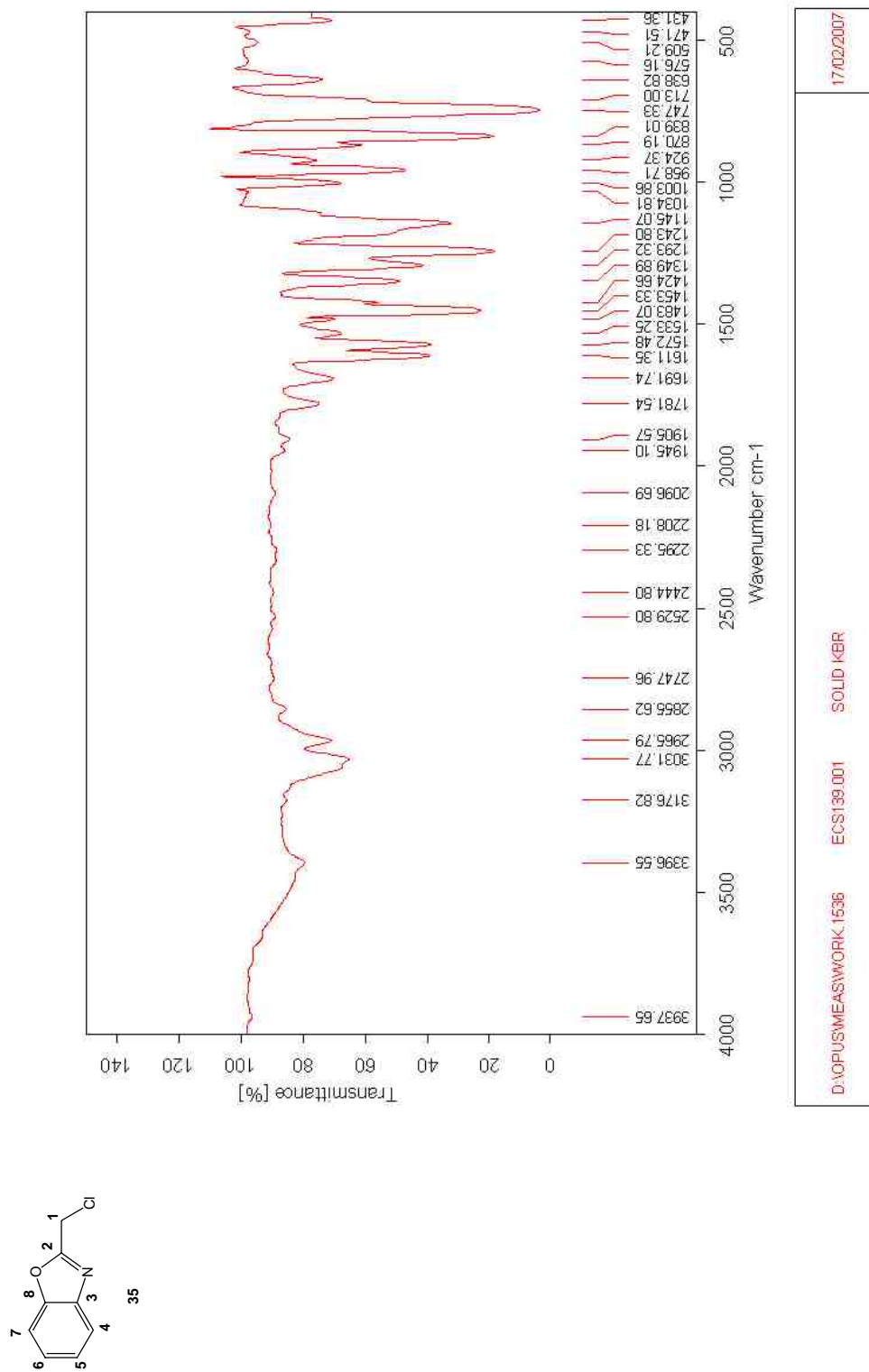**Figure 3.70 Infrared spectrum (KBr, cm^{-1}) for 2-chloromethylbenzoxazole, 35**

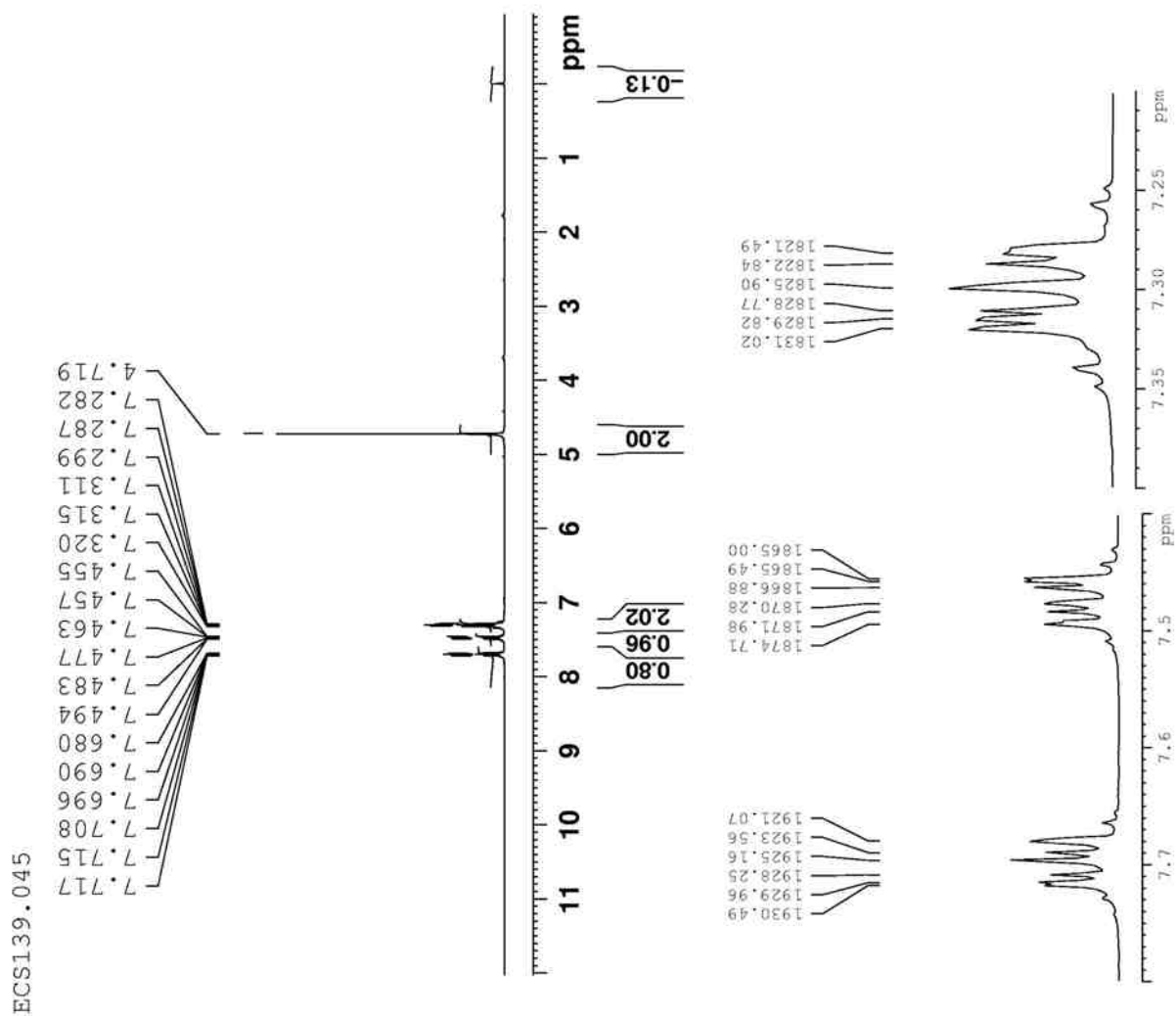**Figure 3.71 250 MHz ^{1}H NMR spectrum for 2-chloromethylbenzoxazole, 35**

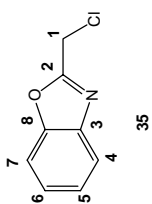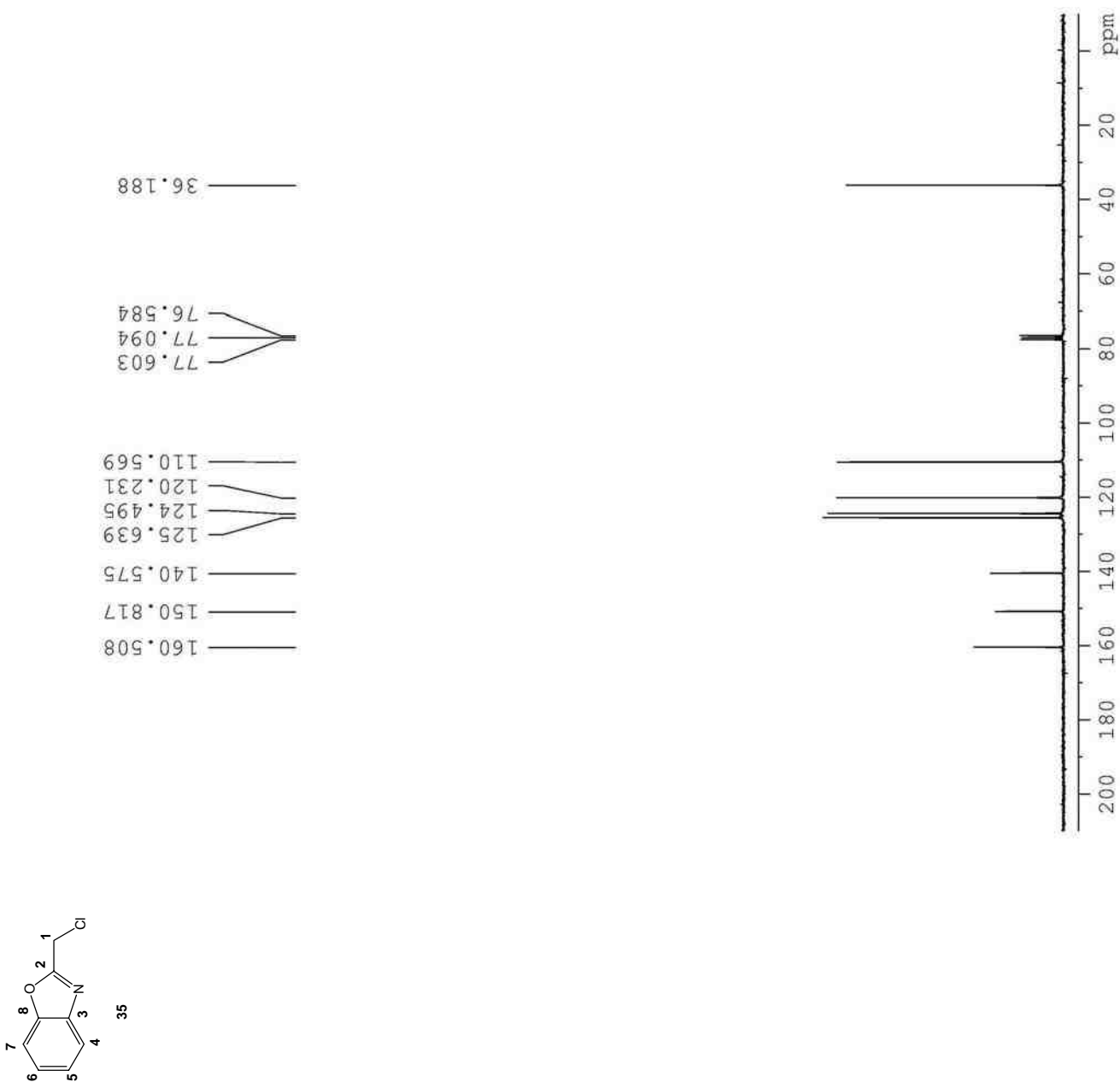**Figure 3.72 62.9 MHz ^{13}C{^{1}H} NMR spectrum for 2-chloromethylbenzoxazole, 35**

Future Directions

Although the syntheses and coordination chemistry of benzoxazole compounds have been examined with Ln(III) ions in the current study, the syntheses of more derivatives is important in order to compare the extraction abilities of these new compounds and probably develop a compound that will show selectivity and high extraction ability to Ln(III)/An(III) ions. In future, compounds **36** and **37** have been proposed. The aim is to explore the coordination chemistry of **36** with Ln(III) ions in order to understand the extent to which the presence of this compound in the extraction of Ln(III)/An(III) may affect the extraction performance of neutral organophosphine oxide ligands. Studies[1, 2] have shown that the neutral organophosphine oxide ligands undergo hydrolysis in acidic solution during the extraction processes to form phosphonic acid derivatives that hinder the extraction ability of neutral organophosphine oxides due to low solubility of the acids in organic phase.

In order to improve the separation of Ln(III)/An(III) in hydrocarbon diluents, compound **37** is also proposed. It is expected that if **37** could be synthesized, having ethylhexyl organic tail, this compound is expected to be more soluble in long carbon chain diluents compared to benzoxazole ligands reported in this study. The stability of these two compounds will be tested in acidic solution.
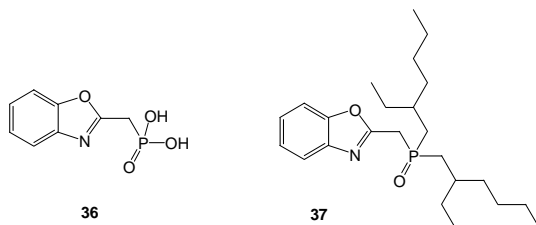
Synthetic directions

The synthesis of **36** involves a multistep synthesis initially adopting the method developed by Minami and co-workers[3] and the hydrolysis reaction will adopt the method developed in our group to synthesize phosphonic acid derivatives.[1, 2]

Scheme 29
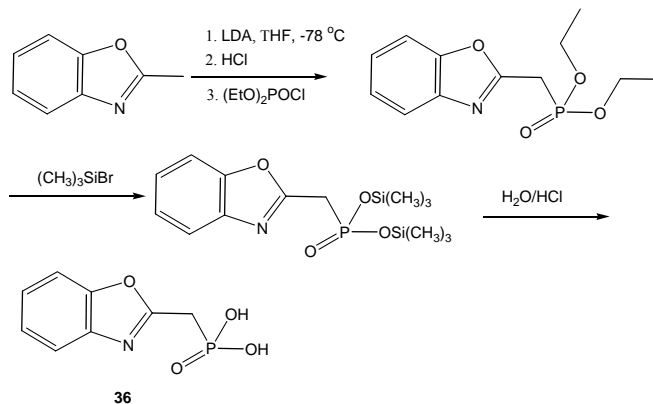
The synthetic approach in the preparation of the ethylhexyl benzoxazole derivative **37** will adopt the Grignard method used in the syntheses of compounds **25a-25d**.[4-9]

Scheme 30
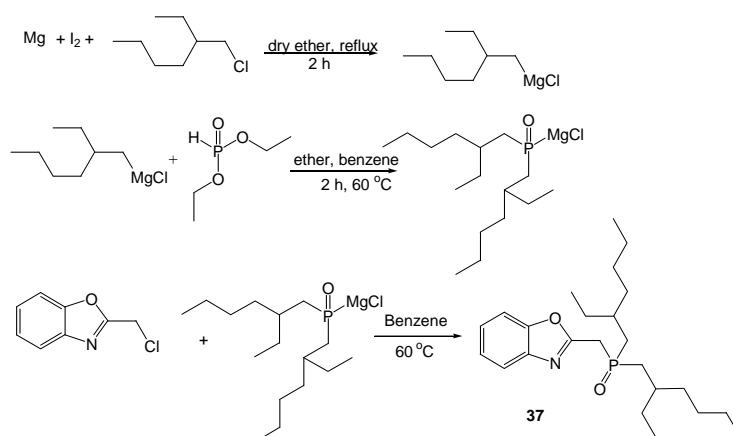
REFERENCES

1. Gan, X.; Binyamin, I.; Pailloux, S.; Duesler, E. N.; and Paine, R. T. *Dalton Trans* **2006,** *45,* 3912.

2. Gan, X.; Rapko, B. M.; Fox, J.; Binyamin, I.; Pailloux, S.; Duesler, E. N.; and Paine, R. T. *Inorganic Chemistry* **2006,** *45,* 3741.

3. Minami, T.; Isonaka, T.; Okada, Y.; and Ichikawa, J. *J. Org. Chem.* **1993,** *58,* 7009.

4. Gan, X. M.; Duesler, E. N.; and Paine, R. T. *Inorg. Chem.* **2001,** *40,* 4420.

5. Tan, Y. C.; Gan, X. M.; Stanchfield, J. L.; Duesler, E. N.; and Paine, R. T. *Inorg. Chem.* **2001,** *40,* 2910.

6. Gan, M. X.; Parveen, S.; Smith, L. Y.; Duesler, E. N.; and Paine, R. T. *Inorg. Chem.* **2000**, *39(20)*, 4591.

7. Gan, X. M.; Duesler, E. N.; and Paine, R. T. *Inorg. Chem.* **2001**, *40*, 4420.

8. Bond, E. M.; Duesla, E. N.; Paine, R. T.; and Nöth, H. *Polyhedron* **2000,** *19,* 2135.

9. Paine, R. T.; Bond, E. M.; Parveen, S.; Donhart, N.; Duesler, E.; Smith, K. A.; and Nöth, H. *Inorg. Chem.* **2002,** *41(2),* 444.